UNIVERSITÄT BAYREUTH

UGC
Umweltgeochemie Bayreuth

Influence of long-term paddy use on arsenic mobility and speciation

Dissertation

submitted to obtain the academic degree
Doctor rerum naturalium (Dr. rer. nat.)

of the Bayreuth Graduate School of Mathematical and Natural Sciences (BayNAT)
of the University of Bayreuth

by
José Miguel G. León Ninin
(MSc. Environmental Chemistry)

born in Mérida, Venezuela

Bayreuth, 2024

This doctoral thesis was prepared at the Environmental Geochemistry Group at the University of Bayreuth from September 2020 until December 2024 and was supervised by Prof. Dr. Britta Planer-Friedrich.

This is a full reprint of the thesis submitted to obtain the academic degree of Doctor of Natural Sciences (Dr. rer. nat.) and approved by the Bayreuth Graduate School of Mathematical and Natural Sciences (BayNAT) of the University of Bayreuth.

Type of thesis: cumulative thesis

Date of submission: 03.12.2024

Admission by the executive board: 11.12.2024

Date of defense: 26.06.2025

Acting director: Prof. Dr. Jürgen Köhler

Doctoral committee:

Prof. Dr. Martin Obst (reviewer)

Prof. Dr. Adrien Mestrot (reviewer)

Prof. Dr. Eva Lehndorff (chair)

Prof. Dr. Stephan Clemens

(additional reviewer: Prof. Dr. Jörg Feldmann)

Acknowledgments

First and foremost, I would like to thank my doctoral supervisor, Prof. Dr. Britta Planer-Friedrich. Thank you for welcoming me into your group, and for your guidance and supervision throughout this project. I am very grateful to you for trusting me and giving me the freedom to figure out things at my own rhythm. Who would have known that a couple of emails in 2016 would lead us here? Thank you for repeatedly correcting “stablished” for “established” and “in” for “on”, in my texts. I hope I did not confuse them here.

I want to extend my most sincere gratitude to the Studienstiftung des deutschen Volkes for supporting me and this project for the last three and a half years. Thanks for the financial support to attend the Geochemistry of the Earth’s Surface symposium in Zürich (2022), the Goldschmidt conference in Lyon (2023), and the Tools in Biogeochemistry workshop in Tübingen (2023). Thanks for allowing me the fulfilling opportunity to design and teach the Chemistry of Climate Change seminar through the Mariane-Plehn Program. Thanks to the Graduate School of the University of Bayreuth for their workshops, get-togethers, and additional financial support for attending the conferences in Lyon and Zürich.

I am also deeply grateful to the Environmental Geochemistry group and its members between 2018 and 2024. You have all contributed to my personal and professional growth, as well as to this project. Thank you for the insightful discussions, celebration cakes, international food Fridays, kayak tours, and hiking trips. Thank you, Niclas, Asel, Grethe, and Alejandra, for the opportunity to supervise your theses, and thank you, Anh, Mila, Eva, Merle, Jens, and Tobi, for your experimental support. Thank you, Sylvia, for all your support in the lab, for Tim (I, II, and III), for the sunflowers, and for helping me get a gaming PC to play Stardew Valley when I was overwhelmed by the PhD.

Special thanks also to the cooperation partners throughout the project, both inside the University of Bayreuth and in other universities and institutes in Germany. Without your expertise and technical support, putting the pieces of this puzzle together would not have been possible. Thank you, Angelika and Livia, for giving me the opportunity to expand on the knowledge of the Cixi chronosequence. Moreover, I would like to extend my gratitude to the technicians who supported me during the measurements and data collection presented and discussed in this thesis. Thank you, Silke, Ilse, Anita, and Paul.

Thank you, Katrin, Andrea, and Jose for proofreading this thesis and keeping me motivated through the final stretch of this journey.

Finally, but most importantly I would like to thank anybody who supported me personally during these last 4 years. To my family (now) in Uruguay who taught me constantly to be brave and to sail for new

adventures, even when afraid. To my friends here in Bayreuth, in Germany, or somewhere else around the world who were and still are my home away from home. Thanks for the coffee, walks, and talks. Thank you, Ale, Philipp, Kevin, Johanna (Danhauser), Johanna (Schmidtmann), Tanu, Katrin, Andrea, Jose, Carolin, Ilvanna, and Rosa.

And thank you, Jon, for being my greatest support along the way, even when I made you come with me to clean the ICP-MS some weekends when we started dating.

Abstract

Rice is traditionally cultivated in flooded paddies under sub-oxic and anoxic conditions where non-aerobic respiration pathways, such as iron (Fe) and sulfur (S) reduction, take place. These conditions trigger arsenic (As) mobilization and, through abiotic and microbially mediated reactions, influence As speciation. The speciation of As influences its mobility, toxicity, uptake by plants, and accumulation in rice grains. Given the importance of rice as a staple food, As exposure through its consumption is a global concern.

Long-term paddy cultivation triggers a specific soil development, characterized by soil organic carbon (SOC) accumulation, formation of amorphous Fe phases, increased microbial biomass, and decreased pH. These are soil properties reported to influence As mobility and speciation. Until now, a clear connection between paddy soil development and aqueous redox biogeochemistry, including As behavior, has not been established.

This thesis aimed to investigate the role of long-term paddy use on As mobility and speciation. Using a paddy soil chronosequence spanning 2000 years of use, the links between changes in soil properties and the biogeochemistry of Carbon (C), Fe, S, and As were evaluated. The influence of long-term paddy use (or paddy soil "age") in the transformation dynamics of well-known As species such as inorganic and methylated oxyarsenic species was assessed. Moreover, pedological and biogeochemical factors influencing the formation of thioarsenates, a group of species recently identified in paddy soils, were also investigated.

Study 1 evaluated how long-term paddy soil development influences As redox dynamics. The formation of amorphous Fe phases with long-term paddy use decreased As mobility. The abundance of bioavailable Fe^{III} in these phases delayed other anaerobic respiration pathways such as sulfate reduction and methanogenesis. Nonetheless, increased SOC supported higher microbial activity, soil respiration, and methanogenesis. This higher microbial activity increased As methylation. Thioarsenate formation was hindered by long-term paddy use due to the high availability of reducible Fe in older soils, which scavenged the sulfide (S^{-II}) required for As thiolation.

Having established that long-term paddy use influences redox biogeochemistry and As dynamics, Studies 2 and 3 evaluated if it also regulates biogeochemical responses to external influences. Considering future climatic scenarios, Study 2 evaluated how higher temperatures influence As biogeochemistry depending on soil development. Increasing temperatures triggered specific risks depending on the soil's developmental stage. Higher temperatures increased As mobilization in newly established and young paddies due to a lack of sorption sites from amorphous Fe phases. Paddies of 100 and 300 years showed higher increases in As methylation, due to an enhanced microbial activity

and SOC pool that supports it. Soil respiration and methanogenesis had the highest relative increase in older soils, risking a positive feedback loop with climate change.

Study 3 evaluated how paddy soils at different stages of development could respond to sulfate fertilization, a practice proposed to limit As mobility. In young paddies with low Fe and SOC availability, sulfate fertilization caused an excess of S^{-II} which increased As thiolation. Older paddies with higher SOC and amorphous Fe phases buffered this increase. In young soils, lower sulfate reduction rates compared to those in older ones, offered a small but constant supply of S^{-II} for As thiolation. Moreover, young paddies had the highest relative increase in As methylation after sulfate fertilization. These results, together with observations from Study 1 suggest changes in the microbial communities related to As methylation with increasing paddy soil age, from sulfate-reducing-bacteria-driven to fermentative-bacteria-driven. Study 3 additionally determined that disruptions to paddy soil development which decrease SOC, Fe availability, and microbial activity, cause their responses to sulfate fertilization to be similar to that in young paddies.

In Studies 1 and 2, thioarsenate formation during incubation stages with low sulfate reduction suggested an alternative source of S^{-II}. Sulfide reoxidation coupled to Fe^{III} reduction (so-called cryptic S cycle, CSC) has been proposed to play a role in As thiolation. In Study 4, the youngest paddy was depleted from excess S, Fe, and As using repetitive redox cycling, to evaluate the role of the CSC as a source of S^{-II} for As thiolation. Zerovalent S and thiosulfate (products of S^{-II} reoxidation) correlated positively with the formation of methylated but not inorganic thioarsenates, suggesting that CSC plays a bigger role in the formation of the former. Results from this Study also suggest that, in S-depleted soils, dethiolation of inorganic thioarsenates takes place to form thermodynamically preferred methylthioarsenates.

The findings of this thesis show that changes in soil properties related to long-term paddy use influence redox processes and, in turn, As mobility and speciation. These findings could help evaluate current and future risks associated with rice production, as well as tailor agronomical practices depending on the specific requirements of each developmental stage. From an As speciation perspective, the findings presented here expand on the current knowledge of the biogeochemical processes influencing the dynamics of methylation and thiolation in paddy soils.

Zusammenfassung

Reis wird traditionell in überfluteten Reisfeldern unter sub- und anoxischen Bedingungen angebaut. Dort finden anaerobe Reaktionen, wie die Reduktion von Eisen (Fe) und Schwefel (S) statt. Dies führt zur Mobilisierung von Arsen (As) und beeinflusst durch abiotische Reaktionen und mikrobielle Prozesse die As-Speziierung. Die Speziierung von As beeinflusst dessen Mobilität, Toxizität, Aufnahme durch Pflanzen und Anreicherung in Reiskörnern. Angesichts seiner Bedeutung als Grundnahrungsmittel ist die As-Exposition durch den Verzehr von Reis ein globales Problem.

Langfristiger Reisanbau löst charakteristische Prozesse im Boden aus. Dazu gehören die Anreicherung von organischem Kohlenstoff (SOC), die Bildung amorpher Fe-Phasen, eine erhöhte mikrobielle Biomasse und ein niedrigerer pH-Wert. Diese Bodeneigenschaften beeinflussen, Studien zufolge, die Mobilität und Speziierung von As. Bislang wurde jedoch kein eindeutiger Zusammenhang zwischen der Bodenentwicklung in Reisfeldern und biogeochemischen Redoxreaktionen, einschließlich der As-Mobililität, im Porenwasser festgestellt.

Das Ziel dieser Doktorarbeit war, die Rolle des langfristigen Reisanbaus für die Mobilität und Speziierung von As zu untersuchen. Anhand von Reisfeldern in einer 2000-jährigen Chronosequenz wurden die Zusammenhänge zwischen den Veränderungen in Bodeneigenschaften und der Biogeochemie von Kohlenstoff (C), Fe, S und As untersucht. Der Einfluss des langfristigen Reisanbaus (oder des „Alters“ der Reisböden) auf die Umwandlung bekannter As-Arten, wie anorganischer und methylierter Oxyarsen-Spezies, wurde bewertet. Darüber hinaus wurden bodenkundliche und biogeochemische Faktoren untersucht, die die Bildung von Thioarsenaten beeinflussen, einer Gruppe von Spezies, die kürzlich in Reisböden identifiziert wurde.

In Studie 1 wurde untersucht, wie die langfristige Entwicklung von Reisböden die Redoxdynamik von As beeinflusst. Die Bildung von amorphen Fe-Phasen bei langfristigem Reisanbau verringerte die As-Mobilität. Das bioverfügbare Fe^{III} in diesen Phasen verzögerte andere anaerobe Atmungswege, wie die Sulfatreduktion und die Methanogenese. Gleichzeitig förderte der erhöhte organische Kohlenstoff die mikrobielle Aktivität, die Bodenatmung und die Methanogenese. Die höhere mikrobielle Aktivität führte zu stärkerer As-Methylierung. Die Bildung von Thioarsenaten wurde durch den langfristigen Reisanbau verlangsamt. Der höhere Gehalt an reduzierbarem Fe in älteren Böden fing den reduzierten sulfid (S^{-II}) ab, der für die Thiolierung von As erforderlich ist.

Basierend auf diesen Ergebnissen wurde in den Studien 2 und 3 untersucht, ob langfristiger Reisanbau die biogeochemischen Reaktionen der Böden auf externe Faktoren beeinflusst. Unter Berücksichtigung künftiger Klimaszenarien wurde in Studie 2 untersucht, wie sich höhere Temperaturen auf die Biogeochemie von As in Abhängigkeit von der Bodenentwicklung auswirken. Höhere Temperaturen verstärkten die As-Mobilisierung in neu angelegten und jungen Reisfeldern, da hier nur wenige

amorphe Fe-Phasen als Sorbenten vorhanden waren. Bei 100 und 300 Jahre alten Anbauflächen stieg die As-Methylierung stärker an. Das ist auf eine höhere mikrobielle Aktivität und einen größeren Pool organischer Substanz zurückzuführen, der die As-Methylierung unterstützt. Die relative Zunahme der Bodenatmung und der Methanogenese war in älteren Böden am größten, was zu einer positive feedback loop mit dem Klimawandel führen könnte.

In Studie 3 wurde untersucht, wie Reisböden in verschiedenen Entwicklungsstadien auf Sulfatdüngung reagieren, eine Maßnahme, die zur Begrenzung der As-Mobilität vorgeschlagen wurde. In jungen Reisfeldern mit geringer Verfügbarkeit von Fe und organischem Kohlenstoff führte die Sulfatdüngung zu einem Überschuss an S^{-II}, was die As-Thiolation erhöhte. Ältere Reisfelder mit mehr organischem Kohlenstoff und amorphen Fe-Phasen pufferten diesen Anstieg ab. In jungen Böden boten die, im Vergleich zu älteren Böden, niedrigeren Sulfatreduktionsraten ein geringes, aber konstantes Angebot an S^{-II} für die As-Thiolierung. In jungen Böden war der relative Anstieg der As-Methylierung nach Sulfatdüngung am höchsten. Diese Ergebnisse deuten zusammen mit den Ergebnissen aus Studie 1 darauf hin, dass sich die mikrobiellen Gemeinschaften, die für die As-Methylierung verantwortlich sind, mit zunehmendem Alter der Reisfelder von sulfatreduzierenden zu fermentativen Bakterien verschieben. In Studie 3 wurde zudem festgestellt, dass Störungen in der Entwicklung von Reisböden, dazu führen, dass die Reaktionen auf die Sulfatdüngung ähnlich sind wie in jungen Reisfeldern. Der Grund dafür ist, dass diese Störungen den organischen Kohlenstoff, die Fe-Verfügbarkeit und die mikrobielle Aktivität verringern.

In den Studien 1 und 2 deutete die Thioarsenatbildung während der Inkubationsphasen mit geringer Sulfatreduktion auf eine alternative Quelle für S^{-II} hin. Möglicherweise spielt die Reoxidation von Sulfid in Verbindung mit der Reduktion von Fe^{III} (so genannter cryptic S cycle, CSC) eine Rolle bei der Thiolierung von As. In Studie 4 wurde im jüngsten Reisfeld überschüssiger S, Fe und As durch wiederholte Redoxzyklen entfernt, um den CSC als Quelle von S^{-II} für die As-Thiolierung zu bewerten. Nullwertiger S und Thiosulfat (Produkte der Sulfidreoxidation) korrelierten positiv mit der Bildung von methylierten, aber nicht von anorganischen Thioarsenaten, was darauf hindeutet, dass der CSC eine wichtige Rolle bei der Bildung von Methylthioarsenaten spielt. Die Ergebnisse dieser Studie deuten darauf hin, dass in S-armen Böden eine Dethiolierung von anorganischen Thioarsenaten stattfindet, um thermodynamisch bevorzugte Methylthioarsenate zu bilden.

Die Ergebnisse dieser Arbeit zeigen, dass Veränderungen der Bodeneigenschaften, die mit langfristigem Reisanbau einhergehen, die Redoxprozesse und damit auch die Mobilität und Speziierung von As beeinflussen. Diese Erkenntnisse könnten dazu beitragen, aktuelle und künftige Risiken im Zusammenhang mit dem Reisanbau zu bewerten und landwirtschaftliche Praktiken auf die spezifischen Anforderungen der Entwicklungsstadien abzustimmen. Aus der Perspektive der As-Speziierung erweitern die hier vorgestellten Ergebnisse das Wissen über die biogeochemischen Prozesse, die die Dynamik der Methylierung und Thiolierung in Reisböden beeinflussen.

Table of Contents

List of Abbreviations

arsM	Arsenite S-adenosylmethionine methyltransferase
AWD	Alternate wet drying
CH_4	Methane
C_{mic}	Microbial carbon
CSC	Cryptic S cycle
DMA	Dimethylarsenate
DMDTA	Dimethyldithioarsenate
DMMTA	Dimethylmonothioarsenate
DOC	Dissolved organic carbon
DSR	Dissimilatory sulfate reduction
dsrA	Dissimilatory sulfite reductase
DTA	Dithioarsenate
FB	Fermentative bacteria
Fe_{DCB}	Dithionite-citrate-bicarbonate extractable Fe
Fe_O	Oxalate extractable Fe
GC-FID	Gas chromatography with flame ionization detector
GHG	Greenhouse gas
GlpF	Aquaglyceroporin channel
HBED	N,N'-Di(2-hydroxybenzyl)ethylenediamine-N,N'-diacetic acid monohydrochloride
HPLC-DAD	High-performance liquid chromatography with diode-array detection
HPLC-RID	High-performance liquid chromatography with refractive index detection
HPLC-UV-Vis	High-performance liquid chromatography with ultraviolet-visible detection
HWHM	Half width at half maximum
IC	Ion Chromatography
ICP-MS	Inductively coupled plasma mass spectrometry
IPCC	International panel for climate change
iThioAs	Inorganic thioarsenates
mcrA	Methyl coenzyme M reductase
MeThioAs	Methylthioarsenates
MMA	Monomethylarsenate
MMDTA	Monomethyldithioarsenate
MMMTA	Monomethylmonothioarsenate
MMTTA	Monomethyltrithioarsenate
MQ	Ultrapure water

MTA	Monothioarsenate
NP	Non-paddy soil
P	Paddy soil
qPCR	Quantitative polymerase chain reaction
SEP	Sequential extraction procedure
SOC	Soil organic carbon
SRB	Sulfate reducing bacteria
SRR	Sulfate reduction rate
TetraTA	Tetrathioarsenate
TRIS	Total reduced inorganic S
TTA	Trithioarsenate
VBF	Voigt Based Fitting
µXRD	Micro X-ray diffraction

List of Tables

List of Figures

Figures 1-6 were created using BioRender.

Extended summary

1. Introduction

1.1. Flooded rice cultivation – Biogeochemical implications and consequences

Rice is a crop of global importance since it is a staple food for half of the world's population, and its consumption is widespread mainly across Asia, Africa, and Latin America.[1,2] The flooded conditions under which rice is traditionally cultivated have direct consequences on soil and porewater biogeochemistry.[3,4] The standing water prevents direct interactions between the soil and the atmosphere, limiting the diffusion of oxygen into the soil.[3] After flooding, aerobic microbial activity readily depletes the porewater from oxygen, decreasing the redox potential and generating sub-oxic and then anoxic conditions.[3] This oxygen depletion triggers dynamic redox processes due to the use of alternative electron acceptors in anaerobic microbial respiration pathways, including sulfur (S) and iron (Fe) reduction, and methanogenesis.[3,5]

These microbially mediated processes are directly linked with the biogeochemistry of arsenic (As) in paddy soils and its accumulation in rice grains. Arsenic accumulation in rice grains is a consequence of increased bioavailability under reducing conditions and the physiology of rice plants, which uptake As through non-specific uptake pathways for phosphorus and silicon.[3,6-8] Thus, rice consumption is considered one of the main dietary exposure sources to As, a well-known carcinogen.[9,10] In comparison to other cereals, such as wheat or barley, rice can contain up to 10 times more As.[11] Considering the high and worldwide spread consumption of rice, exposure to As through accumulation in rice grains is of global concern.[1,2] More importantly, a combination of microbially mediated and abiotic reactions control As speciation, and, thus, its mobility and toxicity for rice plants and consumers.[12-14]

1.1.1. Influence of flooded conditions on As mobility and speciation

Arsenic is ubiquitously present in the environment as a result of the weathering of As-containing minerals, volcanic and geothermal activity, and anthropogenic sources.[15] The global average of As content in soils lies between 5 and 7.5 mg kg^{-1}, but concentrations can reach up to several hundreds of mg kg^{-1} depending on bedrock material or anthropogenic influences from mining activities or the use of As-containing pesticides and fertilizers.[15,16]

Under oxic conditions, As is present in soils mainly as arsenate bound to Fe^{III} (oxy)hydroxide phases, where it is immobile.[17,18] Iron reductive dissolution under flooded conditions releases arsenate into the porewater where it becomes available for plant uptake (Figure 1, lower left).[19] Arsenate can be reduced to arsenite either after release or while it is still adsorbed to mineral phases.[20] Arsenate and arsenite (summarized as inorganic As) are the major species in paddy soil porewater and rice grains.[2,11,21] Being

highly toxic for humans, they are classified as Class A Carcinogens, and their content is regulated in rice grains and products.[22,23]

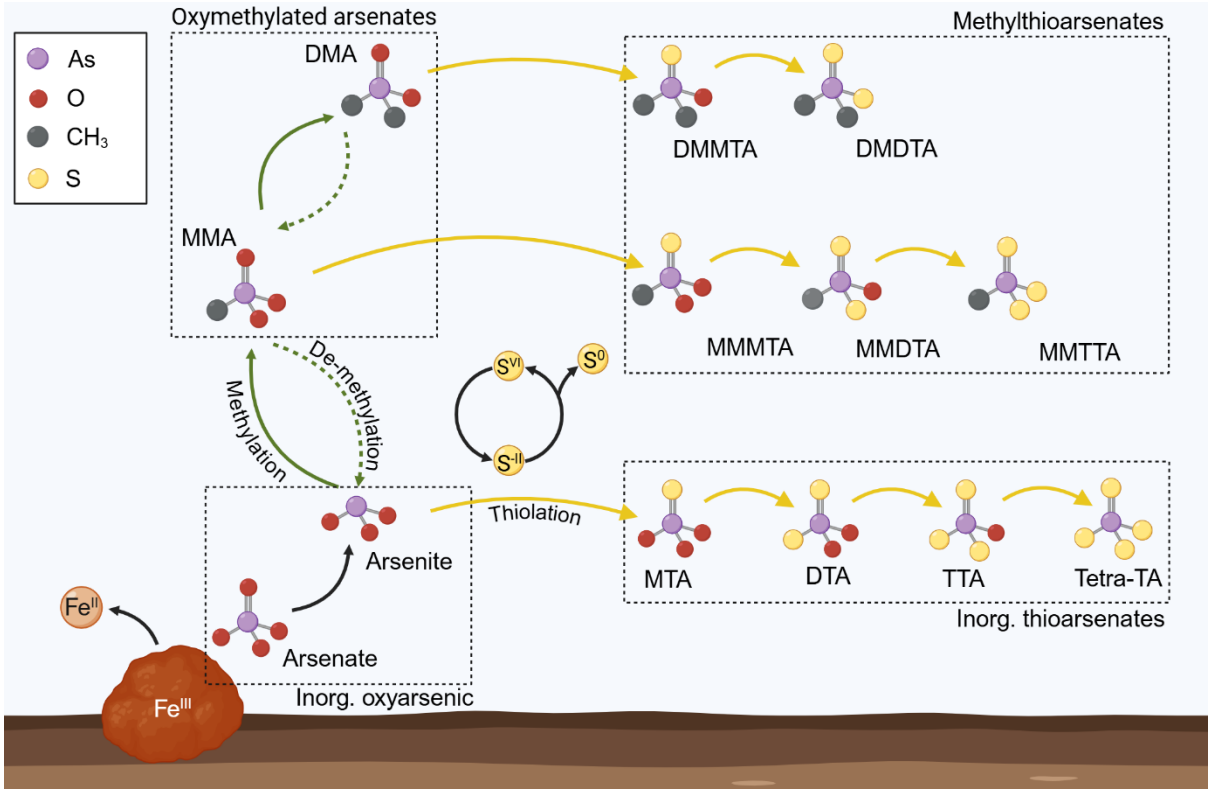

Figure 1: Formation of the different As species discussed in this thesis, and the groups in which they are classified. For simplicity of the depiction, charges, oxidation states, and possible protonation have been omitted.

The second major group of As species in paddy soil porewater are oxymethylated arsenates (Figure 1, upper left).[2,21,24] Soil microbes carrying the S-adenosylmethionine methyltransferase (*arsM*) gene can biotically methylate arsenite in two consecutive steps to form monomethylarsenate (MMA) and dimethylarsenate (DMA).[12,25,26] The two main microbial groups currently associated with As methylation in paddy soils are sulfate reducing bacteria[27,28] (SRB) and fermentative bacteria[29] (FB), although the metabolic advantage behind the methylation process is still largely unknown. Some hypotheses involve detoxification mechanisms[26] or the use of trivalent methylated As species as antibiotics against other microbial groups.[30,31] In paddy soils, oxymethylated arsenates can be demethylated back to arsenite by the activity of some methanogens.[27,32,33] Arsenic methylation dynamics largely influence As accumulation in rice grains. Rice plants have a wide range of As detoxification strategies, such as complexation with glutathione or phytochelatins, which effectively bind arsenate, arsenite, and MMA, and sequester them in the vacuoles.[34,35] However, a lack of effective detoxification mechanisms for DMA causes this species to be enriched in the grains.[36] Although currently considered less toxic for humans than arsenate and arsenite,[37,38] DMA has strong phytotoxic effects, causing so-called straighthead disease which limits grain filling and, thus, plant yield.[39,40]

Besides the species groups mentioned above, thioarsenates have recently been identified in paddy soils,[41,42] rice plants,[43,44] and rice grains.[45,46] In paddy soil porewater, thioarsenate formation has been linked to sulfide (S^{-II}) produced by SRB through dissimilatory sulfate reduction (DSR), which can abiotically thiolate As.[42] Arsenite reaction with S^{-II} and zerovalent S (S^0) in consecutive steps produces the inorganic thioarsenates mono-, di-, tri-, and tetrathioarsenate (MTA, DTA, TTA, and TetraTA, respectively) depending on the S/As ratio (Figure 1, lower right).[47] Similarly, the nucleophilic reaction of MMA or DMA with S^{-II} produces the methylthioarsenates monomethylmonothioarsenate (MMMTA), monomethyldithioarsenate (MMDTA), monomethyltrithioarsenate (MMTTA), dimethylmonothioarsenate (DMMTA), and dimethyldithioarsenate (DMDTA), (Figure 1, upper right).[48,49] Growing evidence shows the toxic effects of thioarsenates on mammalian cells[37,38,50,51] and rice plants,[43,44,52] uptake and accumulation in rice plants and grains,[43,52] and formation during rice product processing.[53] However, under current standard methods for As extraction and speciation determination in rice grain, the highly toxic methylthioarsenates are co-determined as non-regulated oxymethylated arsenates.[45,54] Given the hidden risk that thioarsenates can represent, a better understanding of the redox dynamics influencing As thiolation in paddy soils is urgently needed.[54]

1.1.2. Challenges of studying As speciation in paddy soil porewater

The redox dependency of the reactions regulating As speciation makes species contribution to the aqueous phase highly dynamic. The distribution of As species in paddy soil porewater can be influenced by temporal and spatial variations. For example, the presence of methylated As species is regulated by the net effects of biotically mediated methylation and demethylation reactions, carried out by different microbial groups, which thrive at different redox potentials.[27,32,33,55] Thus, the rates of these reactions can vary, depending on environmental and redox conditions and the availability of substrates that sustain the metabolic processes of the involved microorganisms.[28] Therefore, the content of methylated As in the porewater can peak at a certain point before the rate of demethylation exceeds that of methylation, decreasing then the net content of methylated As.[12,25,32,33,56]

Besides temporal dynamics and transient peaks of species, the spatial distribution of As species might also influence the dominance of species in a sample. In the paddy soil system, these differences are most pronounced when comparing bulk soil and rhizosphere.[57] Root oxygen loss by rice plants increases redox potential around the roots, creating oxic or sub-oxic conditions that contrast with the anoxic ones in the bulk soil.[3,56] Re-oxidation of reduced S species around the rhizosphere, for example, has been shown to play a major role in S redox dynamics in cultivated paddy soils.[57,58] Such conditions around the rice rhizosphere, as well as lower pH due to root exudates, have been shown to increase As mobility and methylation.[41,56,59]

To overcome these challenges, microcosm experiments have been used to study the effects of redox dynamics in paddy soil porewater.[27,28,42] These batch experiments allow a focus on biogeochemical

dynamics through the application of several analytics techniques. Although a simplified system, microcosms avoid influences from environmental and spatial variations, while conveniently allowing regular samplings for evaluating temporal dynamics with an interdisciplinary approach.

Furthermore, since thioarsenates have only been recently identified in paddy soil porewaters, information about the temporal and spatial dynamics influencing their formation in the soil is still largely lacking. Since their formation is linked to S^{-II} availability formed through DSR, they might be also transient signals of thiolation, with dethiolation taking place when S^{-II} is depleted.[41,42] Moreover, there are also analytical challenges related to the study of thioarsenate formation in paddy soils. Arsenic speciation is normally investigated after separation with chromatographic methods.[45,47,48] Most commonly established methods are not suitable for thioarsenate determination since acidic elution conditions transform thioarsenates into their oxyarsenic homologs.[45] Moreover, the sensitivity of thioarsenates to pH, as well as to oxidation, makes common sample stabilization methods such as acidification or oxidation unsuitable for thioarsenate preservation and later determination.[60] Additionally, due to reductive Fe dissolution in paddy soils, porewater samples are often rich in dissolved Fe. The oxidation of Fe^{II} and its reprecipitation as Fe^{III} (oxy)hydroxides form sorption surfaces where some As species are preferentially sorbed, influencing the species distribution in the sample.[61-63] Different Fe complexation agents have been tried to keep the Fe in solution, avoiding reprecipitation. However, the addition of these agents can affect the stability of certain As species, as well as the quality of the chromatographic separation and species recoveries.[42,64,65]

1.2. Influence of soil properties on As mobility and speciation

Global market surveys have shown that there are important variations in the As content and speciation in rice grains, even suggesting, in some cases, geographic patterns.[21,46] Increasing evidence suggests that environmental factors and soil properties are responsible for such differences, rather than genetic variations in rice cultivars.[24,66] As described above, the biogeochemistry of As is closely linked to that of C, S, and Fe.

Under flooded conditions, the main driver of As mobilization is the reductive dissolution of As-bearing Fe^{III} (oxy)hydroxides. Soil oxalate-extractable As has been identified as a good indicator of As mobilization potential, suggesting that As is mainly mobilized from the reductive dissolution of amorphous Fe^{III} phases.[67] Moreover, since the reductive dissolution of Fe is a microbially mediated process, the availability of labile organic matter, including root exudates, can also indirectly influence As mobilization.[68-71] On the contrary, the formation of secondary Fe minerals, such as Fe sulfide phases, has been suggested to limit As mobility in paddy soils due to sorption or incorporation of As.[72-74] Based on this process, sulfate fertilization has been proposed as an agronomic practice to decrease As mobility in paddy soils and accumulation in grains. This practice has, however, shown contrasting results, where no decreases and even increases in As mobilization have been observed after sulfate addition.[75-78] The

variables controlling the effectiveness of sulfate fertilization in decreasing As mobilization remain currently unknown.

Once As is released into the aqueous phase, different soil properties can influence its speciation. Several studies have shown that the addition of different forms of organic carbon increases As methylation.[79-82] Such an increase has been linked to enhanced microbial activity supported by the high availability of labile organic carbon as substrate. Indirectly, the addition of organic matter accelerates the decrease in redox potential, increasing the bioavailability of As for methylation and improving the conditions for the anaerobic microorganisms associated with As methylation.[14,24,26,83] Moreover, Zhao, et al. [14] suggest that although there might be more *arsM*-carrying microbes in soils with neutral to alkaline pH, their activity is higher in acidic soils. Thus, measuring the expression of the *arsM* alone might not be a good indicator of a soil's methylation potential. Additionally, As bioavailability rather than total soil content has been shown to have a major influence on methylation potential.[80] In summary, methylation potential is largely influenced by SOC, microbial community composition, pH, and As bioavailability.

Compared to methylation, much less is known about the properties regulating As thiolation in paddy soil porewater. Until recent years, thioarsenate formation in paddy soils was considered unlikely, since terrestrial systems are assumed to be S-poor.[42,58] Moreover, as mentioned above, difficulties in their analytical determination have hampered the advances of a better understanding of the biogeochemical properties influencing As thiolation in paddy soils.[41,42] Wang, et al. [42] suggest that S^0 accumulation is an important indicator of a soil's potential for the formation of inorganic thioarsenates, while the formation of methylthioarsenates is mainly regulated by the availability of oxymethylated arsenates. The same authors also identified that soil pH is a key parameter regulating the formation of either inorganic or methylated thioarsenates. In alkaline soils, the formation of inorganic thioarsenates was favored, while under acidic conditions, methylated thioarsenates were preferentially formed. Additionally, the authors identified that HCl extractable Fe correlated negatively with thioarsenate concentrations in the aqueous phase. In summary, pH and the availability of Fe and S^{-II} are, until now, the main known properties influencing thioarsenate formation.

Moreover, since sulfate can be readily depleted under anoxic conditions, it has been suggested that the activity of SRB could only account for small fraction of the S^{-II} necessary for thiolation in S-poor paddy soils.[28] Alternatively, the role of a cryptic sulfur cycle (CSC) sustaining thioarsenate formation has been proposed but not studied in detail yet.[42] The cryptic sulfur cycle refers to the partial reoxidation of S^{-II} to S^0, coupled with the reduction of Fe^{III} (oxy)hydroxides (Figure 2).[58] The formed S^0 could be further oxidized to thiosulfate and sulfate, acting again as a substrate for SRB. The CSC offers a constant supply of reducible S, which could support the formation of thioarsenates, even as the main sulfate pool in the soil has been consumed. Studies suggest that the role of the CSC is masked by relatively high S contents in natural systems, making elusive the identification of its importance.[84,85]

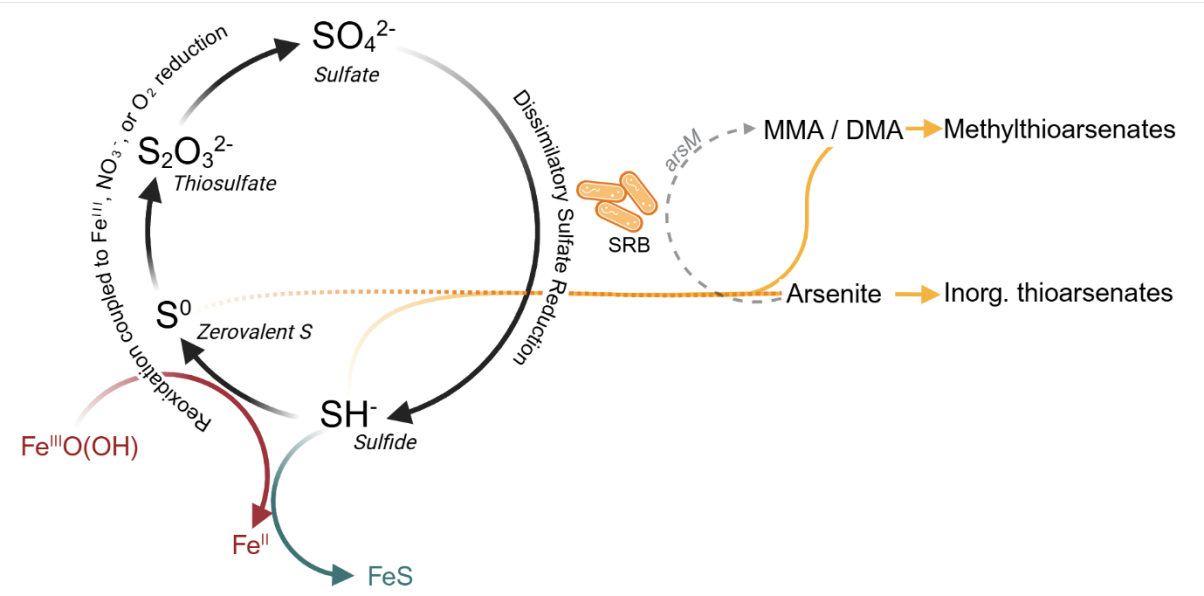

Figure 2: Replenishment of sulfate by S^{-II} reoxidation through the cryptic S cycle and its reported role in the formation of inorganic and methylated thioarsenates in paddy soils.

1.2.1. Alterations to paddy soil biogeochemistry with climate change

Studies have shown that climate change will influence the dynamics of As speciation in paddy soils and rice grains. This effect is related to the microbial processes that govern arsenic biogeochemistry, which are intensified and accelerated by moderate increases in temperature.[13,86-89] For example, incubation experiments carried out by Chen, et al. [28] showed that increasing temperatures accelerated redox dynamics in two Chinese paddy soils, including sulfate reduction and As mobilization and thiolation. In their incubation experiments, the formation of methylated As species, including methylthioarsenates, almost doubled by 5 °C increases in temperature. The same authors observed that increasing temperatures caused As methylation to take place earlier in the incubation time. However, demethylation processes were also enhanced, shifting the temporal dynamics of As methylation. Moreover, in a pot experiment, Muehe, et al. [90] determined that future climatic conditions cause an earlier and higher release of As into the porewater, which translated to a 2-fold increase in inorganic As content in rice grains. In these experiments, grain yield decreased by 39% when rice plants were exposed to a higher temperature and As concentration, compared to only increases in temperature. Temperature also affected As methylation, with a higher share of DMA being present in the grains when the plant-soil system was exposed to a higher temperature. The authors highlight how alterations to the As biogeochemical cycle by climate change pose a risk to food safety and food security in the future.

These studies provide important insights into the influence of climate change-related variables such as temperature and CO_2 concentrations on As mobility and speciation. However, they are limited in the number of soils used and, thus, by the range of soil properties evaluated. As mentioned above, soil properties such as SOC, pH, microbial activity, and Fe mineralogy influence As biogeochemical

dynamics. In this sense, it is key to evaluate how As redox dynamics could be influenced by future climate considering a broad range of soil properties.

Moreover, under the anoxic conditions of paddy cultivation, methanogenic archaea produce CH_4 as a metabolic by-product from the decomposition of organic matter.[91,92] Even though it is produced in trace amounts, CH_4 is an important greenhouse gas (GHG) since it has 27 times the warming potential of CO_2 over a 100-year time frame.[93] Rice is considered the cereal with the largest associated GHG emissions[93-95] and it is estimated that paddy soils globally account for 25 to 40 Tg CH_4 $year^{-1}$, which is equivalent to around 12% of global anthropogenic CH_4 emissions.[96,97] Projections of future climate scenarios show that CH_4 production could increase globally due to moderate increases in temperature and an expansion of flooded areas.[98,99] Thus, accurate estimations of the CH_4 emissions from rice cultivation are necessary for global mitigation efforts. However, there are still important uncertainties in such estimates, which have been related to a lack of data regarding the total area under paddy management and different agricultural practices.[100] Similarly, variations in climatic conditions and soil properties, such as organic matter content and pH, influence microbial communities and, in turn, CH_4 production.[92,101,102]

1.3. Changes in soil properties with long-term paddy use

Chronosequence studies have shown that long-term paddy use on a multiyear scale is characterized by a unique soil development as a direct consequence of redox fluctuations.[103] Several of these studies have been carried out in a chronosequence located in Cixi, province of Zhejiang, China. There, for approximately 2000 years, land reclamation for agriculture has been taking place through the deposition of sediments from the Yangtze River and the building of dikes.[103] The construction records of these structures allow the estimation of the age of the agricultural fields. The Cixi chronosequence represents a unique case where long-term paddy soil development from salt marshes can be studied in soils comprising ages between 50 and 2000 years of flooded rice cultivation. Moreover, the vast literature on the area confirms the robustness of the chronosequence, which allows the identification of trends in soil properties as a consequence of the long-term development of paddy soils.

Studies focused on the soil development in the Cixi chronosequence have shown that long-term paddy use causes the washout of elements such as Ca, Mg, and Na, and the migration of Al, P, Mn, and Fe to deeper soil layers.[104] Moreover, since the anoxic environment under flooded conditions slows down the decomposition of organic matter, the determining characteristic of paddy soil development is the accumulation of SOC in the topsoil.[103-106] Increasing SOC with duration of use (or paddy soil "age") triggers changes in other soil properties, summarized in Figure 3.

Seasonally, once the cultivation period is over and soils are drained shortly before harvest, the increase in redox potential causes the re-oxidation and re-precipitation of Fe^{II} previously produced by Fe

reductive dissolution.[3,107] With increasing paddy soil age, SOC accumulation leads to Fe re-precipitation as amorphous Fe phases,[103] stabilizing SOC and further enhancing its accumulation.[105,106,108] Moreover, SOC accumulation with long-term paddy use has been shown to increase microbial activity and shift microbial community composition.[109-113] Lastly, SOC accumulation lowers paddy soil pH, together with the washout of carbonates.[103]

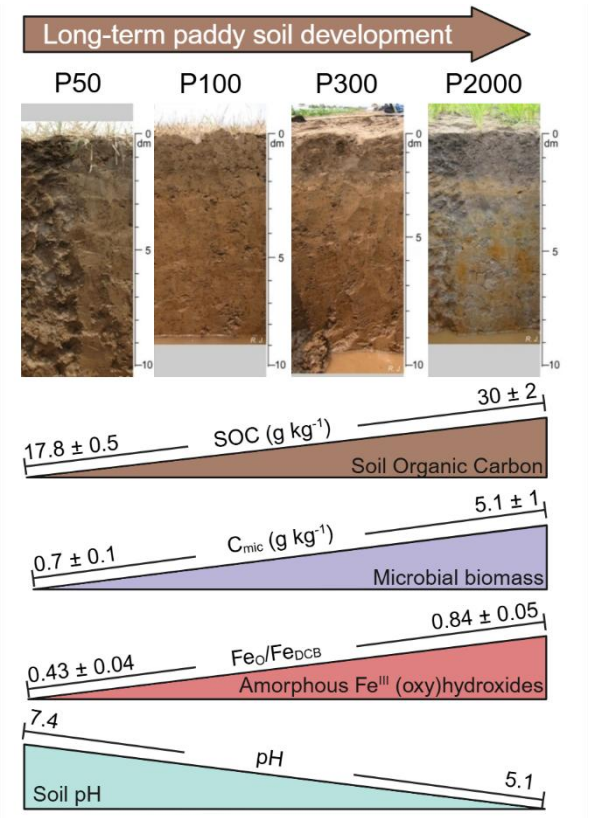

Figure 3: Changes in selected soil properties with long-term paddy use in paddies (P) of 50 to 2000 years of use. Numerical data has been previously reported by Kölbl, et al. [103]. For SOC, Fe_O/Fe_{DCB}, and soil pH, data is presented from a main site and two subsites (mean values ± standard deviation). For microbial C (Cmic), data is given as mean ± standard deviation (n = 5). The standard deviation from soil pH was < 0.01 pH units. Fe_O: oxalate extractable Fe, Fe_{DCB}: dithionite-citrate-bicarbonate extractable Fe.

Based on these changes, Kölbl, et al. [103] divided the pedological development associated with long-term paddy use into three phases. A first phase in the first 50 years of paddy use, is characterized by desalinization and formation of the plough pan. In this phase, paddy-specific microbial communities start to establish in the soil. A second phase, between 100 and 300 years of use is characterized by decalcification and decreases in pH due to washout of carbonates. Microbially, this phase is characterized by increases in microbial biomass, increasing microbial function, and strengthening the structure of the microbial communities. Finally, a third phase in soils used for longer than 700 years is characterized by an acceleration in the rates of SOC accumulation, accompanied by stronger changes

in Fe mineralogy towards amorphous Fe phases.

While previous studies have largely focused on the effects that long-term paddy use has on soil properties, a deep understanding of its effects on redox biogeochemistry and microbially regulated processes is still lacking. Therefore, a comprehensive study is needed to understand how changes in soil properties associated with long-term paddy use influence redox biogeochemistry and As mobility and speciation.

1.4. Objectives

It is well established that soil properties can influence As mobility and speciation in paddy soils. Chronosequence studies have shown that long-term paddy use influences soil development, altering soil properties. However, a linkage between long-term paddy use and changes in soil properties triggering changes in As speciation is still lacking. The overall aim of this thesis was to investigate the impact of long-term paddy use on the As biogeochemical cycle, as well as to obtain a deeper understanding of the general soil properties regulating As methylation and thiolation in paddy soils. Additionally, the influence of long-term paddy use on CH_4 production was investigated.

The specific objectives of this thesis were to:

- Elucidate the effects of long-term paddy use on redox biogeochemistry under flooded conditions, with a focus on As speciation (Study 1).
- Determine if the response of CH_4 production and As mobility and speciation to increased temperatures is influenced by long-term paddy use (Study 2).
- Evaluate the effect of sulfate fertilization on As mobility and speciation in paddy soils at different stages of development (Study 3).
- Investigate the role of cryptic S cycling in the formation of thioarsenates in paddy soils (Study 4).

Study 1 aimed to understand how pedological changes resulting from long-term paddy use affect As mobility and speciation, with an additional focus on microbiological processes associated with As speciation. Study 2 focused on how increased temperatures related to climate change could influence CH_4 production and As mobility and speciation in already established and new paddy soils. Considering the complex links between As and S biogeochemistry, Study 3 evaluated the effects of sulfate fertilization on As biogeochemistry considering different stages of paddy soil development. Moreover, since the cryptic S cycle has been proposed as a source of reducible sulfate for As thiolation in paddy soils, Study 4 was designed to deplete a paddy soil from excess S, Fe, and As to unmask the role of the cryptic S cycle in thioarsenate formation.

2. Methods

2.1. Soils from the paddy soil chronosequence

The soils used throughout studies 1-4 belong to the paddy soil chronosequence located in Cixi, province of Zhejiang, China (30°10′N, 121°14′E). Figure 4 shows a map with the area, indicating the location of the chronosequence soils, highlighting the ones used for this thesis. For all studies, the ≤ 2 mm soil fraction of the Alp horizon of the main sites described by Kölbl, et al. [103] and Cheng, et al. [104] were used. These sites represent paddy soils (P) with 50, 100, 300, and 2000 years of paddy cultivation. These four soils were selected as the main soils for this thesis since they represent the longest uninterrupted paddy soil development. Selected additional soils from the chronosequence were used in studies 2 and 3, depending on the individual objectives. Namely, non-paddy soils (NP) with ages of 50 and 700 years were used in Study 2, and two paddy soils with a disrupted chronosequential development were used in Study 3.

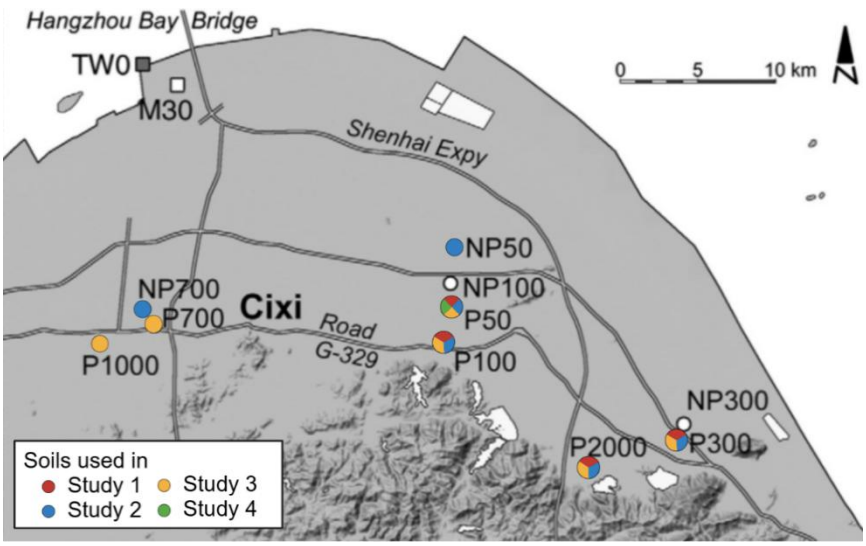

Figure 4: Map of the Cixi chronosequence area indicating the fields from the chronosequence. Colored points indicate the soils used in this thesis for Studies 1-4. Taken and modified from Kölbl, et al. [103].

2.2. Main experimental approach

Since the focus of Studies 1-3 was to investigate the different effects that long-term paddy soil development has on redox biogeochemistry with a focus on mobility and speciation, microcosm incubation experiments were carried out as the main methodological approach. The use of the same experimental setup with varying conditions depending on the objectives of the individual studies allowed direct comparison between them. For Study 4, a different incubation approach was used in order to deplete the soil from bioavailable S, Fe, and As, in order to elucidate the role of cryptic S cycling in As thiolation in paddy soils.

All incubations, as well as the most relevant methods, will be described in this chapter, while further analytical details can be found in the materials and methods sections of each of the studies included in the Publications chapter. Table 1 gives a comprehensive summary of the different methods and analyses carried out in Studies 1-4. All experiments and measurements were carried out in triplicate. Unless stated otherwise, throughout the text, the experimental results are expressed as mean values followed by the standard deviation of the measurements (n = 3).

Table 1: Summary of the methods used in this dissertation.

	Method	Study 1	Study 2	Study 3	Study 4
	Standard incubation	✓	✓	✓	
	Long-term (depletion) incubation				✓
Aqueous phase	GC-FID (CH_4, CO_2)	✓	✓	✓	✓
	ICP-MS (Total Fe, As, S)	✓	✓	✓	✓
	IC-ICP-MS (As and S speciation)	✓	✓	✓	✓
	Photometry (Fe_{tot}, Fe^{II}, S^{-II})	✓	✓	✓	✓
	Redox potential, pH	✓	✓	✓	✓
	DOC determination	✓	✓		
	HPLC-RID (Acetate determination)	✓		✓	
Solid phase	Soil digestion	✓	✓	✓	✓
	Fe_O and Fe_{DCB} extractions	✓	✓	✓	
	HPLC-DAD (S^0 determination)	✓		✓	✓
	DNA & RNA extractions and qPCR analyses	✓			
	Sequential Extraction Procedure		✓	✓	
	Sulfate reduction rate determination			✓	
	Mössbauer spectroscopy and µXRD				✓

Abbreviations are clarified throughout the following text and in the list of abbreviations (page xv).

2.2.1. Standard incubation experiments (Studies 1–3)

Incubation experiments for studies 1-3 were carried out similarly, to compare observations between different setups. Here, the incubation method used for Study 1 will be explained, before describing the variations used for Studies 2 and 3.

The focus of Study 1 was to investigate the effects of long-term paddy use on redox chemistry and As mobility and speciation. For this, incubation experiments were carried out using P50, P100, P300 and P2000. Anoxic incubations were set up in 120 mL septum vials inside a glovebox (COY, 95% N_2, 5% H_2), by adding 10 g of soil and 20 mL of N_2-purged tap water. After closing with butyl rubber stoppers and aluminum caps, the vials were incubated at 30 °C (the average maximum temperature in the Cixi region during the cropping season). Sacrificial samples were taken after 1, 3, 5, 7, 10, and 35 days of incubation. Based on the results from Study 1, it was determined that redox dynamics trends based on paddy soil age were stable after 10 days in the studied conditions. Thus, this was the maximum incubation time selected for Studies 2-4.

Study 2 aimed to evaluate if long-term paddy use influenced the biogeochemical responses to increases in temperature as a consequence of climate change. Incubations for this study were carried out following the same procedure as for Study 1, with increased incubation temperatures (32 and 35 °C), simulating climate change scenarios according to the Intergovernmental Panel on Climate Change (IPCC.)[90,114] In addition to the four paddy soils used for Study 1, two non-paddy soils from the same area were also anoxically incubated at 30, 32, and 35 °C to investigate if the biogeochemical responses on As biogeochemistry and CH_4 production were a consequence of long-term paddy management. Moreover, these two soils aimed to elucidate how freshly reclaimed paddies would react to increasing temperatures in the future.

In the case of Study 3, to investigate how sulfate fertilization could alter As speciation depending on a broad range of soil properties, the aqueous phase used for the incubations were solutions either of sodium sulfate (3 mmol SO_4 kg_{soil}^{-1}, simulating sulfate fertilization) or sodium chloride (as an ionic strength control). Both solutions were prepared using ultrapure water (MQ, ≥18.2 MΩ cm, TOC < 3 µg/L) and purged with N_2 before setting up the incubation as described in Study 1. Besides the four chronosequential paddy soils used in Study 1, two additional paddy soils from the same area of the chronosequence (P700 and P1000) were also incubated for this study. The chronosequential development of these two soils has been affected chemically (by a fossil fuel spillage,[115] P700) and physically (removal of the topsoil,[106,109] P1000). The use of these two additional soils allowed the investigation of how disrupted paddy soil development could influence As mobility, speciation, and their responses to sulfate fertilization.

2.2.2. Long-term soil depletion experiments (Study 4)

In order to elucidate the role of the cryptic S cycle in thioarsenate formation in paddy soils, an alternative approach to the incubation experiments was used, involving repetitive redox cycling to deplete the soil from excess S, Fe, and As. First, a soil with a high potential for As thiolation was selected. Based on the results from Study 1, P50 was used for this study. Incubations were initially set up as described for Study 1, with the addition of 0.13 g of finely milled rice straw as a C source for microbial activity. After

10 days of anoxic incubation at 30 °C, the standing water was removed. The vials were then left standing open in the incubator for an oxic period of 5 days before N_2-purged water was added again inside the glovebox, starting a new cycle. For the following one and a half years, the incubations went through 30 of these redox cycles. After 10, 20, and 30 redox cycles, sacrificial and temporally resolved samplings of the aqueous and solid phases took place on days 1, 3, 5, 7, and 10 of the anoxic incubation period. A constantly anoxic and flooded setup was carried out during the same time as a control.

2.3. Routine analytical methods (Studies 1-4)

Unless stated otherwise, all samples for the analyses described from here onwards were filtered through 0.2 µm cellulose-acetate filters (Chromafil® Xtra). Photometric determinations of total Fe and Fe^{II} (using the ferrozine method[116,117]) and S^{-II} (methylene blue method[118]) were carried out in triplicate using a multiplate reader (Infinite® 200 PRO, Tecan). Colorimetric reactions and analyses were done outside the glovebox after sample stabilization under anoxic conditions according to the methods. If necessary, samples were diluted with MQ.

Methane and CO_2 in the headspace of the incubation vials were measured through Gas Chromatography with a Flame Ionization detector (GC-FID, SRI Instruments 8610C) equipped with a methanizer. A multimeter (HQ40d, Hach) was used to measure pH (PHC301, Ag/AgCl electrode) and redox potential (MTC101) in the filtered aqueous phase. Dissolved Organic Carbon (DOC) was measured (Multi N/C 2100 S, Analytic Jena) after filtration through a 0.45 µm polyamide filter (Chromafil® Xtra) and stabilization with 0.4% HCl.

Total As and S in the aqueous phase were determined by Inductively Coupled Plasma-Mass Spectrometry (ICP-MS, 8900 Triple Quad, Agilent or XSeries2, Thermo-Fisher) using oxygen as reaction cell gas. Samples were stabilized with 0.5% H_2O_2 and 0.8% HNO_3 and diluted before analysis. Arsenic was measured as AsO^+ (m/z = 91) and S as SO^+ (m/z = 48). Rhodium was used as an internal standard to compensate for signal drift, and a certified reference material (TMDA, Environment Canada) was used for quality control.

For the analysis of As speciation, samples were stabilized with the Fe chelator N,N'-Di(2-hydroxybenzyl)ethylenediamine-N,N'-diacetic acid monohydrochloride (HBED, pH 7) to avoid the precipitation of Fe phases. Tests regarding the stability of As species and As recovery in the presence of HBED are described below (see section 2.4.2) and can be additionally found in the Supporting information of Study 1. To ensure the complexation of all the dissolved Fe, an HBED solution of 10 mmol L^{-1} in 10% ethanol at neutral pH was used to stabilize samples with Fe concentrations < 1 mmol L^{-1}, and a 59 mmol L^{-1} solution was used for those with higher Fe concentrations. The stabilized samples were flash-frozen in dry ice and kept at -20 °C until analysis. The samples were thawed anoxically inside the glovebox directly before analysis to avoid changes in

speciation due to oxidation. Arsenic and S species were separated by Ion Chromatography (IC, 940 Professional IC Vario, Metrohm or a Dionex ICS-3000, Thermo-Fisher) and quantified through ICP-MS as described above. For the chromatographic separation, an AS16 column (Dionex AG/AS16 IonPac) was used, with a 2.5 – 100 mM NaOH gradient, 1.2 mL min^{-1} flow rate, and an injection volume of 50 µL.[60] Individual As species were assigned based on previously reported retention times[42,47,48] and concentrations of thiolated As species were calculated based on their oxyarsenic homologues.

Soil samples after incubation were frozen, freeze-dried, and homogenized with a mortar and pestle. These samples were used for the determination of total As, S, and Fe after microwave-assisted digestion (MARS, Xpress, CEM) in Aqua Regia. Additionally, S^0 was determined through HPLC-UV-Vis after a chloroform extraction.[119] Chloroform-extractable S includes zerovalent S in polysulfides and S bound to solid phase, as well as S_8.

2.4. Specific analyses for each Study

Besides general analyses for the understanding of the links between C, S, Fe, and As biogeochemistry, additional analyses were carried out in each study in order to address their specific objectives.

2.4.1. Specific soil characterization and microbial analyses (Study 1)

Arsenic and S contents in the soils prior to incubation were determined by ICP-MS as described above after microwave-assisted digestion (MARS, Xpress, CEM) in Aqua Regia. Iron (III) phases were characterized in the dry soils prior to incubation by dithionate-citrate-bicarbonate[120] (DCB) and oxalate buffer[121] extractions, summarized throughout the text as Fe_{DCB} and Fe_O, respectively. The determination of the extracted Fe was carried out photometrically as described above.

DNA and RNA were extracted following the method reported by Lueders, et al. [122] and analyzed by quantitative polymerase chain reaction (qPCR) from post-incubation soil samples, which had been stored in liquid N_2. Total and active bacteria were based on the amplification of the respective 16S rRNA gene and transcript copy numbers in nucleic acid extracts. Functional genes directly and indirectly related to As biogeochemistry were also amplified and analyzed. Namely, dissimilatory sulfite reductase (*dsrA*) for the activity of SRB, arsenite S-adeno-sylmethyltrransferase (*arsM*), for As methylation capacity, and methyl coenzyme M reductase (*mcrA*), for methanogenic activity. Acetate concentrations in the aqueous phase of the incubations were determined by HPLC with refractive index detection (RID) (Agilent 1200) with a Rezex ROA Organic Acid Column.[123]

Moreover, in Study 1 an additional incubation was carried out to evaluate changes in the demethylating capacity of the soil microbial community with long-term paddy use. For this, incubations were set up as described above, with the exception that the aqueous phase was N_2-purged tap water containing individual spikes of MMA or DMA. The concentration selected for the spikes was 10-fold the maximum

concentration found in the original incubation setup. Non-sacrificial samples were taken with a syringe and needle from the vials after 5, 10, and 33 days of incubation. Arsenic speciation analyses of these samples were carried out as described above.

2.4.2. Evaluation of HBED stabilization method for thioarsenates (Study 1)

The chelating agent HBED has been shown to effectively keep Fe in solution in environmental studies.[124] To test the suitability of HBED to preserve As species, several tests were conducted. All tests described here were carried out anoxically inside the glovebox and using a 10 mmol L^{-1} solution of HBED. Arsenic speciation in the samples described here was measured through IC-ICP-MS as described above, focusing on the recoveries of individual species and total As.

After ensuring that the HBED solution contained no As, the stability of different mixes of As species was evaluated in the presence of the chelating agent. These included first the inorganic and methylated oxyarsenic species used for the IC-ICP-MS calibration (arsenite, arsenate, MMA, and DMA). Next, the stability of a synthetic mix of species at environmentally relevant concentrations, including thioarsenates, was evaluated. Once determined that the species were stable and the chromatographic separation was not hampered by the stabilization method, mixes of species with increasing concentrations of dissolved Fe^{III} were evaluated. Moreover, the stability of the species and HBED mix was evaluated with and without freeze-drying. Finally, the stabilization method was evaluated with samples from incubation experiments as the ones described above. For this, the aqueous phase of two paddy soils with different dissolved Fe concentrations (150 and 850 μmol L^{-1}) were tested.

After the satisfactory evaluation of the HBED stabilization method, it was used for Studies 1-4. Further details regarding the evaluation and results can be found in the supporting information of Study 1.

2.4.3. Effect of long-term paddy use on As binding environment (Studies 2 and 3)

Arsenic binding mechanisms in the paddy and non-paddy soils were characterized through the sequential extraction procedure (SEP) proposed by Fulda, et al. [125]. This method classifies binding mechanisms into five operationally defined fractions. F1 ($CaCl_2$ 0.1 M) – mobile fraction (soluble or exchangeable, and soluble metalorganic complexes); F2 (1M Na-acetate) - easily mobilizable fraction (adsorbed and bound to carbonates or other minerals, weakly bound metalorganic complexes); F3 (0.025 M NH_4-EDTA) - organic fraction (low-affinity sites); F4 (0.2 M NH_4-oxalate) - reducible fraction (bound to amorphous and crystalline Fe and Mn oxides), and F5 (30% H_2O_2, 2 M HNO_3, 3.2 M NH_4-Acetate) - oxidizable fraction (metal sulfides and organically bound to high-affinity sites). Non-extractable As (F6) was calculated by subtracting Σ F1 to F5 of the total As extracted from the original soils by microwave-assisted digestion, as described above.

2.4.4. Effect of long-term paddy use on sulfate reduction rates (Study 3)

Sulfate Reduction Rate (SRR) was determined for the six paddy soils used in Study 3. For this, an anoxically pre-incubated slurry was spiked with ^{35}S-labeled sulfate standard (50 kBq). The spiked slurries were further incubated anoxically for 5 h before halting the microbial activity by injecting 5 mL of a N_2-purged 10% zinc acetate solution through the rubber stopper. Isotopically ^{35}S-labeled products of sulfate reduction were determined from the incubated soil using a scintillation counter (Tri-Carb 2800TR) after standard digestion and distillation procedures for Total Inorganic Reduced Sulfur (TRIS).[126]

2.4.5. Effect of repetitive redox cycling on Fe mineralogy (Study 4)

Changes in Fe mineralogy due to repetitive redox cycling were assessed by Mössbauer spectroscopy. For this, the original and redox-cycled soils were freeze-dried and homogenized manually with mortar and pestle. Dried mineral powders were loaded into Plexiglas holders (area 1 cm^2), forming a thin disc. Holders were inserted into a closed-cycle exchange gas cryostat (Janis cryogenics) under a backflow of He to minimize exposure to air. Spectra were collected at 5 and 77 K using a constant acceleration drive system (WissEL) in transmission mode with a ^{57}Co/Rh source. All spectra were calibrated against a 7 µm thick α-^{57}Fe foil that was measured at room temperature. Analysis was carried out using Recoil (University of Ottawa) and the extended Voigt Based Fitting (VBF) routine.[127] The half width at half maximum (HWHM) was constrained to 0.12 mm/s during fitting. Due to uncertainties regarding the mineral phases of the Fe^{II} and the Fe^{III}(oxy)hydroxide fit components, additional µXRD measurements were carried out. The reference minerals were partly taken from the XRD Match! Software and partly from the mineralogical database “Rruff”.

3. Results and Discussion

3.1. Influence of long-term paddy use on redox chemistry and As biogeochemistry (Study 1)

Paddy soil age directly influenced redox chemistry under flooded conditions. Aqueous phase chemistry showed both differences and similarities to pedological properties typically associated with long-term paddy use. For example, while solid-phase Fe is reported to decrease with soil age (38 mg g^{-1} in P50 vs. 22 mg g^{-1} in P2000),[103] dissolved Fe concentrations increased with paddy soil age. After 7 days of incubation, Fe concentrations peaked at 0.24 ± 0.02 mmol L^{-1} in P50 and 5.4 ± 0.02 mmol L^{-1} in P2000. On the contrary, the reported SOC accumulation with long-term paddy use (17.8 mg g^{-1} in P50 vs. 30 mg g^{-1} in P2000)[106,128] directly translated into higher DOC concentrations in the aqueous phase of the incubations, increasing from 25 ± 4 mmol L^{-1} in P50 to 99 ± 3 mmol L^{-1} in P2000 (data from day 7 to compare with Fe). These two contrasting trends are linked by the changes that SOC accumulation triggers in Fe mineralogy. Crystalline Fe phases repeatedly dissolve and reprecipitate during the redox fluctuations associated with paddy management.[3] The increasing accumulation of SOC with long-term paddy use causes Fe to reprecipitate as amorphous Fe^{III} phases,[103,105] which can easily go through reductive dissolution in the next redox cycle.[129] Briefly, long-term paddy use depletes Fe from soils but enhances the bioavailability of the remaining Fe.

Soil As content decreased with increasing paddy soil age both in the solid phase (17 ± 2 mg kg^{-1} in P50 vs. 11 ± 1 mg kg^{-1} in P2000) and in the aqueous phase (1.81 ± 0.05 µmol L^{-1} in P50 vs. 0.5 ± 0.1 µmol $L^{-}1$ in P2000, data from day 7 to compare with Fe and DOC data above). Even though Fe reductive dissolution is considered the main source of As in the aqueous phase,[19,20] fewer moles of As were released per mole of dissolved Fe with increasing paddy soil age. The formation of amorphous Fe phases due to the SOC accumulation likely immobilizes As more effectively due to the increased availability of sorption sites.[63] These results from Study 1 suggest that long-term paddy use decreases As mobility.

Paddy soil age also affected As speciation. Inorganic arsenic species (mainly arsenate and arsenite, but also inorganic thioarsenates) dominated total As, especially in younger soils, and ranged between 90.9 ± 0.5% (P50, day 5) and 48 ± 2% (P2000, day 7). The highest inorganic thioarsenate contribution to total As was found in P50 at day 3 (8.8 ± 0.8%), decreasing sharply with paddy soil age. Moreover, the share of inorganic thioarsenates to As speciation decreased with longer incubation time in all soils. While the higher contribution of inorganic As in young paddy soils can be related to the absence of methylation (see below), the formation of inorganic thioarsenates was regulated by the availability of S^{-II} linked to DSR.

Although free S^{-II} was not detected throughout the experiment, DSR was indirectly assessed by the decreases in porewater S concentrations over time. Decreases in aqueous S started on day 3 for P50 but

only after day 5 for P2000, showing that paddy soil age delays DSR, postponing the formation of thioarsenates. This delay with increasing paddy soil age, which also affected the start of methanogenesis, was likely related to the higher availability of reducible Fe as a thermodynamically preferred electron acceptor.[130,131] As an additional indicator, redox potential had a slower decrease with increasing paddy soil age.

Principal component analysis revealed a strong negative correlation between thioarsenate formation and soil age, DOC, and dissolved Fe. Inorganic thioarsenates contributed > 2% to total As only when Fe^{II} and DOC concentrations were below 1 mmol L^{-1} and 50 mmol L^{-1}, respectively. Higher dissolved Fe^{II} concentrations with increasing paddy soil age likely scavenged S^{-II} through the formation of FeS phases, hindering thioarsenate formation.[78,132] Similarly, S^{-II} could have also been scavenged through reactions with SOC and DOC to thiolate organic compounds.[133,134] Moreover, acidification with increasing paddy soil age (due to carbonate washout and SOC accumulation)[103] was an additional limitation to inorganic thioarsenate formation, which is thermodynamically favored at neutral to alkaline conditions.[48,49] These results show that long-term paddy management limits thioarsenate formation mainly because of a decreased availability of S^{-II} as a consequence of increasing DOC and reducible Fe.

The contribution of methylated species to total As increased sharply during early paddy soil development, from 9.6 ± 0.3% in P50 to 38 ± 4% in P300 (day 35, equilibrated system). Increases in As methylation have been previously associated with increased microbial activity related to high C availability.[14,56,80,135] The results showed that the accumulation of SOC and increased availability of DOC with paddy soil age increased microbial respiration, methanogenesis, and 16S rRNA copy numbers. However, considering the trend of increased As methylation between P50 and P300, P2000 showed lower net methylation potential than expected. While it could be argued that the high methanogenic activity in P2000 could decrease net As methylation due to demethylation,[33,55] incubations with MMA and DMA addition showed that P2000 had the lowest demethylating capacity. The low total As concentrations in P2000 likely decreased methylation due to a diminished need for detoxification or lower effectiveness of methylated As species as antibiotics.[30] Additionally, the high DOC concentration in P2000 may have triggered carbon catabolite repression, under which microbes downregulate enzymes related to the uptake of small organic molecules. These enzymes include, for example, the aquaglyceroporin channel (GlpF), which is also related to arsenite uptake in bacteria.[136,137] This downregulation has been recently shown to decrease As uptake by bacterial cells[138] and to decrease As methylation potential.[139]

Higher *arsM* gene copy numbers (associated to As methylation) were positively correlated with aqueous As concentrations. However, a significant correlation between *arsM* copy numbers and methylated As was only found when excluding P50. It has been reported that, although there might be more methylating microbes in alkaline soils like P50, their activity is higher under acidic conditions,[24] as

found in older soils. Additionally, a strong positive correlation was found between *dsrA* (linked to DSR) and *arsM* genes, supporting previous reports that SRB are important As methylators in paddy soils.[27,28,140] This correlation weakened with increasing soil age. Acetate concentrations (a byproduct of fermentation), correlated with As methylation in older soils. Earlier studies related fermentative bacteria with As methylation in paddy soils.[29] This observation suggests that, as paddy soils age, fermentative bacteria might become more relevant methylators than SRB. Overall, Study 1 showed that the increased microbial activity and SOC accumulation with long-term paddy use enhances the formation of methylated As species. Moreover, statistical observations suggested that there might be a shift from the main microbial groups related to As methylation from SRB-driven to fermentative-bacteria-driven.

Once formed, methylated oxyarsenates were readily thiolated. Methylthioarsenates were detected in all soils at all incubation times, except for P2000 where they were only found from day 5 onwards, coinciding with the start of DSR. Methylthioarsenate formation was initially limited by the availability of MMA and DMA as precursors, as reported previously by Wang, et al. [42]. Once MMA or DMA were formed, the formation of methylthioarsenates was limited by the decreasing availability of S^{-II} with increasing soil age as described above for the formation of inorganic thioarsenates. However, the acidic to neutral conditions in the aqueous phase favored the thiolation of oxymethylated arsenates over that of arsenite.[48,49,60] Even in spiked incubations with a 10-fold excess of oxymethylated arsenates, up to 98% of DMA was thiolated compared to 22% of inorganic As species. Methylthioarsenates continued to form in the later stages of the incubation when no DSR was taking place. We suggested that cryptic S cycling provided the S^{-II} necessary for methylthioarsenate formation.

In summary, Study 1 showed that paddy soil age influences the redox chemistry in the aqueous phase after flooding. This influence can be coupled to the changes in soil properties with paddy soil age (increased DOC coupled to increased SOC), or not (increased aqueous Fe concentrations in contrast to Fe depletion in soil). Long-term paddy use also influences anoxic respiration pathways, delaying DSR and methanogenesis due to the increased availability of reducible Fe. Regarding As (see Publications chapter, Study 1, Figure 5), long-term paddy use decreases its mobility due to the formation of amorphous Fe phases, increases the potential for methylation due to increased microbial activity, and decreases the thiolation potential due to excess of SOC and reducible Fe which can scavenge S^{-II}.

3.2. Influence of long-term paddy use on biogeochemical responses to increasing temperature (Study 2)

Increasing incubation temperature (compared to the 30 °C used in Study 1) accelerated biotically mediated processes in all paddy soils. The magnitude of this acceleration depended on soil age. Increasing the temperature by +2 °C to 32 °C had generally more significant effects on biogeochemistry than a further +3 °C increase to 35 °C. Unless stated otherwise, the comparison between 30-32 °C incubations will be referred to from here onwards.

Higher temperatures accelerated Fe reductive dissolution and increased dissolved Fe concentrations in paddy soils. Young paddy soils showed a lower relative change compared to older ones (median increase of 31% in P50, compared to 88% in P2000). In comparison, non-paddy soils showed much lower dissolved Fe concentrations than paddy soils. At 30 °C on day 7 (as reported above for the paddy soils in Study 1), non-paddy soils had dissolved Fe concentrations of 0.082 ± 0.002 mmol L^{-1}, and 0.106 ± 0.004 mmol L^{-1} for NP50 and NP700, respectively. These concentrations were around a third of the one in P50 under the same conditions. Moreover, with increasing temperature, dissolved Fe concentrations decreased in non-paddy soils, which translated into a negative relative change.

Higher incubation temperatures increased the release and microbial consumption of DOC in paddy soils, yielding small relative changes in DOC concentrations. However, the increased microbial consumption of organic substrates caused higher CO_2 production in all paddy soils, even when comparing 30-35 °C setups. After 10 days of incubation, P50 produced 13 ± 2 µmol CO_2 g_{soil}^{-1} at 30 °C, compared with 23 ± 2 µmol CO_2 g_{soil}^{-1} at 35 °C, meaning a 1.7-fold increase. In the case of P2000, after 10 days at 30 °C, 34 ± 5 µmol CO_2 g_{soil}^{-1} were produced, compared with 63 ± 3 µmol CO_2 g_{soil}^{-1} at 35 °C, yielding a 1.9-fold increase. Non-paddy soils had around half the DOC concentration compared to P50 incubations at 30 °C. When comparing non-paddy soil incubations at 30 and 35 °C, NP50 and NP700 showed relative increases in CO_2 production of only 1.5- and 1.6-fold, respectively.

The differences between the responses of paddy and non-paddy soils to higher temperatures can be attributed to pedological changes due to long-term paddy use. Amorphous Fe phases that form with long-term paddy use are more sensitive to Fe reductive dissolution when exposed to higher temperatures than crystalline phases.[129] Accumulation of SOC also supports higher microbial activity, increasing the response of biotically mediated processes in paddy soils to increasing temperatures.[88,141] In contrast, non-paddy soils, subjected to different agricultural practices such as tillage, show less SOC accumulation, limiting changes in Fe mineralogy and microbial activity.[103,142] Additionally, the microbial community in non-paddy soils is likely not well adapted to sub-oxic and anoxic environments, which could further limit their activity under flooded conditions.[91,143] Based on these contrasting results between paddy and non-paddy soils, it was determined that long-term paddy use does influence how soils respond to changes in temperature under flooded conditions.

Higher temperatures increased CH_4 production in all paddy soils, showing higher positive relative changes with increasing paddy soil age. At 30 °C, P50 produced 4.2 ± 0.5 µmol CH_4 g_{soil}^{-1}, compared to 12 ± 1 µmol CH_4 g_{soil}^{-1} at 35 °C (2.9-fold increase). In the case of P2000, 6.7 ± 0.9 µmol CH_4 g_{soil}^{-1} were produced at 30 °C, compared to 41 ± 3 µmol CH_4 g_{soil}^{-1} at 35 °C, yielding a 6.1-fold increase. Non-paddy soils had a much lower CH_4 production (around 10% of the production of P50 under the same conditions) and even a decrease under higher incubation temperatures. For all soils, a linear correlation was observed between the final CH_4 production and incubation temperature. The slope of this

correlation (with units μmol CH_4 g_{soil}^{-1} $°C^{-1}$) increased with paddy soil age, indicating higher temperature sensitivity with long-term paddy use. A similar correlation was found for CO_2. Increased CH_4 and CO_2 production in future climatic scenarios, especially in old paddy soils with high C stocks, could risk the role of paddies as net C sinks,[3,144] causing a positive feedback loop with climate change.

The increased CH_4 and CO_2 production with temperature rise in paddy soils was driven by SOC accumulation supporting higher microbial biomass in older soils.[108,110-112,145] Since the incubations were carried out with topsoil, it is likely that the increased consumption of labile organic matter was responsible for the increases in microbial respiration rather than the consumption of recalcitrant compounds with higher temperature sensitivity.[146,147] Moreover, higher and earlier reductive Fe dissolution might have shortened the period of methanogenesis inhibition by Fe^{III} (oxy)hydroxides.[148,149] In younger paddy soils, the low DOC concentrations could have limited increases in methanogenic activity. In these soils, labile DOC could have been consumed in the early stages of incubation, when other respiration pathways were thermodynamically preferred.

Arsenic mobility increased with higher temperatures in all soils, particularly in the early incubation phase. However, older paddy soils exhibited smaller relative changes, suggesting that long-term paddy use, despite promoting Fe reductive dissolution, still limits As mobility by forming amorphous Fe phases that offer additional sorption sites. Non-paddy soils, with a larger proportion of weakly sorbed As according to the SEP results, showed a higher As release at elevated temperatures.

Temperature also influenced As speciation. The contribution of methylated arsenates (MMA and DMA) to total As increased sharply under higher incubation temperatures, doubling in some cases and surpassing inorganic As species as the main species. Higher methylation capacity with increasing temperature has been reported before and has been related to an increase in microbial activity and *arsM* copy numbers.[13,28] While the concentrations of methylated arsenates steadily increased at 30 °C, higher temperatures caused the concentrations of these species to peak and then decline. This change indicates that the demethylation rate overtook that of methylation, possibly due to increased methanogen activity.[32,33,55] In non-paddy soils, methylation was low and decreased even more with increasing temperature, likely due to the limited microbial adaptation to flooded conditions. The formation of inorganic and methylated thioarsenates was hindered by higher temperatures in all soils, likely due to the increased scavenging of S^{-II} caused by the higher Fe reductive dissolution. Although the thiolation potential was hindered throughout the incubation, methylthioarsenate formation was observed in older soils in late stages of the incubation, possibly due to cryptic sulfur cycling.

Overall, Study 2 showed that climate change poses different risks to paddy soils depending on their developmental stage (see Publications chapter, Graphical Abstract of Study 2). Young paddy soils, and newly reclaimed soils for paddy cultivation could show a relatively higher As mobilization with increasing temperatures, risking food safety. In established paddy soils with high SOC and functional

microbial communities, the highest risk is the one associated with higher As methylation, which could risk grain yield through straighthead disease, endangering food security. Finally, while older soils show lower relative changes in As mobilizatioin and methylation, their GHG emissions showed the highest relative increase at higher temperatures. Such increase could risk the role of paddies as net C sinks, and act as a positive feedback loop with climate change.

3.3. Influence of long-term paddy soil development on the response of As speciation to sulfate fertilization (Study 3)

Sulfate addition caused a decrease of 8 – 20% in total aqueous As concentration after 10 days of incubation, with no trends related to paddy soil age. While paddy soil age did not affect the effectiveness of sulfate addition in removing As from the aqueous phase, it did influence the response of As speciation. Briefly, sulfate addition increased As methylation and thiolation. However, paddy soil age had an important control in regulating the magnitude of those increases. Before evaluating how long-term paddy soil development influences the response of As mobility and speciation to sulfate fertilization, the effects that physical and chemical disruptions to soil development could have on redox chemistry and As biogeochemistry will be discussed.

Soils in which the chronosequential development had been disrupted (P700 and P1000) showed higher As mobilization compared to soils with normal soil development related to long-term paddy use. P700 had a high share (7.5%) of weakly bound As compared to the rest of the chronosequence soils (5.3% on average), potentially related to the oil spill that it was affected by. Moreover, P700 had a lower microbial activity, as shown by higher Eh values and low dissolved Fe concentrations. This suggests that in this soil, there was no effective formation of secondary FeS phases which could limit the already high As mobilization into the aqueous phase. In P1000, where the topsoil was removed, the soil As content was almost double that in the other chronosequence soils (38 mg kg^{-1}). Kölbl, et al. [103] have shown the migration of redox-sensitive elements (such as Mn and Fe) towards deeper soil layers due to the redox fluctuations associated with long-term paddy use. We suggest that the removal of the topsoil in P1000 exposed a deeper soil layer that had been enriched with As. This newly exposed layer lacked the characteristic development of the topsoil and thus had lower SOC and Fe amorphous phases.[103] These characteristics limited the available sorption sites, the microbial activity (reflected in higher Eh values), and the formation of secondary Fe phases that could immobilize As in P1000.

In all soils, sulfate addition stimulated As methylation. This effect was particularly higher in young paddy soils compared to older ones (1.6-fold increase in P50 vs. 1.1-fold in P2000). This suggests that sulfate addition has a stronger effect on the methylating microbial community in younger paddy soils. According to the preliminary observations from Study 1, SRB might play a primary role in As methylation in soils at the early stages of paddy soil development. In older soils, higher acetate concentrations correlated with a lower relative increase in As methylation following sulfate addition,

supporting a shift in microbial function towards fermentative bacteria. In both disrupted soils, the contribution of methylated species to total As was low (8.2 ± 0.6% in P700, and 10.1 ± 0.3% in P1000, even lower than P50 under the same conditions). These soils had low acetate concentrations, and sulfate addition caused a high relative increase in methylation (1.6 and 1.7-fold increase for P700 and P1000, respectively), suggesting it was mainly driven by SRB.

In younger soils, inorganic thioarsenate formation increased sharply after sulfate addition. However, as paddy soils aged, this effect became much weaker (a 4.2-fold increase in P50, followed by an increase of only 1.9-fold in P100). P2000 even showed a decrease in inorganic thioarsenate formation after sulfate addition. Younger paddy soils with less amorphous Fe had lower dissolved Fe^{II} concentrations, meaning that after sulfate addition there was an excess of S^{-II} available for As thiolation. In contrast, higher dissolved Fe^{II} in older paddy soils decreased the S^{-II} availability, acting as a buffer. With the addition of sulfate, S^0 concentrations in the soil after incubation increased, particularly in younger soils. Higher S^0 levels correlated with a greater proportion of inorganic thioarsenates, as previously suggested by Wang, et al. [42]. Moreover, the determination of the sulfate reduction rate suggests that young paddy soils with slower SRR (5.3 ± 0.1 nmol mL^{-1} d^{-1}) offer a slow but constant supply of S^{-II} for thiolation, compared to a pulse of higher concentration in older paddy soils with higher SRR (15.7 ± 0.7 nmol mL^{-1} d^{-1}). In this sense, the results suggested that in paddy soil systems, S availability at the right time might be more relevant for thiolation than a high-concentration pulse.

The formation of methylthioarsenates also increased with sulfate addition, driven by the increased availability of S^{-II} and oxymethylated arsenates. Similar to the formation of inorganic thioarsenates, younger soils showed a higher relative increase (1.7-fold for P50, 1.3-fold for P100 and P300, and a slight decrease of 0.96 for P2000). However, the effect of age in this relative change showed a less steep decline than the one for the formation of inorganic thioarsenates. We suggested that, as S^{-II} becomes less available with increasing paddy soil age due to the increasing dissolved Fe^{II} concentrations, inorganic thiolation will be hampered first since the formation of methylthioarsenates is favored under paddy soil neutral to acidic conditions.[49,60]

In the soils where the paddy soil development was disrupted, sulfate addition increased the formation of inorganic thioarsenates (2.8- and 2.2-fold for P700 and P1000, respectively) and methylthioarsenates (1.8-fold for both soils). Lower Fe reductive dissolution, both by hampered microbial activity and removal of amorphous Fe phases (in P1000), decreased Fe^{II} concentrations in the aqueous phase, limiting the buffering effect described above with normal paddy soil development.

Study 3 highlights the importance of knowing soil history and considering soil properties when deciding on agronomical practices such as sulfate fertilization. Here, it was shown that depending on the developmental stage of paddy soils, sulfate fertilization could cause unwanted secondary effects. Namely, sulfate fertilization could increase As methylation and thiolation in young paddy soils with an

SRB-driven As methylation, low SOC, and low Fe availability (see Publications chapter, Study 3, Figure 4). These changes in speciation could hamper the effectiveness of sulfate fertilization on limiting As uptake by rice plants, and have rather the opposite effect, given the high mobility and phytotoxicity of methylthioarsenates.[44,52] Moreover, long-term paddy soil development was shown to buffer changes in As speciation after sulfate addition, emphasizing the importance of sustaining the properties related with a healthy paddy soil development.

3.4. The role of the cryptic S cycle on thioarsenate formation in a S depleted paddy soil (Study 4)

Through repeated redox cycling, P50 (referred to as C0 in this Study) was depleted from excess S, Fe, and As. After 30 redox cycles (C30), dissolved concentrations of S, Fe, and As were decreased by 96, 61, and 94%, respectively, compared to C0. This depletion was coupled with an increased contribution of inorganic and methylated thioarsenates to total As. Compared to contributions of 0.6 and 3% of inorganic and methylated thioarsenates, respectively, depleted soils had contributions up to 25 and 24% of each thioarsenate group. This increase was correlated to higher S/As molar ratios driving higher inorganic thiolation, while the formation of methylthioarsenates was still governed by the availability of oxymethylated arsenates.

Besides increases in thioarsenate contribution to total As, and despite lower S content in the soil, increased redox cycling caused an increase in the formation of highly thiolated inorganic thioarsenates (DTA and TTA) in the early stages of the 10-day anoxic incubation. Increased incubation time caused their dethiolation, at the same time as oxymethylated arsenates were produced and readily thiolated. These (de)thiolation behavior suggest that inorganic thioarsenates formed mainly at a moment of high SRB activity, which produced high concentrations of S^{-II} while consuming the soil's original “primary” sulfate pool. A temporary S^{-II} excess drove the equilibrium toward the formation of highly thiolated species. Once the primary sulfate pool was consumed, S^{-II} became less available, and the equilibrium was shifted towards dethiolation. At the same incubation time, even though dethiolation suggests low S^{-II} availability, methylthioarsenates formed. While the contribution of inorganic thioarsenates to total As decreased and the one from methylthioarsenates increased, total thiolated As remained relatively constant. These observations suggest that under S^{-II} limited conditions, like the ones in the depleted soil, the formation of MMA and DMA could trigger the dethiolaion of inorganic thioarsenates. Briefly, the release of S^{-II} by the dethiolation of inorganic thioarsenates could react with MMA or DMA to form methylthioarsenates, which are stable under lower S^{-II} concentrations and thus thermodynamically preferred products than inorganic thioarsenates at neutral and acidic pH.[49,60]

Products of the partial reoxidation of S^{-II} were found in the incubations. Zerovalent S was found in the solid phase, accumulating independently from the depletion of the aqueous phase S. The S^0 pool had a relatively stable concentration throughout the incubation 10-day anoxic incubation period. Thiosulfate

was also found, with concentrations peaking at the beginning of the 10-day anoxic incubation. These concentrations can be related to the partial reoxidation of sulfide phases during the oxic incubation period. Nonetheless, thiosulfate was still found at the end of each anoxic cycle, indicating its production under anoxic conditions. The stable pool of S^0 and thiosulfate concentrations correlated positively and significantly (Pearson correlation, $p < 0.05$) with aqueous phase sulfate, thus indicating cryptic S cycling in the depleted soils. According to these results, S^{-II} reoxidation through the CSC produces a secondary sulfate pool which is available for reduction and thiolation after the primary sulfate pool is consumed.

For CSC to take place, a redox partner undertaking reduction is needed, with Fe^{III} (oxy)hydroxides being widely reported.[84,85] Increasing concentrations of dissolved Fe in the aqueous phase, of which > 85% on average was observed to be Fe^{II}, indicate Fe reduction. Although the reduction of Fe can take place biotically, the production of CH_4 production offers indirect evidence that abiotic Fe reduction dominates over biotically mediated Fe reductive dissolution. Methanogenesis can be inhibited by bioavailable Fe^{III} phases, since Fe reduction is a thermodynamically preferred respiration pathway than CH_4 production.[149,150] In such cases, CH_4 production has a lag phase while Fe reduction dominates respiration, and once Fe^{III} is consumed, CH_4 production shows exponential growth.[151,152] This lag phase was observed in C0, but not in the depleted soils, where CH_4 production had a linear growth, suggesting low availability of other electron acceptors such as Fe and sulfate. Moreover, Mössbauer spectroscopy showed the availability of reducible Fe^{III} phases in the solid phase. Previous studies have suggested that Fe phases with low bioavailability support CSC.[84,85]

The formation of methylthioarsenates correlated positively and significantly (Pearson correlation, $p < 0.05$) with excess S^0 and thiosulfate over oxymethylated As. This ratio considers the precursors (S^0 and thiosulfate as precursors of sulfate, which can be then reduced by DSR), and reactants (MMA and DMA) needed for methylthioarsenate formation. Such correlations were not found for the formation of inorganic thioarsenates and the excess S^0 and thiosulfate over arsenite ratio. The absence of this correlation suggests that S^{-II} produced by the reduction of a secondary sulfate pool formed through CSC, preferentially thiolate oxymethylated arsenates in S-depleted systems.

The evaluation of thioarsenate formation by reaction of arsenite or oxymethylated As with S^{-II} was not possible, since the latter was not detected during the experiment. Low S^{-II} has been previously linked to the CSC since the small and constant amounts of S^{-II} produced readily react and, thus, do not accumulate.[57,84] Correlations were carried out using sulfate, assuming its complete availability for DSR. Such correlations do not consider, however, that not all produced S^{-II} is available for thiolation due to, for example, FeS precipitation. Excess sulfate over arsenite significantly correlated (Pearson correlation, $p < 0.05$) positively with inorganic thioarsenate formation in highly depleted soils (C20 and C30). In the case of sulfate excess over oxymethylated arsenates, a negative correlation was found.

These results support the above-described interpretation that the consumption of the primary sulfate pool is related to the formation of inorganic thioarsenates in the early stages of the 10-day anoxic incubation. Once this pool is depleted, sulfate produced by CSC would also be available for reduction and thiolation. While theoretically, the S^{-II} produced through the reduction of the secondary sulfate pool could be available for inorganic thioarsenate formation, the thiolation of MMA and DMA requires a lower S^{-II} excess under the experimental conditions, making their thiolation preferred to that of inorganic thioarsenates.[49,60]

Through observations in an artificially depleted paddy soil, Study 4 suggests that there are two main phases related to the formation of thioarsenates in paddy soil (see Publications chapter, Study 4, Figure 6). First, the consumption of a primary sulfate pool generates a S^{-II} excess that reacts with arsenite, forming highly thiolated inorganic thioarsenates. Decreasing S^{-II} concentrations due to consumption of most of the primary pool and FeS precipitation, cause dethiolation. However, the CSC offers a secondary sulfate pool that is available for reduction and thiolation, which will preferentially form methylthioarsenates due to their lower S^{-II} requirements compared to their inorganic homologs. In the context of the chronosequence, the role of the secondary sulfate pool for As thiolation could be more relevant in older soils where the higher SRR consume the primary pool faster. This interpretation correlates with the formation of methylthioarsenates in late incubation stages in Studies 1 and 2, where cryptic S cycling could offer sulfate for reduction and thiolation.

4. General conclusions and Outlook

Rice is a major dietary source of As. Arsenic content and speciation in rice grains are influenced by soil properties that regulate As bioavailability, mobility, and toxicity through abiotic and microbially mediated reactions. This thesis aimed to investigate how changes in soil properties as a consequence of long-term paddy use influence As mobility and speciation. Since As biogeochemistry is largely regulated by interactions with C, S, and Fe, this thesis also evaluated changes in the redox chemistry of these elements with long-term paddy use. The studies presented here were carried out to better understand to which extent long-term paddy cultivation under flooded conditions influences risks for rice production and consumers. The main results from Studies 1-3 are summarized in Figure 5.

The findings of Study 1 were central to identifying that long-term paddy use affects the soil's redox chemistry. More specifically, SOC accumulation with long-term paddy use increased DOC availability, soil respiration, and Fe availability. In turn, these changes in aqueous chemistry had a direct influence on As mobility and speciation, increasing As methylation through enhanced microbial activity but decreasing thiolation through a limited availability of S^{-II}.

To strengthen the links between the results from this thesis based on the Cixi chronosequence and global trends of As content and speciation in rice, the following steps should be taken:

(1) Field studies in the Cixi chronosequence: While the observations carried out in our incubation experiments are central to understanding redox biogeochemical dynamics in paddy soils, the next step should be to evaluate these parameters in the field. Ideally, experiments should be carried out on-site rather than transporting material that would disturb the horizons and soil development. These experiments should follow redox dynamics throughout the cultivation period, evaluating As speciation in the aqueous phase at different stages in plant growth. This study would additionally consider the interactions between temporal, spatial, and environmental factors in the context of the plant-soil system.

(2) Survey of the grains from Cixi: In order to evaluate to which extent the changes in redox dynamics with long-term paddy use affect As accumulation in rice, grain samples should be collected from the paddies in Cixi and evaluated for As content and speciation. Ideally, this sampling could be done after the cultivation period of the above-described experiment so a direct comparison between As behavior at different stages in plant growth can be linked to the final As content in the grain.

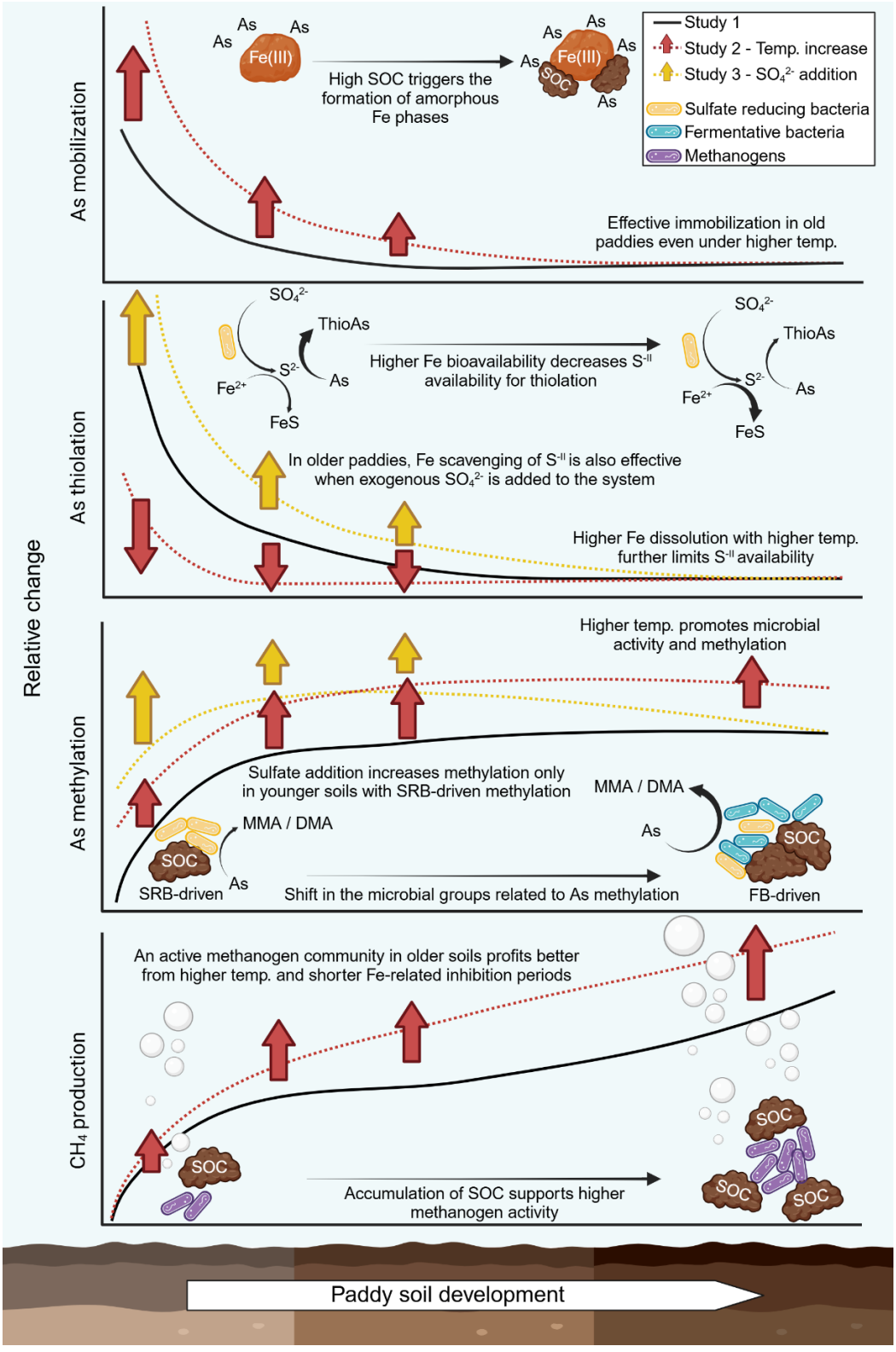

Figure 5: Conceptual model of results from Studies 1-3, indicating changes in As mobility, speciation, and CH_4 production along the chronosequence. The size of the arrows qualitatively indicates relative change with higher temperature (Study 2) or sulfate addition (Study 3), in comparison to Study 1. No significant changes were observed for As mobilization and CH_4 production in Study 3. FB: fermentative bacteria, SRB: sulfate reducing bacteria.

(3) *Global survey of paddy soil biogeochemistry and link to rice As content and speciation distribution:* This thesis suggests a range of soil properties that can be directly linked between paddy soil development and As speciation. For example, high SOC and a high potential for As methylation, or high content of amorphous Fe and a low potential for thiolation. The extension and applicability of these observations in the broader context of global rice production could be evaluated by studying soils from different rice cultivation areas around the world. These studies should include, ideally, incubation experiments to understand biogeochemical interactions, field studies for extrapolation, and comparison with either new or already existent global surveys of rice As content and speciation.

Study 2 identified specific risks associated with climate change and different stages of paddy soil development. Under higher temperatures in the future, young and newly reclaimed paddy soils established to feed growing populations could show high As mobilization. Grains with higher inorganic As content could represent a risk to food safety. Paddy soils with an already established microbial community and SOC accumulation could see an increase in As methylation, risking food security due to lower yields caused by straighthead disease due to the phytotoxic effects of DMA. Rice agriculture has seen exponential growth in the last century. Around two-thirds of the area currently used for rice cultivation is under 100 years old. These would be susceptible to the specific risk of decreased yield due to increased As methylation. Lastly, while in older paddy soils As mobilization is decreased, the main risk associated with these soils would be a strong increase in CH_4 production, causing a positive feedback loop with climate change. More importantly, these increased biogeochemical responses took place with a +2 °C increase in temperature, with an additional +3 °C showing small changes. These results show that even small increases in temperature could have important effects on the As and CH_4 biogeochemistry in paddy soil systems, adding to the need to limit warming under 1.5 °C above pre-industrial levels. Moreover, studies that allow the extrapolation of the observations from Study 2 considering field conditions and plant-soil interactions are needed:

(4) *Changes in microbial communities and dynamics with long-term paddy use:* Using samples from the chronosequence soils, the specific changes in microbial communities and functional genes with long-term paddy use could be evaluated. This study could focus on GHG emissions, additionally exploring biogeochemical parameters related to the nitrogen cycle, in order to expand on GHG emission trends based on N_2O production. Additionally, this study could offer further insights into the change from SRB-driven to FB-driven As methylation.

(5) *Field studies in Cixi under future climate scenarios:* Field experiments using climate chambers that simulate higher temperatures and atmospheric CO_2 concentrations could expand in the findings from Study 2. The suggested study could have a particular focus on changes in the dynamics of emissions of important GHG gases such as CO_2, CH_4, and N_2O. Moreover, this study could evaluate changes in the role of paddy soils as C sinks or sources under higher temperatures or CO_2

concentrations. From a food safety and security perspective, the study could evaluate if there are increases in rice As content due to enhanced As mobility, or if the cases of straighthead disease increase in paddies between 100 and 300 years.

These suggested future studies could help expand on the results from Studies 1 and 2 and identify current and future risk factors for rice production related to the stages of paddy soil development. In turn, this knowledge could help inform management practices that mitigate the specific risks associated with each field. A clear example of how agricultural practices could benefit from understanding soil properties associated with long-term paddy management comes from Study 3. These results show how an understanding of selected soil properties such as Fe availability, pH, and SOC content, could avoid unwanted effects from sulfate fertilization. According to Study 3, older paddy soils could benefit more from sulfate fertilization without having secondary effects related to increases in As methylation and thiolation. However, the question remains of which agricultural management practices could help limit high As mobilization and methylation in paddies where sulfate fertilization might not be beneficial according to the results of Study 3. Young soils could benefit from other practices such as alternate wet drying (AWD) to increase redox potential or organic carbon addition to increase SOC accumulation and formation of amorphous Fe phases. The evaluation of different mitigation strategies could be carried out in the following suggested study:

(6) Targeted mitigation strategies depending on age-related risks: Using soil samples from the chronosequence it could be evaluated how GHG emission and As mobility and speciation respond to other agricultural management practices. These could include the addition of different sources of C, such as plant material, manure, or biochar. In theory, these practices could help increase the formation of Fe-SOC associations that limit As mobility, while biochar is reported to decrease CH_4 production. These practices could, however, risk an increase in As methylation. Moreover, the direct addition of amorphous Fe phases could offer sorption sites to limit As mobility and inhibit methanogenesis. While such evaluation could start in incubation experiments, it could be further expanded to include field trials, and evaluation of grain As content and speciation.

From an agricultural management perspective, AWD has been shown to decrease CH_4 production, As mobility, and As methylation. This practice could then minimize the risks associated with constantly flooded paddy management. It would be interesting to evaluate if AWD could influence paddy soil development:

(7) Does AWD accelerate paddy soil development? The application of AWD would increase the number of redox fluctuations that a soil goes through during a single cultivation season. Accelerated redox dynamics could enhance processes related to long-term paddy soil development, such as washout of soluble salts, migration of redox-sensitive elements towards deeper soil layers, formation of Fe-SOC associations, and decreases in soil pH. These changes could, in turn, limit As

mobility. Moreover, the increase in As methylation and CH_4 production normally associated with long-term paddy use would be limited with the increase in redox potential during the drying phase of AWD. So far, the understanding of paddy soil development is limited to specific rates and redox dynamics. It should be further evaluated how the duration of the flooded and drying periods during AWD influence soil development rates.

Moreover, Study 4 addressed the knowledge gap regarding the role of the cryptic S cycle in thioarsenate formation. According to the results of this Study, the reduction of the primary sulfate pool of the soil causes a spike in S^{-II} concentrations, which favors the formation of inorganic thioarsenates. Sulfate recycled through CSC supports the formation of methylthioarsenates, even though dethiolation of inorganic thioarsenates suggests low S^{-II} availability. Thus, Study 4 proposes an adjusted role of the CSC on As thiolation (Figure 6), and additionally broadens the knowledge related to the temporal trends of thiolation and dethiolation in paddy soils. Furthermore, the results suggest that in S-depleted systems, there could be competitive thiolation, where methylthioarsenates would be preferred to their inorganic homologs. This observation could be evaluated with batch experiments using thioarsenate solutions.

(8) Evaluation of competitive thiolation between arsenite and oxymethylated arsenates: A solution of an inorganic thioarsenate standard, such as DTA, could be titrated with MMA, DMA, or a mixture of both to evaluate changes in As speciation. First, methylthioarsenates would form through reaction with the excess S^{-II} in the inorganic thioarsenate standard. However, once this excess becomes limited, the dethiolation of inorganic thioarsenates could be observed to favor the formation of methylthioarsenates. A control being titrated with ultrapure water should be considered to account for changes in speciation due to dilution of the inorganic thioarsenate standard solution. Further experiments could include more complex matrixes with, for example, the addition of Fe^{II} to further limit S^{-II} availability, and trigger changes in the species distribution, as well as evaluating a range of pH values due to its important control on As thiolation.

Overall, the results of this thesis show the links between long-term paddy use and aqueous phase redox chemistry, including As mobility and speciation. Through a better understanding of how soil properties can be linked to abiotic and microbially mediated reactions, Studies 1-3 expand on the existing knowledge of As methylation and thiolation dynamics in paddy soils. The insights generated here contribute to safeguarding rice as a safe and secure crop, both today and in the future. Moreover, the results presented here illustrate the major influence that varying soil properties have on the biogeochemical effects of agricultural practices and environmental changes such as increasing temperatures. This knowledge serves as a foundation for tailoring agricultural practices to the specific needs and risks associated with specific characteristics of paddy soil systems.

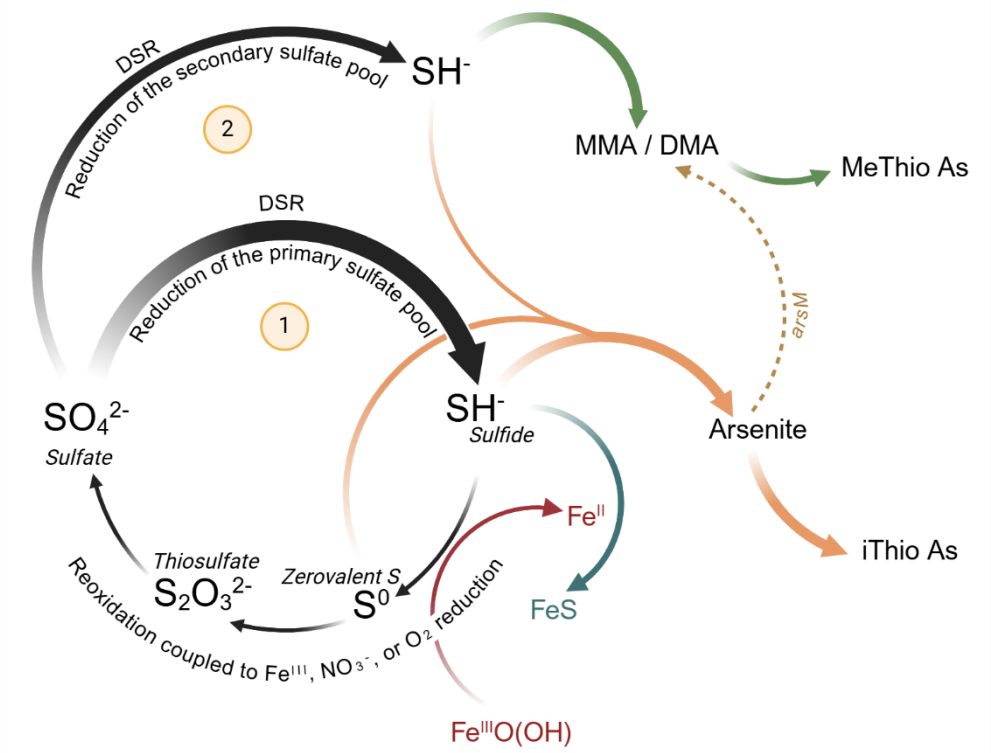

Figure 6: Adjusted role of the cryptic sulfur cycle in thioarsenate formation according to the results from Study 4. The figure shows the biogeochemical reactions involved in the production of S^{-II} and thioarsenates through the consumption of a primary (1) or secondary (2) sulfate pool. The thickness of the arrows qualitatively illustrates the importance of a reaction. Sulfur species are protonated assuming pH 7, reflecting the neutral values during the experiment. iThioAs: inorganic thioarsenates, MeThioAs: methylthioarsenates.

References

1 FAO. Food and Agriculture Organization of the United Nations: FAOSTAT-Food and agriculture. (2022).

2 Meharg, A. A. *et al.* Geographical variation in total and inorganic arsenic content of polished (white) rice. *Environmental Science & Technology* **43**, 1612-1617 (2009).

3 Kögel-Knabner, I. *et al.* Biogeochemistry of paddy soils. *Geoderma* **157**, 1-14 (2010). https://doi.org/10.1016/j.geoderma.2010.03.009

4 Meharg, A. A. & Zhao, F. J. *Arsenic & Rice*. (Springer Netherlands, 2012).

5 Sethunathan, N., Rao, V., Adhya, T. & Raghu, K. Microbiology of rice soils. *CRC Critical Reviews in Microbiology* **10**, 125-172 (1982).

6 Clemens, S. Safer food through plant science: reducing toxic element accumulation in crops. *Journal of Experimental Botany* **70**, 5537-5557 (2019). https://doi.org/10.1093/jxb/erz366

7 Wu, Z., Ren, H., McGrath, S. P., Wu, P. & Zhao, F.-J. Investigating the contribution of the phosphate transport pathway to arsenic accumulation in rice *Plant Physiology* **157**, 498-508 (2011). https://doi.org/10.1104/pp.111.178921

8 Ma, J. F. *et al.* Transporters of arsenite in rice and their role in arsenic accumulation in rice grain. *Proceedings of the National Academy of Sciences* **105**, 9931-9935 (2008). https://doi.org/10.1073/pnas.0802361105

9 Davis, M. A. *et al.* Assessment of human dietary exposure to arsenic through rice. *Science of The Total Environment* **586**, 1237-1244 (2017). https://doi.org/10.1016/j.scitotenv.2017.02.119

10 Mantha, M. *et al.* Estimating inorganic arsenic exposure from U.S. rice and total water intakes. *Environmental Health Perspectives* **125**, 057005 (2017). https://doi.org/10.1289/EHP418

11 Williams, P. N. *et al.* Greatly enhanced arsenic shoot assimilation in rice leads to elevated grain levels compared to wheat and barley. *Environmental Science & Technology* **41**, 6854-6859 (2007). https://doi.org/10.1021/es070627i

12 Lomax, C. *et al.* Methylated arsenic species in plants originate from soil microorganisms. *New Phytologist* **193**, 665-672 (2012). https://doi.org/10.1111/j.1469-8137.2011.03956.x

13 Müller, V., Chavez-Capilla, T., Feldmann, J. & Mestrot, A. Increasing temperature and flooding enhance arsenic release and biotransformations in Swiss soils. *Science of The Total Environment* **838**, 156049 (2022). https://doi.org/10.1016/j.scitotenv.2022.156049

14 Zhao, F.-J. *et al.* Arsenic methylation in soils and its relationship with microbial arsM }abundance and diversity, and As speciation in rice. *Environmental Science & Technology* **47**, 7147-7154 (2013). https://doi.org/10.1021/es304977m

15 Trevors, J. T. & Alloway, B. J. Heavy Metals in Soils: Trace Metals and Metalloids in Soils and their Bioavailability. *Heavy Metals in Soils* (2013).

16 Matschullat, J. Arsenic in the geosphere—a review. *Science of the Total Environment* **249**, 297-312 (2000).

17 Goldberg, S. & Johnston, C. T. Mechanisms of arsenic adsorption on amorphous oxides evaluated using macroscopic measurements, vibrational spectroscopy, and surface complexation modeling. *Journal of colloid and Interface Science* **234**, 204-216 (2001).

18 Takahashi, Y. *et al.* Arsenic behavior in paddy fields during the cycle of flooded and non-flooded periods. *Environmental Science & Technology* **38**, 1038-1044 (2004). https://doi.org/10.1021/es034383n

19 Smedley, P. L. & Kinniburgh, D. G. A review of the source, behaviour and distribution of arsenic in natural waters. *Applied Geochemistry* **17**, 517-568 (2002). https://doi.org/10.1016/S0883-2927(02)00018-5

20 Zobrist, J., Dowdle, P. R., Davis, J. A. & Oremland, R. S. Mobilization of arsenite by dissimilatory reduction of adsorbed arsenate. *Environmental Science & Technology* **34**, 4747-4753 (2000). https://doi.org/10.1021/es001068h

21 Williams, P. *et al.* Variation in arsenic speciation and concentration in paddy rice related to dietary exposure. *Environmental science & technology* **39**, 5531-5540 (2005).

22 Arsenic, metals, fibres, and dusts. *IARC Monogr Eval Carcinog Risks Hum* **100**, 11-465 (2012).

23 Stone, R. Arsenic and paddy rice: A neglected cancer risk? *Science* **321**, 184-185 (2008). https://doi.org/10.1126/science.321.5886.184

24 Zhao, F.-J., Zhu, Y.-G. & Meharg, A. A. Methylated arsenic species in rice: geographical variation, origin, and uptake mechanisms. *Environmental Science & Technology* **47**, 3957-3966 (2013). https://doi.org/10.1021/es304295n

25 Qin, J. *et al.* Arsenic detoxification and evolution of trimethylarsine gas by a microbial arsenite S-adenosylmethionine methyltransferase. *Proceedings of the National Academy of Sciences* **103**, 2075-2080 (2006). https://doi.org/10.1073/pnas.0506836103

26 Viacava, K. *et al.* Variability in arsenic methylation efficiency across aerobic and anaerobic microorganisms. *Environmental Science & Technology* **54**, 14343-14351 (2020). https://doi.org/10.1021/acs.est.0c03908

27 Chen, C. *et al.* Sulfate-reducing bacteria and methanogens are involved in arsenic methylation and demethylation in paddy soils. *The ISME Journal* **13**, 2523-2535 (2019). https://doi.org/10.1038/s41396-019-0451-7

28 Chen, C. *et al.* Sulfate addition and rising temperature promote arsenic methylation and the formation of methylated thioarsenates in paddy soils. *Soil Biology and Biochemistry* **154**, 108129 (2021). https://doi.org/10.1016/j.soilbio.2021.108129

29 Reid, M. C. *et al.* Arsenic methylation dynamics in a rice paddy soil anaerobic enrichment culture. *Environmental Science & Technology* **51**, 10546-10554 (2017). https://doi.org/10.1021/acs.est.7b02970

30 Chen, J. & Rosen, B. P. The arsenic methylation cycle: how microbial communities adapted methylarsenicals for use as weapons in the continuing war for dominance. *Frontiers in Environmental Science* **8** (2020). https://doi.org/10.3389/fenvs.2020.00043

31 Chen, J., Yoshinaga, M. & Rosen, B. P. The antibiotic action of methylarsenite is an emergent property of microbial communities. *Molecular Microbiology* **111**, 487-494 (2019). https://doi.org/10.1111/mmi.14169

32 Chen, C., Li, L., Wang, Y., Dong, X. & Zhao, F.-J. Methylotrophic methanogens and bacteria synergistically demethylate dimethylarsenate in paddy soil and alleviate rice straighthead disease. *The ISME Journal* (2023). https://doi.org/10.1038/s41396-023-01498-7

33 Zhang, X. & Reid, M. C. Inhibition of methanogenesis leads to accumulation of methylated arsenic species and enhances arsenic volatilization from rice paddy soil. *Science of The Total Environment* **818**, 151696 (2022). https://doi.org/10.1016/j.scitotenv.2021.151696

34 Lemos Batista, B. *et al.* Identification and quantification of phytochelatins in roots of rice to long-term exposure: evidence of individual role on arsenic accumulation and translocation. *Journal of experimental botany* **65**, 1467-1479 (2014).

35 Mishra, S., Mattusch, J. & Wennrich, R. Accumulation and transformation of inorganic and organic arsenic in rice and role of thiol-complexation to restrict their translocation to shoot. *Scientific Reports* **7**, 40522 (2017).

36 Schmoger, M. E., Oven, M. & Grill, E. Detoxification of arsenic by phytochelatins in plants. *Plant Physiology* **122**, 793-802 (2000).

37 Moe, B. *et al.* Comparative cytotoxicity of fourteen trivalent and pentavalent arsenic species determined using real-time cell sensing. *Journal of Environmental Sciences* **49**, 113-124 (2016). https://doi.org/10.1016/j.jes.2016.10.004

38 Naranmandura, H. *et al.* Comparative Toxicity of Arsenic Metabolites in Human Bladder Cancer EJ-1 Cells. *Chemical Research in Toxicology* **24**, 1586-1596 (2011). https://doi.org/10.1021/tx200291p

39 Wang, Y.-J., Dong, C.-Y., Tang, Z. & Zhao, F.-J. Translocation, enzymatic reduction and toxicity of dimethylarsenate in rice. *Plant Physiology and Biochemistry* **207**, 108393 (2024). https://doi.org/10.1016/j.plaphy.2024.108393

40 Zheng, M.-Z., Li, G., Sun, G.-X., Shim, H. & Cai, C. Differential toxicity and accumulation of inorganic and methylated arsenic in rice. *Plant and Soil* **365**, 227-238 (2013).

41 Wang, J. *et al.* Redox dependence of thioarsenate occurrence in paddy soils and the rice rhizosphere. *Environmental Science & Technology* **54**, 3940-3950 (2020). https://doi.org/10.1021/acs.est.9b05639

42 Wang, J. *et al.* Thiolated arsenic species observed in rice paddy pore waters. *Nature Geoscience* **13**, 282-287 (2020). https://doi.org/10.1038/s41561-020-0533-1

43 Kerl, C. F., Rafferty, C., Clemens, S. & Planer-Friedrich, B. Monothioarsenate uptake, transformation, and translocation in tice plants. *Environmental Science & Technology* **52**, 9154-9161 (2018). https://doi.org/10.1021/acs.est.8b02202

44 Pischke, E. *et al.* Dimethylmonothioarsenate is highly toxic for plants and readily translocated to shoots. *Environmental Science & Technology* **56**, 10072-10083 (2022). https://doi.org/10.1021/acs.est.2c01206

45 Colina Blanco, A. E., Kerl, C. F. & Planer-Friedrich, B. Detection of thioarsenates in rice grains and rice products. *Journal of Agricultural and Food Chemistry* **69**, 2287-2294 (2021). https://doi.org/10.1021/acs.jafc.0c06853

46 Dai, J. *et al.* Widespread occurrence of the highly toxic dimethylated monothioarsenate (DMMTA) in rice globally. *Environmental Science & Technology* **56**, 3575-3586 (2022). https://doi.org/10.1021/acs.est.1c08394

47 Wallschläger, D. & Stadey, C. J. Determination of (oxy)thioarsenates in sulfidic waters. *Analytical Chemistry* **79**, 3873-3880 (2007). https://doi.org/10.1021/ac070061g

48 Wallschläger, D. & London, J. Determination of methylated arsenic-sulfur compounds in groundwater. *Environmental Science & Technology* **42**, 228-234 (2008). https://doi.org/10.1021/es0707815

49 Conklin, S. D., Fricke, M. W., Creed, P. A. & Creed, J. T. Investigation of the pH effects on the formation of methylated thio-arsenicals, and the effects of pH and temperature on their stability. *Journal of Analytical Atomic Spectrometry* **23**, 711-716 (2008). https://doi.org/10.1039/B713145C

50 Naranmandura, H., Ibata, K. & Suzuki, K. T. Toxicity of dimethylmonothioarsinic acid toward human epidermoid carcinoma A431 cells. *Chemical research in toxicology* **20**, 1120-1125 (2007).

51 Ochi, T. *et al.* Cytotoxic, genotoxic and cell-cycle disruptive effects of thio-dimethylarsinate in cultured human cells and the role of glutathione. *Toxicology and Applied Pharmacology* **228**, 59-67 (2008).

52 Kerl, C. F. *et al.* Methylated thioarsenates and monothioarsenate differ in uptake, transformation, and contribution to total arsenic translocation in rice plants. *Environmental Science & Technology* **53**, 5787-5796 (2019). https://doi.org/10.1021/acs.est.9b00592

53 Colina Blanco, A. E., Higa Mori, A. & Planer-Friedrich, B. Widespread occurrence of dimethylmonothioarsenate (DMMTA) in rice cakes: Effects of puffing and storage. *Food Chemistry* **436**, 137723 (2024). https://doi.org/10.1016/j.foodchem.2023.137723

54 Planer-Friedrich, B., Kerl, C. F., Colina Blanco, A. E. & Clemens, S. Dimethylated thioarsenates: a potentially dangerous blind spot in current worldwide regulatory limits for arsenic in rice. *Journal of Agricultural and Food Chemistry* **70**, 9610-9618 (2022). https://doi.org/10.1021/acs.jafc.2c02425

55 Chen, C. *et al.* Suppression of methanogenesis in paddy soil increases dimethylarsenate accumulation and the incidence of straighthead disease in rice. *Soil Biology and Biochemistry* **169**, 108689 (2022). https://doi.org/10.1016/j.soilbio.2022.108689

56 Jia, Y. *et al.* Microbial arsenic methylation in soil and rice rhizosphere. *Environmental Science & Technology* **47**, 3141-3148 (2013). https://doi.org/10.1021/es303649v

57 Wind, T. & Conrad, R. Sulfur compounds, potential turnover of sulfate and thiosulfate, and numbers of sulfate-reducing bacteria in planted and unplanted paddy soil. *FEMS Microbiology Ecology* **18**, 257-266 (1995). https://doi.org/10.1111/j.1574-6941.1995.tb00182.x

58 Wind, T. & Conrad, R. Localization of sulfate reduction in planted and unplanted rice field soil. *Biogeochemistry* **37**, 253-278 (1997). https://doi.org/10.1023/A:1005760506957

59 Ma, R. *et al.* Impact of agronomic practices on arsenic accumulation and speciation in rice grain. *Environmental Pollution* **194**, 217-223 (2014). https://doi.org/10.1016/j.envpol.2014.08.004

60 Planer-Friedrich, B., London, J., McCleskey, R. B., Nordstrom, D. K. & Wallschläger, D. Thioarsenates in geothermal waters of Yellowstone National Park: determination, preservation, and geochemical importance. *Environmental Science & Technology* **41**, 5245-5251 (2007). https://doi.org/10.1021/es070273v

61 Kerl, C. F., Ballaran, T. B. & Planer-Friedrich, B. Iron plaque at rice roots: no barrier for methylated thioarsenates. *Environmental Science & Technology* **53**, 13666-13674 (2019). https://doi.org/10.1021/acs.est.9b04158

62 Yan, K. *et al.* Effects of thiolation and methylation on arsenic sorption to geothermal sediments. *Science of The Total Environment* **827**, 154016 (2022). https://doi.org/10.1016/j.scitotenv.2022.154016

63 Dixit, S. & Hering, J. G. Comparison of arsenic(V) and arsenic(III) sorption onto iron oxide minerals: implications for arsenic mobility. *Environmental Science & Technology* **37**, 4182-4189 (2003). https://doi.org/10.1021/es030309t

64 Suess, E., Wallschläger, D. & Planer-Friedrich, B. Stabilization of thioarsenates in iron-rich waters. *Chemosphere* **83**, 1524-1531 (2011). https://doi.org/10.1016/j.chemosphere.2011.01.045

65 Suess, E., Mehlhorn, J. & Planer-Friedrich, B. Anoxic, ethanolic, and cool – An improved method for thioarsenate preservation in iron-rich waters. *Applied Geochemistry* **62**, 224-233 (2015). https://doi.org/10.1016/j.apgeochem.2014.11.017

66 Khan, M. A., Stroud, J. L., Zhu, Y.-G., McGrath, S. P. & Zhao, F.-J. Arsenic bioavailability to rice is elevated in Bangladeshi paddy soils. *Environmental Science & Technology* **44**, 8515-8521 (2010).

67 Xu, X., Chen, C., Wang, P., Kretzschmar, R. & Zhao, F.-J. Control of arsenic mobilization in paddy soils by manganese and iron oxides. *Environmental Pollution* **231**, 37-47 (2017). https://doi.org/10.1016/j.envpol.2017.07.084

68 Borch, T. *et al.* Biogeochemical redox processes and their impact on contaminant dynamics. *Environmental Science & Technology* **44**, 15-23 (2010). https://doi.org/10.1021/es9026248

69 Lovley, D. R. *et al.* Humic substances as a mediator for microbially catalyzed metal reduction. *Acta hydrochimica et hydrobiologica* **26**, 152-157 (1998).

70 Williams, P. N. *et al.* Organic matter-solid phase interactions are critical for predicting arsenic release and plant uptake in bangladesh paddy soils. *Environmental science & technology* **45**, 6080-6087 (2011).

71 Jiang, O. *et al.* Root exudates increased arsenic mobility and altered microbial community in paddy soils. *Journal of Environmental Sciences* **127**, 410-420 (2023). https://doi.org/10.1016/j.jes.2022.05.036

72 Burton, E. D., Johnston, S. G. & Kocar, B. D. Arsenic mobility during flooding of contaminated soil: the effect of microbial sulfate reduction. *Environmental Science & Technology* **48**, 13660-13667 (2014). https://doi.org/10.1021/es503963k

73 Farquhar, M. L., Charnock, J. M., Livens, F. R. & Vaughan, D. J. Mechanisms of arsenic uptake from aqueous solution by interaction with goethite, lepidocrocite, mackinawite, and pyrite: an X-ray absorption spectroscopy study. *Environmental Science & Technology* **36**, 1757-1762 (2002). https://doi.org/10.1021/es010216g

74 Bostick, B. C. & Fendorf, S. Arsenite sorption on troilite (FeS) and pyrite (FeS2). *Geochimica et Cosmochimica Acta* **67**, 909-921 (2003). https://doi.org/10.1016/S0016-7037(02)01170-5

75 Wisawapipat, W. *et al.* Sulfur amendments to soil decrease inorganic arsenic accumulation in rice grain under flooded and nonflooded conditions: Insights from temporal dynamics of porewater chemistry and solid-phase arsenic solubility. *Science of The Total Environment* **779**, 146352 (2021). https://doi.org/10.1016/j.scitotenv.2021.146352

76 Yan, S. *et al.* Arsenic and cadmium bioavailability to rice (Oryza sativa L.) plant in paddy soil: Influence of sulfate application. *Chemosphere* **307**, 135641 (2022). https://doi.org/10.1016/j.chemosphere.2022.135641

77 Fang, X. *et al.* Simultaneously decreasing arsenic and cadmium in rice by soil sulfate and limestone amendment under intermittent flooding. *Environmental Pollution* **347**, 123786 (2024). https://doi.org/10.1016/j.envpol.2024.123786

78 Xu, X. *et al.* Microbial sulfate reduction decreases arsenic mobilization in flooded paddy soils with high potential for microbial Fe reduction. *Environmental Pollution* **251**, 952-960 (2019). https://doi.org/10.1016/j.envpol.2019.05.086

79 Huang, H., Jia, Y., Sun, G.-X. & Zhu, Y.-G. Arsenic speciation and volatilization from flooded paddy soils amended with different organic matters. *Environmental science & technology* **46**, 2163-2168 (2012).

80 Mestrot, A. *et al.* Field fluxes and speciation of arsines emanating from soils. *Environmental science & technology* **45**, 1798-1804 (2011).

81 Mestrot, A. *et al.* Quantitative and qualitative trapping of arsines deployed to assess loss of volatile arsenic from paddy soil. *Environmental science & technology* **43**, 8270-8275 (2009).

82 Yan, M. *et al.* Dissolved organic matter differentially influences arsenic methylation and volatilization in paddy soils. *Journal of Hazardous Materials* **388**, 121795 (2020). https://doi.org/10.1016/j.jhazmat.2019.121795

83 Gao, A.-X. *et al.* Soil redox status governs within-field spatial variation in microbial arsenic methylation and rice straighthead disease. *The ISME Journal* **18** (2024). https://doi.org/10.1093/ismejo/wrae057

84 Holmkvist, L., Ferdelman, T. G. & Jørgensen, B. B. A cryptic sulfur cycle driven by iron in the methane zone of marine sediment (Aarhus Bay, Denmark). *Geochimica et Cosmochimica Acta* **75**, 3581-3599 (2011). https://doi.org/10.1016/j.gca.2011.03.033

85 Hansel, C. M. *et al.* Dominance of sulfur-fueled iron oxide reduction in low-sulfate freshwater sediments. *The ISME Journal* **9**, 2400-2412 (2015). https://doi.org/10.1038/ismej.2015.50

86 Weber, F.-A., Hofacker, A. F., Voegelin, A. & Kretzschmar, R. Temperature dependence and coupling of iron and arsenic reduction and release during flooding of a contaminated soil. *Environmental Science & Technology* **44**, 116-122 (2010). https://doi.org/10.1021/es902100h

87 Castro, H. F., Classen, A. T., Austin, E. E., Norby, R. J. & Schadt, C. W. Soil microbial community responses to multiple experimental climate change drivers. *Applied and Environmental Microbiology* **76**, 999-1007 (2010). https://doi.org/10.1128/AEM.02874-09

88 Bradford, M. A. *et al.* Thermal adaptation of soil microbial respiration to elevated temperature. *Ecology Letters* **11**, 1316-1327 (2008). https://doi.org/10.1111/j.1461-0248.2008.01251.x

89 Frey, S., Drijber, R., Smith, H. & Melillo, J. Microbial biomass, functional capacity, and community structure after 12 years of soil warming. *Soil Biology and Biochemistry* **40**, 2904-2907 (2008). https://doi.org/10.1016/j.soilbio.2008.07.020

90 Muehe, E. M., Wang, T., Kerl, C. F., Planer-Friedrich, B. & Fendorf, S. Rice production threatened by coupled stresses of climate and soil arsenic. *Nature Communications* **10**, 4985 (2019). https://doi.org/10.1038/s41467-019-12946-4

91 Conrad, R. Methane production in soil environments—anaerobic biogeochemistry and microbial life between flooding and desiccation. *Microorganisms* **8**, 881 (2020). https://doi.org/10.3390/microorganisms8060881

92 Conrad, R. in *Advances in Agronomy* Vol. 96 1-63 (Academic Press, 2007).

93 Forster, P. *et al.* Chapter 7: The Earth's energy budget, climate feedbacks, and climate sensitivity. Climate Change 2021: The Physical Science Basis. Contribution of Working Group I to the Sixth Assessment Report of the Intergovernmental Panel on Climate Change. (2021).

94 Carlson, K. M. *et al.* Greenhouse gas emissions intensity of global croplands. *Nature Climate Change* **7**, 63-68 (2017). https://doi.org/10.1038/nclimate3158

95 Linquist, B., van Groenigen, K. J., Adviento-Borbe, M. A., Pittelkow, C. & van Kessel, C. An agronomic assessment of greenhouse gas emissions from major cereal crops. *Global Change Biology* **18**, 194-209 (2012). https://doi.org/10.1111/j.1365-2486.2011.02502.x

96 Canadell, J. *et al.* Climate change 2021: The physical science basis. Contribution of working group I to the sixth assessment report of the intergovernmental panel on climate change. *Cambridge Univ. Press* (2021).

97 Ciais, P. *et al.* The physical science basis. Contribution of working group I to the fifth assessment report of the intergovernmental panel on climate change. *Change, IPCC climate* **10** (2013).

98 Cao, M., Gregson, K. & Marshall, S. Global methane emission from wetlands and its sensitivity to climate change. *Atmospheric environment* **32**, 3293-3299 (1998).

99 Ringeval, B. *et al.* Climate-CH_4 feedback from wetlands and its interaction with the climate-CO_2 feedback. *Biogeosciences* **8**, 2137-2157 (2011).

100 Van Amstel, A. Methane. A review. *Journal of Integrative Environmental Sciences* **9**, 5-30 (2012). https://doi.org/10.1080/1943815X.2012.694892

101 Yang, S.-S. & Chang, H.-L. Effect of environmental conditions on methane production and emission from paddy soil. *Agriculture, Ecosystems & Environment* **69**, 69-80 (1998). https://doi.org/10.1016/S0167-8809(98)00098-X

102 Yan, X., Yagi, K., Akiyama, H. & Akimoto, H. Statistical analysis of the major variables controlling methane emission from rice fields. *Global Change Biology* **11**, 1131-1141 (2005). https://doi.org/10.1111/j.1365-2486.2005.00976.x

103 Kölbl, A. *et al.* Accelerated soil formation due to paddy management on marshlands (Zhejiang Province, China). *Geoderma* **228-229**, 67-89 (2014). https://doi.org/10.1016/j.geoderma.2013.09.005

104 Cheng, Y.-Q., Yang, L.-Z., Cao, Z.-H., Ci, E. & Yin, S. Chronosequential changes of selected pedogenic properties in paddy soils as compared with non-paddy soils. *Geoderma* **151**, 31-41 (2009). https://doi.org/10.1016/j.geoderma.2009.03.016

105 Wissing, L. *et al.* Organic carbon accumulation on soil mineral surfaces in paddy soils derived from tidal wetlands. *Geoderma* **228-229**, 90-103 (2014). https://doi.org/10.1016/j.geoderma.2013.12.012

106 Wissing, L. *et al.* Organic carbon accumulation in a 2000-year chronosequence of paddy soil evolution. *CATENA* **87**, 376-385 (2011). https://doi.org/10.1016/j.catena.2011.07.007

107 Schulz, K. *et al.* Contact with soil impacts ferrihydrite and lepidocrocite transformations during redox cycling in a paddy soil. *Environmental Science: Processes & Impacts* **25**, 1945-1961 (2023). https://doi.org/10.1039/D3EM00314K

108 Bannert, A. *et al.* Changes in diversity and functional gene abundances of microbial communities involved in nitrogen fixation, nitrification, and denitrification in a tidal wetland versus paddy soils cultivated for different time periods. *Applied and Environmental Microbiology* **77**, 6109-6116 (2011). https://doi.org/10.1128/AEM.01751-10

109 Roth, P. J. *et al.* Accumulation of nitrogen and microbial residues during 2000 years of rice paddy and non-paddy soil development in the Yangtze River Delta, China. *Global Change Biology* **17**, 3405-3417 (2011). https://doi.org/10.1111/j.1365-2486.2011.02500.x

110 Wang, P. *et al.* Long-term rice cultivation stabilizes soil organic carbon and promotes soil microbial activity in a salt marsh derived soil chronosequence. *Scientific Reports* **5**, 15704 (2015). https://doi.org/10.1038/srep15704

111 Wang, F. *et al.* Succession of bacterial community composition in coastal agricultural soils along a 1000-year reclamation chronosequence in Hangzhou Bay, China. *Ecological Indicators* **121**, 106972 (2021). https://doi.org/10.1016/j.ecolind.2020.106972

112 Ho, A., Lüke, C., Cao, Z. & Frenzel, P. Ageing well: methane oxidation and methane oxidizing bacteria along a chronosequence of 2000 years. *Environmental Microbiology Reports* **3**, 738-743 (2011).

113 Li, D. *et al.* Exploring microbial dynamics, metabolic functions and microbes–metabolites correlation in a millennium paddy soil chronosequence using metabolome and microbiome. *Chemical and Biological Technologies in Agriculture* **11**, 146 (2024). https://doi.org/10.1186/s40538-024-00673-y

114 Le Quéré, C. *et al.* Global carbon budget 2017. *Earth System Science Data* **10**, 405-448 (2018). https://doi.org/10.5194/essd-10-405-2018

115 Mueller-Niggemann, C., Bannert, A., Schloter, M., Lehndorff, E. & Schwark, L. Intra- versus inter-site macroscale variation in biogeochemical properties along a paddy soil chronosequence. *Biogeosciences* **9**, 1237-1251 (2012). https://doi.org/10.5194/bg-9-1237-2012

116 Stookey, L. L. Ferrozine---a new spectrophotometric reagent for iron. *Analytical Chemistry* **42**, 779-781 (1970). https://doi.org/10.1021/ac60289a016

117 Hegler, F., Posth, N. R., Jiang, J. & Kappler, A. Physiology of phototrophic iron(II)-oxidizing bacteria: implications for modern and ancient environments. *FEMS Microbiology Ecology* **66**, 250-260 (2008). https://doi.org/10.1111/j.1574-6941.2008.00592.x

118 Cline, J. D. Spectrophotometric determination of hydrogen sulfide in natural waters. *Limnology and Oceanography* **14**, 454-458 (1969).

119 Lohmayer, R., Kappler, A., Lösekann-Behrens, T. & Planer-Friedrich, B. Sulfur species as redox partners and electron shuttles for ferrihydrite reduction by Sulfurospirillum deleyianum.

Applied and Environmental Microbiology **80**, 3141-3149 (2014). https://doi.org/10.1128/aem.04220-13

120 Mehra, O. P. & Jackson, M. L. Iron oxide removal from soils and clays by a dithionite-citrate system buffered with sodium bicarbonate. *Clays and Clay Minerals* **7**, 317-327 (1958). https://doi.org/10.1346/CCMN.1958.0070122

121 McKeague, J. A. & Day, J. H. Dithionite- and oxalate-extractable Fe and Al as aids in differentiating various classes of soils. *Canadian Journal of Soil Science* **46**, 13-22 (1966). https://doi.org/10.4141/cjss66-003

122 Lueders, T., Manefield, M. & Friedrich, M. W. Enhanced sensitivity of DNA- and rRNA-based stable isotope probing by fractionation and quantitative analysis of isopycnic centrifugation gradients. *Environmental Microbiology* **6**, 73-78 (2004). https://doi.org/10.1046/j.1462-2920.2003.00536.x

123 Zeibich, L., Schmidt, O. & Drake, H. L. Protein- and RNA-enhanced fermentation by gut microbiota of the earthworm *Lumbricus terrestris*. *Applied and Environmental Microbiology* **84**, e00657-00618 (2018). https://doi.org/doi:10.1128/AEM.00657-18

124 López-Rayo, S., Hernández, D. & Lucena, J. J. Chemical Evaluation of HBED/Fe^{3+} and the novel HJB/Fe^{3+} chelates as fertilizers to alleviate iron chlorosis. *Journal of Agricultural and Food Chemistry* **57**, 8504-8513 (2009). https://doi.org/10.1021/jf9019147

125 Fulda, B., Voegelin, A., Ehlert, K. & Kretzschmar, R. Redox transformation, solid phase speciation and solution dynamics of copper during soil reduction and reoxidation as affected by sulfate availability. *Geochimica et Cosmochimica Acta* **123**, 385-402 (2013). https://doi.org/10.1016/j.gca.2013.07.017

126 Fossing, H. & Jørgensen, B. B. Measurement of bacterial sulfate reduction in sediments: evaluation of a single-step chromium reduction method. *Biogeochemistry* **8**, 205-222 (1989).

127 Lagarec, K. & Rancourt, D. G. Extended Voigt-based analytic lineshape method for determining N-dimensional correlated hyperfine parameter distributions in Mössbauer spectroscopy. *Nuclear Instruments and Methods in Physics Research Section B: Beam Interactions with Materials and Atoms* **129**, 266-280 (1997). https://doi.org/10.1016/S0168-583X(97)00284-X

128 Kalbitz, K. *et al.* The carbon count of 2000 years of rice cultivation. *Global Change Biology* **19**, 1107-1113 (2013). https://doi.org/10.1111/gcb.12080

129 Schwertmann, U. Solubility and dissolution of iron oxides. *Plant and Soil* **130**, 1-25 (1991). https://doi.org/10.1007/BF00011851

130 Snoeyink, V. L. & Jenkins, D. *Water Chemistry*. (Wiley, 1980).

131 Achtnich, C., Bak, F. & Conrad, R. Competition for electron donors among nitrate reducers, ferric iron reducers, sulfate reducers, and methanogens in anoxic paddy soil. *Biology and Fertility of Soils* **19**, 65-72 (1995). https://doi.org/10.1007/BF00336349

132 Gramp, J. P., Bigham, J. M., Jones, F. S. & Tuovinen, O. H. Formation of Fe-sulfides in cultures of sulfate-reducing bacteria. *Journal of Hazardous Materials* **175**, 1062-1067 (2010). https://doi.org/10.1016/j.jhazmat.2009.10.119

133 Spratt Jr, H. G. & Morgan, M. D. Sulfur cycling in a cedar-dominated, freshwater wetland. *Limnology and Oceanography* **35**, 1586-1593 (1990).

134 Yu, Z.-G., Peiffer, S., Göttlicher, J. & Knorr, K.-H. Electron transfer budgets and kinetics of abiotic oxidation and incorporation of aqueous sulfide by dissolved organic matter. *Environmental Science & Technology* **49**, 5441-5449 (2015). https://doi.org/10.1021/es505531u

135 Yang, Y.-P. *et al.* Microbe mediated arsenic release from iron minerals and arsenic methylation in rhizosphere controls arsenic fate in soil-rice system after straw incorporation. *Environmental Pollution* **236**, 598-608 (2018). https://doi.org/10.1016/j.envpol.2018.01.099

136 Meng, Y.-L., Liu, Z. & Rosen, B. P. As(III) and Sb(III) Uptake by GlpF and efflux by ArsB in *Escherichia coli**. *Journal of Biological Chemistry* **279**, 18334-18341 (2004). https://doi.org/10.1074/jbc.M400037200

137 Rosen, B. P. & Liu, Z. Transport pathways for arsenic and selenium: A minireview. *Environment International* **35**, 512-515 (2009). https://doi.org/10.1016/j.envint.2008.07.023

138 Yoon, H. *et al.* Time-dependent biosensor fluorescence as a measure of bacterial arsenic uptake kinetics and its inhibition by dissolved organic Matter. *Applied and Environmental Microbiology* **88**, e00891-00822 (2022). https://doi.org/10.1128/aem.00891-22

139 Yoon, H. *et al.* Repression of microbial arsenite uptake and methylation by dissolved organic carbon. *Environmental Science & Technology Letters* **11**, 838-844 (2024). https://doi.org/10.1021/acs.estlett.4c00400

140 Klein, M. *et al.* Multiple lateral transfers of dissimilatory sulfite reductase genes between major lineages of sulfate-reducing prokaryotes. *Journal of Bacteriology* **183**, 6028-6035 (2001). https://doi.org/10.1128/jb.183.20.6028-6035.2001

141 Frey, S. D., Lee, J., Melillo, J. M. & Six, J. The temperature response of soil microbial efficiency and its feedback to climate. *Nature Climate Change* **3**, 395-398 (2013). https://doi.org/10.1038/nclimate1796

142 Dimassi, B. *et al.* Long-term effect of contrasted tillage and crop management on soil carbon dynamics during 41 years. *Agriculture, Ecosystems & Environment* **188**, 134-146 (2014). https://doi.org/10.1016/j.agee.2014.02.014

143 Wei, L. *et al.* Paddy soils have a much higher microbial biomass content than upland soils: A review of the origin, mechanisms, and drivers. *Agriculture, Ecosystems & Environment* **326**, 107798 (2022). https://doi.org/10.1016/j.agee.2021.107798

144 Chen, X. *et al.* Contrasting pathways of carbon sequestration in paddy and upland soils. *Global Change Biology* **27**, 2478-2490 (2021). https://doi.org/10.1111/gcb.15595

145 Liu, Y. *et al.* Divergent accumulation of microbial and plant necromass along paddy soil development in a millennium scale. *Soil and Tillage Research* **232**, 105769 (2023). https://doi.org/10.1016/j.still.2023.105769

146 Wei, L. *et al.* Labile carbon matters more than temperature for enzyme activity in paddy soil. *Soil Biology and Biochemistry* **135**, 134-143 (2019).

147 Su, R. *et al.* Carbon availability and microbial activity manipulate the temperature sensitivity of anaerobic degradation in a paddy soil profile. *Environmental Research*, 118453 (2024). https://doi.org/10.1016/j.envres.2024.118453

148 Luo, D. *et al.* A joint role of iron oxide and temperature for methane production and methanogenic community in paddy soils. *Geoderma* **433**, 116462 (2023). https://doi.org/10.1016/j.geoderma.2023.116462

149 van Bodegom, P. M., Scholten, J. C. M. & Stams, A. J. M. Direct inhibition of methanogenesis by ferric iron. *FEMS Microbiology Ecology* **49**, 261-268 (2004). https://doi.org/10.1016/j.femsec.2004.03.017

150 Lovley, D. R. & Phillips, E. J. Competitive mechanisms for inhibition of sulfate reduction and methane production in the zone of ferric iron reduction in sediments. *Applied and Environmental Microbiology* **53**, 2636-2641 (1987). https://doi.org/10.1128/aem.53.11.2636-2641.1987

151 Ponnamperuma, F. N. in *Advances in Agronomy* Vol. 24 (ed N. C. Brady) 29-96 (Academic Press, 1972).

152 Patrick Jr., W. H. & Jugsujinda, A. Sequential reduction and oxidation of inorganic nitrogen, manganese, and iron in flooded soil. *Soil Science Society of America Journal* **56**, 1071-1073 (1992). https://doi.org/10.2136/sssaj1992.03615995005600040011x

Publications: Studies 1-4

Published Studies:

Study 1

León Ninin, J.M.; Muehe, E.M.; Kölbl, A.; Higa Mori, A.; Nicol A.; Gilfedder, B.; Pausch, J.; Urbanski, L.; Lueders, T.; Planer-Friedrich, B. Changes in arsenic mobility and speciation across a 2000-year-old paddy soil chronosequence. *Sci. Total Environ.* **2024**, *908*, 168351. https://doi.org/10.1016/j.scitotenv.2023.168351

Study 2

León Ninin, J.M.; Higa Mori, A.; Pausch, J.; Planer-Friedrich, B. Long-term paddy use influences response of methane production, arsenic mobility and speciation to future higher temperatures. *Sci. Total Environ.* **2024**, *943*, 173793. https://doi.org/10.1016/j.scitotenv.2024.173793

Study 3

León Ninin, J.M.; Kryschak, N.; Peiffer, S.; Planer-Friedrich, B. Long-term paddy soil development buffers the increase in arsenic methylation and thiolation after sulfate fertilization. *J. Agric. Food Chem.* **2024** 72 (45), 25045-25053. https://doi.org/10.1021/acs.jafc.4c09537

Study 4

León Ninin, J.M.; Dreher, C.; Kappler, A.; Planer-Friedrich, B. Sulfur depletion through repetitive redox cycling unmasks the role of the cryptic sulfur cycle in (methyl)thioarsenate formation in paddy soils. *Environmental Sciences: Processes & Impacts.* **2025** (Advance article). https://doi.org/10.1039/d4em00764f

Study 1: Changes in arsenic mobility and speciation across a 2000-year-old paddy soil chronosequence

José M. León Ninin, E. Marie Muehe, Angelika Kölbl, Alejandra Higa Mori, Alan Nicol, Ben Gilfedder, Johanna Pausch, Livia Urbanski, Tillmann Lueders, and Britta Planer-Friedrich

Reprinted with permission from

Science of The Total Environment (*908*, pp. 168351)

Own contribution to Study 1:	
Concept and study design	90%
Data acquisition	80%
Analyses of samples	85%
Data analysis and figure preparation	95%
Discussion of results	90%
Manuscript writing	90%

This study was designed by J.M.L.N. and B.P.-F.; experiments were carried out by J.M.L.N with the support of A.H.M. and A.N.; analysis of samples was carried out by J.M.L.N. with the support of E.M.M., A.H.M., A.N., and a master student (see acknowledgments); original soil samples were provided by A.K. and L.U.; access to analytical facilities was provided by B.G., J.P., and T.L.; data analyses, discussion of results, and manuscript writing were carried out by J.M.L.N. with the support of B.P.-F.; all authors contributed to the revisions of the published manuscript.

Science of the Total Environment 908 (2024) 168351

Contents lists available at ScienceDirect

Science of the Total Environment

journal homepage: www.elsevier.com/locate/scitotenv

Changes in arsenic mobility and speciation across a 2000-year-old paddy soil chronosequence

José M. León Ninin [a], E. Marie Muehe [b,c], Angelika Kölbl [d], Alejandra Higa Mori [a], Alan Nicol [a], Ben Gilfedder [e], Johanna Pausch [f], Livia Urbanski [g], Tillmann Lueders [h], Britta Planer-Friedrich [a,*]

[a] Environmental Geochemistry, Bayreuth Center for Ecology and Environmental Research (BayCEER), University of Bayreuth, 95440 Bayreuth, Germany
[b] Department of Environmental Microbiology, Helmholtz Centre for Environmental Research (UFZ), 04318 Leipzig, Germany
[c] Department of Geosciences, University of Tübingen, 72076 Tübingen, Germany
[d] Soil Science and Soil Protection, Martin Luther University Halle-Wittenberg, 06120 Halle (Saale), Germany
[e] Limnological Research Station, Bayreuth Center for Ecology and Environmental Research (BayCEER), University of Bayreuth, 95440 Bayreuth, Germany
[f] Agroecology, Bayreuth Center for Ecology and Environmental Research (BayCEER), University of Bayreuth, 95440 Bayreuth, Germany
[g] Chair of Soil Science, TUM School of Life Sciences Weihenstephan, Technical University of Munich, Emil-Ramann-Str. 2, 85354 Freising, Germany
[h] Ecological Microbiology, Bayreuth Center of Ecology and Environmental Research (BayCEER), University of Bayreuth, 95448 Bayreuth, Germany

HIGHLIGHTS

- Pedologic changes with long-term paddy use alter redox chemistry after flooding.
- Arsenic (As) mobility decreases with increasing paddy soil age.
- Increasing microbial activity and organic C promote As methylation in older paddies.
- Long-term paddy use limits As thiolation due to high dissolved Fe and organic C.
- Methylthioarsenates formed in all soils across the studied chronosequence.

GRAPHICAL ABSTRACT

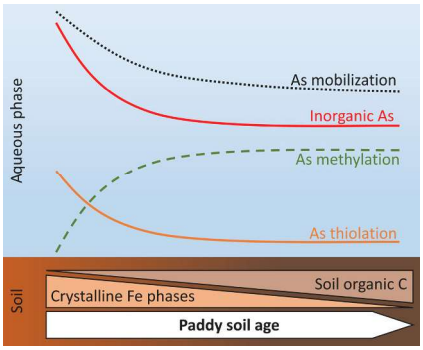

ARTICLE INFO

Editor: Filip M.G. Tack

Keywords:
Methylation
Thiolation
Soil development
Redox chemistry
Rice

ABSTRACT

Rice accumulates arsenic (As) when cultivated under flooded conditions in paddy soils threatening rice yield or its safety for human consumption, depending on As speciation. During long-term paddy use, repeated redox cycles systematically alter soil biogeochemistry and microbiology. In the present study, incubation experiments from a 2000-year-old paddy soil chronosequence revealed that As mobilization and speciation also change with paddy soil age. Younger paddies (≤100 years) showed the highest total As mobilization, with speciation dominated by carcinogenic inorganic oxyarsenic species and highly mobile inorganic thioarsenates. Inorganic thioarsenates formed by a high availability of reduced sulfur (S) due to low concentrations of reducible iron (Fe) and soil organic carbon (SOC). Long-term paddy use (>100 years) resulted in higher microbial activity and SOC, increasing the share of phytotoxic methylated As. Methylated oxyarsenic species are precursors for cytotoxic

* Corresponding author.
E-mail address: b.planer-friedrich@uni-bayreuth.de (B. Planer-Friedrich).

https://doi.org/10.1016/j.scitotenv.2023.168351
Received 13 September 2023; Received in revised form 3 November 2023; Accepted 3 November 2023
Available online 6 November 2023

methylated thioarsenates. Methylated thioarsenates formed in soils of all ages being limited either by the availability of methylated As in young soils or that of reduced-S in older ones. The present study shows that via a linkage of As to the biogeochemistry of Fe, S, and C, paddy soil age can influence the kind and the extent of threat that As poses for rice cultivation.

1. Introduction

Rice is traditionally cultivated under flooded conditions which cause porewater oxygen-depletion by microbial respiration, directly affecting the biogeochemistry and microbiology of paddy soils (Kögel-Knabner et al., 2010). Oxygen depletion triggers arsenic (As) mobilization through reductive dissolution of As-bearing iron (Fe) minerals, mainly as the inorganic species arsenate (Smedley and Kinniburgh, 2002) (Fig. 1), or through direct arsenate reduction to arsenite on mineral surfaces (Zobrist et al., 2000). Both arsenate and arsenite are class I carcinogens (Stone, 2008), and especially the latter can be taken up by rice plants and accumulate in rice grains, making rice consumption one of the main dietary sources of As (Zobrist et al., 2000; Ma et al., 2008; Meharg and Hartley-Whitaker, 2002; Zavala et al., 2008). Although arsenite and arsenate typically dominate porewater speciation in paddy soils, arsenite can also be biotically transformed into the oxymethylated As species monomethylarsenate (MMA) and dimethylarsenate (DMA). Arsenic can be methylated in paddy soils by microbes with an active expression of arsenite S-adenosylmethionine methyltransferase genes (*arsM*) (Lomax et al., 2012; Qin et al., 2006), likely as detoxification mechanism or as antibiotic reaction against other microbial groups (Chen et al., 2019a; Viacava et al., 2020; Chen and Rosen, 2020). Chen et al. (2019b) suggested that sulfate-reducing bacteria (SRB) contribute to As methylation and methylotrophic methanogens to As demethylation, while other authors found no contribution of SRB, but fermenting bacteria to methylate As (Reid et al., 2017). The main reasons for As methylation and the communities ruling (de)methylation in paddy soils thus remain controversial. Dimethylarsenate has a strong phytotoxic effect on rice plants and has been associated to causing straight-head disease (Zheng et al., 2013) and, due to its high root-grain translocation, DMA can dominate As speciation in rice grains (Zhao et al., 2013a). However, DMA shows lower toxicity for humans than inorganic As and is thus not regulated in rice products (Zheng et al., 2013; Jia et al., 2013a; Planer-Friedrich et al., 2022). Since As speciation determines its mobility, uptake, translocation, and accumulation in rice plants as well as its toxicity, great efforts have been made to understand the dynamics of these four major oxyarsenic species (OxyAs) in paddy soil porewater, their association to soil minerals, rice plants, and rice grains (Zobrist et al., 2000; Ma et al., 2008; Zavala et al., 2008; Raab et al., 2007).

In the presence of reduced sulfur (e.g., through dissimilatory sulfate reduction, DSR, carried out by SRB) (Stauder et al., 2005), both inorganic and oxymethylated As species can be abiotically thiolated to form inorganic and methylated thioarsenates, respectively. Inorganic thiolation is favored in systems with neutral to alkaline pH where arsenite reacts with S^{-II} or S^0 in consecutive steps to form mono-, di-, or trithioarsenate (MTA, DTA, and TTA, respectively), depending on the S/As ratio (Wallschläger and Stadey, 2007). Methylthiolation requires the oxymethylarsenates, MMA or DMA, as precursors. Consecutive nucleophilic reactions with S^{-II} in acidic to neutral pH lead to formation of mono- or dithiolated species (monomethylmonothioarsenate, MMMTA; monomethyldithioarsenate, MMDTA; dimethylmonothioarsenate, DMMTA; and dimethyldithioarsenate, DMDTA) (Conklin et al., 2008; Wallschläger and London, 2008). Thioarsenates have recently been identified in paddy soils (Wang et al., 2020), rice plants (Kerl et al., 2019), and rice products (Colina Blanco et al., 2021) since traditional sampling and analytical methods mask them as their respective oxyarsenic analogues (Planer-Friedrich et al., 2022). Especially

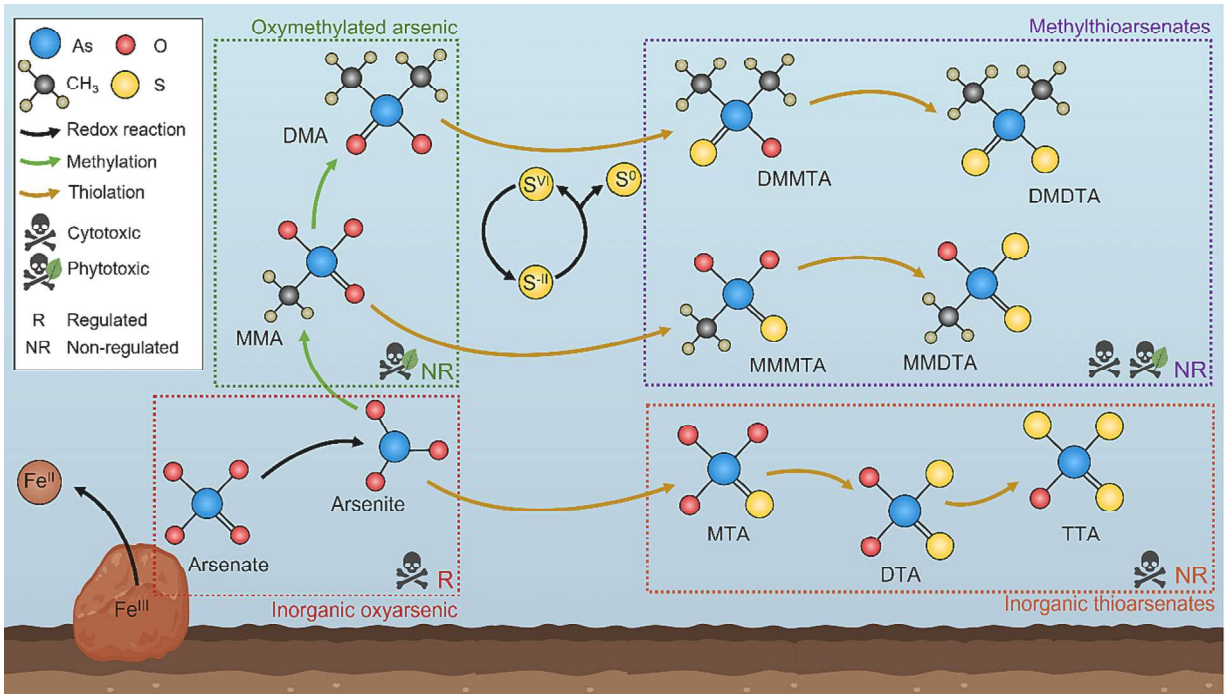

Fig. 1. Formation of the As species discussed in the present study, through reduction, methylation, and thiolation; they are grouped into the four categories discussed here: Inorganic oxyarsenic species, inorganic thioarsenates, oxymethylated arsenic species, and methylthioarsenates. R: regulated under food guidelines, NR: non-regulated. For simplicity of the depiction, charges, oxidation states, and possible protonation of O have been omitted.

dimethylated thioarsenates represent a hidden risk because their toxicity is similar to or even higher than that of arsenite for rice plants and mammalian cells (Planer-Friedrich et al., 2022; Naranmandura et al., 2011; Moe et al., 2016; Pischke et al., 2022).

Besides seasonal effects on As speciation through decreases in the redox potential, chronosequence studies have confirmed that repeated flooding and draining of paddy soils triggers a characteristic and unique long-term soil development (Kölbl et al., 2014). The duration of use as paddy soils (paddy soil "age") leads to continuous changes in pedogenic properties (Kölbl et al., 2014; Huang et al., 2015), including accumulation of organic carbon in the topsoil, increased formation of amorphous Fe phases, decreases in soil pH, and adaptation of microbial communities with increased activity (Roth et al., 2011; Cheng et al., 2009; Wissing et al., 2011; Kalbitz et al., 2013; Wu et al., 2023). We hypothesize that these long-term biogeochemical changes also affect As mobilization and speciation and thus, paddy soil age can influence the kind and the extent of threat that As poses for rice cultivation.

For the present study, four topsoils of an intensively studied 2000-year-old chronosequence representing paddy soils (P) of 50, 100, 300, and 2000 years of paddy use were selected. The use of a chronosequence with a limited number of samples could carry constraints regarding representativity and potential additional effects aside from age which cannot be fully excluded, especially with a chronosequence which spans 2000 years. However, based on the results of numerous previous studies (Kölbl et al., 2014; Cheng et al., 2009; Wissing et al., 2011; Kalbitz et al., 2013; Wissing et al., 2014), we consider our selected soils as representative for changes that are caused primarily by typical paddy soil aging. The selected soils were incubated and time-resolved sampling after 1, 3, 5, 7, 10, and 35 days helped unravel changes in abiotic and biotic reaction kinetics of different redox-sensitive elements and their influence on the overall As availability and speciation in each soil and translate this to characteristic age-dependent biogeochemical trends.

2. Materials and methods

2.1. Short description of the chronosequence

The soils used for this study come from the coastal paddy cultivation area around Cixi in the province of Zhejiang, China, located in the delta of the Yangtze River (30°10′N, 121°14′E). There, land reclamation has taken place since approximately 2000 years by river sediment deposition and by the building of dikes, allowing the transformation of coastal marshlands to agricultural fields. The construction records of these structures allow the estimation of the age of arable land and paddy soils. Details on the sampling campaign carried out in 2008 are given by Cheng et al. (2009) and Kölbl et al. (2014). In this study, we used the ≤2 mm soil fraction of the Alp horizon of the main sites of the paddy soils (P) with 50, 100, 300, and 2000 years of rice cultivation. The soils were air-dried and stored in the dark until use for the present study. Dry storage might raise concerns regarding loss of sample representativity and potential of re-activating representative microbial communities upon incubation. However, longer dry periods are part of the characteristic conditions in paddy fields and previous research has shown that intermittent flooding of paddy soils makes their microbial communities particularly resistant to long periods of desiccation (Conrad, 2020). Similarly, although changes in the oxidation state of organic compounds might have occurred during storage, the same processes that allow the accumulation of SOC with long-term paddy use (Wissing et al., 2011; Wissing et al., 2014) likely protect the carbon pool in the stored samples from excessive degradation.

2.2. Incubation experiments

Anaerobic incubations were carried out using the above-described soils. In triplicate, 10 g of soil and 20 mL of N_2-purged tap water were added to 120 mL serum vials inside an anaerobic chamber (95 % N_2, 5 % H_2, COY). The vials were sealed with butyl rubber stoppers and aluminum caps, mixed manually, and left standing in an incubator at 30 °C until sampling. Sacrificial triplicates were taken at 1, 3, 5, 7, 10, and 35 days of incubation. Similar time spans have been used before to study As speciation dynamics (Chen et al., 2019b; Chen et al., 2022).

For sampling, the corresponding vials were taken out of the incubator, shaken, and allowed to reach room temperature before measuring the gas pressure inside the vial using a handheld pressure-meter (Greisinger GMH, 3100 Series). With a gas-tight syringe and a needle, 5 mL of headspace was taken from each vial, injected into an evacuated 5 mL glass vial (approx. -500 mbar), and stored in the dark until quantification of CH_4 and CO_2 via gas chromatography coupled to a Flame Ionization Detector (GC-FID, SRI Instruments 8610C) equipped with a methanizer.

After gas phase sampling, the vials were taken into the anaerobic chamber, shaken, and opened. The homogeneous mix of soil and aqueous phase was transferred to 50 mL centrifuge tubes. The tubes were closed and wrapped with parafilm before being centrifuged outside the glovebox (4000 rpm, 10 min) and brought back into the anaerobic chamber. The aqueous phase was separated from the soil using syringe and needle, filtered, and accordingly stabilized to carry out the analyses described in the following section. Unless stated otherwise, all aqueous phase samples were filtered through 0.2 μm acetate-cellulose syringe filters (Macherey-Nagel).

2.3. Aqueous phase analyses

To determine the total concentration of As and S in the aqueous phase, a 2 mL aliquot was stabilized with 30 μL of 9.8 M H_2O_2 and 40 μL of 8 M HNO_3, diluted, and measured by inductively coupled plasma mass spectrometry (ICP-MS, XSeries2, Thermo-Fisher) after in-cell reaction with an O_2/He mixture (10/90 %). Arsenic was determined as AsO^+ ($m/z = 91$) and S as SO^+ (m/z = 48). A reference material (TMDA 62.2, Environment Canada) was used for quality control, and rhodium (Rh) was used as internal standard to correct signal drift.

Photometric determinations of Fe (Fe_{tot}, Fe^{II}) and S^{-II} were carried out using the ferrozine method (Stookey, 1970; Hegler et al., 2008) and the methylene blue method (Cline, 1969), respectively. All samples for photometric determinations were diluted when required, carried out in triplicate, and measured using a multiplate reader (Infinite 200 PRO, TECAN).

Immediately after knowing the Fe_{tot} concentration, 700 μL aliquots were taken for As speciation and stabilized with 100 μL of a 10 mM solution of the iron complexing agent HBED (N,N′-Di(2-hydroxybenzyl) ethylenediamine-N,N′-diacetic acid monohydrochloride) in 10 % ethanol at neutral pH (adjusted using 0.1 M NaOH). In case of Fe concentrations >1 mM, a 55 mM HBED solution was used for stabilization in the same ratio. Further details on the HBED stabilization method can be found in the Supporting Information (see supplementary discussion). The samples were flash-frozen on dry ice and kept at −20 °C until analysis by ion chromatography (IC, Dionex ICS-200, with an AG/AS16 IonPac column), using a 0.1 M NaOH gradient with a flow rate of 1.2 mL min^{-1} coupled to inductively coupled plasma mass spectrometry (IC-ICP-MS) (Planer-Friedrich et al., 2007). Further details regarding the As speciation method can be found in the Supporting Information (see supplementary methods).

Dissolved organic carbon (DOC) was determined from a 2 mL aliquot filtered through a 0.45 μm polyamide syringe filter (Macherey-Nagel), stabilized with 40 μL of 6 M HCl and kept at 4 °C until analysis (Multi N/C 2100 S, Analytik Jena). An additional 2 mL aliquot for acetate determination was taken and kept frozen until analysis by HPLC-RID (Agilent 1200) with a Rezex ROA Organic Acid column (Zeibich et al., 2018). Acetate analyses were carried out for incubation days 1, 3, 5, and 10.

Redox potential and pH were measured using a multiparameter (HQ40d, Hach) with the corresponding electrodes (PHC301, Ag/AgCl

electrode, and MTC101, respectively). Electrical conductivity was measured with a conductivity meter (Winlab Data Line, Windaus) attached to an LCV 0.35/21 electrode (Meinsberger Elektroden).

2.4. Solid phase analyses

Total content of As and S in the original dry soil were determined by ICP-MS after microwave-assisted digestion (MARS Xpress, CEM) in 10 mL aqua regia. The digested samples were filtered and diluted 1:10 with ultrapure deionized water (Millipore, 18.2 MΩ cm) before analysis. Iron (III) phases were also characterized in the dry soils before the incubations using the dithionite-citrate-bicarbonate (DCB) (Mehra and Jackson, 1958) and oxalate buffer methods (McKeague and Day, 1966). Iron determination after each extraction was carried out photometrically as described above for aqueous phase Fe.

Triplicate soil samples of each incubation at 1, 3, 5, and 10 days were separated into cryovials and flash-frozen in liquid nitrogen for microbial analyses. DNA and RNA were extracted following the protocol described by Lueders et al. (2004) (described in detail in supplementary methods). The extracts were stored at −80 °C until analysis. Specific qPCR standards for each gene of interest were created from paddy soil using the In-Fusion® Snap Assembly cloning system (TaKaRa Bio Inc.) according to the manual and cloned into a pUC19 vector. Total and active bacteria were based on amplification of the respective 16S rRNA gene and transcript copy numbers in nucleic acid extracts. Total and active sulfate-reducing microbes, arsenic methylating microbes, and methanogenic microbes were approximated with respective amplification of the *dsrA* (dissimilatory sulfite reductase), *arsM* (arsenite *S*-adenosylmethyltransferase) and *mcrA* (methyl coenzyme M reductase) genes and transcripts (see supplementary methods). Gene and transcript copies were quantified with qPCR. While 16S rRNA transcripts were quantifiable, *dsrA*, *arsM,* and *mcrA* were below quantification limit. The average copy numbers were calculated from triplicate extractions.

The remaining soil from each incubation was stored frozen and later freeze-dried for the determination of zerovalent sulfur (S^0) via HPLC-UV-Vis (Lohmayer et al., 2014). Methodologically, soil-extracted S^0 in this study is operationally defined as chloroform-extractable S, which includes zerovalent S in polysulfides and S bound to solid phase, as well as S_8.

2.5. Oxymethylated As-spiked incubations

To better understand the dynamics of As (de)methylation in the chronosequence, a second batch of non-sacrificial incubations was carried out as described before. The tap water used for these incubations was amended with MMA or DMA in a 10-fold excess of the concentrations of methylated As found in the original setup. This excess was selected to have a concentration of species high enough to discern between small changes in the As speciation. Thus, P50 and P2000 were amended with 100 μg L^{-1} of MMA or DMA, while concentrations of 250 μg L^{-1} were used for P100 and P300. Samples for As speciation were taken with syringe and needle from each incubation bottle after 5, 10 and 33 days of incubation in the same conditions as the original batch. Speciation stabilization and analyses were carried out as described previously.

2.6. Statistical analyses

Mean and standard deviation were calculated for each measured variable. Principal component analyses (PCA) were carried out for the complete dataset. Pearson correlation coefficients were used to assess the significance of all variable correlations presented. All PCA and Pearson correlation analyses were carried out using the Rstudio software (R Development Core Team, 2008).

3. Results and discussion

3.1. Arsenic content and availability through the chronosequence

Incubation experiments confirmed that paddy soil age does not only cause distinct trends in solid phase biogeochemistry, such as the well documented accumulation of soil organic carbon (SOC) (Kölbl et al., 2014; Kalbitz et al., 2013) or a decrease in Fe content (Kölbl et al., 2014) (Fig. 2a), but also in aqueous phase chemistry (Fig. 2b), with general trends developing slowly during the first 300 years of paddy development but with parameters being highly distinctive from those of P2000. Principal component analyses showed that after flooding, dissolved Fe, Fe^{II}, and dissolved organic carbon (DOC) concentrations were the parameters most closely associated to paddy soil age (Fig. SI1). Flooding triggered reductive Fe^{III} mineral dissolution, releasing Fe^{II} and associated SOC (Wissing et al., 2014) into the aqueous phase (Fig. SI2). While SOC accumulation (due to fertilization with animal manure, and dry or charred crop residues (Kölbl et al., 2014)) directly translated to an increase in DOC (Fig. 2b), solid-phase Fe depletion was outcompeted by the accumulation of amorphous Fe phases (Table SI2) which are easily dissolved (Kölbl et al., 2014; Schwertmann, 1991), causing higher dissolved Fe concentrations with increasing age. These close dynamics between Fe and DOC are likely related to the stabilization of SOM due to mineral associations with amorphous Fe phases (Kölbl et al., 2014; Wissing et al., 2011; Wissing et al., 2014).

Arsenic concentrations in the aqueous phase decreased with age, particularly in P2000, similar to As concentrations in the solid phase (Fig. 2a and Table SI2). Previous studies on the chronosequence have shown a general mobilization of elements towards deeper soil layers or washout with soil drainage each cultivation season (Kölbl et al., 2014). The higher availability of reducible Fe with increasing age caused a strong decrease of the As/Fe ratio in the aqueous phase with paddy soil age (compared to the relatively stable values from the solid phase), meaning that more moles of As are released per mole of Fe in younger soils. Arsenic release was coupled to the dissolution of Fe^{III} mineral phases, with concentrations increasing over the first 10 incubation days and decreasing after 35 days (Fig. SI2), likely because of sorption to newly formed FeS phases (Xu et al., 2019; Hoffmann et al., 2013).

In the equilibrated aqueous phase (after 35 days), As concentrations decreased with age (Fig. SI2). This could be related to As in older paddies being associated with remaining Fe crystalline phases which are not so readily accessible for reductive dissolution. In this sense, although As concentrations in the solid phase showed only a relatively small overall decrease with increasing age, As mobilization decreased with increasing paddy soil age.

3.2. Highly toxic and mobile inorganic As dominates early stages of paddy development

The high As mobilization in younger paddies is a source of concern since As can become bioavailable for plant uptake and eventually accumulate in rice grains. For all soils and incubation times, arsenic speciation was dominated by inorganic species. Their contribution to the sum of species largely varied between 91 % (P50, day 5) and 48 % (P2000, day 7), overall being higher in younger paddies (Fig. SI3). Inorganic oxyAs, and especially arsenate had a higher proportion, but arsenite was found in all soils at all incubation times, together with up to 9 % of inorganic thioarsenates (P50, day 3). Using day 35 as a representative equilibrated system, inorganic As contribution decreased strongly with age (Fig. 3a), while the contribution of inorganic thioarsenates additionally decreased with incubation time (Fig. SI4).

While the accumulation of inorganic oxyAs was mostly caused by the absence of biotic methylation (the second most dominant group of As species, see Section 3.3), the formation of inorganic thioarsenates was regulated by geochemical factors in the aqueous phase that are strongly affected by paddy soil age.

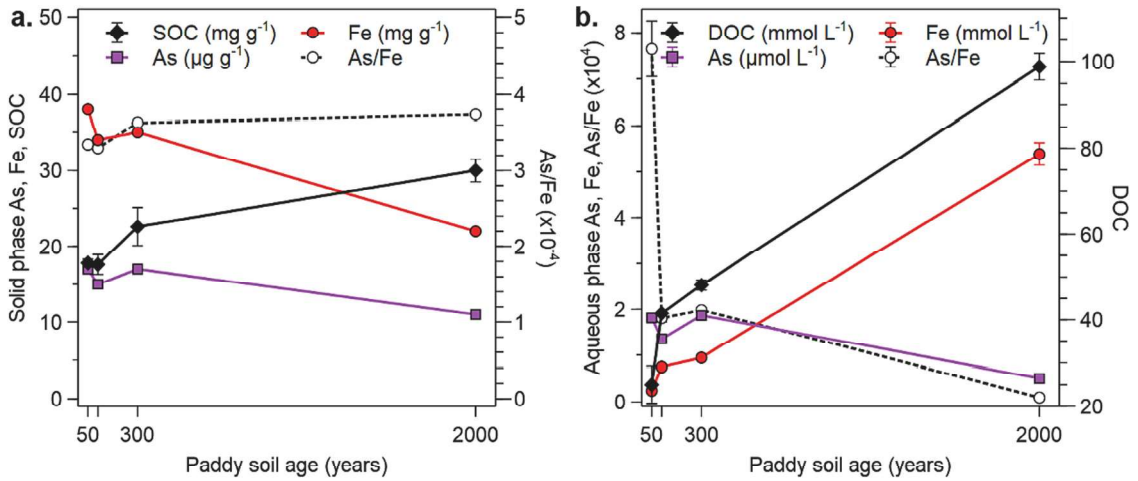

Fig. 2. Differences in solid and aqueous phase As, Fe and C in the chronosequence. Soil content (a) and aqueous phase after 7 days of flooding (time selected to reflect peak of Fe release) (b). Data for SOC and soil Fe content are taken from Kölbl et al. (2014) for a main site and two subsites (mean values ± standard error). For DOC, As, and aqueous Fe data points represent mean values, while error bars represent the standard deviation ($n = 3$).

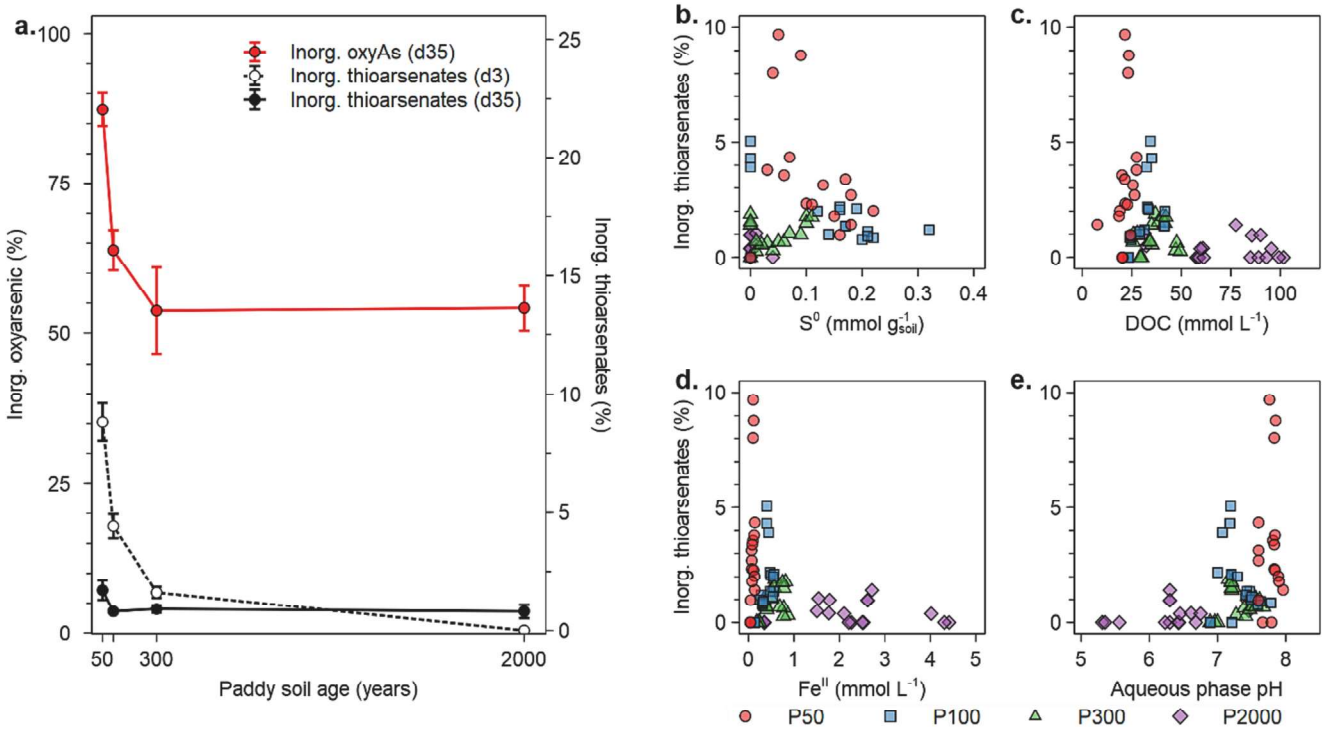

Fig. 3. Effect of paddy soil evolution on inorganic As species. Decrease of inorganic As species with increasing age (a) and effects of different biogeochemical factors on inorganic thioarsenate formation: Accumulation of S^0 in the soil (b), DOC (c), Fe^{II} (d), and pH (e). Data points on (a) represent mean values while error bars represent the standard deviation ($n = 3$).

Inorganic thioarsenate formation requires reduced sulfur, with dissimilatory sulfate reduction being its main source in paddy soil porewater (Sethunathan et al., 1982; Wind and Conrad, 1995). Free S^{-II} was not detected in the aqueous phase of any incubation setup, but total S concentration decreased with incubation time (Fig. SI5), indicating precipitation of sulfide phases. Although observed in paddy soils of all ages, the start of DSR showed a delay with increasing age. In younger soils, it started as early as day 3 (P50), and in the older ones, as late as day 5 (P2000). This delay is likely due to the higher availability of reducible Fe^{III} (as seen in Fig. SI2) in older paddies, since Fe^{III} reduction has a higher energy yield and is thermodynamically preferred to S reduction (Snoeyink and Jenkins, 1980). Inorganic thioarsenates were detected in P2000 after day 5, coinciding with the start of DSR in this soil (Fig. SI4).

Sulfate reduction was also assessed as the accumulation of S^0 in the soils after incubation, with younger paddies showing higher accumulation compared to older paddies (Fig. SI6). Although S^0 has been previously reported as the best proxy for the formation of thioarsenates in paddy soil porewater (Wang et al., 2020), no direct correlation between its accumulation and inorganic thioarsenate formation was found (Fig. 3b). Our results suggest that the higher availability of SOC and reduced Fe in the aqueous phase with increasing paddy soil age scavenged reduced sulfur for thiolation of organic matter (Spratt Jr and Morgan, 1990) or precipitation of FeS phases (Xu et al., 2019),

decreasing its availability for As thiolation. The quick and early formation of inorganic thioarsenates could be related to a peak in the availability of reduced sulfur during a phase of strong DSR before it was scavenged by the major release of Fe^{II} into the aqueous phase taking place by day 5 or 7, depending on the soil, or due to the absence of more favorable substrates for thiolation (see Section 3.3).

Supporting these observations, contributions to the sum of species > 2 % of inorganic thioarsenates were only observed under incubation conditions that had DOC concentrations <50 mmol L^{-1} and dissolved Fe^{II} concentrations <1 mmol L^{-1} (Fig. 3c and d, respectively). Our PCA (Fig. SI1) also showed how formation of inorganic thioarsenates was negatively correlated to paddy soil age, DOC, and dissolved Fe. Another environmental factor that has been reported to strongly control inorganic thiolation is pH with more alkaline pH causing higher inorganic thiolation (Stauder et al., 2005). Contributions >2 % of inorganic thioarsenates were observed for aqueous phase pH values above 7 (Fig. 3e). The accumulation of organic carbon, as well as the washout of carbonates with increasing soil age, generally decrease soil and porewater pH under paddy management (Kölbl et al., 2014), allowing inorganic As thiolation in younger paddies with more circumneutral pH values.

Our results suggest that the high availability of inorganic As species (including thioarsenates) in young paddy soils could represent a higher risk for the consumption of rice products coming from fields that have been under paddy use for 100 years or less. Additionally, paddy soil evolution hampers the formation of inorganic thioarsenates, which form preferentially in young paddies with lower dissolved Fe and SOC contents.

3.3. Higher As methylation in mature paddies

Arsenic methylation showed a sharp increase in the first 300 years of paddy evolution (Fig. 4a). After 35 days of incubation, the contribution

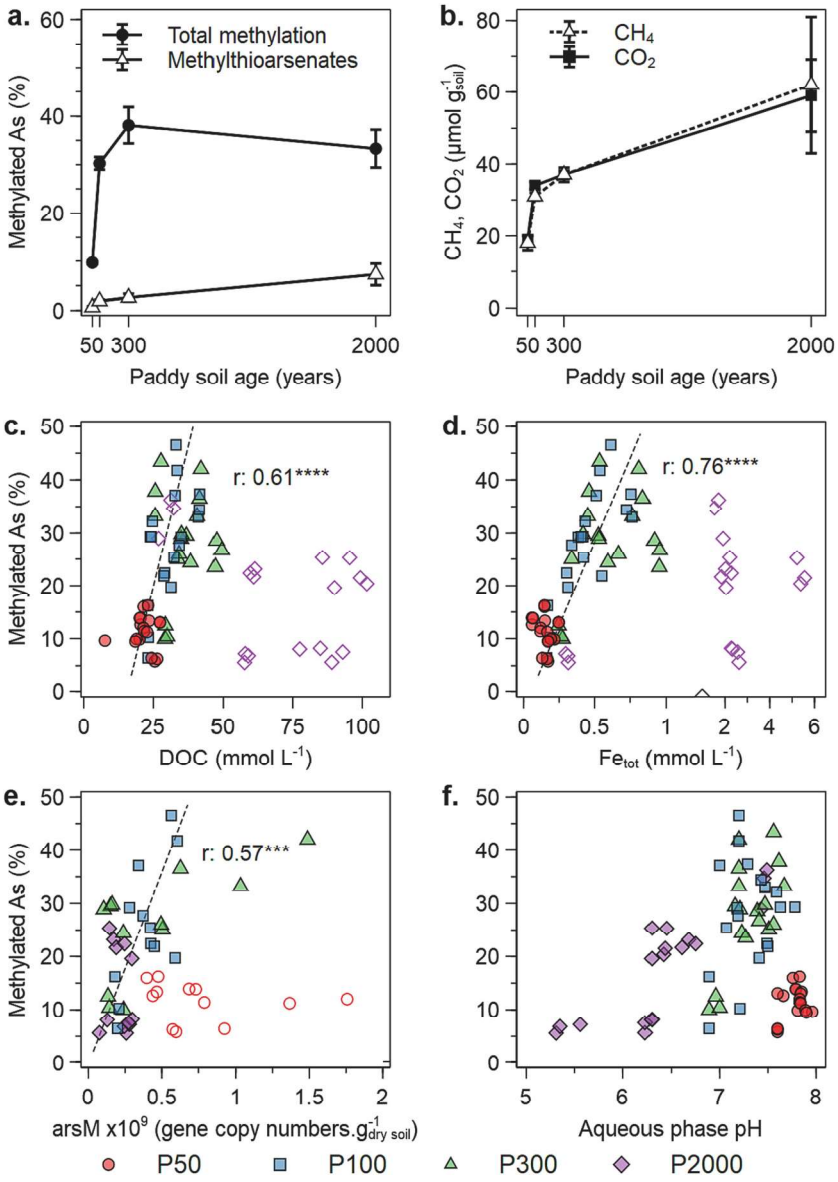

Fig. 4. Effect of paddy soil evolution on As methylation. Contribution of methylated As species (including MMA, DMA, MMMTA, MMDTA, DMMTA, and DMDTA) to the sum of species in different soils after 35 days of incubation (a). Increased CO_2 and CH_4 release with paddy soil age by day 35 of incubation (b). Data points on (a) and (b) represent mean values while error bars represent the standard deviation ($n = 3$). Parameters that are related to As methylation: DOC (c), Fe (d), *arsM* gene copy numbers (e), and aqueous phase pH (f). Empty symbols indicate data not taken for Pearson correlation in the case of P2000 (c, d) due to an unidentified limitation in methylation and for P50 (f) because of low methylation potential. Asterisks indicate the Pearson significance levels (p): *** = $p < 0.001$; **** = $p < 0.0001$. For (c), (d) and (f), $n = 54$, while for (e), $n = 36$.

of methylated As (which includes oxymethylated species and their thiolated analogs) to the sum of species increased from 9.6 ± 0.3 % in P50 to 38 ± 4 % in P300. These values represent the net effect of formation and consumption (i.e., de-methylation) carried out simultaneously by different microbial communities which drive contribution of methylated species to the aqueous phase speciation (Fig. SI7).

The increase of the methylation potential with paddy soil age can be explained together with other biogeochemical parameters that showed similar trends. The general potential for microbial activity and respiration in the paddy soils strongly increased during the first 300 years (Fig. SI8a and b), likely due to the accumulation of bioavailable organic substrates and, as reported before for the chronosequence, increases in the microbial biomass, alongside the establishment of specific microbial communities (Kölbl et al., 2014; Wang et al., 2015a; Ho et al., 2011; Bannert et al., 2011). Additionally, DOC release and efficient microbial consumption caused increased CO_2 and CH_4 production with soil age (Fig. 4b). On all sampling days, older soils showed a higher CO_2 production than younger ones (Fig. SI8b). In the case of CH_4, its production was strongly delayed in older soils. While younger soils showed between 0.08 and 0.29 % of their final CH_4 production after 3 days of incubation, P2000 produced only around 0.005 % of its final value, being the lowest CH_4 producer up to day 7 (Fig. SI8c). This delayed CH_4 production was again likely related to the high amount of reducible Fe^{III} in the system with increasing age, which has been reported to suppress methanogenesis (van Bodegom et al., 2004), possible competition with other microbial groups (Lovley and Phillips, 1987), or due to the low energy yield of methanogenesis (Snoeyink and Jenkins, 1980). This delay is also represented by a slower decrease of the redox potential in P2000 when compared to younger soils (Fig. SI9). Nonetheless, the high accumulation of organic C and likely a well-adapted methanogenic community (Conrad, 2020) made P2000 the highest CH_4 producer after 35 days of incubation.

Arsenic methylation in P50, P100, and P300 showed positive Pearson correlations with DOC ($r = 0.61$, $p < 0.0001$) and aqueous phase Fe ($r = 0.76$, $p < 0.0001$) (Fig. 4c and d, respectively), suggesting a higher abundance of organic substrates for microbial activity from the reductive dissolution of amorphous Fe phases. A similar correlation of high methylation and DOC has been reported before (Zhao et al., 2013b), and other studies have seen an increase in As methylation in organic matter-amended treatments (Jia et al., 2013b; Yang et al., 2018). The oldest paddy soil, P2000, showed lower methylation values than expected if assuming a continuously increasing trend from P50 over P100 and P300. The aforementioned three soils had aqueous phase As concentrations of around 2 μmol L^{-1}, compared to 0.5 μmol L^{-1} in P2000 (Fig. SI2). P2000 also showed generally lower *arsM* copy numbers than the other soils, especially when normalized to 16S rRNA (Fig. SI10 a and b), suggesting that microbes in this soil are less prone to methylation. This lower methylation potential could be related to several factors. On the one side, the lower As concentrations in porewater when compared to younger paddies could mean that detoxification mechanisms are not needed in P2000 as much as they would be in younger paddies. Similarly, it could also mean that the use of methylated As species as an antibiotic is less efficient in P2000 due to a lack of porewater As. On the other hand, Conrad (2020) has also suggested that frequently drained soil environments show less population changes than permanently flooded ones. Long-term paddy use could result in a stable microbial community where warfare could be less necessary or methylated As could be less effective. Lastly, it has been shown that in systems with high availability of labile organic C like P2000, Carbon Catabolite Repression takes place, meaning a down-regulation of catabolic enzymes such as the aquaglyceroporin channel (GlpF). The down-regulation of this specific channel, which can also uptake arsenite, could affect the uptake of As into the cells and thus, indirectly, decrease the methylation potential in soils with particularly high SOC (Yoon et al., 2022).

While strong de-methylation due to high methanogenic activity could also be an option (Chen et al., 2019b) (decreasing the net methylated As in P2000), incubation experiments with spiked MMA and DMA showed that P2000 had the lowest demethylating capacity of all soils with up to 50 % of the MMA spike remaining as methylated species after 5 days, compared to 18 % of the same spike in P50 (Fig. SI11). These observations only highlight the difficulties of assessing (de)methylation dynamics. Having in mind the different possibilities and the still open questions regarding As methylation dynamics in paddy soils in general, it is particularly difficult to determine which exact changes in microbial dynamics are affecting the methylation capacity in P2000.

Although higher *arsM* abundances were found with higher aqueous phase As concentrations (Fig. SI10a), a significant correlation between *arsM* gene counts and methylated As ($r = 0.57$, $p < 0.001$) was only found when excluding P50 (Fig. 4e). It has been observed that although there may be more methylating microbes in soils with higher pH values, their activity is higher at lower pH (Zhao et al., 2013b). This pH dependency was observed in P50, which had higher pH values (Fig. 4f) and *arsM* copy numbers but showed lower methylation potential. The *arsM* copy numbers and soil pH decreased with age, while the contribution of methylated As to As speciation increased. Additional observations related to possible changes of microbial communities responsible for As methylation (from SRB-driven to fermenter-driven) with increasing paddy soil age are discussed in the supplementary discussion. Throughout all incubations and for all soils, monomethylated species had higher contributions to the sum of species than dimethylated ones. It is not clear if this difference from field observations (where dimethylated species usually dominate the share of methylated species), is an artifact of our incubation experiments. Such dominance of monomethylated species has been previously observed and attributed to different microbial capacities and the activity of different enzyme systems carrying out the first or second methylation steps (Wang et al., 2015b; Wang et al., 2014; Chen and Rosen, 2023). A recent study by Qiao et al. (2023) also identified a predominance of MMA over DMA in paddy soil extracts.

Furthermore, once formed, oxymethylated As (MMA and DMA) can lead to the formation of methylthioarsenates through their abiotic reaction with S^{-II}. Methylthioarsenates were detected in all soils at all incubation times except for P2000, where they were only found after 5 days of incubation (in the same way as the delayed formation of inorganic thioarsenates related to the delay in DSR) (Fig. SI12). According to our data, as soon as oxymethylated As species are formed, they are readily thiolated when reduced sulfur is available in the system. Additionally, in most soils, oxymethylated species continued to be thiolated even when there was no more inorganic thiolation, especially in P100 (Figs. SI4 and SI12). This suggests that in paddy soil porewater, the formation of methylthioarsenates is preferred over their inorganic homologs. The enhanced thiolation of methylated As species could be related to the pH conditions in paddy soil porewater, where acidic to neutral pH are more prevalent than the alkaline conditions that allow the thiolation of inorganic oxyAs. This preferential thiolation was also confirmed by the spiked incubations, particularly for those spiked with DMA where (even with a 10-fold excess compared to non-spiked concentrations), up to 98 % of the present DMA was thiolated compared to only up to 22 % of inorganic As being present as thioarsenates (Fig. S13).

Methylthioarsenates contribution to As speciation through paddy soil age (Fig. S14a) behaved similarly to inorganic thioarsenates in the short term (3 days of incubation), decreasing strongly with age (with the exception of P50, where there was low availability of oxymethylated precursors). The same factors decreasing the availability of reduced sulfur for the formation of inorganic thioarsenates with increasing age would also affect the formation of methylthioarsenates. Interestingly, the contribution of methylthioarsenates to As speciation after 35 days of incubation was very similar to that of oxymethylated As. This means that in the early stages of incubation, the formation of methylthioarsenates is limited by the availability of MMA or DMA as precursors, but as soon as oxymethylated species become available, their formation is limited only

by the availability of reduced sulfur.

The contribution of methylthioarsenates to speciation with respect to oxymethylated As can be seen in Fig. SI14b. A few data points of P50, P100, and P300 are over the 1:1 line which indicates that methylthiolated species had higher contributions than the oxymethylated ones in these paddies. These points correspond to early incubation days with relatively low methylation, but high availability of reduced sulfur, while older paddies (and later incubation times) with higher levels of methylation and limited availability of reduced sulfur for thiolation fell under the 1:1 line.

Interestingly, P2000 showed a low but constant formation of methylated and inorganic thioarsenates even by day 35 (Figs. SI4 and SI12). It has been suggested that the presence of a cryptic S-cycle constantly supplies small amounts of reduced sulfur to the system for constant As thiolation and is related to the reduction of Fe^{III} oxyhydroxides (Wang et al., 2020; Wind and Conrad, 1997). More specifically, the cryptic-S cycle involves sulfide re-oxidation to S^0 coupled to the reduction of Fe^{III} (oxy)hydroxides, forming mixed $Fe^{II}Fe^{III}$ minerals, pyrite, and release Fe^{II} into the porewater (Saalfield and Bostick, 2009). The high availability of amorphous Fe^{III} phases increasing with age could provide a sort of "S battery" for later As thiolation, especially in very old soils like P2000, where these phases are most abundant. Supporting this idea, a slight accumulation of S^0 in the long term took place in P2000 after 35 days of incubation.

In summary, although in early stages of incubation, younger paddies showed a higher share of methylthioarsenates with respect to their oxymethylated counterparts, older paddies offer a larger potential for methylthiolation in the long-term. Furthermore, our observations show that as soils age and As is methylated, methylthioarsenates will definitely contribute to the As speciation, to an extent depending on the environmental factors governing the availability of reduced S. This represents not only a risk for plant yield through the phytotoxicity of DMA, but also a potential risk for human consumption from DMMTA and DMDTA formation.

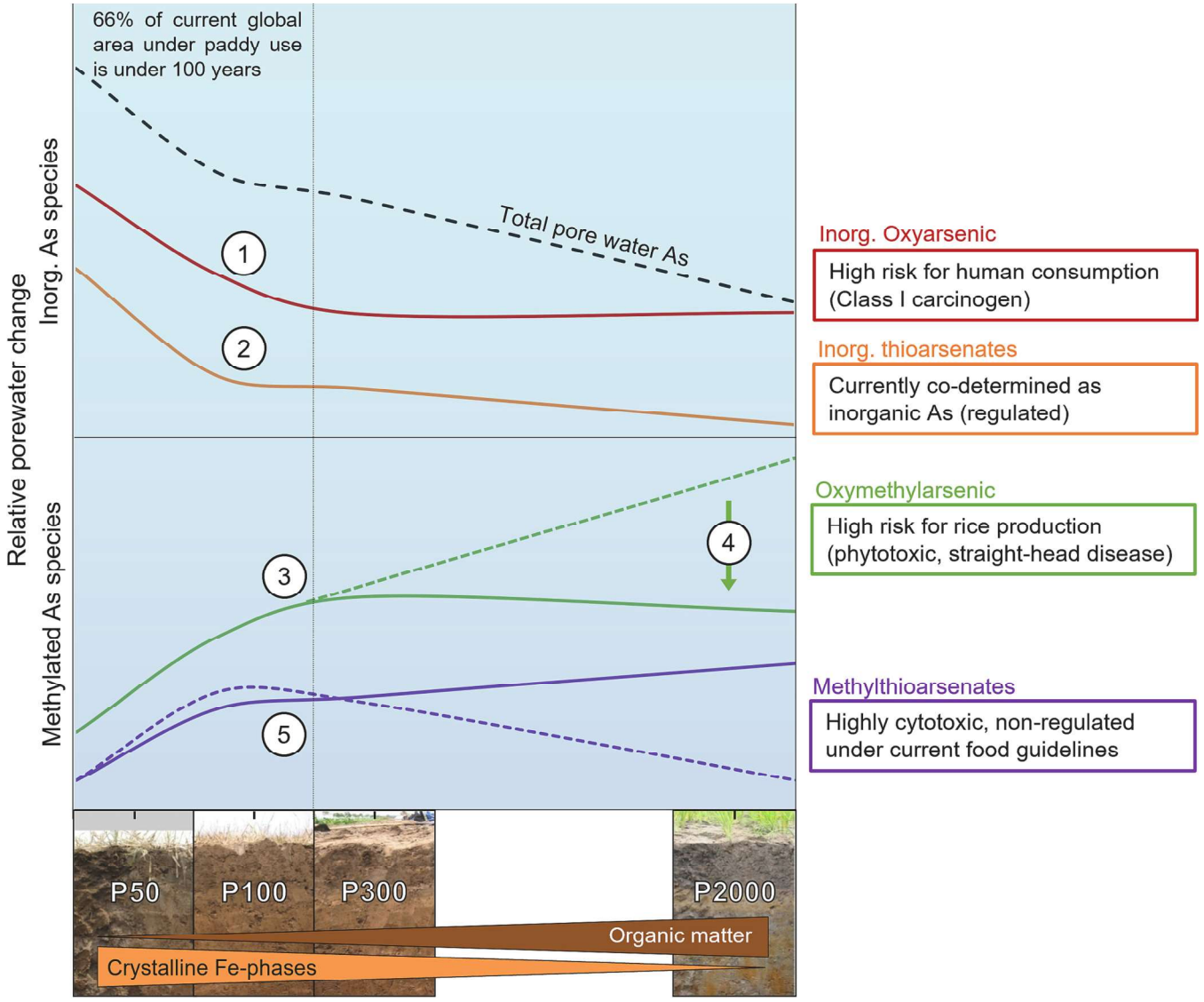

Fig. 5. Conceptual model representing the relative change in the contribution of inorganic (top) and organic (bottom) As species to aqueous phase speciation with increasing paddy soil age, together with challenges associated to each group (right). Total aqueous phase As is represented as a dashed black line for reference. Numbers represent: (1) Decrease in inorganic oxyAs. (2) Decrease in inorganic thiolation due to accumulation of SOM and amorphous Fe minerals. (3) Increased methylation with the accumulation of SOM and increased microbial activity. (4) Decrease in measured methylated species with respect to the expected value (dashed line) due to an unidentified limitation on methylation. (5) Transitioning soils between young and mature, showing high potential for the formation of methylthioarsenates, being limited by the availability of reduced sulfur (dashed line) or methylated As (solid line). Pictures from soil profiles show the upper 50 cm (taken and modified from Kalbitz et al. (2013)).

4. Conclusions

Our study presents, to the best of our knowledge, the first linkages between paddy soil age and As speciation. Although the paddy soils of the chronosequence used in this work originate from coastal marshlands (Cheng et al., 2009) and the extent or rates to which paddy soil evolution affects As speciation might change according to the parent material, environmental conditions or number of harvests per year, general processes described here should be transferable to other paddy soils of different origins (Winkler et al., 2016). Following up on the age-related effects on As biogeochemistry observed in the present chronosequence, further chronosequence studies should be carried out to evaluate the extent to which these observations are transferable to other soil types and different age spans.

For our chronosequence, the high As availability in porewater of young soils (≤ 100 years), dominated by inorganic oxyAs species, suggests that these soils have an increased risk for high inorganic As concentrations in porewater (Fig. 5, process 1). If porewater As speciation directly links to speciation in rice grains, cultivation on these younger soils could pose a higher risk for the consumption of the respective rice products. Currently, worldwide, 118 million ha are estimated to be under paddy use, with around 66 % of these soils being younger than 100 years (Klein Goldewijk et al., 2017). Based on the results from our study, there could also be a high potential for inorganic thiolation in such soils. Although currently co-determined in rice grains as inorganic As (and thus, regulated), inorganic thioarsenates (particularly MTA, the dominant inorganic thioarsenate species during most of our experiments) show lower adsorption to Fe minerals than inorganic oxyarsenic species, increasing As mobility (Couture et al., 2013; Suess and Planer-Friedrich, 2012). In the context of rice cultivation, MTA shows lower uptake but higher root-to-shoot translocation in rice plants, which translates into a higher contribution to inorganic As enrichment in rice grains (Kerl et al., 2019; Kerl et al., 2018). Our data suggests that as paddy soil development takes place, the geochemical changes in the soil decrease the potential for As thiolation (Fig. 5, process 2).

Regarding methylation, we found correlation with biogeochemical parameters related to paddy soil age. However, from a microbiological perspective, formation and consumption of methylated As species is not completely clear, yet. Here, we showed how long-term paddy use enhances As methylation mainly due to the accumulation of organic matter, increased microbial activity, and decreasing soil pH (Fig. 5, process 3). Furthermore, older paddies with lower As mobilization could also have a lower methylating capacity related to lower *arsM* expression or other unidentified limitations (Fig. 5, process 4). Moreover, older paddies produced higher greenhouse gas emissions due to their higher microbial activity, including that of methanogens. Our results show that as soon as methylation takes place and reduced sulfur is available in the system, methylthioarsenates will form. Particularly in early stages of soil evolution (>50 years) there is enough availability of methylated As and reduced S to make methylthioarsenate species contribution highly relevant in the paddy soil porewater (up to ca. 20 % for P100 at day 7) (Fig. 5, process 5). Methylthiolated As species should not only be considered an issue in young paddies transitioning to mature ones but also in old ones where they were present and increasing after 35 incubation days, likely associated to cryptic S-cycling.

Observations from the present laboratory study certainly need to be verified in the field, either with the present chronosequence, others of its kind with different parent material, or in soils where the time of rice cultivation is known. Field studies will help to understand how the age-related dynamics presented here change in systems with plant-soil interactions and in the context of a cropping season, as well as how the changes in aqueous phase As speciation observed here translate into As accumulation in rice grains. Looking at the bigger picture, these observations could help decide which agricultural practices or rice varieties to use at different sites to mitigate the most prominent risk factors for each soil age group. For example, a mature soil in which high contents of methylated species are found will profit from a rice variety with a lower yield but higher resistance to straight-head disease (Yan et al., 2005). Similarly, rice straw can be removed from these soils to limit the methylation potential or greenhouse gas emissions, as well as applying intermittent flooding, which has been reported to decrease As accumulation in grain and CH_4 production (Liu et al., 2021; Somenahally et al., 2011). Likewise, younger paddies could profit from a higher addition of rice straw or other forms of organic matter to enhance the methylation potential, according to previous observations (Jia et al., 2013b; Yang et al., 2018). Overall, paddy soil age is a factor that requires more attention in future studies, as it has the potential to influence the kind and the extent of threat that As poses for rice cultivation.

CRediT authorship contribution statement

José M. León Ninin: Conceptualization, Methodology, Software, Validation, Formal analysis, Data curation, Writing – Original draft, Visualization. **E. Marie Muehe:** Methodology, Validation, Resources. **Angelika Kölbl:** Resources. **Alejandra Higa Mori:** Investigation. **Alan Nicol:** Methodology, Software, Validation, Investigation, Data curation. **Ben Gilfedder:** Resources. **Johanna Pausch:** Resources. **Livia Urbanski:** Resources. **Tillman Lueders:** Resources. **Britta Planer-Friedrich:** Conceptualization, Methodology, Resources, Supervision, Project administration, Funding acquisition, Writing – Original draft. **All co-authors contributed to Writing - Reviewing and Editing**.

Declaration of competing interest

The authors declare the following financial interests/personal relationships which may be considered as potential competing interests:

Jose M. Leon Ninin reports financial support was provided by the German Academic Scholarship Foundation. Britta Planer-Friedrich reports financial support was provided by the Federal Ministry of Education and Research.

Data availability

The data generated and analyzed for the current study are also available from the corresponding author on reasonable request.

Acknowledgements

We acknowledge financial support for J.M.L.N. from the German Academic Scholarship Foundation in the form of doctoral funding and funding within the Federal Ministry of Education and Research project BMBF #031B0840 to B.P.-F. We thank Asel Traut for her help with the early laboratory work, Paul Richter for carrying out the qPCR analyses, Anita Gößner for the help with HPLC analyses, and Dr. Carolin Kerl and Philipp Knobloch for their assistance with plotting and statistics. Fig. 1 was created using Biorender.

Appendix A. Supplementary data

Further details on materials and methods (As speciation; DNA and RNA extraction and quantification). Biogeochemical and microbial data supporting the above-described observations and discussion. Additional discussion regarding HBED stabilization method and changes in microbial communities involved in As methylation. Supplementary data to this article can be found online at doi:https://doi.org/10.1016/j.scitotenv.2023.168351.

References

Bannert, A., et al., 2011. Changes in diversity and functional gene abundances of microbial communities involved in nitrogen fixation, nitrification, and denitrification in a tidal wetland versus paddy soils cultivated for different time

periods. Appl. Environ. Microbiol. 77, 6109–6116. https://doi.org/10.1128/AEM.01751-10.
van Bodegom, P.M., Scholten, J.C.M., Stams, A.J.M., 2004. Direct inhibition of methanogenesis by ferric iron. FEMS Microbiol. Ecol. 49, 261–268. https://doi.org/10.1016/j.femsec.2004.03.017.
Chen, C., et al., 2019b. Sulfate-reducing bacteria and methanogens are involved in arsenic methylation and demethylation in paddy soils. ISME J. 13, 2523–2535. https://doi.org/10.1038/s41396-019-0451-7.
Chen, C., et al., 2022. Suppression of methanogenesis in paddy soil increases dimethylarsenate accumulation and the incidence of straighthead disease in rice. Soil Biol. Biochem. 169, 108689 https://doi.org/10.1016/j.soilbio.2022.108689.
Chen, J., Rosen, B.P., 2020. The arsenic methylation cycle: how microbial communities adapted methylarsenicals for use as weapons in the continuing war for dominance. Front. Environ. Sci. 8 https://doi.org/10.3389/fenvs.2020.00043.
Chen, J., Rosen, B.P., 2023. Arsenite methyltransferase diversity and optimization of methylation efficiency. Environ. Sci. Technol. https://doi.org/10.1021/acs.est.3c00966.
Chen, J., Yoshinaga, M., Rosen, B.P., 2019a. The antibiotic action of methylarsenite is an emergent property of microbial communities. Mol. Microbiol. 111, 487–494. https://doi.org/10.1111/mmi.14169.
Cheng, Y.-Q., Yang, L.-Z., Cao, Z.-H., Ci, E., Yin, S., 2009. Chronosequential changes of selected pedogenic properties in paddy soils as compared with non-paddy soils. Geoderma 151, 31–41. https://doi.org/10.1016/j.geoderma.2009.03.016.
Cline, J.D., 1969. Spectrophotometric determination of hydrogen sulfide in natural waters 1. Limnol. Oceanogr. 14, 454–458.
Colina Blanco, A.E., Kerl, C.F., Planer-Friedrich, B., 2021. Detection of thioarsenates in rice grains and rice products. J. Agric. Food Chem. 69, 2287–2294. https://doi.org/10.1021/acs.jafc.0c06853.
Conklin, S.D., Fricke, M.W., Creed, P.A., Creed, J.T., 2008. Investigation of the pH effects on the formation of methylated thio-arsenicals, and the effects of pH and temperature on their stability. J. Anal. At. Spectrom. 23, 711–716. https://doi.org/10.1039/B713145C.
Conrad, R., 2020. Methane production in soil environments—anaerobic biogeochemistry and microbial life between flooding and desiccation. Microorganisms 8, 881.
Couture, R.-M., et al., 2013. Sorption of arsenite, arsenate, and thioarsenates to iron oxides and iron sulfides: a kinetic and spectroscopic investigation. Environ. Sci. Technol. 47, 5652–5659.
Hegler, F., Posth, N.R., Jiang, J., Kappler, A., 2008. Physiology of phototrophic iron(II)-oxidizing bacteria: implications for modern and ancient environments. FEMS Microbiol. Ecol. 66, 250–260. https://doi.org/10.1111/j.1574-6941.2008.00592.x.
Ho, A., Lüke, C., Cao, Z., Frenzel, P., 2011. Ageing well: methane oxidation and methane oxidizing bacteria along a chronosequence of 2000 years. Environ. Microbiol. Rep. 3, 738–743.
Hoffmann, M., Mikutta, C., Kretzschmar, R., 2013. Arsenite binding to natural organic matter: spectroscopic evidence for ligand exchange and ternary complex formation. Environ. Sci. Technol. 47, 12165–12173. https://doi.org/10.1021/es4023317.
Huang, L.-M., et al., 2015. The use of chronosequences in studies of paddy soil evolution: a review. Geoderma 237, 199–210.
Jia, Y., et al., 2013a. Microbial arsenic methylation in soil and rice rhizosphere. Environ. Sci. Technol. 47, 3141–3148. https://doi.org/10.1021/es303649v.
Jia, Y., et al., 2013b. Microbial arsenic methylation in soil and rice rhizosphere. Environ. Sci. Technol. 47, 3141–3148. https://doi.org/10.1021/es303649v.
Kalbitz, K., et al., 2013. The carbon count of 2000 years of rice cultivation. Glob. Chang. Biol. 19, 1107–1113. https://doi.org/10.1111/gcb.12080.
Kerl, C.F., Rafferty, C., Clemens, S., Planer-Friedrich, B., 2018. Monothioarsenate uptake, transformation, and translocation in rice plants. Environ. Sci. Technol. 52, 9154–9161. https://doi.org/10.1021/acs.est.8b02202.
Kerl, C.F., et al., 2019. Methylated thioarsenates and monothioarsenate differ in uptake, transformation, and contribution to total arsenic translocation in rice plants. Environ. Sci. Technol. 53, 5787–5796. https://doi.org/10.1021/acs.est.9b00592.
Klein Goldewijk, K., Beusen, A., Doelman, J., Stehfest, E., 2017. Anthropogenic land use estimates for the Holocene – HYDE 3.2. Earth Syst. Sci. Data 9, 927–953. https://doi.org/10.5194/essd-9-927-2017.
Kögel-Knabner, I., et al., 2010. Biogeochemistry of paddy soils. Geoderma 157, 1–14.
Kölbl, A., et al., 2014. Accelerated soil formation due to paddy management on marshlands (Zhejiang Province, China). Geoderma 228-229, 67–89. https://doi.org/10.1016/j.geoderma.2013.09.005.
Liu, Q., et al., 2021. Alternating wet–dry cycles rather than sulfate fertilization control pathways of methanogenesis and methane turnover in rice straw-amended paddy soil. Environ. Sci. Technol. 55, 12075–12083. https://doi.org/10.1021/acs.est.1c03149.
Lohmayer, R., Kappler, A., Lösekann-Behrens, T., Planer-Friedrich, B., 2014. Sulfur species as redox partners and electron shuttles for ferrihydrite reduction by Sulfurospirillum deleyianum. Appl. Environ. Microbiol. 80, 3141–3149. https://doi.org/10.1128/aem.04220-13.
Lomax, C., et al., 2012. Methylated arsenic species in plants originate from soil microorganisms. New Phytol. 193, 665–672. https://doi.org/10.1111/j.1469-8137.2011.03956.x.
Lovley, D.R., Phillips, E.J., 1987. Competitive mechanisms for inhibition of sulfate reduction and methane production in the zone of ferric Iron reduction in sediments. Appl. Environ. Microbiol. 53, 2636–2641. https://doi.org/10.1128/aem.53.11.2636-2641.1987.
Lueders, T., Manefield, M., Friedrich, M.W., 2004. Enhanced sensitivity of DNA- and rRNA-based stable isotope probing by fractionation and quantitative analysis of isopycnic centrifugation gradients. Environ. Microbiol. 6, 73–78. https://doi.org/10.1046/j.1462-2920.2003.00536.x.
Ma, J.F., et al., 2008. Transporters of arsenite in rice and their role in arsenic accumulation in rice grain. Proc. Natl. Acad. Sci. 105, 9931–9935. https://doi.org/10.1073/pnas.0802361105.
McKeague, J.A., Day, J.H., 1966. Dithionite- and oxalate-extractable Fe and Al as aids in differentiating various classes of soils. Can. J. Soil Sci. 46, 13–22. https://doi.org/10.4141/cjss66-003.
Meharg, A.A., Hartley-Whitaker, J., 2002. Arsenic uptake and metabolism in arsenic resistant and nonresistant plant species. New Phytol. 154, 29–43.
Mehra, O.P., Jackson, M.L., 1958. Iron oxide removal from soils and clays by a dithionite-citrate system buffered with sodium bicarbonate. Clay Clay Miner. 7, 317–327. https://doi.org/10.1346/CCMN.1958.0070122.
Moe, B., et al., 2016. Comparative cytotoxicity of fourteen trivalent and pentavalent arsenic species determined using real-time cell sensing. J. Environ. Sci. 49, 113–124. https://doi.org/10.1016/j.jes.2016.10.004.
Naranmandura, H., et al., 2011. Comparative toxicity of arsenic metabolites in human bladder cancer EJ-1 cells. Chem. Res. Toxicol. 24, 1586–1596. https://doi.org/10.1021/tx200291p.
Pischke, E., et al., 2022. Dimethylmonothioarsenate is highly toxic for plants and readily translocated to shoots. Environ. Sci. Technol. 56, 10072–10083. https://doi.org/10.1021/acs.est.2c01206.
Planer-Friedrich, B., London, J., McCleskey, R.B., Nordstrom, D.K., Wallschläger, D., 2007. Thioarsenates in geothermal waters of Yellowstone National Park: determination, preservation, and geochemical importance. Environ. Sci. Technol. 41, 5245–5251. https://doi.org/10.1021/es070273v.
Planer-Friedrich, B., Kerl, C.F., Colina Blanco, A.E., Clemens, S., 2022. Dimethylated thioarsenates: a potentially dangerous blind spot in current worldwide regulatory limits for arsenic in rice. J. Agric. Food Chem. 70, 9610–9618. https://doi.org/10.1021/acs.jafc.2c02425.
Qiao, J., et al., 2023. Prevalence of methylated arsenic and microbial arsenic methylation genes in paddy soils of the Mekong Delta. Environ. Sci. Technol. https://doi.org/10.1021/acs.est.3c00210.
Qin, J., et al., 2006. Arsenic detoxification and evolution of trimethylarsine gas by a microbial arsenite S-adenosylmethionine methyltransferase. Proc. Natl. Acad. Sci. 103, 2075–2080. https://doi.org/10.1073/pnas.0506836103.
Raab, A., Williams, P., Meharg, A., Feldmann, J., 2007. Uptake and translocation of inorganic and methylated arsenic species by plants. Environ. Chem. 4 https://doi.org/10.1071/EN06079.
Reid, M.C., et al., 2017. Arsenic methylation dynamics in a rice paddy soil anaerobic enrichment culture. Environ. Sci. Technol. 51, 10546–10554. https://doi.org/10.1021/acs.est.7b02970.
Roth, P.J., et al., 2011. Accumulation of nitrogen and microbial residues during 2000 years of rice paddy and non-paddy soil development in the Yangtze River Delta, China. Glob. Chang. Biol. 17, 3405–3417. https://doi.org/10.1111/j.1365-2486.2011.02500.x.
Saalfield, S.L., Bostick, B.C., 2009. Changes in iron, sulfur, and arsenic speciation associated with bacterial sulfate reduction in ferrihydrite-rich systems. Environ. Sci. Technol. 43, 8787–8793. https://doi.org/10.1021/es901651k.
Schwertmann, U., 1991. Solubility and dissolution of iron oxides. Plant Soil 130, 1–25. https://doi.org/10.1007/BF00011851.
Sethunathan, N., Rao, V., Adhya, T., Raghu, K., 1982. Microbiology of rice soils. CRC Crit. Rev. Microbiol. 10, 125–172.
Smedley, P.L., Kinniburgh, D.G., 2002. A review of the source, behaviour and distribution of arsenic in natural waters. Appl. Geochem. 17, 517–568. https://doi.org/10.1016/S0883-2927(02)00018-5.
Snoeyink, V.L., Jenkins, D., 1980. Water Chemistry. Wiley.
Somenahally, A.C., Hollister, E.B., Loeppert, R.H., Yan, W., Gentry, T.J., 2011. Microbial communities in rice rhizosphere altered by intermittent and continuous flooding in fields with long-term arsenic application. Soil Biol. Biochem. 43, 1220–1228. https://doi.org/10.1016/j.soilbio.2011.02.011.
Spratt Jr., H.G., Morgan, M.D., 1990. Sulfur cycling in a cedar-dominated, freshwater wetland. Limnol. Oceanogr. 35, 1586–1593.
Stauder, S., Raue, B., Sacher, F., 2005. Thioarsenates in sulfidic waters. Environ. Sci. Technol. 39, 5933–5939. https://doi.org/10.1021/es048034k.
Stone, R., 2008. Arsenic and paddy rice: a neglected cancer risk? Science 321, 184–185. https://doi.org/10.1126/science.321.5886.184.
Stookey, L.L., 1970. Ferrozine—a new spectrophotometric reagent for iron. Anal. Chem. 42, 779–781. https://doi.org/10.1021/ac60289a016.
Suess, E., Planer-Friedrich, B., 2012. Thioarsenate formation upon dissolution of orpiment and arsenopyrite. Chemosphere 89, 1390–1398.
Viacava, K., et al., 2020. Variability in arsenic methylation efficiency across aerobic and anaerobic microorganisms. Environ. Sci. Technol. 54, 14343–14351. https://doi.org/10.1021/acs.est.0c03908.
Wallschläger, D., London, J., 2008. Determination of methylated arsenic-sulfur compounds in groundwater. Environ. Sci. Technol. 42, 228–234. https://doi.org/10.1021/es0707815.
Wallschläger, D., Stadey, C.J., 2007. Determination of (oxy)thioarsenates in sulfidic waters. Anal. Chem. 79, 3873–3880. https://doi.org/10.1021/ac070061g.
Wang, J., et al., 2020. Thiolated arsenic species observed in rice paddy pore waters. Nat. Geosci. 13, 282–287. https://doi.org/10.1038/s41561-020-0533-1.
Wang, P., et al., 2015a. Long-term rice cultivation stabilizes soil organic carbon and promotes soil microbial activity in a salt marsh derived soil chronosequence. Sci. Rep. 5, 15704. https://doi.org/10.1038/srep15704.
Wang, P.P., Bao, P., Sun, G.X., 2015b. Identification and catalytic residues of the arsenite methyltransferase from a sulfate-reducing bacterium, *Clostridium* sp. BXM. FEMS Microbiol. Lett. 362, 1–8. https://doi.org/10.1093/femsle/fnu003.

Wang, P.-P., Sun, G.-X., Zhu, Y.-G., 2014. Identification and characterization of Arsenite methyltransferase from an archaeon, *Methanosarcina acetivorans* C2A. Environ. Sci. Technol. 48, 12706–12713. https://doi.org/10.1021/es503869k.

Wind, T., Conrad, R., 1995. Sulfur compounds, potential turnover of sulfate and thiosulfate, and numbers of sulfate-reducing bacteria in planted and unplanted paddy soil. FEMS Microbiol. Ecol. 18, 257–266. https://doi.org/10.1111/j.1574-6941.1995.tb00182.x.

Wind, T., Conrad, R., 1997. Localization of sulfate reduction in planted and unplanted rice field soil. Biogeochemistry 37, 253–278. https://doi.org/10.1023/A:1005760506957.

Winkler, P., et al., 2016. Response of vertisols, andosols, and alisols to paddy management. Geoderma 261, 23–35. https://doi.org/10.1016/j.geoderma.2015.06.017.

Wissing, L., et al., 2011. Organic carbon accumulation in a 2000-year chronosequence of paddy soil evolution. CATENA 87, 376–385. https://doi.org/10.1016/j.catena.2011.07.007.

Wissing, L., et al., 2014. Organic carbon accumulation on soil mineral surfaces in paddy soils derived from tidal wetlands. Geoderma 228-229, 90–103. https://doi.org/10.1016/j.geoderma.2013.12.012.

Wu, B., Meng, X., Yao, H., Amelung, W., 2023. Iron dynamics and isotope fractionation in soil and rice during 2000 years of rice cultivation. Plant Soil. https://doi.org/10.1007/s11104-023-06352-5.

Xu, X., et al., 2019. Microbial sulfate reduction decreases arsenic mobilization in flooded paddy soils with high potential for microbial Fe reduction. Environ. Pollut. 251, 952–960. https://doi.org/10.1016/j.envpol.2019.05.086.

Yan, W., et al., 2005. Differential response of rice germplasm to straighthead induced by arsenic. Crop Sci. 45, 1223–1228.

Yang, Y.-P., et al., 2018. Microbe mediated arsenic release from iron minerals and arsenic methylation in rhizosphere controls arsenic fate in soil-rice system after straw incorporation. Environ. Pollut. 236, 598–608. https://doi.org/10.1016/j.envpol.2018.01.099.

Yoon, H., et al., 2022. Time-dependent biosensor fluorescence as a measure of bacterial Arsenic uptake kinetics and its inhibition by dissolved organic matter. Appl. Environ. Microbiol. 88, e00822–e00891. https://doi.org/10.1128/aem.00891-22.

Zavala, Y.J., Gerads, R., Gürleyük, H., Duxbury, J.M., Arsenic in Rice: II., 2008. Arsenic speciation in USA grain and implications for human health. Environ. Sci. Technol. 42, 3861–3866. https://doi.org/10.1021/es702748q.

Zeibich, L., Schmidt, O., Drake, H.L., 2018. Protein- and RNA-enhanced fermentation by gut microbiota of the earthworm *Lumbricus terrestris*. Appl. Environ. Microbiol. 84, e00618–e00657. https://doi.org/10.1128/AEM.00657-18.

Zhao, F.-J., Zhu, Y.-G., Meharg, A.A., 2013a. Methylated arsenic species in rice: geographical variation, origin, and uptake mechanisms. Environ. Sci. Technol. 47, 3957–3966. https://doi.org/10.1021/es304295n.

Zhao, F.-J., et al., 2013b. Arsenic methylation in soils and its relationship with microbial arsM abundance and diversity, and as speciation in rice. Environ. Sci. Technol. 47, 7147–7154. https://doi.org/10.1021/es304977m.

Zheng, M.-Z., Li, G., Sun, G.-X., Shim, H., Cai, C., 2013. Differential toxicity and accumulation of inorganic and methylated arsenic in rice. Plant Soil 365, 227–238.

Zobrist, J., Dowdle, P.R., Davis, J.A., Oremland, R.S., 2000. Mobilization of arsenite by dissimilatory reduction of adsorbed arsenate. Environ. Sci. Technol. 34, 4747–4753. https://doi.org/10.1021/es001068h.

Supporting information

Changes in arsenic mobility and speciation across a 2000-year-old paddy soil chronosequence

José M. León Ninin[1], E. Marie Muehe[2,3], Angelika Kölbl[4], Alejandra Higa Mori[1], Alan Nicol[1], Ben Gilfedder[5], Johanna Pausch[6], Livia Urbanski[7], Tillmann Lueders[8], Britta Planer-Friedrich[1]*.

[1] Environmental Geochemistry, Bayreuth Center for Ecology and Environmental Research (BayCEER), University of Bayreuth, 95440 Bayreuth, Germany

[2] Department of Environmental Microbiology, Helmholtz Centre for Environmental Research (UFZ), 04318 Leipzig, Germany

[3] Department of Geosciences, University of Tübingen, 72076 Tübingen, Germany

[4] Soil Science and Soil Protection, Martin Luther University Halle-Wittenberg, 06120 Halle (Saale), Germany

[5] Limnological Research Station, Bayreuth Center for Ecology and Environmental Research (BayCEER), University of Bayreuth, 95440 Bayreuth, Germany

[6] Agroecology, Bayreuth Center for Ecology and Environmental Research (BayCEER), University of Bayreuth, 95440 Bayreuth, Germany

[7] Chair of Soil Science, TUM School of Life Sciences Weihenstephan, Technical University of Munich, Emil-Ramann-Str. 2, 85354 Freising, Germany

[8] Ecological Microbiology, Bayreuth Center of Ecology and Environmental Research (BayCEER), University of Bayreuth, 95448 Bayreuth, Germany

* Corresponding author. Phone: +49-921-553999; E-mail address: b.planer-friedrich@uni-bayreuth.de (B. Planer-Friedrich).

Number of pages: 23

Number of Tables: 2

Number of figures: 21

Contents:

Supplementary Materials and Methods

Details on As speciation analyses

Inorganic arsenic (arsenite and arsenate), methylated oxyarsenates (MMA and DMA), inorganic thioarsenates (MTA, DTA, and TTA), and methylthioarsenates (MMMTA, MMDTA, DMMTA, and DMDTA) were separated with an ion chromatograph coupled to an ICP-MS detector, as described before[1]. Peak assignment was done based on previously reported retention times[1,2]. Calculation of concentrations was done by calibration containing arsenite ($NaAsO_2$, Fluka), arsenate ($Na_2HAsO_4 \times 7H_2O$, Fluka), MMA ($CH_3AsNa_2O_3 \times 6H_2O$, Supelco), and DMA ($C_2H_6AsNaO_2 \times 3H_2O$, Sigma-Aldrich). Concentrations of thiolated As species were calculated based on their oxyAs homologues: MTA, DTA, and TTA were calibrated with arsenate, MMMTA and MMDTA with MMA, and DMMTA and DMDTA with DMA.

Details on DNA and RNA extractions and transcript quantification

Cell material was lysed from approximately 0.6 g of wet soil by bead-beating in sodium phosphate and dodecyl sulfate solutions. DNA and RNA were co-extracted from the soil slurry with phenol-chloroform-isoamyl alcohol (PCI) and chloroform-isoamyl alcohol (CI), precipitated overnight in polyethylene glycol, washed with 70% ethanol, and dissolved in 100 µL TE buffer. Nucleic acid quality was determined with a 1% ethidium bromide dyed gel and with nanodrop-based absorbance ratios at 260/280 and 260/230 nm (NanoDrop 1000, Peqlab). Nucleic acid quantity was assessed with Qubit® 3.0 Fluorometer (life technologies, Germany).

For transcript quantification, DNA was digested with the Invitrogen Turbo DNA free Kit (Invitrogen), and cDNA produced via the SuperScript III reverse transcription kit (Invitrogen). Quantitative PCR was performed using the SsoAdvanced Universial SYBR Green supermix (Bio-Rad Laboratories GmbH, Munich, Germany) on an CFX96™ Real-Time PCR Detection System (Bio-Rad Laboratories, Germany) and analyzed using the CFX Manager™ software. Primers, reaction mixtures and cycling programs are given for each gene in Table SI1.

Table SI1: Primers, reaction mixtures and cycling programs for the qPCR quantification of 16S rRNA, *dsrA*, *ArsM* and *mcrA* genes and partially transcripts.

<table>
<tr><td colspan="2"><u>16S rRNA gene and transcript</u></td></tr>
<tr><td>Forward primer:</td><td>341F: 5’-CCTACGGGAGGCAGCAG-3’ (Ref: [3])</td></tr>
<tr><td>Reverse primer:</td><td>797R: 5’-GGACTACCAGGGTATCTAATCCTGTT-3’ (Ref: [4])</td></tr>
<tr><td>qPCR reaction mix</td><td>
<table>
<tr><th>Reagent</th><th>Stock conc.</th><th>1 x</th></tr>
<tr><td>Sso Advanced SYBR green master mix</td><td>5x</td><td>5 µL</td></tr>
<tr><td>PCR-grade water</td><td></td><td>3.4 µL</td></tr>
<tr><td>Forward primer</td><td>5 µM</td><td>0.15 µL</td></tr>
<tr><td>Reverse primer</td><td>5 µM</td><td>0.45 µL</td></tr>
<tr><td>Template DNA</td><td>1-20 ng/µL</td><td>1 µL</td></tr>
<tr><td>Total volume</td><td></td><td>10 µL</td></tr>
</table>
</td></tr>
<tr><td>qPCR cycling program</td><td>
<table>
<tr><td>98°C</td><td>98°C</td><td>60°C</td><td>98°C</td><td>55-95°C 0.5°C steps</td></tr>
<tr><td>3 min</td><td>15 sec</td><td>30 sec</td><td>15 sec</td><td>0.05 sec</td></tr>
<tr><td>1x</td><td colspan="2">40 x</td><td>1 x</td><td>1x</td></tr>
</table>
</td></tr>
<tr><td colspan="2"><u>dsrA gene and transcript</u></td></tr>
<tr><td>Forward primer:</td><td>dsr-F+: 5’-ACSCACTGGAAGCACGGCGG-3’ (Ref: [5,6])</td></tr>
<tr><td>Reverse primer:</td><td>dsr-R: 5’-GTGGMRCCGTGCAKRTTGG-3’ (Ref: [5,6])</td></tr>
<tr><td>qPCR reaction mix</td><td>
<table>
<tr><th>Reagent</th><th>Stock conc.</th><th>1 x</th></tr>
<tr><td>Sso Advanced SYBR green master mix</td><td>5x</td><td>5 µL</td></tr>
<tr><td>PCR-grade water</td><td></td><td>2.76 µL</td></tr>
<tr><td>BSA</td><td>2.5 mg / mL</td><td>0.6 µL</td></tr>
<tr><td>Forward primer</td><td>5 µM</td><td>0.32 µL</td></tr>
<tr><td>Reverse primer</td><td>5 µM</td><td>0.32 µL</td></tr>
<tr><td>Template DNA</td><td>1-20 ng/µL</td><td>1 µL</td></tr>
<tr><td>Total volume</td><td></td><td>10 µL</td></tr>
</table>
</td></tr>
<tr><td>qPCR cycling program</td><td>
<table>
<tr><td>95°C</td><td>95°C</td><td>60°C</td><td>72°C</td><td>95°C</td><td>55-95°C 0.5°C steps</td></tr>
<tr><td>10 min</td><td>30 sec</td><td>30 sec</td><td>30 sec</td><td>30 sec</td><td>0.05 sec</td></tr>
<tr><td>1x</td><td colspan="3">40 x</td><td>1x</td><td>1x</td></tr>
</table>
</td></tr>
<tr><td colspan="2"><u>ArsM gene and transcript</u></td></tr>
<tr><td>Forward primer:</td><td>arsMF1: 5’-TCYCTCGGCTGCGGCAAYCCVAC-3’ (Ref: [7])</td></tr>
<tr><td>Reverse primer:</td><td>arsMF2: 5’-CGWCCGCCWGGCTTWAGYACCCG-3’ (Ref: [7])</td></tr>
</table>

qPCR reaction mix

Reagent	Stock conc.	1 x
Sso Advanced SYBR green master mix	5x	5 µL
PCR-grade water		3.2 µL
Forward primer	5 µM	0.4 µL
Reverse primer	5 µM	0.4 µL
Template DNA	1-20 ng/µL	1
Total volume		**10 µL**

qPCR cycling program

95°C	98°C	61°C	72°C	72°C	98°C	55-95°C 0.5°C steps
10 min	30 sec	45 sec	30 sec	7 min	30 sec	0.05 sec
1x	40 x				1 x	1x

***mcrA* gene and transcript**

Forward primer: mlas: 5'-GGTGGTGTMGGDTTCACMCARTA-3' (Ref: [6,8])

Reverse primer: mcrA-rev: 5'-CGTTCATBGCGTAGTTVGGRTAGT-3' (Ref: [6,8])

qPCR reaction mix

Reagent	Stock conc.	1 x
Sso Advanced SYBR green master mix	5x	5 µL
BSA	2.5 mg mL^{-1}	0.4 µL
PCR-grade water		2.8 µL
Forward primer	5 µM	0.4 µL
Reverse primer	5 µM	0.4 µL
Template DNA	1-20 ng/µL	1 µL
Total volume		**10 µL**

qPCR cycling program

95°C	95°C	48°C Ramp 0.1°C/sec	72°C	95°C	55°C	72°C	72°C
3 min	30 sec	45 sec	30 sec	30 sec	45 sec	30 sec	10 min
1x	5 Zyklen			30 x			1x

Supplementary results

Table SI2: Selected soil properties of the top soils from the chronosequence used in this study.

Paddy soil age (years)	Horizon*	Horizon depth (cm)*	Soil pH*	Soil Org. C* ($g\ kg^{-1}$)	Soil Fe* ($g\ kg^{-1}$)	Soil As ($mg\ kg^{-1}$)	Soil S ($g\ kg^{-1}$)	Fe_O/Fe_{DCB}
50	Alp1	0 - 7	7.4	17.8 ± 0.5	38	17	3.52	0.43 ± 0.04
100	Alp1**	0 - 9	5.0	17.6 ± 1.3	34	15 ± 2	2.64 ± 0.06	0.44 ± 0.04
100	Alp2**	9 - 15	5.8	15.3 ± 1.1	35			
300	Alp	0 - 18	5.8	22.6 ± 2.5	35	17	2.77	0.46 ± 0.06
2000	Alp	0 - 15	5.1	30.0 ± 1.5	22	11	2.57	0.84 ± 0.05

*Data from Kölbl, et al. [9]. SOC = (TC – TIC) analyzed by dry combustion (TC) and infrared detection of evolving CO_2 after carbonate dissolution (TIC). ** For this work, horizons Alp1 and Alp2 from P100 were mixed to obtain a material representative of the complete Alp horizon. Fe_O: Oxalate extractable iron, Fe_{DCB}: Dithionate-citrate-bicarbonate extractable iron. A complete characterization of all soils and horizons from this chronosequence can be found in Kölbl, et al. [9].

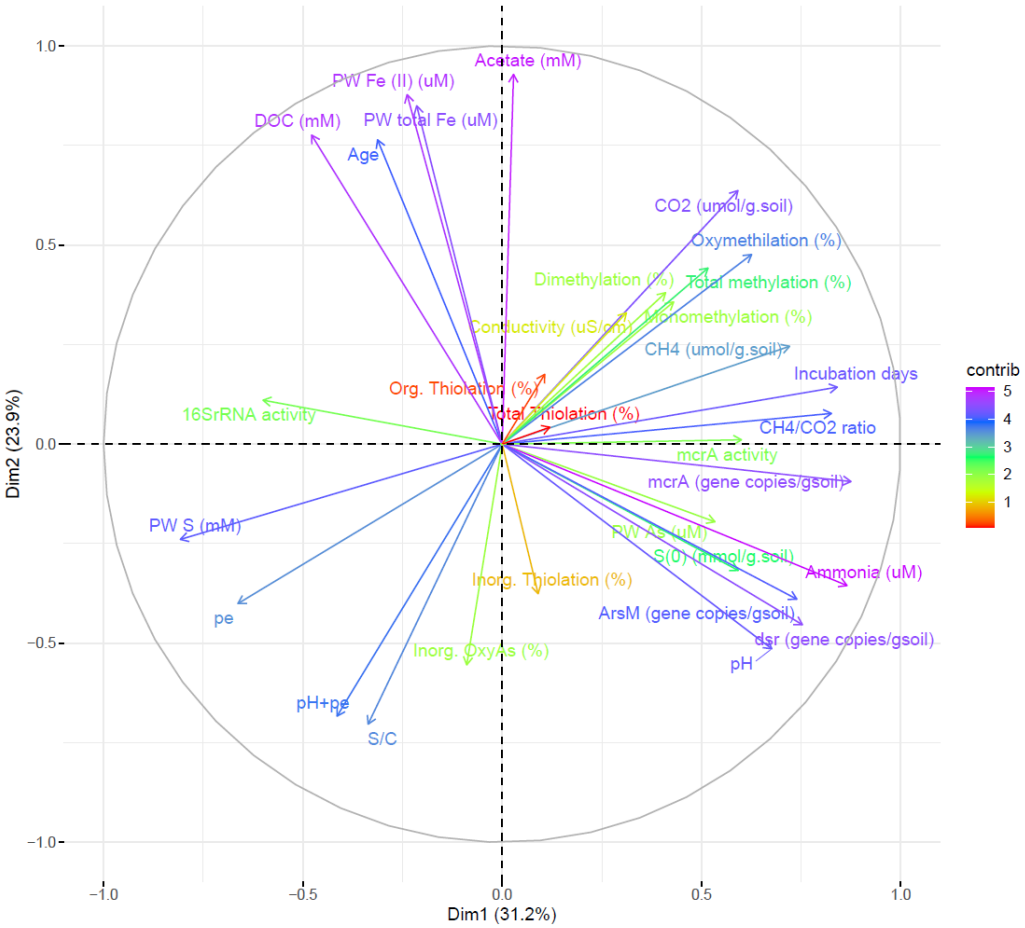

Figure SI1: Principal Component Analysis for the complete dataset. The axes Dim1 and Dim2 represent the two principal components (PC) explaining 31.2 and 23.9% of the variance of the dataset, respectively. Colored arrows represent the original variables introduced. The more parallel an arrow is to Dim1 or Dim2, the more it contributes to that PC. The length of the arrow is associated to how much of the variability of the variable is represented by both PCs in the plot. Furthermore, the angle between two arrows is associated to the correlation between the variables they represent, with smaller angles representing high positive correlations, and opposite angles representing high negative correlations.

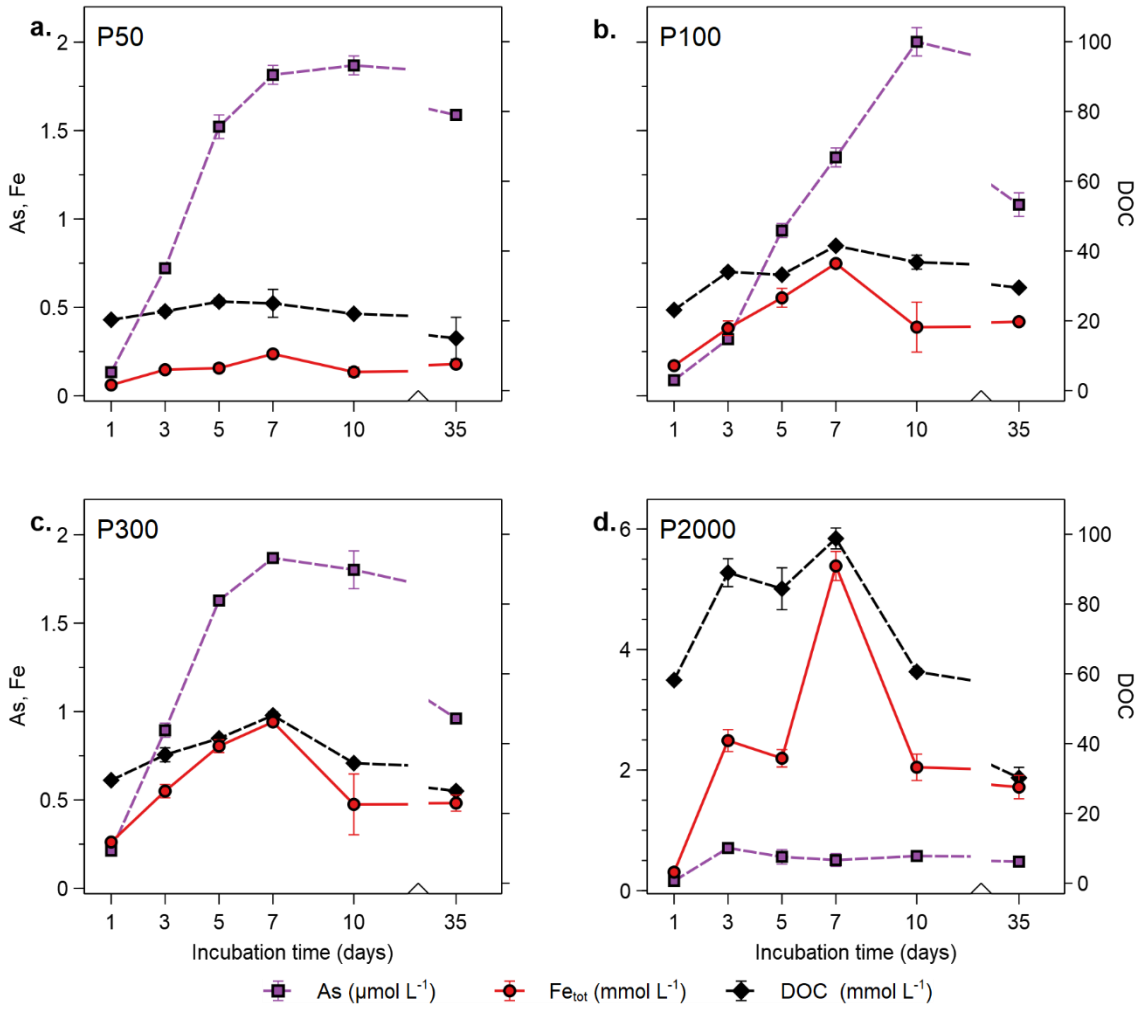

Figure SI2: Dynamics of Fe, As, and DOC in paddy soils of different ages. Note the different primary y-axis for P2000 (d). Points represent mean values and error bars their standard deviation (n=3).

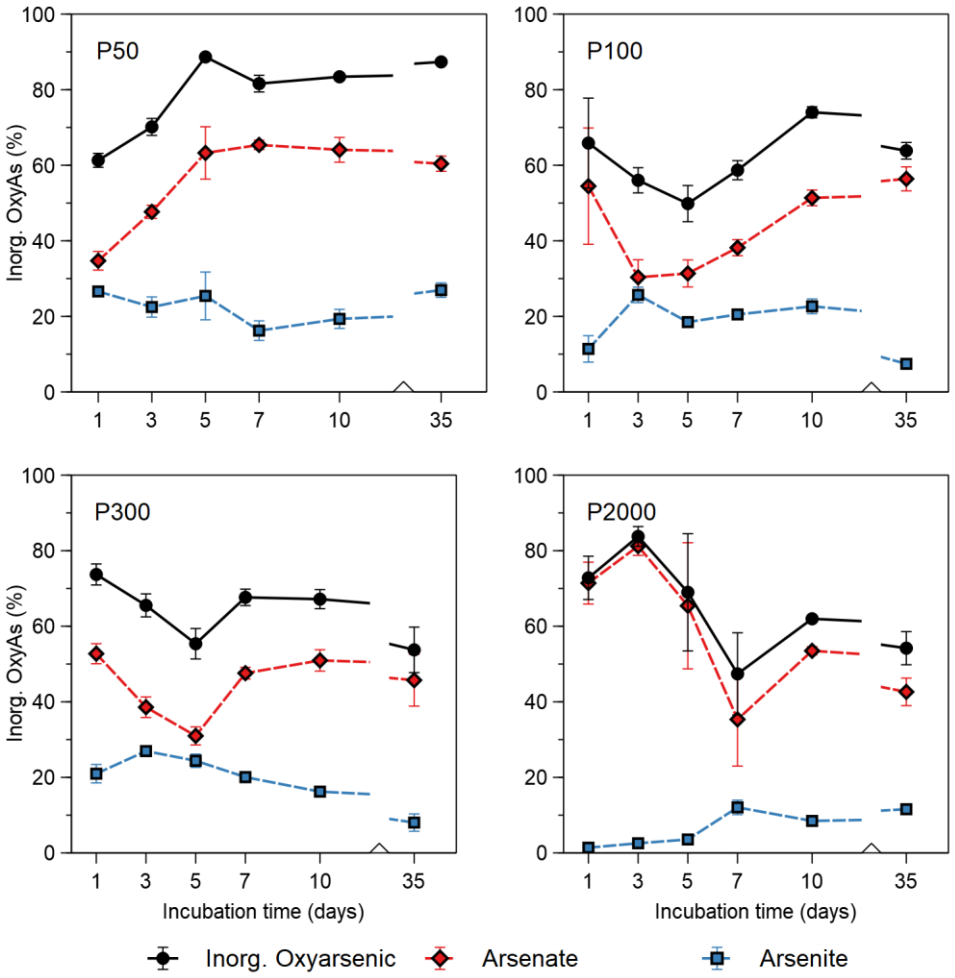

Figure SI3: Contribution of inorganic oxyarsenic species to As pore water speciation for all soils over incubation time. Points represent mean values and error bars their standard deviation (n=3).

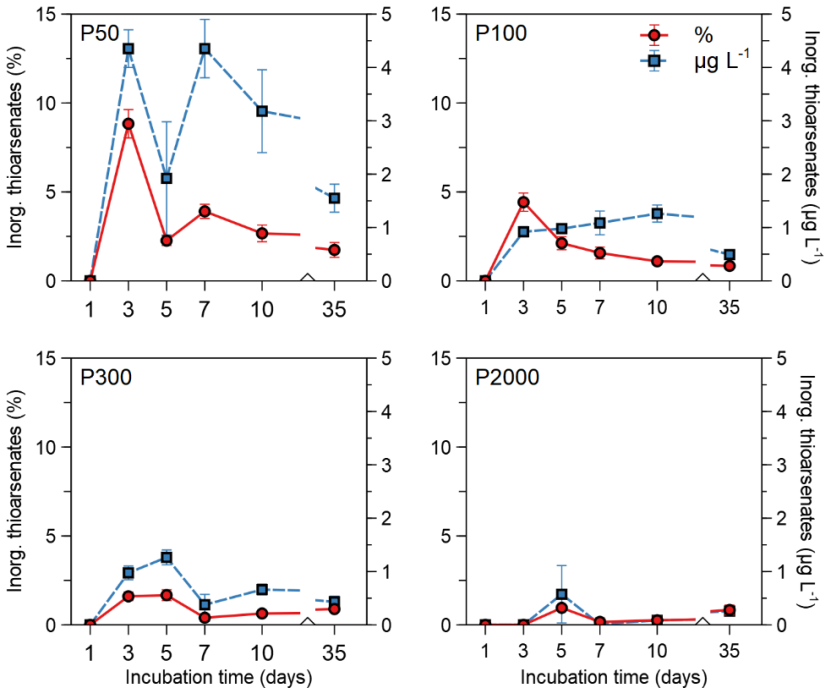

Figure SI4: Contribution of inorganic thioarsenates to As pore water speciation for all soils over incubation time. Points represent mean values and error bars their standard deviation (n=3).

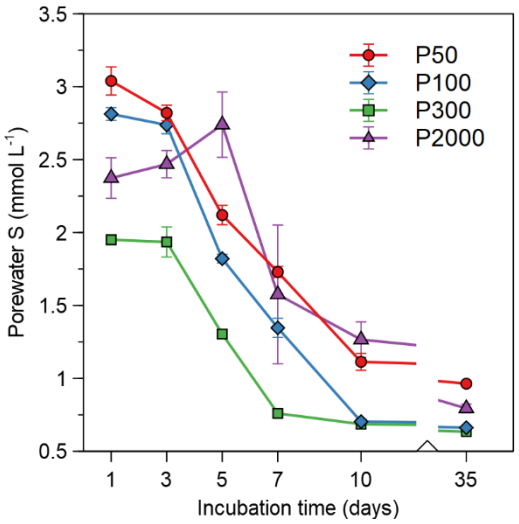

Figure SI5: Consumption of porewater S in soils of different ages indicating dissimilative sulfate reduction. Points represent mean values and error bars their standard deviation (n=3).

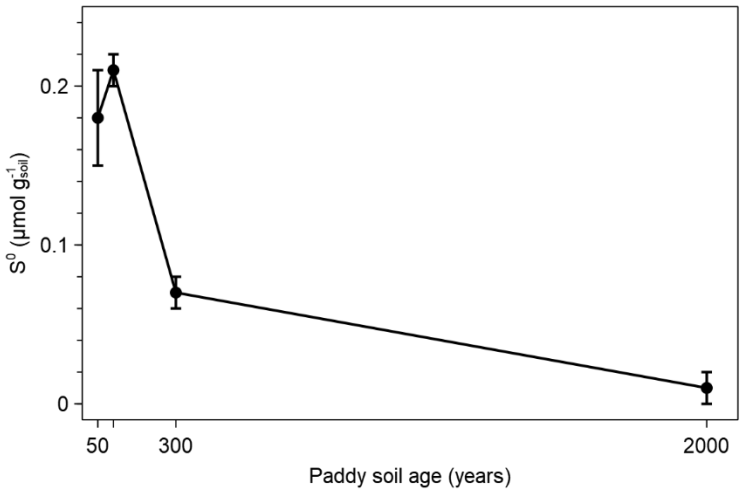

Figure SI6: Accumulation of S^0 in paddy soils of different ages after 35 days of incubation. Points represent mean values and error bars their standard deviation (n=3).

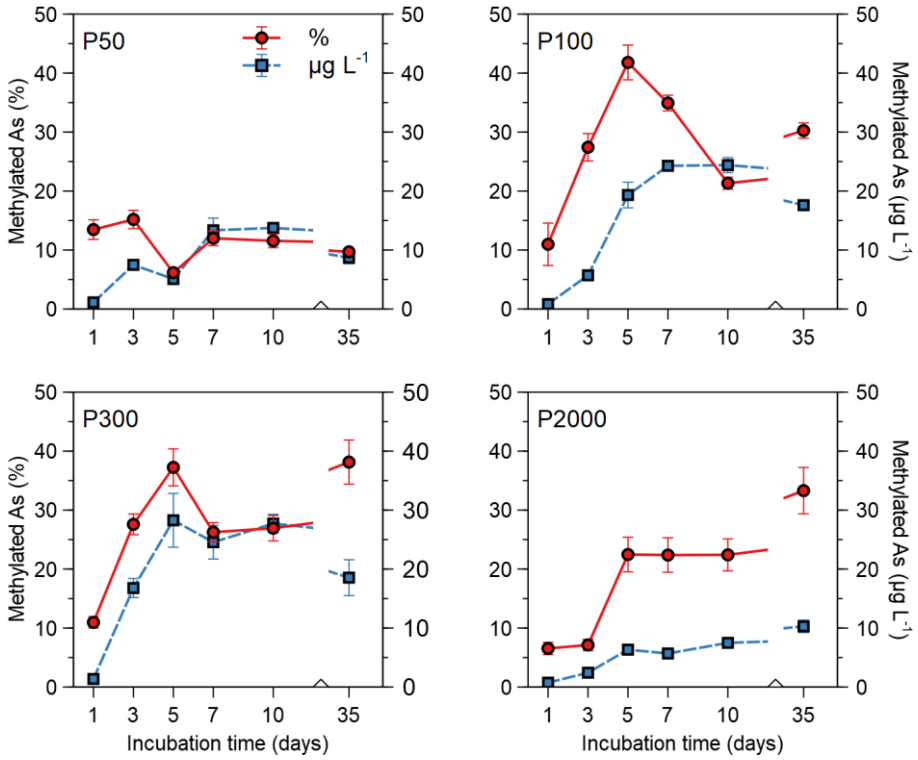

Figure SI7: Contribution of methylated As to total pore water As speciation for all soils over incubation time. Points represent mean values and error bars their standard deviation (n=3).

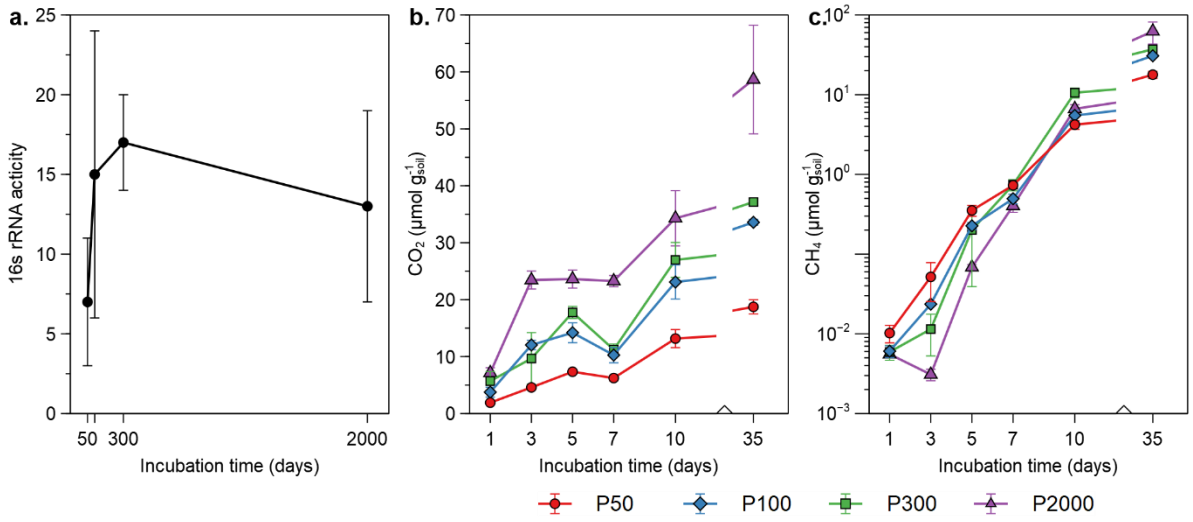

Figure SI8: Increasing potential microbial activity in paddy soils with increasing age. Potential activity of the soil microbiome based on 16S rRNA transcript quantification by day 5 of incubation (a), respiratory CO_2 (b) and CH_4 (c) production in each soil during the 35 days of the experiment. Note the logarithmic scale for (c). Points represent mean values and error bars their standard deviation (n=3).

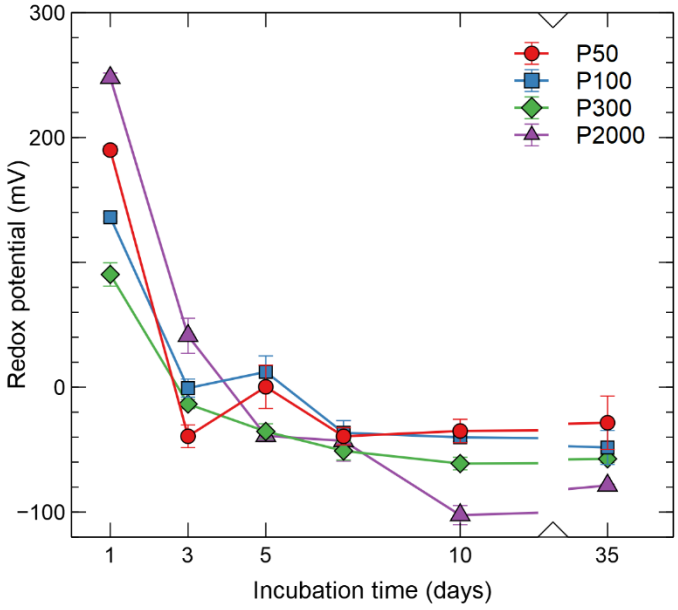

Figure SI9: Redox potential values for the chronosequence soils during flooded incubation.

Points represent mean values and error bars their standard deviation (n=3).

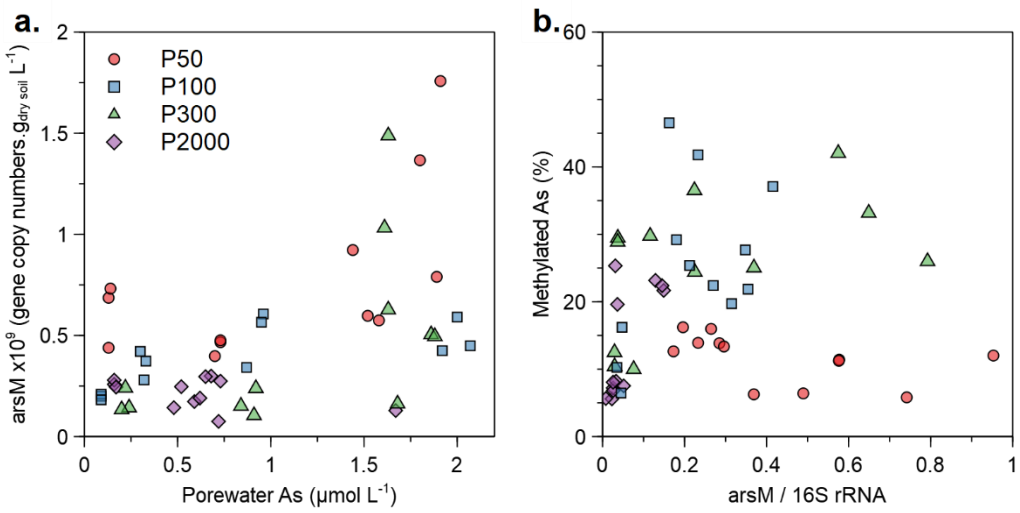

Figure SI10: *arsM* gene copy numbers present in different soils related to their porewater total As concentration (a). Methylated As contribution in reference to arsM gene copy numbers normalized by 16S rRNA gene copy numbers (b).

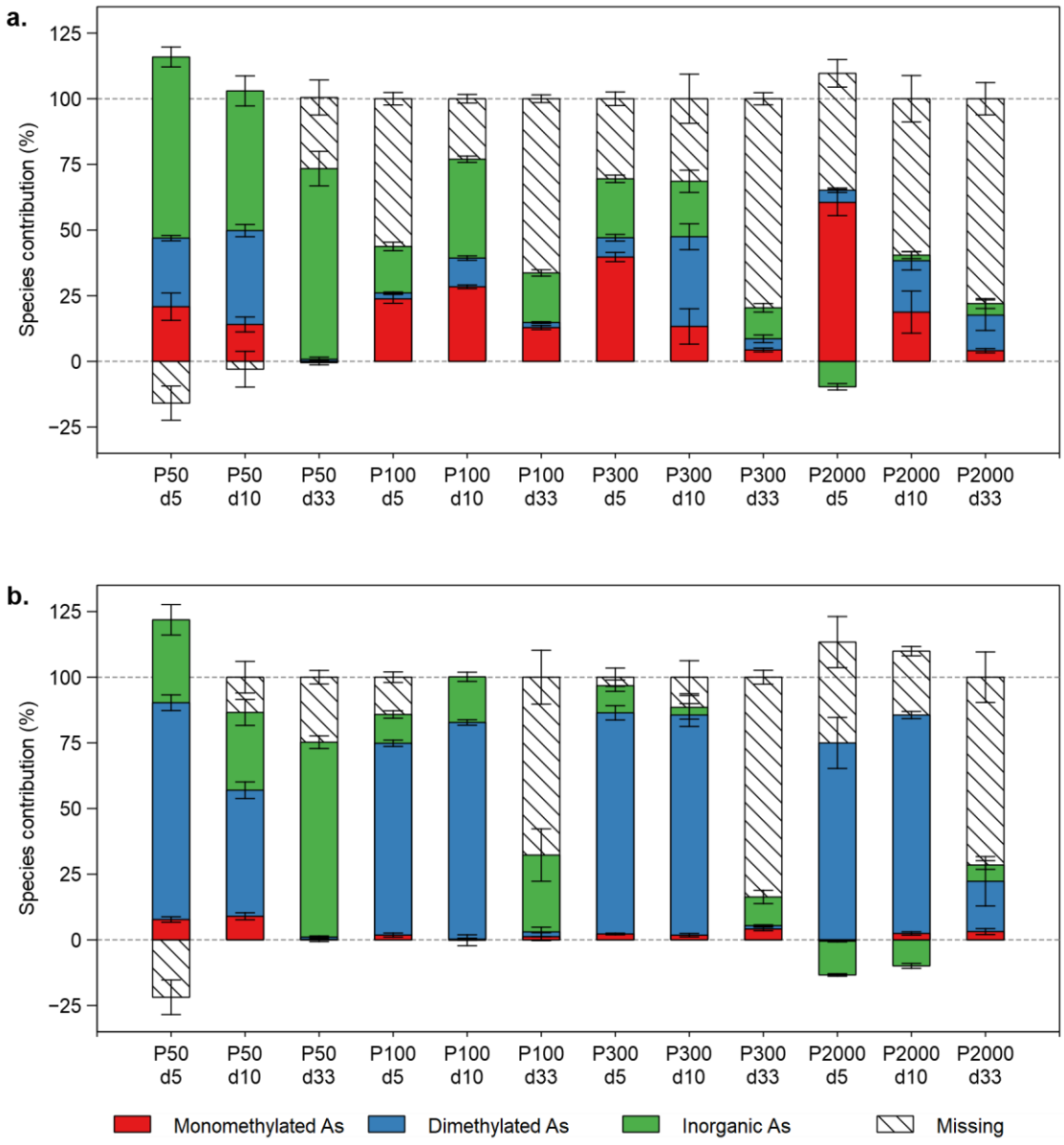

Figure SI11: Contribution of As species in the incubation experiments amended with MMA (a) and DMA (b). Each bar section represents the sum of oxy and thiolated As species corresponding to each group (e.g., Dimethylated As corresponds to the sum of the contributions of DMA, DMMTA and DMDTA). Each species group was corrected by subtracting the concentration found in the original incubation setup (hence the appearance of negative values). The "missing" section corresponds to the difference between the spiked As and the sum of species, likely due to adsorption.

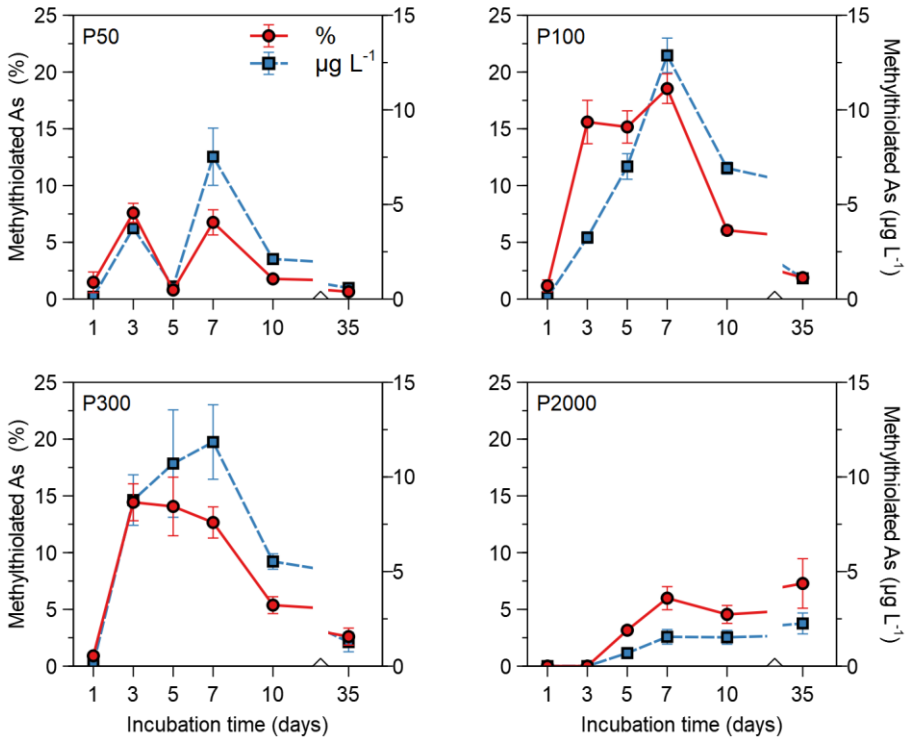

Figure SI12: Contribution of methylthioarsenates to total pore water As speciation for all soils over incubation time. Points represent mean values and error bars their standard deviation (n=3).

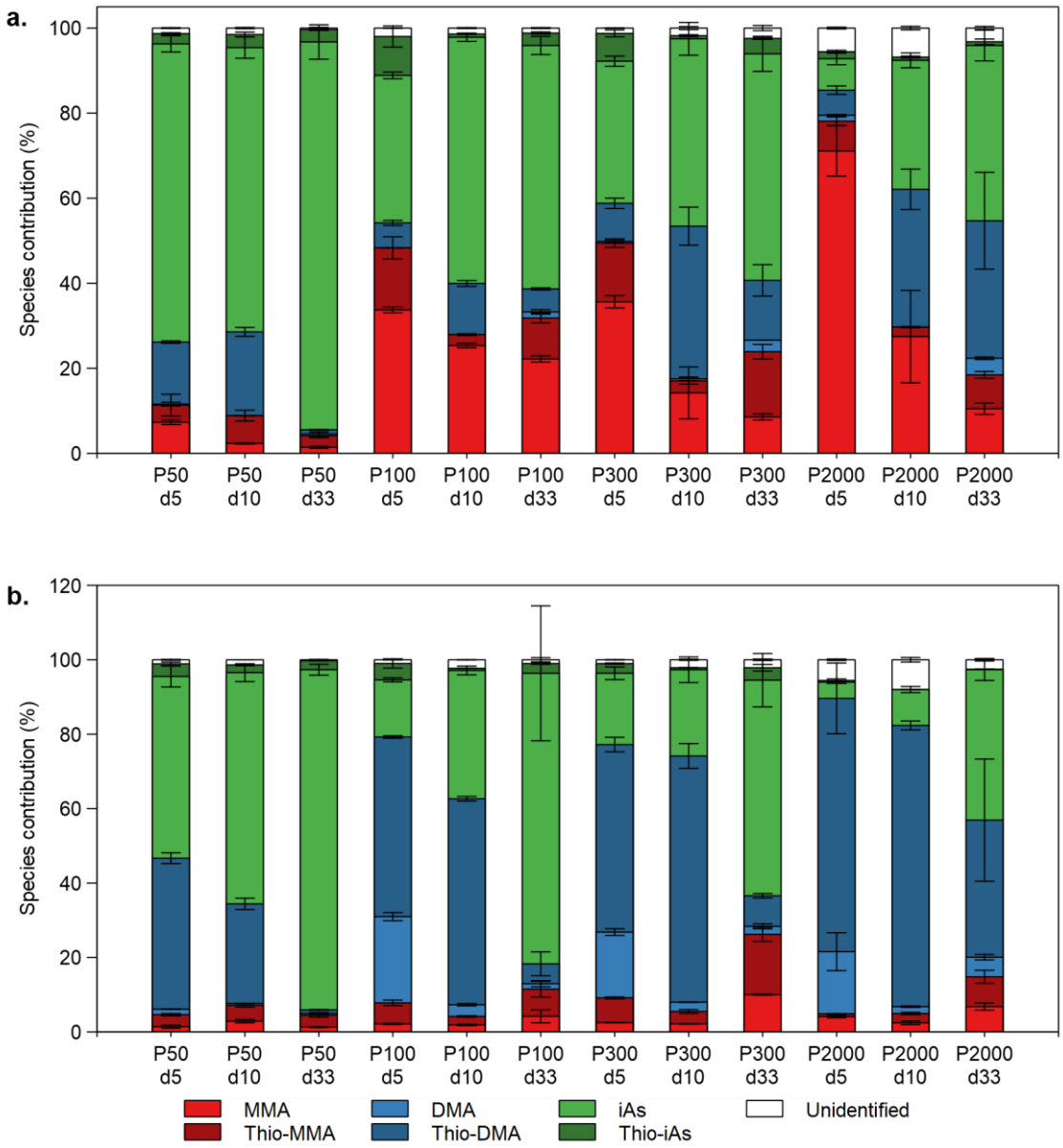

Figure SI13: Contribution of thiolated As species in reference to their oxy analogues in the incubation experiments amended with MMA (a) and DMA (b). Each bar labeled as "Thio-" represents the sum of the contribution of the related thiolated species (e.g., Thio-DMA is the sum of the contributions of DMMTA and DMDTA). "Unidentified" corresponds to a group of non-identifiable As species that elute in the dead volume during the chromatographic separation.

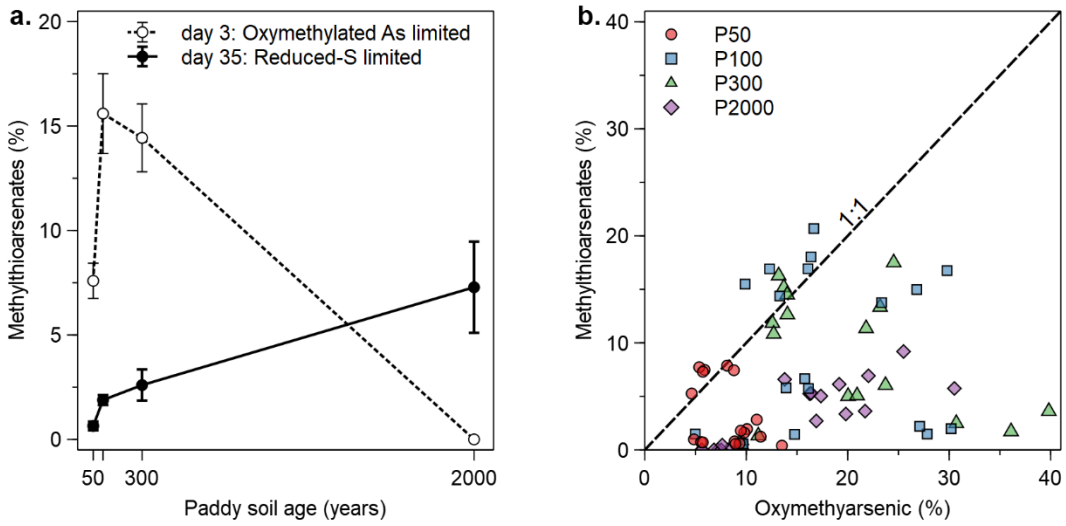

Figure SI14: Effect of paddy soil evolution on formation of methylthioarsenates. Effect of two stages of soil incubation: Oxymethylated-As-limited and reduced-sulfur-limited (a); contribution of methylthiolated species with comparison to their oxymethylated precursors (b). Data points on (a) represent mean values while error bars represent the standard deviation (n=3).

Figures S15 to S18 support the supplementary discussion (see below).

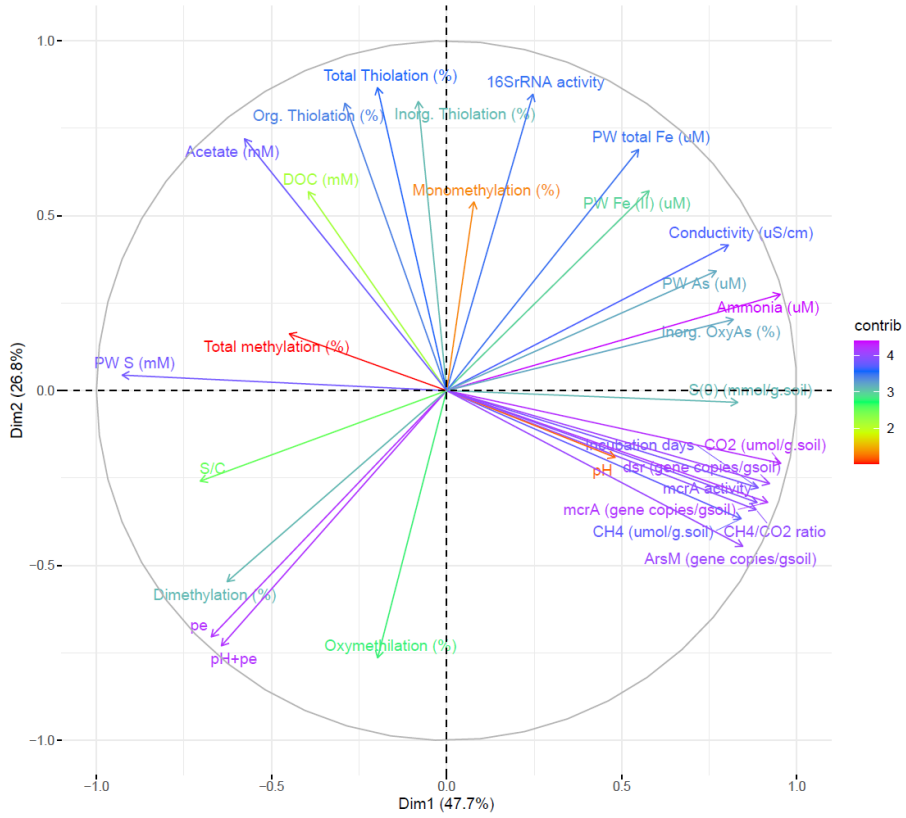

Figure SI15: Principal Component Analysis for P50. See Supplementary Fig. 1 for interpretation.

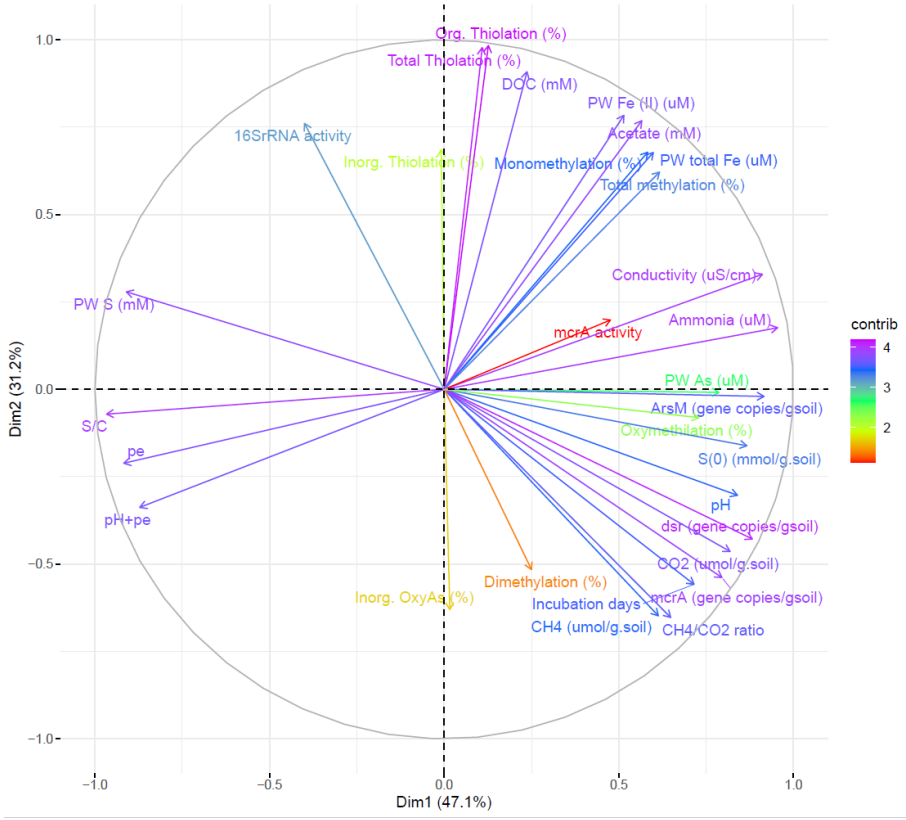

Figure SI16: Principal Component Analysis for P100. See Supplementary Fig. 1 for interpretation.

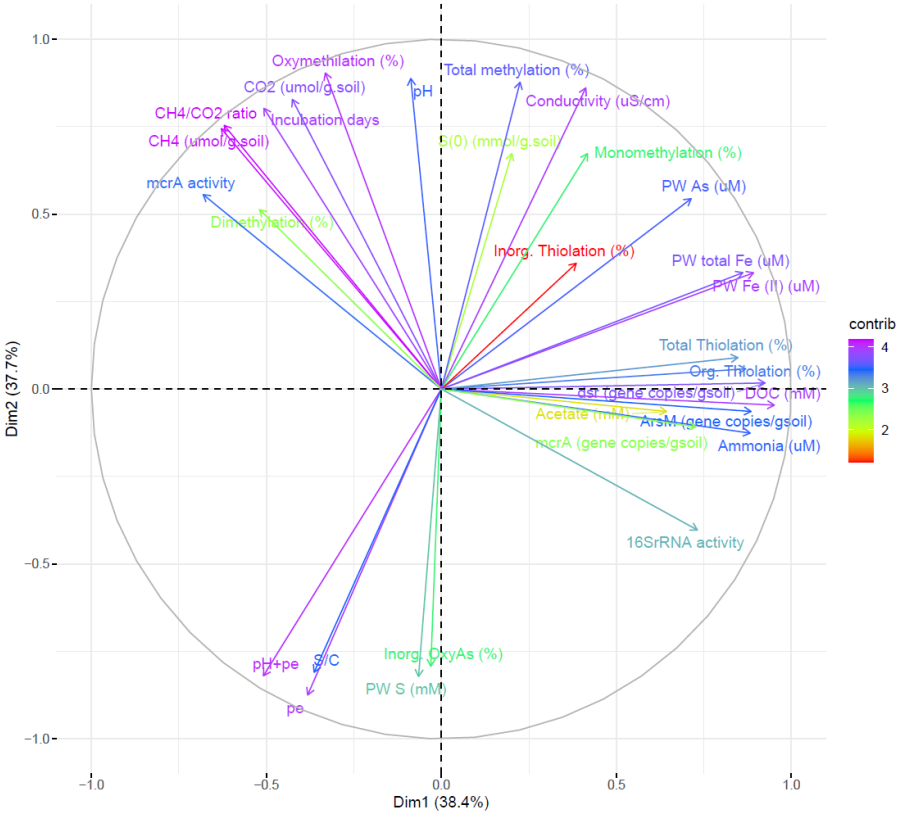

Figure SI17: Principal Component Analysis for P300. See Supplementary Fig. 1 for interpretation.

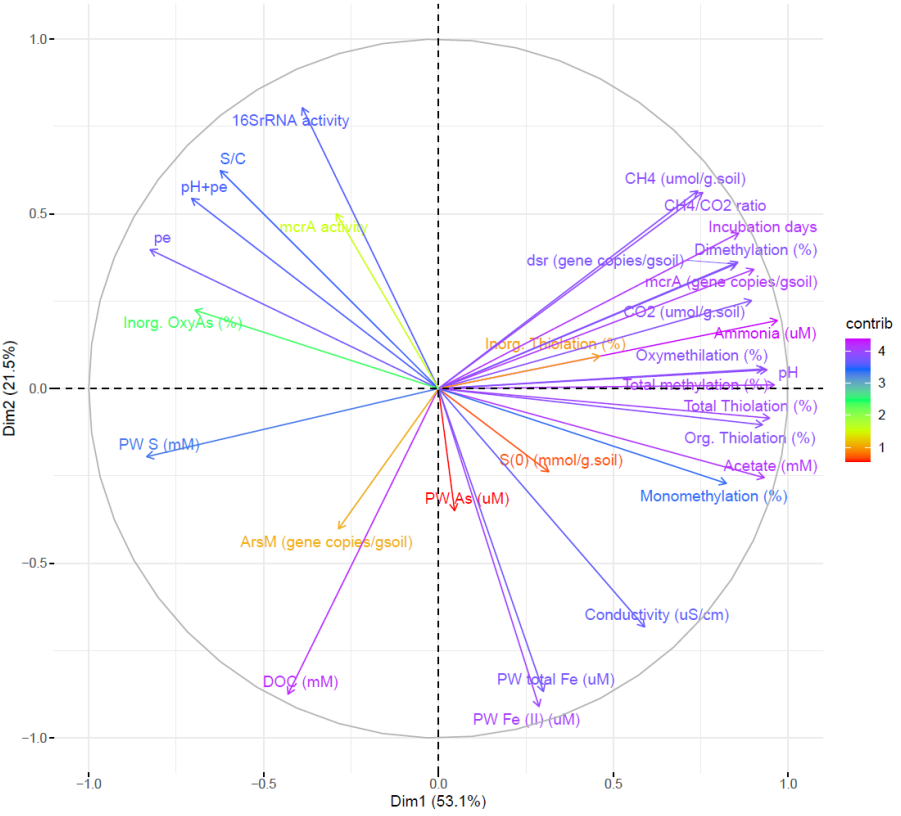

Figure SI18: Principal Component Analysis for P2000. See Supplementary Fig. 1 for interpretation.

Supplementary discussion

HBED for stabilization of As speciation samples

When determining As speciation, precipitation of Fe in the sample is unwanted since some of the As species show high adsorption to Fe phases, hampering the analysis. For this reason, methods which avoid the precipitation of Fe and do not affect the As speciation and the later chromatographic separation are required.

The chelating agent hydroxybenzyl ethylenediamine (HBED) has previously been proven effective in keeping Fe in solution in environmentally relevant laboratory experiments[10]. Although other Fe chelators, such as diethylenetriamine-pentaacetic acid (DTPA), have been used previously when determining thioarsenates in paddy soil porewaters, they have shown low levels of recovery[2]. In order to prove that HBED is an adequate Fe chelator for As speciation samples, different experiments were carried out. The HBED solution used here was initially measured for total As to assess if it contained As. Once verified that the solution´s As background concentrations were below detection limit (0.03 µg/L), HBED was tested in different mixes of As species and paddy soil aqueous phase samples. For all experiments described in this section, 630 µL of the As species mix or samples were stabilized with 70 µL of an HBED 10 mM solution prepared as stated in the main manuscript´s materials and methods section. All tests were carried out inside the anaerobic glovebox, including mixing and sealing of the samples.

First, a mix of the As species used for calibrating the IC-ICP-MS was prepared to evaluate if HBED changed the peak shape or retention times of oxyAs species during chromatography. Arsenite, arsenate, MMA, and DMA were mixed to a final nominal concentration of 5 µg L^{-1} each (20 µg L^{-1} in total). The mix was measured for As speciation with and without adding HBED. The recovery for the mix stabilized with HBED was 101.1% when compared to the non-stabilized one. Arsenic speciation was not affected by HBED addition and peak shapes in the chromatograms did not show significant changes.

Secondly, the stability of As species was tested with different Fe^{III} concentrations in the presence of HBED. For this, a mixed solution of As species in environmentally relevant concentrations was used, which contained 50 µg L^{-1} of arsenite and arsenate each, 10 µg L^{-1} of MMA and DMA each, 15 µg L^{-1} of a mix of methylthioarsenates (including MMMTA, MMDTA, DMMTA, and DMDTA), and 2 µg L^{-1} of MTA, as

representative of inorganic thioarsenates. This mix was combined with a solution of Fe^{III} ($FeCl_3$) in different concentrations (0.005, 0.05, and 0.5 mM) and subdivided into two aliquots. The first aliquot was analyzed immediately, while the second was flash frozen (FF) in dry ice, stored for 4 h, and thawed inside the glovebox before being analyzed for As speciation. This test aimed to evaluate if thawing the samples affected the As speciation (through, for example, precipitation of Fe^{III} phases or de-thiolation of thioarsenates). The speciation analyses of these tests are shown in Figure SI19. No changes were observed in the speciation composition, and the recovery of As in these analyses varied between 98.6 and 105%, compared to the same mix measured without HBED. This test shows that HBED is a suitable chelator agent to avoid Fe-related losses and species transformations when measuring As speciation in paddy soil porewater, including thioarsenates.

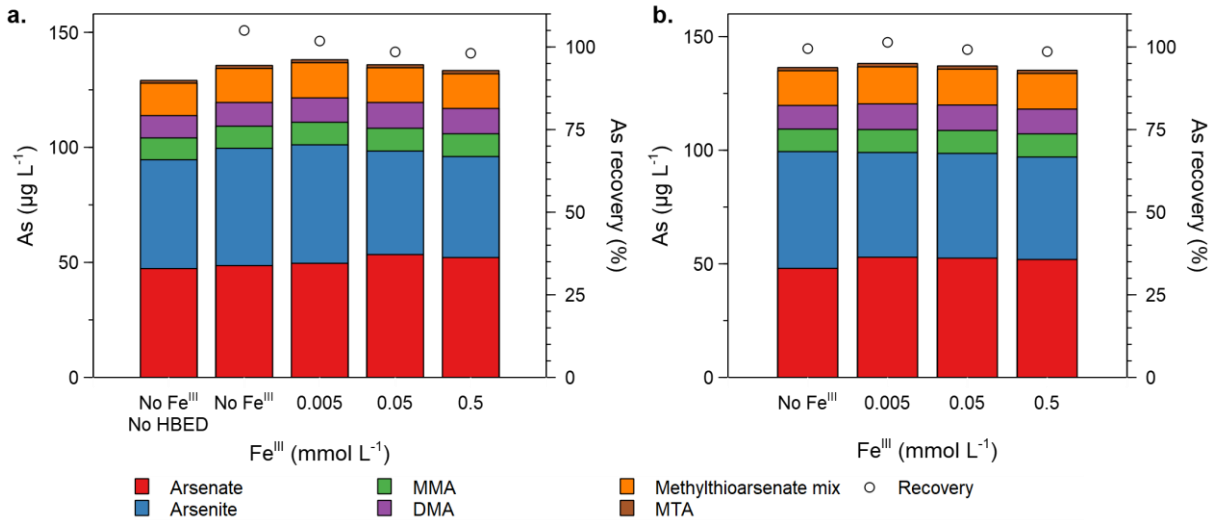

Figure SI19: Stability test of As species in environmentally relevant concentrations in HBED, stabilized with HBED in the presence of different Fe^{III} concentrations, measured immediately (a) and after flash freezing in dry ice and thawing anoxically right before analysis (b).

Stabilization with HBED was tested on two paddy soil aqueous phase samples from incubation experiments like the ones carried out in this study: sample A with a low porewater Fe content (150 µM) and sample B with a higher Fe content (850 µM). Samples A and B had similar, low contents of total As (5.1 and 5.8 µg L^{-1}, respectively), as we intended to show that HBED stabilization is also appropriate for lower As concentrations. Sample A was taken and measured immediately with and without adding HBED. Sample B was taken and split into five aliquots: the first aliquot was measured immediately without stabilization. The second and third were measured immediately with HBED in two different concentrations (0.1 mM and 1 mM). The fourth

and fifth aliquots were flash-frozen with and without HBED, respectively. Sample A (Figure SI20a) showed the improved recovery when using HBED (101.9 vs. 88.2% in the non-stabilized sample) and that, in natural samples, the composition of thioarsenates was not affected by the addition of HBED. Sample B (Figure SI20b), although it showed no thioarsenates content (due to the high Fe content in the porewater), proved that there is a lower recovery when not using HBED or concentrations that are not high enough to complex all available Fe.

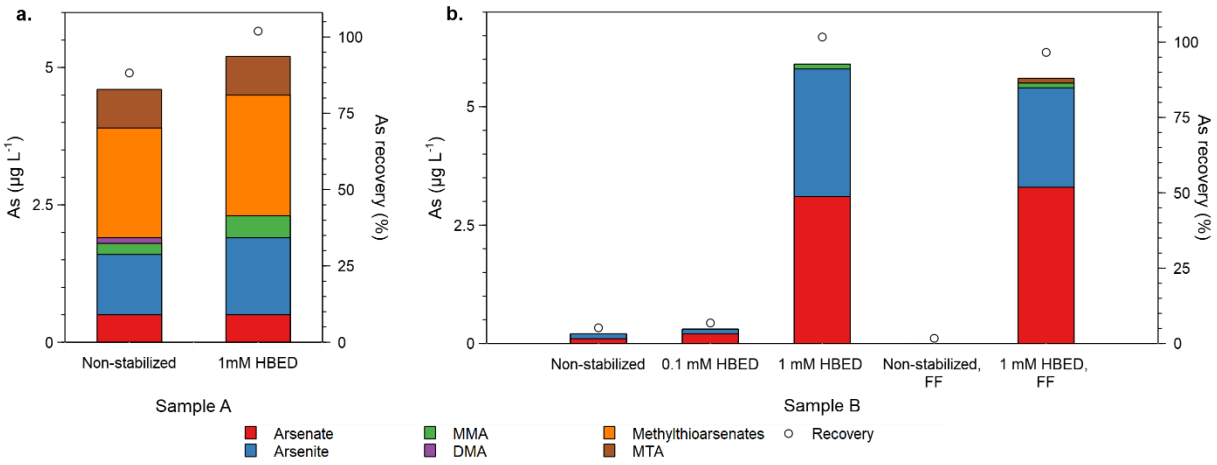

Figure SI20: Stability test of paddy soil aqueous phase samples with HBED. Sample A (a) with low Fe content shows the stability of thioarsenates when adding HBED to natural samples, while sample B (b) with higher Fe content shows the effects of no stabilization or a deficit of HBED on As recovery with and without flash freezing (FF).

Changes in methylating microbial communities with soil evolution

A positive correlation was found between copy numbers of dissimilatory sulfite reductase alpha subunit (*dsrA*, encoding the key enzyme of DSR[11]) and *ArsM* copy numbers (Figure SI21a), which agrees with the observations by Chen et al. [6], that SRB play a significant role in As methylation. However, looking at the absolute concentration of methylated As species rather than their contribution to the sum of species through incubation time for different soils (Figure SI7), their formation in P2000 was not as delayed as sulfate reduction, meaning both processes are not directly coupled, which has been previously suggested by Reid, et al. [12]. Additionally, although the concentration of methylated As started to plateau with increasing methanogenic activity (day 7), methylated As species were still found during the highly methanogenic phase at the end of the experiment (day 35). For P2000, there was even a late increase

in methylated As by day 35, when the soil had the highest methanogenic activity and no further sulfate reduction was taking place (Figure SI5 and SI8c). The occurrence of methylated As species before DSR and their persistence even throughout strong methanogenesis implies that other microbial groups are also importantly related to As (de-)methylation beyond those suggested by Chen et al. [6] Additionally, PCA done for each soil individually (Figures SI15 to SI18) showed that the correlation between *dsrA* and *ArsM* decreased with paddy soil evolution (as the angle between the vectors of both parameters increased with age, suggesting the level of correlation between these two variables decreases). This change suggests that SRB are important for As methylation in early phases of paddy soil development, while other groups may gain relevance with increasing soil age. One of the groups gaining relevance with further soil development could be fermenting bacteria, as proposed by Reid, et al. [12]. Principal component analysis of our complete dataset (Figure SI1) indicated a high correlation between acetate concentration, a major product of fermentative processes, and As methylation. However, direct changes in this correlation with increasing paddy soil age were not observed in the individual PCAs.

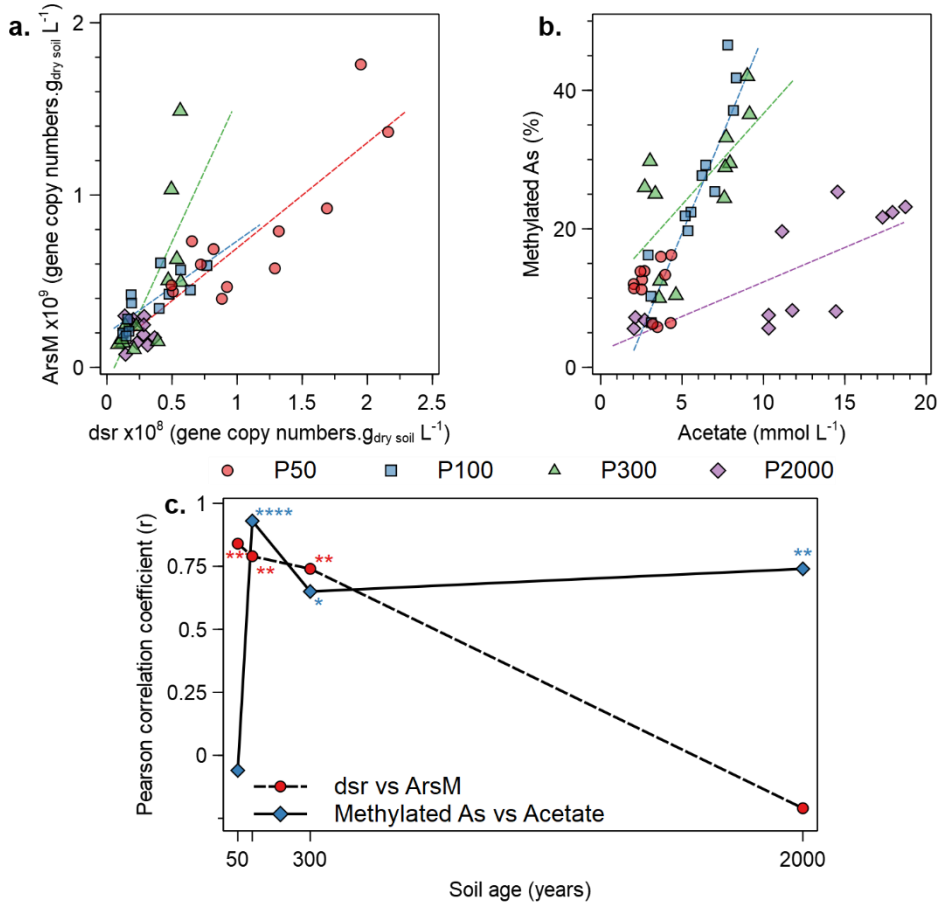

Figure SI21: Shift of microbial activities related to As methylation. Correlation between ArsM and dsr gene copy numbers (a), and correlation between the contribution of methylated As species and aqueous phase acetate concentrations (b). Comparison of the r values for each soil (c). Asterisks indicate the Pearson significance levels (p): * = p < 0.05; ** = p < 0.01; *** = p < 0.001; **** = p < 0.0001. No significant correlation for P2000 was found on ArsM vs. dsr and for P50 on methylated As vs. Acetate. Each Pearson correlation in (a) and (b) has n = 12.

To further statistically assess these changes, Pearson correlation coefficients (r) were obtained from the correlations between *dsrA* and *ArsM* (21a), and for the contribution of methylated As species and acetate concentration in the aqueous phase (Figure SI21b) for each soil, and their changes were compared (Figure SI21c). The correlation between *dsrA* and *ArsM* decreased with age until being not significant for P2000 ($p>0.05$), while the correlation between acetate and As methylation started as not significant for P50 but increased strongly with age. The concept that the microbial community responsible for As methylation in paddy soils shifts with long-term use (e.g., as suggested here, from SRB-driven to fermenter-driven) would reconcile observations from previous studies[6,12] and should be further investigated.

Supplementary references

1 Wallschläger, D. & London, J. Determination of methylated arsenic-sulfur compounds in groundwater. *Environmental Science & Technology* **42**, 228-234 (2008). https://doi.org:10.1021/es0707815

2 Wang, J. *et al.* Thiolated arsenic species observed in rice paddy pore waters. *Nature Geoscience* **13**, 282-287 (2020). https://doi.org:10.1038/s41561-020-0533-1

3 Muyzer, G., Teske, A., Wirsen, C. O. & Jannasch, H. W. Phylogenetic relationships ofThiomicrospira species and their identification in deep-sea hydrothermal vent samples by denaturing gradient gel electrophoresis of 16S rDNA fragments. *Archives of Microbiology* **164**, 165-172 (1995).

4 Nadkarni, M. A., Martin, F. E., Jacques, N. A. & Hunter, N. Determination of bacterial load by real-time PCR using a broad-range (universal) probe and primers set. *Microbiology* **148**, 257-266 (2002).

5 Kondo, R., Nedwell, D. B., Purdy, K. J. & Silva, S. Q. Detection and enumeration of sulphate-reducing bacteria in estuarine sediments by competitive PCR. *Geomicrobiology Journal* **21**, 145-157 (2004).

6 Chen, C. *et al.* Sulfate-reducing bacteria and methanogens are involved in arsenic methylation and demethylation in paddy soils. *The ISME Journal* **13**, 2523-2535 (2019). https://doi.org:10.1038/s41396-019-0451-7

7 Jia, Y. *et al.* Microbial Arsenic Methylation in Soil and Rice Rhizosphere. *Environmental Science & Technology* **47**, 3141-3148 (2013). https://doi.org:10.1021/es303649v

8 Steinberg, L. M. & Regan, J. M. Phylogenetic Comparison of the Methanogenic Communities from an Acidic, Oligotrophic Fen and an Anaerobic Digester Treating Municipal Wastewater Sludge. *Applied and Environmental Microbiology* **74**, 6663-6671 (2008). https://doi.org:doi:10.1128/AEM.00553-08

9 Kölbl, A. *et al.* Accelerated soil formation due to paddy management on marshlands (Zhejiang Province, China). *Geoderma* **228-229**, 67-89 (2014). https://doi.org:https://doi.org/10.1016/j.geoderma.2013.09.005

10 López-Rayo, S., Hernández, D. & Lucena, J. J. Chemical Evaluation of HBED/Fe3+ and the Novel HJB/Fe3+ Chelates as Fertilizers to Alleviate Iron Chlorosis. *Journal of Agricultural and Food Chemistry* **57**, 8504-8513 (2009). https://doi.org:10.1021/jf9019147

11 Klein, M. *et al.* Multiple lateral transfers of dissimilatory sulfite reductase genes between major lineages of sulfate-reducing prokaryotes. *Journal of Bacteriology* **183**, 6028-6035 (2001). https://doi.org:10.1128/jb.183.20.6028-6035.2001

12 Reid, M. C. *et al.* Arsenic methylation dynamics in a rice paddy soil anaerobic enrichment culture. *Environmental Science & Technology* **51**, 10546-10554 (2017). https://doi.org:10.1021/acs.est.7b02970

Study 2: Long-term paddy use influences response of methane production, arsenic mobility and speciation to future higher temperatures.

José M. León Ninin, Alejandra Higa Mori, Johanna Pausch, and Britta Planer-Friedrich

Reprinted with permission from

Science of The Total Environment (*943*, pp. 173793)

Own contribution to Study 2:	
Concept and study design	90%
Data acquisition	40%
Analyses of samples	40%
Data analysis and figure preparation	60%
Discussion of results	70%
Manuscript writing	90%

This study was designed by J.M.L.N. and B.P.-F.; experiments and analyses of samples were carried out by A.H.M, with the support of J.M.L.N. and a master student (see acknowledgments); access to analytical facilities was provided by J.P. and additional analyses were carried out at the Limnological Research Station of the University of Bayreuth (see acknowledgments); data analyses, figure preparation, discussion of results, and manuscript writing were carried out by J.M.L.N. with the support of A.H.M. and B.P.-F.; all authors contributed to the revisions of the published manuscript.

Science of the Total Environment 943 (2024) 173793

Contents lists available at ScienceDirect

Science of the Total Environment

journal homepage: www.elsevier.com/locate/scitotenv

Long-term paddy use influences response of methane production, arsenic mobility and speciation to future higher temperatures

José M. León Ninin [a], Alejandra Higa Mori [a], Johanna Pausch [b], Britta Planer-Friedrich [a,*]

[a] Environmental Geochemistry, Bayreuth Center for Ecology and Environmental Research (BayCEER), University of Bayreuth, 95440 Bayreuth, Germany
[b] Agroecology, Bayreuth Center for Ecology and Environmental Research (BayCEER), University of Bayreuth, 95440 Bayreuth, Germany

HIGHLIGHTS

- Biogeochemical responses to higher temperatures differ between paddies and non-paddies.
- Paddies of long-term use show increased methane production at higher temperatures.
- Paddies of short-term use show higher arsenic mobility at higher temperatures.
- Higher temperatures increase arsenic methylation in all paddies, regardless of age.
- Higher temperatures increase dissolved iron, which limits arsenic thiolation.

GRAPHICAL ABSTRACT

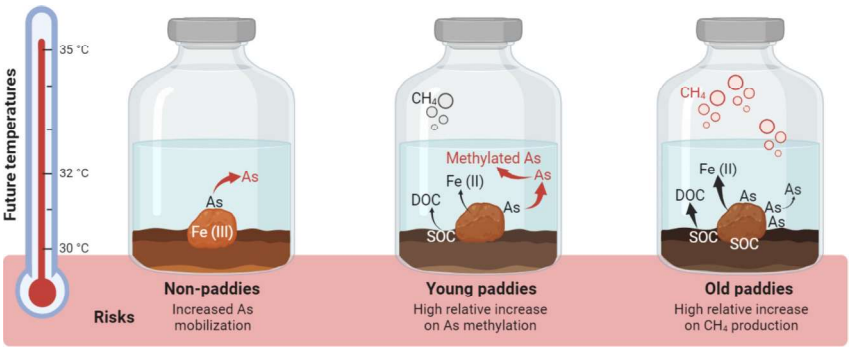

ARTICLE INFO

Editor: Jan Vymazal

Keywords:
Soil development
Biogeochemistry
Chronosequence
Climate change
Methylation
Thiolation

ABSTRACT

Anaerobic microbial metabolisms make flooded paddy soils a major source of the greenhouse gas methane (CH_4) and mobilize toxic arsenic (As), threatening rice production and consumption. Increasing temperatures due to climate change enhance these microbially mediated processes, increasing their related threats. Chronosequence studies show that long-term paddy use ("age") changes soil properties and redox biogeochemistry through soil organic carbon (SOC) accumulation, its association to amorphous iron (Fe) phases, and increased microbial activity. Using paddy and non-paddy soils from a chronosequence as proxies of soil development and incubating them at different temperatures, we show that paddy soil age influences the response of paddies to changes in temperature. Older paddies showed up to a 6-fold higher CH_4 production with increasing temperature, compared to a 2-fold increase in young ones. Contrarily, changes in As mobility were higher in non-paddies and young paddies due to a lack of Fe-SOC-sorption sites. Temperature increased the formation of phytotoxic methylated As in all paddies, posing a risk for rice production. Mitigation strategies for future maintenance, abandonment, or management of paddy soils should include the consideration that history of use shapes the soils' biogeochemistry and microbiology and can influence the response of paddy soils to future temperature increases.

* Corresponding author.
E-mail address: b.planer-friedrich@uni-bayreuth.de (B. Planer-Friedrich).

https://doi.org/10.1016/j.scitotenv.2024.173793
Received 5 April 2024; Received in revised form 14 May 2024; Accepted 3 June 2024
Available online 6 June 2024

1. Introduction

Rice is a crop of global importance, feeding over half of the World's population. In contrast to other cereals, rice is cultivated under flooded conditions in paddy soils (Kögel-Knabner et al., 2010; Meharg and Zhao, 2012). Biogeochemically, these soils undergo strong redox fluctuations, since the standing water and active microbes deplete it from oxygen after flooding (Kögel-Knabner et al., 2010). This depletion creates an anoxic environment where microbial groups use alternative anaerobic respiratory pathways, such as sulfur (S) and iron (Fe) reduction, and methanogenesis (Kögel-Knabner et al., 2010; Sethunathan et al., 1982). In the long-term, the redox fluctuations associated with paddy use alter pedologic properties (Kalbitz et al., 2013; Kölbl et al., 2014; Wissing et al., 2014; Wissing et al., 2011), for example by storing carbon (C) as soil organic carbon (SOC), lowering soil pH, and increasing the share of amorphous Fe phases. In a recent study using a 2000-year old chronosequence we have shown that long-term paddy use (i.e., paddy soil "age") also influences redox biogeochemistry and the above-mentioned respiratory pathways, increasing, among others, the rates of soil respiration, methanogenesis, and Fe reductive dissolution (León Ninin et al., 2024). With increasing paddy soil age, amorphous Fe^{III} phases accumulate and stabilize SOC by mineral associations (Kölbl et al., 2014; León Ninin et al., 2024; Lalonde et al., 2012). The reductive dissolution of these Fe^{III}-SOC associations releases high amounts of Fe^{II} and dissolved organic carbon (DOC) into the aqueous phase, supporting an increased microbial activity (León Ninin et al., 2024).

The alternative respiratory pathways used by microbes under anoxic conditions are responsible for two main concerns related to paddy use. First, methanogenic archaea thrive in paddy soils and release methane (CH_4) as a metabolic by-product (Le Mer and Roger, 2001; Bridgham et al., 2013). Methane is a greenhouse gas with high relevance for climate change since, although it is produced in trace amounts, it has 27 times the warming potential of CO_2 over a 100 year time frame (Forster et al., 2021). Paddies are a major anthropogenic CH_4 source, responsible for the emission of 24 to 31 Tg $year^{-1}$ (11 % of annual agricultural CH_4 emissions) (Forster et al., 2021; FAO, 2022; Qian et al., 2023). Our previous study showed that long-term paddy use increases CH_4 production (León Ninin et al., 2024), due to SOC accumulation, increased microbial biomass and activity, and likely a well-established community of methanogens (Conrad, 2020; Ho et al., 2011).

Secondly, anaerobic microbial activity drives different aspects of the biogeochemistry of arsenic (As). Arsenic is a toxic trace element that accumulates in rice plants and grains, affecting plant yield and representing a risk of As exposure from rice consumption (Stone, 2008; Ma et al., 2008; Zheng et al., 2013). Iron reduction controls the availability of As in the porewater for plant uptake, since the reductive dissolution of As-bearing Fe minerals releases carcinogenic inorganic oxyarsenic species, arsenate and arsenite (Stone, 2008; Smedley and Kinniburgh, 2002; Zobrist et al., 2000). Sulfate reducing bacteria (Chen et al., 2019) (SRB) as well as other microbial groups (Reid et al., 2017) have been proposed as As methylators. Methylated As species (mono- and di-methylarsenate, MMA and DMA, respectively) represent a lower risk for humans but have been reported to cause plant sterility (Zheng et al., 2013; Zhao et al., 2013). The reduced S produced as a by-product of SRB respiration can thiolate As to form thioarsenates. Inorganic and methylated thioarsenates are usually-overlooked, highly mobile and cytotoxic As species that have been found in paddy soil porewater (León Ninin et al., 2024; Wang et al., 2020; Chen et al., 2021a), rice grains, and products (Colina Blanco et al., 2021; Dai et al., 2022; Colina Blanco et al., 2024). Lastly, methanogenesis also has been previously reported as a biogeochemical process affecting As speciation through de-methylation (Chen et al., 2019; Chen et al., 2022; Chen et al., 2023; Zhang and Reid, 2022). Our previous study in the chronosequence showed that long-term paddy use decreases As mobility due to the formation of amorphous Fe^{III}-SOC associations that act as effective sorption sites. Additionally, the increased microbial activity and SOC accumulation with increasing paddy soil age enhances As methylation, particularly during the first 300 years of paddy use (León Ninin et al., 2024). Regarding As thiolation, increased SOC and dissolved Fe^{II} with long-term paddy use scavenge reduced S, decreasing its availability for thioarsenate formation.

The rates of these microbially mediated processes are reported to be enhanced by temperature (Frey et al., 2008; Castro et al., 2010; Bradford et al., 2008). In the context of anthropogenic climate change, several studies have shown how higher temperatures could increase As mobility, methylation and thiolation (Chen et al., 2021a; Muehe et al., 2019; Farhat et al., 2021; Neumann et al., 2017; Müller et al., 2022), while the reports regarding CH_4 production are contradictory and depend on agricultural practices (van Groenigen et al., 2011; Cheng et al., 2006; Tokida et al., 2011; Gaihre et al., 2013). These observations have been partially attributed to SOC being an important factor determining soil responses to changes in temperature (Wei et al., 2019; Su et al., 2024). However, it remains unknown how the systematic accumulation of SOC as a cause of long-term paddy use can affect these temperature responses. More generally, a better understanding of how the pedologic and redox changes related to paddy soil aging could be influenced by increasing temperatures in the future is lacking.

Here, we incubated soils from a well characterized 2000-year-old paddy soil chronosequence at different temperatures. The advantage of using selected soils of such a chronosequence is that they provide a range of stages in paddy development, which allow a broad understanding of paddy soil biogeochemistry. Our aim was to investigate whether there is a link between long-term paddy use and the degree to which CH_4 and As biogeochemistry are affected by increasing temperatures. In this sense, we are using this chronosequence as a tool to understand how intrinsic pedological changes associated with paddy management affect their response to increasing temperatures. We hypothesize that higher temperatures will accelerate microbial processes to a greater extent in older paddies, with more active microbes sustained by higher SOC, leading to increased methanogenesis and As methylation. However, we expect older paddies to remain unaffected by temperature increase in terms of As mobility due to abundant Fe^{III}-SOC sorption sites. Additionally, we used non-paddy soils to understand how the development of new fields could be affected by future warmer temperatures, as well as to determine if such a response to increasing temperatures is indeed related to long-term paddy use.

2. Materials and methods

2.1. Incubations from soil chronosequence

Incubation experiments were carried out with soils from a paddy soil chronosequence located around Cixi, in the delta of the Yangtze River in the province of Zhejiang, China (Kölbl et al., 2014; Cheng et al., 2009). Through sedimentation and dike building, land reclamation for agricultural purposes has been taking place from saltmarshes since approximately 2000 years. The building dates of the dikes allow an estimation of the age of the arable land and its management as paddies and non-paddies. For this study, the ≤2 mm fraction of the topsoil of the main sites described by Cheng et al. (2009) and Kölbl et al. (2014) were used, representing paddies (P) with ages of 50, 100, 300 and 2000 years. Two additional non-paddy soils (NP) from the same chronosequence, used for upland agriculture and with ages of 50 and 700 years, were also incubated as representatives of upland systems. The soils were characterized for As binding mechanisms by sequential extraction procedures (SEP), proposed by Fulda et al. (2013). A detailed description of the procedure can be found in the supporting information (supplementary methods, Table SI1). Selected soil properties can be found in Table SI2.

For the incubations, 10 g of soil and 20 mL of N_2-purged tap water were added into 120 mL septum vials in triplicate under anoxic conditions inside a glovebox (95 % N_2, 5 % H_2, COY). The vials were closed with butyl rubber stoppers and aluminum caps, shaken to mix the slurry and incubated standing at 30, 32, and 35 °C. While 30 °C represents the

average maximum temperature in Cixi during the cropping season between April and September, 32 °C and 35 °C correspond to +2 °C and + 5 °C increases in air temperature for IPCC scenarios SSP2–4.5 and SSP5–8.5 in the region, respectively (Muehe et al., 2019; Le Quéré et al., 2018). Data used in this publication for the paddy soils incubated at 30 °C has been previously published in León Ninin et al. (2024).

2.2. Sampling

The corresponding triplicate vials were sampled sacrificially after 1, 3, 5, 7, and 10 days of incubation. These days were selected based on the dynamics of redox processes that we described before in the chronosequence (León Ninin et al., 2024). The vials were removed from the water bath, shaken, and allowed to reach room temperature (20 °C) before measuring the inner pressure of the vials using a handheld pressuremeter (Greisinger GMH, 3100 Series), followed by sampling the headspace with a gas-tight syringe and needle. Approximately 5 mL of headspace were sampled from each vial and stored in evacuated glass vials until CH_4 and CO_2 determination using a gas chromatograph with a Flame Ionization Detector (GC-FID, SRI Instruments 8610C) equipped with a methanizer.

The vials were then brought into the glovebox and shaken to form a homogeneous slurry that was transferred into 50 mL centrifuge tubes. The tubes were closed and wrapped in Parafilm before being centrifuged for 10 min at 4000 rpm outside the glovebox. The tubes were brought back into the glovebox and the aqueous phase was separated from the soil with syringe and needle. The aqueous phase was split into different aliquots for different geochemical analyses described below.

2.3. Aqueous phase analyses

To measure dissolved organic carbon (DOC), 2 mL of aqueous phase were filtered through a 0.45 μm polyamide filter (Chromafil® Xtra), acidified with 40 μL of 6 M HCl and kept at 4 °C until analysis (Multi N/C 2100 S, Analytik Jena). For the rest of the analyses, the aqueous phase was filtered through 0.2 μm cellulose-acetate filters (Chromafil® Xtra). Inside the glovebox, a multiparameter (HQ40d, Hach) connected to the respective electrodes was used to measure pH (PHC301, Ag/AgCl electrode) and redox potential (MTC101).

Photometric determinations following the Ferrozine method (Stookey, 1970; Hegler et al., 2008) for total Fe and the methylene blue method (Cline, 1969) for sulfide were carried out. After stabilization, colorimetric reactions and measurements were done outside the glovebox. All photometric determinations were carried out in triplicate using a multiplate reader (Infinite® 200 PRO, Tecan). Samples were diluted, if necessary, with ultrapure deionized water (Millipore, 18.2 MΩ cm).

Total As and S were determined by Inductively Coupled Plasma-Mass Spectrometry (ICP-MS, 8900 Triple Quad, Agilent) in reaction mode with O_2. Arsenic was measured as AsO^+ (*m/z* 91) and S as SO^+ (m/z 48). Detection limits were 0.01 μg L^{-1} for As and 21 μg L^{-1} for S. For this analysis, a 2 mL aliquot was stabilized with 0.5 % H_2O_2 and 0.8 % HNO_3 and diluted before analysis. Rhodium was used as internal standard to compensate for signal drift and a certified reference material (TMDA 62.2, Environment Canada) was used for quality control.

For the determination of As speciation, a 700 μL aliquot was stabilized with 100 μL of hydroxybenzylethylenediamin (HBED, pH 7) (León Ninin et al., 2024). An HBED solution of 10 mmol L^{-1} was used to stabilize samples with Fe concentrations <1 mmol L^{-1} and a 59 mmol L^{-1} solution was used for those with higher Fe concentrations. Stabilized samples were frozen with dry ice and stored at −20 °C until analysis. Arsenic speciation was determined by ICP-MS after chromatographic separation by ion chromatography (IC, 940 Professional IC Vario Metrohm). The chromatographic separation was done using an AS16 column (Dionex AG/AS16 IonPac column), with a 2.5–100 mM NaOH gradient, 1.2 mL min^{-1} flow rate, and an injection volume of 50 μL (Planer-Friedrich et al., 2007). Samples were thawed inside the glovebox before analyses to avoid changes in speciation due to oxidation. Individual As species were assigned based on previously reported retention times (Wang et al., 2020; Wallschläger and London, 2008; Wallschläger and Stadey, 2007). Concentrations were calculated through a linear calibration containing arsenite (NaAsO2, Fluka), arsenate ($Na_2HAsO_4 \times 7H_2O$, Fluka), MMA ($CH_3AsNa_2O_3 \times 6H_2O$, Supelco), and DMA ($C_2H_6AsNaO_2 \times 3H_2O$, Sigma-Aldrich). Detection limit for As species was 0.02 μg L^{-1}. Because of the unavailability of commercial standards for thioarsenates, concentrations of thiolated As species were calculated based on their oxyarsenic homologues: inorganic thioarsenates (mono-, di-, and trithioarsenate) were calibrated through arsenate, monomethylated thioarsenates (monomethyl mono-, di-, and trithioarsenate) through MMA, and dimethylated thioarsenates (dimethyl mono- and dithioarsenate) through DMA. Throughout the following text, rather than describing the species individually, they will be grouped as inorganic oxyarsenic, oxymethylarsenates, inorganic thioarsenates and methylthioarsenates. An example chromatogram, names, abbreviations, and grouping can be found on Figure SI1.

2.4. Statistical analyses

Mean and standard deviation were calculated for each measured variable. Relative change of biogeochemical parameters with temperature was calculated by dividing the absolute difference of said parameter at both temperatures by the value of the parameter at the higher temperature. These values are shown in percentages throughout the text and figures. One- or Two-way-ANOVAs were used to determine the individual or combined effects of paddy soil age and incubation temperature (*P*-values are summarized in Tables SI 3 and 4, and additional statistical data can be found in the supplementary files). ANOVAs were carried out using the "Analysis ToolPak" Add-In for Microsoft Excel. Pearson correlation coefficients were used to assess the significance of the presented correlations, and done using RStudio (R Development Core Team, 2008).

3. Results and discussion

3.1. Temperature effect on general redox (biogeo)chemistry

Previous studies have established that increases in temperature enhance microbially mediated processes in redox dynamic soils (Weber et al., 2010). The results of our incubations using the 2000-year-old paddy soil chronosequence revealed that the magnitude of such enhancement is strongly influenced by soil age. Fig. 1a and b show dissolved Fe concentrations at 30 °C versus 32 °C (from now on referred as 30–32 °C), and 32 °C versus 35 °C (32–35 °C), respectively. Concentrations of dissolved Fe increased from non-paddies to paddies with increasing age as reported before (León Ninin et al., 2024). Moreover, deviations from the 1:1 line indicate that there was a temperature effect on Fe reductive dissolution. These deviations are presented as relative change in Fig. 1c for 30–32 °C and Fig. 1d for 32–35 °C. Fig. 1c shows that non-paddies had a negative relative change, indicating an average decrease on dissolved Fe concentrations, while the positive relative change in paddies indicates enhanced Fe reductive dissolution. Furthermore, the relative change in dissolved Fe concentration in paddies increased with soil age. Relative change was larger between 30–32 °C (Fig. 1c) than between 32–35 °C (Fig. 1d). Two-way ANOVA confirmed that paddy soil age and incubation temperature had a significant individual effect on dissolved Fe concentrations, as well as a significant interaction between both factors ($p < 0.05$). Dissolved Fe concentrations over incubation time (Fig. SI2a-d), were enhanced both in magnitude (higher peaks) and kinetics (earlier peaks) at the higher temperatures. Across the non-paddy incubations there was a constant increase of dissolved Fe concentrations with incubation time (Fig. SI3a, b), opposite to the bell-shape observed in paddy soils (Fig. SI2a-d).

Similar to what was observed for Fe, DOC concentrations increased

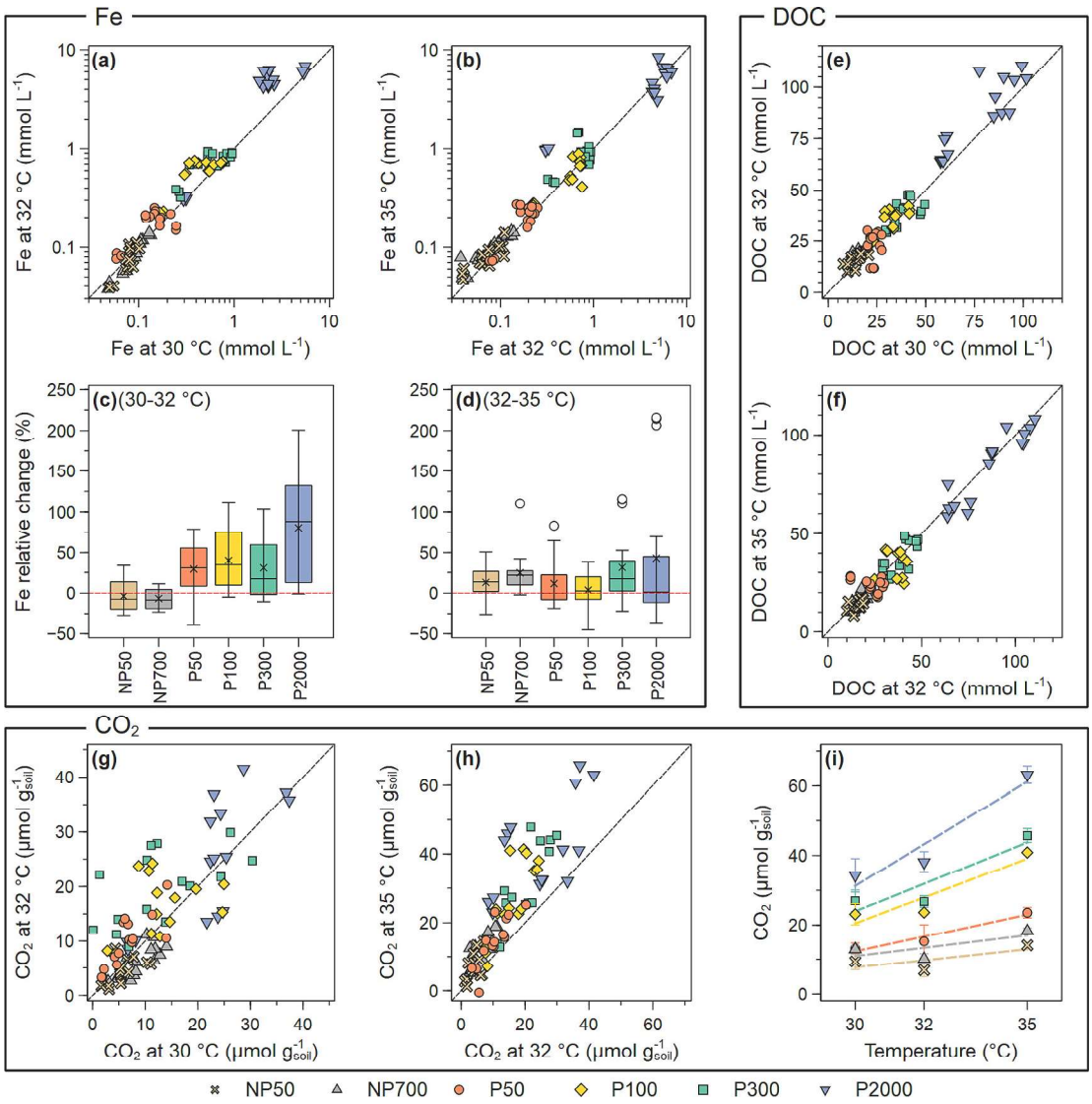

Fig. 1. Changes in selected biogeochemical parameters through the chronosequence with increasing temperature. Comparison of dissolved Fe concentrations between 30–32 °C (a) and between 32–35 °C (b). Relative change in dissolved Fe concentration, integrated over all incubation times, based on both temperature comparisons (c, d). Comparison of DOC concentrations between 30–32 °C (e) and between 32–35 °C (f). Comparison of CO_2 production between 30–32 °C (g) and between 32–35 °C (h). Effect of incubation temperature on CO_2 production by the end of the experiment (day 10) (i). For c and d, each box summarizes the results of triplicates through the incubation time ($n = 15$), with "x" showing the mean value and white circles showing outliers (1.5 IQR). For i, data points represent averaged results and error bars show standard deviation ($n = 3$). For the rest of the plots, data is displayed as individual results of experimental triplicates from all 5 incubation times (n = 15), color-coded per soil. The black dotted line represents a 1:1 line. Note logarithmic scale for (a) and (b).

from non-paddies to paddies with increasing age (Fig. 1e,f). Temperature showed only small effects on DOC concentrations, slightly enhancing them for a 2 °C increase (30–32 °C) (Fig. 1e, Fig. SI4), while for a further 3 °C increase (32–35 °C) the relative change was around the zero % line (Figs. 1f, SI4). Looking at the temporal resolution (Fig. SI2e-h for paddies, Fig. SI3 c,d for non-paddies), higher temperatures slightly increased DOC release in early days in the incubation, but also caused a stronger and earlier decrease.

Higher incubation temperature also caused an increased CO_2 production in all paddies (Fig. 1g,h), especially when incubated at 35 °C (Fig. SI5). A two-way ANOVA confirmed that the CO_2 production by the end of the experiment (day 10) was significantly ($p < 0.05$) affected individually by paddy soil age and temperature, and by the interaction of both factors. When plotting the final CO_2 produced by day 10 against the incubation temperature (Fig. 1i), all paddies showed a positive slope which increased with paddy soil age, indicating that older soils with higher soil C stocks have a greater response on CO_2 production at high temperatures. Soil respiration in non-paddies was only half of the values observed in paddy soils. Temperature had contrasting effects on the CO_2 production in non-paddies, with 32 °C causing generally lower respiration and being distinctively different from the effect of temperature in paddy soils, and with 35 °C enhancing it (Fig. SI5). For non-paddies, a two-way ANOVA showed that temperature and age had individual significant effects ($p < 0.05$) on the final CO_2 production but no significant interaction between both factors.

The above-described observations can be explained when considering paddy soil development. Increased Fe dissolution with paddy soil age is related to the formation of amorphous Fe^{III} phases with SOC accumulation, which changes the structure of Fe oxyhydroxides upon reprecipitation (Kölbl et al., 2014). These Fe^{III}-phases are known to be more easily reduced at higher temperatures (Schwertmann, 1991), explaining why the magnitude of the increase of dissolved Fe is higher with increasing temperature and age. A significant Pearson correlation between dissolved Fe and DOC (r: 0.9, $p < 0.0001$; Fig. SI6), as well as

their similar temporal dynamics (Fig. SI2) suggests that DOC is mainly released from the reductive dissolution of Fe-SOC mineral associations. However, this could also indicate that the increased availability of DOC with increasing soil age enhances Fe reductive dissolution. The effective removal of DOC from the paddy incubations with increasing time at higher temperatures suggests effective microbial consumption of organic substrates, supported by the increased CO_2 production. Increased soil respiration in paddies indicates that their role as C sinks (Kögel-Knabner et al., 2010; Chen et al., 2021b) could be negatively affected by increasing temperatures, particularly in older paddies where more SOC is stored.

Non-paddy soils are subject to different agricultural practices like tillage, which aerates the soil releasing accumulated SOC as CO_2 into the atmosphere, lowering the SOC pool and hampering the formation of amorphous Fe^{III} phases (Kölbl et al., 2014; Rhoton et al., 2002) (Table SI2). Non-paddy soils are thus generally less dynamic systems once they are flooded and exposed to different temperatures. The constant increase of Fe concentrations in the aqueous phase of the non-paddy incubations can be explained when considering that the main mechanism removing reduced Fe from solution is the precipitation of Fe–S phases (Xu et al., 2019; Saalfield and Bostick, 2009), once SRB perform dissimilatory sulfate reduction (DSR). A decrease of total aqueous phase S with incubation time in paddies and non-paddies (Fig. SI7) indicates effective DSR. The amount of S in non-paddies was lower than in paddies, meaning that there was less reduced S available to precipitate dissolved Fe and remove it from the aqueous phase. This lower availability of reduced S in non-paddies explains the constantly increasing dissolved Fe concentrations in these soils, compared to the bell-shaped curve described for paddies (Figs. SI2a-d and SI3a,b). Furthermore, the lower DOC concentrations in non-paddies, as well as a different microbial community which is likely not adapted to anoxic and suboxic environments, decreases microbial activity under flooded conditions in comparison to paddies (Wei et al., 2022). The lower microbial activity in the incubations of flooded non-paddies was reflected in lower

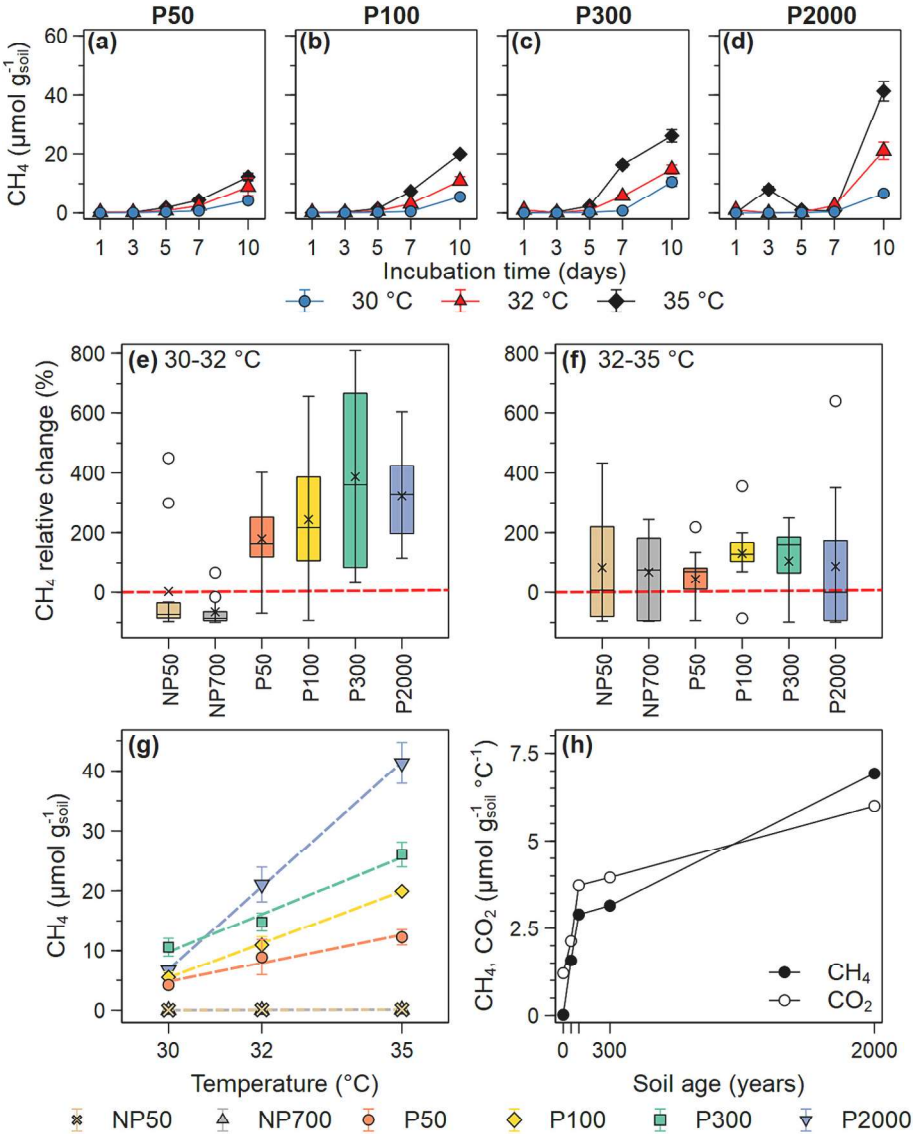

Fig. 2. Methane production in the paddy soils at different temperatures over time (a-d). Relative change in the CH_4 production between 30–32 °C (e) and between 32–35 °C (f), integrated over all incubation times. Effect of incubation temperature on CH_4 production by the end of the experiment (day 10) (g). Response of CH_4 and CO_2 production to changes in temperature in paddy soils (h), based on the slopes of (g) and Fig. 1i. Averaged values of NP50 and NP700 are used in (h) to represent a paddy soil of 0 years. For a-d, and g, data points represent averaged results and error bars show standard deviation ($n = 3$). For e and f, each box summarizes results of triplicates through the incubation time ($n = 15$), with "x" representing the mean value and white circles showing outliers (1.5 IQR). Data for CH_4 production in non-paddies is found in Fig. SI9.

CO_2 production and in higher Eh values, when compared to those in paddies (Fig. SI8).

Considering that increased temperature had stronger effects on the biogeochemistry of Fe and C in paddy soils than in non-paddies, we suggest that it is long term paddy management that creates the temperature-induced differences under flooded conditions. In the following sections, we will describe how these differences in biogeochemistry with long-term paddy use also influence the response of CH_4 production, As release, and affect As speciation to changes in temperature.

3.2. Temperature effect on methane production

Increasing incubation temperature caused higher CH_4 production in all paddies (Fig. 2a-d). The relative magnitude of this increase depended on the age of the paddies when considering 30–32 °C (Fig. 2e). Non-paddies showed a much lower CH_4 production than paddies (Fig. SI9) and even a negative relative change in CH_4 production at 30–32 °C (Fig. 2e). Further increasing the incubation temperature to 35 °C enhanced CH_4 production in all soils (Fig. 2f), including non-paddies, but overall showing a lower relative change when comparing 32–35 °C to 30–32 °C and not being systematic with paddy soil age.

A two-way ANOVA showed that the amount of CH_4 produced by day 10 was significantly influenced by paddy soil age and incubation temperature, as well as by the interaction of both factors ($p < 0.05$). Non-paddies showed no significant difference in their final CH_4 production with increasing temperature. Methane produced by day 10 showed a positive correlation with incubation temperature for all paddies (Fig. 2g), with slopes increasing with paddy soil age (Fig. 2h), indicating that the magnitude of the response to produce more CH_4 per increasing °C is highly dependent on soil age. This age-related trend was also found for CO_2 (based on results from Fig. 1i).

The increased response with paddy age to produce more CH_4 and CO_2 could have several explanations. Long-term paddy use enhances microbial biomass (Table SI5) and activity, meaning that older soils generally have a higher microbial activity that could respond to changes in temperature (Ho et al., 2011; Wang et al., 2021; Wang et al., 2015; Bannert et al., 2011; Liu et al., 2023). Increased microbial activity with paddy soil age can be observed in our experiments when comparing CO_2 production (as a proxy of microbial respiration) at a fixed temperature across paddy soil ages (Fig. SI2). It has been separately reported that long-term paddy use (Conrad, 2020; Ho et al., 2011) and increased temperature (Zhang et al., 2023; Mohanty et al., 2007; Lee et al., 2014) promote CH_4 production through enhanced activity of methanogens. To the best of our knowledge, this is the first time that both these parameters have been studied together. Older paddies also have a bigger pool of organic substrates that can support higher microbial activity, including that of methanogens (Table SI2, Fig. 1e,f). The importance of labile organic substrates regarding soil response to increased CH_4 and CO_2 production with temperature changes has previously been studied in batch experiments amended with C sources (Wei et al., 2019), where it was shown that the effect of temperature change is limited by labile C availability. The labile DOC from P50 may have been consumed rapidly by microorganisms with increasing temperature, before redox conditions for methanogenesis were reached, leading to a lower CH_4 production and lower relative change to increased CH_4 production. In contrast, we have previously reported (León Ninin et al., 2024) that P2000 has a high amount of labile organic C. This pool of labile C was likely still available for methanogens once other preferred metabolic pathways were exhausted. Additionally, we had previously reported that the high availability of Fe^{III} (oxy)hydroxides with increasing age delayed the start of methanogenesis at 30 °C (León Ninin et al., 2024; Luo et al., 2023; van Bodegom et al., 2004). Under higher temperatures, an accelerated reductive dissolution of Fe^{III} phases shortened this inhibition period. For non-paddies, it is likely that there is no established methanogenic community to be affected by changes in temperature (Liu et al., 2018). Furthermore, non-paddies also showed lower levels of DOC, which as mentioned above, is a limiting factor on how sensitive soils are to show changes in CH_4 production at different temperatures (Wei et al., 2019).

Moreover, according to the Carbon-Quality Temperature (CQT) hypothesis, recalcitrant C compounds have a higher sensitivity to changes in temperature, based on their activation energies (Craine et al., 2010; Davidson and Janssens, 2006). Previous studies carried out in the Cixi chronosequence focused on SOC accumulation and soil development, with contrasting reports regarding SOC quality. While some studies report no significant difference in C quality across the chronosequence (Hanke et al., 2013; Zhou et al., 2014), others find accumulation of lignin phenols and humic substances (Wang et al., 2015; Liu et al., 2023). A recent study from Su et al. (2024) determined that, in paddy soils, the effects of the CQT hypothesis are more relevant with increasing depth, as recalcitrant compounds become more abundant. In the topsoil of paddies (like the ones used in our study), the degradation of labile organic matter was the determining factor increasing the response of CH_4 production with higher temperatures.

The effect of long-term paddy use on the response of CH_4 production to increased temperature can be linked to previous contrasting results. While some studies have shown none (Wang et al., 2022), slightly positive (Yun et al., 2012), or negative (Ziska et al., 1998) effects on CH_4 production when exposing paddy soils to higher temperatures, most studies have reported increases (Pereira et al., 2013; Tokida et al., 2010; Xu et al., 2020). Although cropping systems and climate have been proposed as reasons for these contrasting responses (Zhang et al., 2023), we suggest based on our results that paddy soil age can also be a contributing factor since it is directly reflected in methanogenic communities, SOC as substrate and Fe^{III}-phases as a possible inhibitor of methanogenesis. It must be noted, however, that although paddy soil development is a general process for all flooded rice fields, the rates at which changes take place also depend on climate and cropping practices.

Our results show that as paddy soils develop, the accumulated C and increased microbial activity increases CH_4 production in paddies compared to non-paddies with lower SOC contents. The C accumulated through long-term paddy use provides methanogens (and other bacterial groups) with substrates, increasing their response to changes in temperature, and thus, soil response to CH_4 and CO_2 production. These results are particularly important when considering CH_4 emission models and future predictions related to climate change. The current CH_4 emission estimations from paddy soils are between 31 and 112 Tg $year^{-1}$. The broad range of this estimation comes from lack of data regarding total irrigation area and differences in emissions with different agricultural practices (Van Amstel, 2012). It has also been reported that environmental parameters such as organic matter content, pH and redox potential affect CH_4 emissions from paddy soils and affect the precision of such predictions (Yang and Chang, 1998). Since long-term paddy use affects these parameters, considering paddy soil age in models is necessary to get more accurate predictions both for today's climate and for future climatic conditions. Since determining paddy soil age is currently difficult (in the absence of a record like the one existing for the Cixi chronosequence), we suggest that in the meantime, models should try to include the potential increase in CH_4 production not only because of increasing temperature, but also as a consequence of paddy soil aging itself. In the case of CO_2 production, our results suggest that older paddy soils with higher C stocks could be more sensitive to release stored C under future higher temperatures, having negative implications for paddy soils acting as C sinks.

3.3. Temperature effect on As mobility

Higher temperatures generally mobilized more As from all soils (Fig. 3a,b). The aqueous As concentrations were significantly higher ($p < 0.05$) at 32 °C and 35 °C compared to 30 °C, particularly in the early

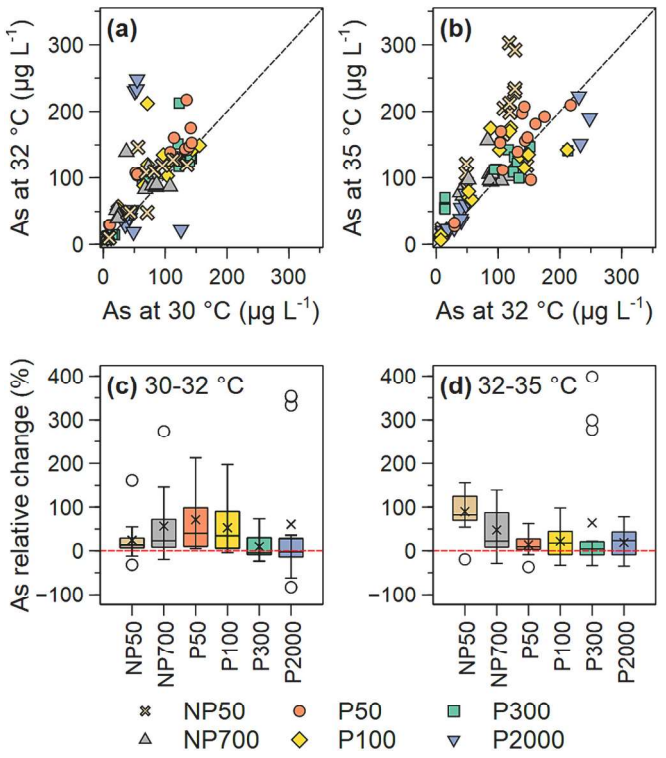

Fig. 3. Changes in aqueous phase As with incubation temperature across the chronosequence. Comparisons are done between 30–32 °C (a) and between 32–35 °C (b). Relative change in As concentration, integrated over all incubation times, based on both temperature comparisons (c, d). For a and b, data is displayed as individual results of experimental triplicates from all 5 incubation times ($n = 15$), color-coded per soil. The black dotted line represents a 1:1 line. For c and d, each box summarizes the results of triplicates through the incubation time for each soil (n = 15), with "x" showing the mean value and white circles showing outliers (1.5 IQR).

stages of the incubation (between days 1 and 5) (Fig. SI10). The relative changes in As mobility when comparing 30–32 °C (Fig. 4c) were particularly high in non-paddies and in young paddies (P50 and P100). When comparing 32–35 °C, the relative change on As mobility was increased further in non-paddies, while paddies showed lower relative changes and no age-related effect (Fig. 4d). The lower As mobility with increasing soil age is related to the high share of amorphous Fe^{III}-phases that form due to SOC accumulation. These phases act as sorption sites, lowering As mobility even under anoxic conditions. Non-paddies and young paddies, with less proportion of amorphous Fe^{III}-phases have less sorption sites, so As is easily mobilized when exposed at higher temperatures under flooded conditions.

An interesting observation is how much more As is mobilized from NP50 at 35 °C compared to 30 °C and 32 °C (Figs. 3a,b, SI10). Sequential extractions (Fig. SI11) showed that NP50 had the highest contributions of easily mobilizable As (F2, Table SI1), and around 5.0 % of the total solid phase As was classified as weakly bound (theoretically defined as ΣF1 - F3), compared to 3.4 % of NP700. This higher proportion of easily mobilizable As is likely related to its early stages of soil development, since long-term paddy use causes wash out of different elements, including As (Kölbl et al., 2014). The wash out of As likely takes longer in non-paddies compared to paddies, since they are not exposed to the high volumes of water used in paddy management.

A second interesting observation is on P2000, which showed a 4.4-fold and 3.5-fold increased As concentration at day 3 when incubated at 32 °C and 35 °C, respectively, compared to the incubations at 30 °C (Fig. SI10). This high mobilization corresponds to the period of high Fe reductive dissolution. The fast rate of dissolution of a high proportion of amorphous Fe^{III}-SOC phases likely releases bound As into the aqueous phase. Supporting this observation, the sequential extraction (Fig. SI11) showed that P2000 had the highest contribution of weakly bound As (8.1 %) meaning that even though Fe^{III}-SOC associations are an effective sink for As, their fast reductive dissolution under increasing temperatures could act as an As source. However, the As concentrations then decrease strongly by day 5 (Fig. SI10), being even lower than those in the incubations at 30 °C. This drop corresponds to the start of DSR in P2000 (Fig. SI7), so the precipitation of secondary mineral phases such as Fe-S, As-Fe-S, and As-S could be responsible for the rapid removal of As from the aqueous phase (Xu et al., 2019; Burton et al., 2014; Burton et al., 2013). In contrast, non-paddies with lower S concentrations and less effective DSR had no effective sink for aqueous phase As over the time of our experiments. This is reflected in the constantly increasing concentrations of aqueous phase Fe (Fig. SI3a) and As (Fig. SI10a) in NP50.

In summary, we have previously shown that paddy soil development generally decreases As mobility due to effective sorption to amorphous Fe^{III}-SOC associations, together with reprecipitation as or sorption to secondary mineral phases. This is also effective in future warmer temperatures, with older paddies showing the least relative changes in As mobility. Younger paddies and soils that have never been used as paddies before were more sensitive to show an increased As mobility. According to our results, As mobility is highly dependent on temperature in freshly reclaimed non-paddies when first flooded, so there could be particular risks of high As mobilization when transforming upland soils or marshlands (like the chronosequence used in the present study) into paddies. Moreover, the specific risk that this mobilization will inflict on rice production is highly dependent on the As speciation.

3.4. Temperature effect on As speciation

Enhanced microbial activity with higher incubation temperature caused a significantly higher ($p < 0.05$) share of methylated As in the aqueous phase in all paddy soils compared to the incubations at 30 °C. This temperature effect on total As methylation was higher for the first +2 °C increase (Fig. 4a), compared to the additional +3 °C (Fig. 4b). This increase was particularly high for P100 (Fig. SI12), which at 30 °C was also the soil with the highest methylation potential among all the studied paddy soils (León Ninin et al., 2024). Since the changes in total As methylation were stronger with the initial +2 °C increase, when discussing the species subgroups (oxymethylarsenates and methylthioarsenates) we will focus on the changes between 30–32 °C. The data comparing 32–35 °C is presented in Fig. SI13. The contribution of oxymethylated As (MMA and DMA) showed a sharp increase when incubated at 32 °C (Fig. 4c). While the maximum contribution of oxymethylated species to As speciation were at around 30 % at 30 °C, their share almost doubled with higher temperatures. In some cases, there was a 4-fold increase in oxymethylated As at higher temperatures when compared to 30 °C, becoming the dominating species group over inorganic oxyarsenic (Fig. SI14a,b). Arsenic methylation was not only enhanced by higher temperatures but also started earlier in the incubation time (Fig. SI15). Furthermore, while in the incubations at 30 °C the concentration of methylated As constantly increased or eventually stabilized, at 32 °C and 35 °C their concentrations peaked at some point of the incubation before decreasing. The formation of methylthioarsenates (Fig. 4d, Fig SI13b) and inorganic thioarsenates (Fig. SI13c,d) was significantly hampered ($p < 0.05$) by higher temperatures.

Since the biogeochemical cycles described in previous sections showed little differences between both non-paddies, only one of them (NP700) was selected for As speciation analyses. In NP700, As speciation was generally dominated by inorganic oxyarsenic species (Fig. SI16a) and contrary to what was observed in paddies, increasing temperature decreased the share of methylated species to total As (Fig. SI16b). Formation of thioarsenates showed a general decrease with increasing

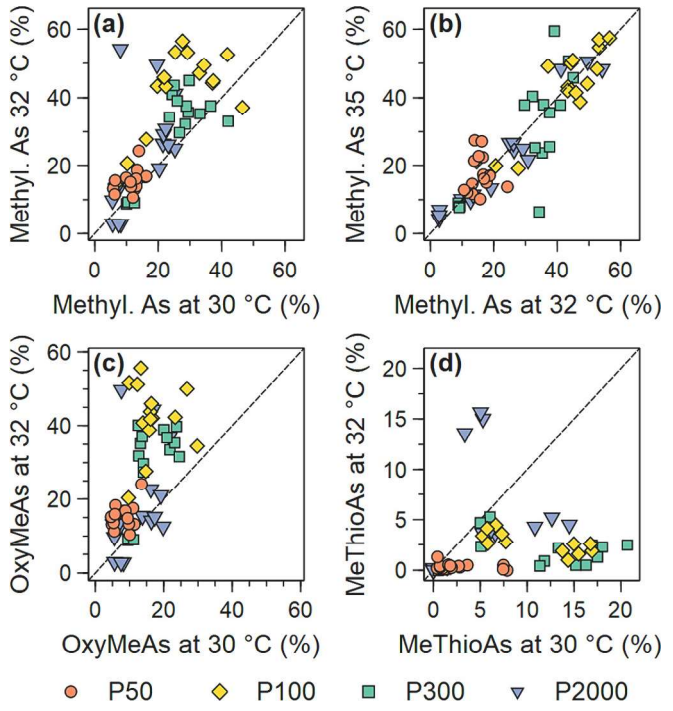

Fig. 4. Comparison of total As methylation between 30–32 °C (a), and between 32–35 °C (b) in the aqueous phase of the paddy soil chronosequence incubations. Comparison between both methylated As subgroups at 30 °C and 32 °C: oxymethylarsenates (c) and methylthioarsenates (d). Fig. SI1 shows how the individual As species have been grouped. The data is displayed as individual results of experimental triplicates from all 5 incubation times ($n = 15$), color-coded per paddy soil age. The black dotted line represents a 1:1 line.

incubation temperature, with some samples showing an increase at days 1 and 3 (Fig. SI16c,d). This period coincides with DSR in the non-paddies (Fig. SI7), suggesting a high availability of reduced S for thiolation.

Increased As methylation with higher temperature in paddy soils has been reported before and related to an increase in both bacterial activity (bacterial 16S rRNA) and abundance of the gene related to As methylation (arsenite S-adenosylmethionine methyltransferase, *arsM*) (Chen et al., 2021a; Müller et al., 2022). In non-paddies, like suggested above for methanogenesis, methylation could be limited by the low SOC and likely microbial communities not adapted to flooded conditions.

The temporal changes in the contribution of methylated As species observed at any time point is the net effect of methylation and de-methylation reactions. A net decrease in methylated As at a certain time point in the incubations at higher temperatures indicates a change in the rates of these reactions, yielding more active de-methylation. Methylotrophic methanogens have previously been suggested as playing an active role on As de-methylation (Chen et al., 2019; Chen et al., 2022; Chen et al., 2023) and considering the important increase on methanogenesis observed at higher temperatures, it is likely that they are contributing to As de-methylation.

Considering As uptake and accumulation by rice plants, and the high toxicity that inorganic As has on humans, an overall increasing share of methylated As species in paddies with future higher temperatures could be regarded as a meliorating effect. Methylated As species are, however, highly phytotoxic and reported to lead to plant sterility where no grains are produced (straight-head disease) (Zheng et al., 2013; Yan et al., 2005). Thus, when extrapolating the observations of our incubations to a soil-plant system, grain yield could decrease in paddies with already established microbial communities and a SOC pool that sustains them, but particularly in soils like P100, with high methylation potential. Most of the soils currently under paddy management are younger than 100 years old (Klein Goldewijk et al., 2017). Continued use of these paddies might increase the risk of high As methylation (as observed in P100) in a higher share of soils until the end of the century. Extent and kinetics of this shift will also depend on other factors such as individual agricultural practices or specific environmental factors.

If reduced S is available in the system, oxymethylated As species can readily go through abiotic thiolation to form methylthioarsenates (León Ninin et al., 2024; Wang et al., 2020). Considering the general increase in oxymethylated As and no major changes in pH when incubating the soils at different temperatures (Fig. SI17), the limiting factor for such a decrease in the formation of inorganic and methyl-thioarsenates can only be the lower availability of reduced S. While S reduction was observed in the aqueous phase (Fig. SI7), we suggest that the higher amount of reduced Fe with increasing temperatures scavenged the reduced S from the aqueous phase. Supporting this, no free sulfide was detected in any incubation. We have also suggested this Fe-related limitation on reduced S before, with paddies of increasing age showing a decrease in As thiolation (León Ninin et al., 2024). Interestingly, by the end of our 32 °C and 35 °C incubations, P2000 showed an increase of methylthioarsenates compared to the incubations at 30 °C. We have previously suggested that the high amount of Fe^{III} (oxy)hydroxides present in P2000 could support an active cryptic-S cycle, in which sulfide re-oxidation to S^0 is coupled to the reduction of Fe^{III} (oxy) hydroxides (Wang et al., 2020; Wind and Conrad, 1997), supplying small amounts of reduced S to the system. This supply of reduced S could support As thiolation in later stages of the incubations, even though no active DSR is taking place (León Ninin et al., 2024; Saalfield and Bostick, 2009). In non-paddies, the formation of methylthioarsenates was additionally limited by the decrease in oxymethylated arsenates as substrate.

In summary, non-paddies show a high share of inorganic oxyarsenic species, in contrast to paddies with a higher share of methylated As. While higher temperatures showed small effects in As speciation in non-paddies, +2 °C increased As methylation and decreased thiolation in all paddies. An additional +3 °C had little effect on As speciation. In the context of rice production, newly reclaimed soils and young paddies are at a major risk of showing increased As mobility when exposed to higher temperatures. These paddy soils in early stages of development also show a higher contribution of carcinogenic inorganic As to their speciation. Higher temperatures during the ripening stage and full maturation of rice plants have been correlated with higher As in rice grains (Arao et al., 2018; Dhar et al., 2023; Dhar et al., 2020; Farhat et al., 2023). The consumption of rice produced in these fields could present a risk for high inorganic As ingestion. Thus, it is key to understand how elevated temperatures will alter the dynamics of As mobility in the field (and eventual uptake by rice plants) depending on soil properties that are affected by paddy soil age. On the other hand, while older soils are less affected by increased As mobility, their higher SOC pool and microbial activity increased As methylation to an important extent. While considered to be less toxic to humans, methylated As can be phytotoxic and decrease grain yield, being a possible risk for securing sufficient yield.

4. Conclusions

The results obtained by our incubation experiments show that long-term paddy use leads to different biogeochemical responses related to increased temperature, both in terms of kinetics (accelerating processes or overruling delays) and magnitude of effect. While we focused here on two major issues related to paddy use, namely CH_4 production and As mobility and speciation, the dynamics of these processes are closely linked to the biogeochemistry of other major elements in paddy soils and their aqueous phase, mainly as a consequence of SOC accumulation with long-term paddy use. While it has been previously shown that organic C is an important parameter determining the response of soils to changes in temperature (Wei et al., 2019), this is, to the best of our knowledge, the first report considering a systematic accumulation of SOC related to long-term paddy use, rather than exogenous addition of labile C

substrates. Furthermore, another advantage of our study is that we studied the endogenous As concentrations in the soil, instead of amending them with higher As concentrations which could lead to changes in the partition of its natural binding environment. Additionally, by comparing the distinctive responses between paddies and non-paddy soils we were able to confirm that long-term paddy management modifies the response of CH_4 production to changes in temperature, As mobility and changes in As speciation. We focused here on the highly dynamic first 10 days of incubation to better elucidate changes in C, S, Fe and As redox chemistry. Next steps should include studies focusing on such changes in the field and on a temporal scale related to the cropping season, as well as considering daily temperature variations.

The last IPCC projections show that the previously established worst-case scenario is not likely and that the effects of climate change by the end of the century lay between +1.4 °C (SSP1–1.9) and + 2.7 °C (SSP2–4.5) increases in air temperature (Lee et al., 2023). It must be noted that in the context rice cultivation, the overlying water over the paddies would act as a temperature buffer, dampening the effect of air temperature on the soils. However, our results showed that the difference between current temperatures and + 2 °C is higher than between +2 and + 5 °C, so even small changes in temperature have an important effect mainly on As mobility and speciation, but also on CH_4 production. Thus, our results support previous claims of the important feedback between rice cultivation in a future climate and increased CH_4 emissions, as well as the additional constraints that altered biogeochemical dynamics could pose on food security (Muehe et al., 2019; Liu et al., 2020; Dijkstra et al., 2012).

CRediT authorship contribution statement

José M. León Ninin: Writing – review & editing, Writing – original draft, Visualization, Validation, Software, Methodology, Investigation, Formal analysis, Data curation, Conceptualization. **Alejandra Higa Mori:** Writing – review & editing, Validation, Methodology, Investigation, Formal analysis, Data curation, Conceptualization. **Johanna Pausch:** Writing – review & editing, Resources. **Britta Planer-Friedrich:** Writing – review & editing, Writing – original draft, Supervision, Resources, Project administration, Funding acquisition, Conceptualization.

Declaration of competing interest

The authors declare the following financial interests/personal relationships which may be considered as potential competing interests:

Britta Planer-Friedrich reports financial support was provided by the Federal Ministry of Education and Research Bonn Office. Jose M. Leon Ninin reports financial support was provided by German National Merit Foundation. If there are other authors, they declare that they have no known competing financial interests or personal relationships that could have appeared to influence the work reported in this paper.

Data availability

The data generated and analyzed for the current study are also available from the corresponding author on reasonable request.

Acknowledgements

We thank the German Academic Scholarship Foundation for the doctoral funding support for J.M.L.N and funding within the Federal Ministry of Education and Research project BMBF #031B0840 to B.P.-F. We thank Livia Urbanski and Angelika Kölbl for providing the chronosequence soils, Asel Traut for her help with the early lab work, Dr. Ben Gilfedder for providing access to CH_4 and CO_2 measurements, and Ilse Thaufelder for her assistance with the DOC analyses. The graphical abstract was created using Biorender.

Appendix A. Supplementary data

Supplementary methods with a detailed protocol for the Sequential Extraction Procedure (SEP) and example chromatogram indicating As species grouping. Supplementary data and figures showing biogeochemical data supporting the above-described observations and discussion. Supplementary files with additional statistical information from the one- and two-way-ANOVAs. Supplementary data to this article can be found online at https://doi.org/10.1016/j.scitotenv.2024.173793.

References

Arao, T., Makino, T., Kawasaki, A., Akahane, I., Kiho, N., 2018. Effect of air temperature after heading of rice on the arsenic concentration of grain. Soil Sci. Plant Nutr. 64, 433–437. https://doi.org/10.1080/00380768.2018.1438811.

Bannert, A., et al., 2011. Changes in diversity and functional gene abundances of microbial communities involved in nitrogen fixation, nitrification, and denitrification in a tidal wetland versus paddy soils cultivated for different time periods. Appl. Environ. Microbiol. 77, 6109–6116. https://doi.org/10.1128/AEM.01751-10.

van Bodegom, P.M., Scholten, J.C.M., Stams, A.J.M., 2004. Direct inhibition of methanogenesis by ferric iron. FEMS Microbiol. Ecol. 49, 261–268. https://doi.org/10.1016/j.femsec.2004.03.017.

Bradford, M.A., et al., 2008. Thermal adaptation of soil microbial respiration to elevated temperature. Ecol. Lett. 11, 1316–1327. https://doi.org/10.1111/j.1461-0248.2008.01251.x.

Bridgham, S.D., Cadillo-Quiroz, H., Keller, J.K., Zhuang, Q., 2013. Methane emissions from wetlands: biogeochemical, microbial, and modeling perspectives from local to global scales. Glob. Chang. Biol. 19, 1325–1346. https://doi.org/10.1111/gcb.12131.

Burton, E.D., Johnston, S.G., Planer-Friedrich, B., 2013. Coupling of arsenic mobility to sulfur transformations during microbial sulfate reduction in the presence and absence of humic acid. Chem. Geol. 343, 12–24. https://doi.org/10.1016/j.chemgeo.2013.02.005.

Burton, E.D., Johnston, S.G., Kocar, B.D., 2014. Arsenic mobility during flooding of contaminated soil: the effect of microbial sulfate reduction. Environ. Sci. Technol. 48, 13660–13667. https://doi.org/10.1021/es503963k.

Castro, H.F., Classen, A.T., Austin, E.E., Norby, R.J., Schadt, C.W., 2010. Soil microbial community responses to multiple experimental climate change drivers. Appl. Environ. Microbiol. 76, 999–1007. https://doi.org/10.1128/AEM.02874-09.

Chen, C., et al., 2019. Sulfate-reducing bacteria and methanogens are involved in arsenic methylation and demethylation in paddy soils. ISME J. 13, 2523–2535. https://doi.org/10.1038/s41396-019-0451-7.

Chen, C., et al., 2021a. Sulfate addition and rising temperature promote arsenic methylation and the formation of methylated thioarsenates in paddy soils. Soil Biol. Biochem. 154, 108129 https://doi.org/10.1016/j.soilbio.2021.108129.

Chen, C., et al., 2022. Suppression of methanogenesis in paddy soil increases dimethylarsenate accumulation and the incidence of straighthead disease in rice. Soil Biol. Biochem. 169, 108689 https://doi.org/10.1016/j.soilbio.2022.108689.

Chen, C., Li, L., Wang, Y., Dong, X., Zhao, F.-J., 2023. Methylotrophic methanogens and bacteria synergistically demethylate dimethylarsenate in paddy soil and alleviate rice straighthead disease. ISME J. https://doi.org/10.1038/s41396-023-01498-7.

Chen, X., et al., 2021b. Contrasting pathways of carbon sequestration in paddy and upland soils. Glob. Chang. Biol. 27, 2478–2490. https://doi.org/10.1111/gcb.15595.

Cheng, W., Yagi, K., Sakai, H., Kobayashi, K., 2006. Effects of elevated atmospheric CO2 concentrations on CH4 and N2O emission from rice soil: an experiment in controlled-environment chambers. Biogeochemistry 77, 351–373. https://doi.org/10.1007/s10533-005-1534-2.

Cheng, Y.-Q., Yang, L.-Z., Cao, Z.-H., Ci, E., Yin, S., 2009. Chronosequential changes of selected pedogenic properties in paddy soils as compared with non-paddy soils. Geoderma 151, 31–41. https://doi.org/10.1016/j.geoderma.2009.03.016.

Cline, J.D., 1969. Spectrophotometric determination of hydrogen sulfide in natural waters 1. Limnol. Oceanogr. 14, 454–458.

Colina Blanco, A.E., Kerl, C.F., Planer-Friedrich, B., 2021. Detection of thioarsenates in rice grains and rice products. J. Agric. Food Chem. 69, 2287–2294. https://doi.org/10.1021/acs.jafc.0c06853.

Colina Blanco, A.E., Higa Mori, A., Planer-Friedrich, B., 2024. Widespread occurrence of dimethylmonothioarsenate (DMMTA) in rice cakes: effects of puffing and storage. Food Chem. 436, 137723 https://doi.org/10.1016/j.foodchem.2023.137723.

Conrad, R., 2020. Methane production in soil environments—anaerobic biogeochemistry and microbial life between flooding and desiccation. Microorganisms 8, 881. https://doi.org/10.3390/microorganisms8060881.

Craine, J.M., Fierer, N., McLauchlan, K.K., 2010. Widespread coupling between the rate and temperature sensitivity of organic matter decay. Nat. Geosci. 3, 854–857. https://doi.org/10.1038/ngeo1009.

Dai, J., et al., 2022. Widespread occurrence of the highly toxic dimethylated monothioarsenate (DMMTA) in rice globally. Environ. Sci. Technol. 56, 3575–3586. https://doi.org/10.1021/acs.est.1c08394.

Davidson, E.A., Janssens, I.A., 2006. Temperature sensitivity of soil carbon decomposition and feedbacks to climate change. Nature 440, 165–173. https://doi.org/10.1038/nature04514.

Dhar, P., et al., 2020. The increase in the arsenic concentration in brown rice due to high temperature during the ripening period and its reduction by silicate material treatment. Agriculture 10, 289.
Dhar, P., et al., 2023. Factors causing the increase in arsenic concentration in brown rice due to high temperatures during the ripening period and its reduction by applying converted furnace slag. J. Plant Nutr. 46, 2652–2675. https://doi.org/10.1080/01904167.2022.2160746.
Dijkstra, F.A., et al., 2012. Effects of elevated carbon dioxide and increased temperature on methane and nitrous oxide fluxes: evidence from field experiments. Front. Ecol. Environ. 10, 520–527. https://doi.org/10.1890/120059.
FAO, 2022. Food and Agriculture Organization of the United Nations. FAOSTAT-Food and Agriculture.
Farhat, Y.A., Kim, S.-H., Seyfferth, A.L., Zhang, L., Neumann, R.B., 2021. Altered arsenic availability, uptake, and allocation in rice under elevated temperature. Sci. Total Environ. 763, 143049.
Farhat, Y.A., Kim, S.-H., Neumann, R.B., 2023. When does temperature matter? Response of rice arsenic to heat exposure during different developmental stages. Plant Soil. https://doi.org/10.1007/s11104-023-06122-3.
Forster, P., et al., 2021. Chapter 7: The Earth's energy budget, climate feedbacks, and climate sensitivity. In: Climate Change 2021: The Physical Science Basis. Contribution of Working Group I to the Sixth Assessment Report of the Intergovernmental Panel on Climate Change.
Frey, S., Drijber, R., Smith, H., Melillo, J., 2008. Microbial biomass, functional capacity, and community structure after 12 years of soil warming. Soil Biol. Biochem. 40, 2904–2907. https://doi.org/10.1016/j.soilbio.2008.07.020.
Fulda, B., Voegelin, A., Ehlert, K., Kretzschmar, R., 2013. Redox transformation, solid phase speciation and solution dynamics of copper during soil reduction and reoxidation as affected by sulfate availability. Geochim. Cosmochim. Acta 123, 385–402. https://doi.org/10.1016/j.gca.2013.07.017.
Gaihre, Y.K., Wassmann, R., Villegas-Pangga, G., 2013. Impact of elevated temperatures on greenhouse gas emissions in rice systems: interaction with straw incorporation studied in a growth chamber experiment. Plant Soil 373, 857–875. https://doi.org/10.1007/s11104-013-1852-4.
van Groenigen, K.J., Osenberg, C.W., Hungate, B.A., 2011. Increased soil emissions of potent greenhouse gases under increased atmospheric CO2. Nature 475, 214–216. https://doi.org/10.1038/nature10176.
Hanke, A., Cerli, C., Muhr, J., Borken, W., Kalbitz, K., 2013. Redox control on carbon mineralization and dissolved organic matter along a chronosequence of paddy soils. Eur. J. Soil Sci. 64, 476–487. https://doi.org/10.1111/ejss.12042.
Hegler, F., Posth, N.R., Jiang, J., Kappler, A., 2008. Physiology of phototrophic iron(II)-oxidizing bacteria: implications for modern and ancient environments. FEMS Microbiol. Ecol. 66, 250–260. https://doi.org/10.1111/j.1574-6941.2008.00592.x.
Ho, A., Lüke, C., Cao, Z., Frenzel, P., 2011. Ageing well: methane oxidation and methane oxidizing bacteria along a chronosequence of 2000 years. Environ. Microbiol. Rep. 3, 738–743.
Kalbitz, K., et al., 2013. The carbon count of 2000 years of rice cultivation. Glob. Chang. Biol. 19, 1107–1113. https://doi.org/10.1111/gcb.12080.
Klein Goldewijk, K., Beusen, A., Doelman, J., Stehfest, E., 2017. Anthropogenic land use estimates for the Holocene–HYDE 3.2. Earth System Science Data 9, 927–953. https://doi.org/10.5194/essd-9-927-2017.
Kögel-Knabner, I., et al., 2010. Biogeochemistry of paddy soils. Geoderma 157, 1–14. https://doi.org/10.1016/j.geoderma.2010.03.009.
Kölbl, A., et al., 2014. Accelerated soil formation due to paddy management on marshlands (Zhejiang Province, China). Geoderma 228-229, 67–89. https://doi.org/10.1016/j.geoderma.2013.09.005.
Lalonde, K., Mucci, A., Ouellet, A., Gélinas, Y., 2012. Preservation of organic matter in sediments promoted by iron. Nature 483, 198–200. https://doi.org/10.1038/nature10855.
Le Mer, J., Roger, P., 2001. Production, oxidation, emission and consumption of methane by soils: a review. Eur. J. Soil Biol. 37, 25–50. https://doi.org/10.1016/S1164-5563(01)01067-6.
Le Quéré, C., et al., 2018. Global carbon budget 2017. Earth System Science Data 10, 405–448. https://doi.org/10.5194/essd-10-405-2018.
Lee, H., et al., 2023. IPCC, 2023: Climate Change 2023: Synthesis Report. Contribution of Working Groups I, II and III to the Sixth Assessment Report of the Intergovernmental Panel on Climate Change, pp. 33–115 (IPCC, 2023).
Lee, H.J., Kim, S.Y., Kim, P.J., Madsen, E.L., Jeon, C.O., 2014. Methane emission and dynamics of methanotrophic and methanogenic communities in a flooded rice field ecosystem. FEMS Microbiol. Ecol. 88, 195–212. https://doi.org/10.1111/1574-6941.12282.
León Ninin, J.M., et al., 2024. Changes in arsenic mobility and speciation across a 2000-year-old paddy soil chronosequence. Sci. Total Environ. 908, 168351 https://doi.org/10.1016/j.scitotenv.2023.168351.
Liu, P., Klose, M., Conrad, R., 2018. Temperature effects on structure and function of the methanogenic microbial communities in two paddy soils and one desert soil. Soil Biol. Biochem. 124, 236–244. https://doi.org/10.1016/j.soilbio.2018.06.024.
Liu, Y., et al., 2020. Impacts of 1.5 and 2.0°C global warming on rice production across China. Agric. For. Meteorol. 284, 107900 https://doi.org/10.1016/j.agrformet.2020.107900.
Liu, Y., et al., 2023. Divergent accumulation of microbial and plant necromass along paddy soil development in a millennium scale. Soil Tillage Res. 232, 105769 https://doi.org/10.1016/j.still.2023.105769.
Luo, D., et al., 2023. A joint role of iron oxide and temperature for methane production and methanogenic community in paddy soils. Geoderma 433, 116462. https://doi.org/10.1016/j.geoderma.2023.116462.
Ma, J.F., et al., 2008. Transporters of arsenite in rice and their role in arsenic accumulation in rice grain. Proc. Natl. Acad. Sci. 105, 9931–9935. https://doi.org/10.1073/pnas.0802361105.
Meharg, A.A., Zhao, F.J., 2012. Arsenic & Rice. Springer, Netherlands.
Mohanty, S.R., Bodelier, P.L.E., Conrad, R., 2007. Effect of temperature on composition of the methanotrophic community in rice field and forest soil. FEMS Microbiol. Ecol. 62, 24–31. https://doi.org/10.1111/j.1574-6941.2007.00370.x.
Muehe, E.M., Wang, T., Kerl, C.F., Planer-Friedrich, B., Fendorf, S., 2019. Rice production threatened by coupled stresses of climate and soil arsenic. Nat. Commun. 10, 4985. https://doi.org/10.1038/s41467-019-12946-4.
Müller, V., Chavez-Capilla, T., Feldmann, J., Mestrot, A., 2022. Increasing temperature and flooding enhance arsenic release and biotransformations in Swiss soils. Sci. Total Environ. 838, 156049 https://doi.org/10.1016/j.scitotenv.2022.156049.
Neumann, R.B., Seyfferth, A.L., Teshera-Levye, J., Ellingson, J., 2017. Soil warming increases arsenic availability in the rice rhizosphere. Agricultural & Environmental Letters 2, 170006. https://doi.org/10.2134/ael2017.02.0006.
Pereira, J., et al., 2013. Effects of elevated temperature and atmospheric carbon dioxide concentration on the emissions of methane and nitrous oxide from Portuguese flooded rice fields. Atmos. Environ. 80, 464–471. https://doi.org/10.1016/j.atmosenv.2013.08.045.
Planer-Friedrich, B., London, J., McCleskey, R.B., Nordstrom, D.K., Wallschläger, D., 2007. Thioarsenates in geothermal waters of Yellowstone National Park: determination, preservation, and geochemical importance. Environ. Sci. Technol. 41, 5245–5251. https://doi.org/10.1021/es070273v.
Qian, H., et al., 2023. Greenhouse gas emissions and mitigation in rice agriculture. Nature Reviews Earth & Environment 4, 716–732. https://doi.org/10.1038/s43017-023-00482-1.
Reid, M.C., et al., 2017. Arsenic methylation dynamics in a rice paddy soil anaerobic enrichment culture. Environ. Sci. Technol. 51, 10546–10554. https://doi.org/10.1021/acs.est.7b02970.
Rhoton, F.E., Shipitalo, M.J., Lindbo, D.L., 2002. Runoff and soil loss from midwestern and southeastern US silt loam soils as affected by tillage practice and soil organic matter content. Soil Tillage Res. 66, 1–11. https://doi.org/10.1016/S0167-1987(02)00005-3.
Saalfield, S.L., Bostick, B.C., 2009. Changes in iron, sulfur, and arsenic speciation associated with bacterial sulfate reduction in ferrihydrite-rich systems. Environ. Sci. Technol. 43, 8787–8793. https://doi.org/10.1021/es901651k.
Schwertmann, U., 1991. Solubility and dissolution of iron oxides. Plant Soil 130, 1–25. https://doi.org/10.1007/BF00011851.
Sethunathan, N., Rao, V., Adhya, T., Raghu, K., 1982. Microbiology of rice soils. CRC Crit. Rev. Microbiol. 10, 125–172.
Smedley, P.L., Kinniburgh, D.G., 2002. A review of the source, behaviour and distribution of arsenic in natural waters. Appl. Geochem. 17, 517–568. https://doi.org/10.1016/S0883-2927(02)00018-5.
Stone, R., 2008. Arsenic and paddy rice: a neglected cancer risk? Science 321, 184–185. https://doi.org/10.1126/science.321.5886.184.
Stookey, L. L. Ferrozine—a new spectrophotometric reagent for iron. Anal. Chem. 42, 779–781 (1970). doi:https://doi.org/10.1021/ac60289a016.
Su, R., et al., 2024. Carbon availability and microbial activity manipulate the temperature sensitivity of anaerobic degradation in a paddy soil profile. Environ. Res. 118453 https://doi.org/10.1016/j.envres.2024.118453.
Tokida, T., et al., 2010. Effects of free-air CO2 enrichment (FACE) and soil warming on CH4 emission from a rice paddy field: impact assessment and stoichiometric evaluation. Biogeosciences 7, 2639–2653. https://doi.org/10.5194/bg-7-2639-2010.
Tokida, T., et al., 2011. Methane and soil CO2 production from current-season photosynthates in a rice paddy exposed to elevated CO2 concentration and soil temperature. Glob. Chang. Biol. 17, 3327–3337. https://doi.org/10.1111/j.1365-2486.2011.02475.x.
Van Amstel, A., 2012. Methane. A review. J. Integr. Environ. Sci. 9, 5–30. https://doi.org/10.1080/1943815X.2012.694892.
Wallschläger, D., London, J., 2008. Determination of methylated arsenic-sulfur compounds in groundwater. Environ. Sci. Technol. 42, 228–234. https://doi.org/10.1021/es0707815.
Wallschläger, D., Stadey, C.J., 2007. Determination of (oxy)thioarsenates in sulfidic waters. Anal. Chem. 79, 3873–3880. https://doi.org/10.1021/ac070061g.
Wang, F., et al., 2021. Succession of bacterial community composition in coastal agricultural soils along a 1000-year reclamation chronosequence in Hangzhou Bay, China. Ecol. Indic. 121, 106972 https://doi.org/10.1016/j.ecolind.2020.106972.
Wang, H., et al., 2022. Effects of free-air temperature increase on grain yield and greenhouse gas emissions in a double rice cropping system. Field Crop Res. 281, 108489 https://doi.org/10.1016/j.fcr.2022.108489.
Wang, J., et al., 2020. Thiolated arsenic species observed in rice paddy pore waters. Nat. Geosci. 13, 282–287. https://doi.org/10.1038/s41561-020-0533-1.
Wang, P., et al., 2015. Long-term rice cultivation stabilizes soil organic carbon and promotes soil microbial activity in a salt marsh derived soil chronosequence. Sci. Rep. 5, 15704. https://doi.org/10.1038/srep15704.
Weber, F.-A., Hofacker, A.F., Voegelin, A., Kretzschmar, R., 2010. Temperature dependence and coupling of iron and arsenic reduction and release during flooding of a contaminated soil. Environ. Sci. Technol. 44, 116–122. https://doi.org/10.1021/es902100h.
Wei, L., et al., 2019. Labile carbon matters more than temperature for enzyme activity in paddy soil. Soil Biol. Biochem. 135, 134–143.
Wei, L., et al., 2022. Paddy soils have a much higher microbial biomass content than upland soils: a review of the origin, mechanisms, and drivers. Agric. Ecosyst. Environ. 326, 107798 https://doi.org/10.1016/j.agee.2021.107798.

Wind, T., Conrad, R., 1997. Localization of sulfate reduction in planted and unplanted rice field soil. Biogeochemistry 37, 253–278. https://doi.org/10.1023/A:1005760506957.

Wissing, L., et al., 2011. Organic carbon accumulation in a 2000-year chronosequence of paddy soil evolution. CATENA 87, 376–385. https://doi.org/10.1016/j.catena.2011.07.007.

Wissing, L., et al., 2014. Organic carbon accumulation on soil mineral surfaces in paddy soils derived from tidal wetlands. Geoderma 228-229, 90–103. https://doi.org/10.1016/j.geoderma.2013.12.012.

Xu, X., et al., 2019. Microbial sulfate reduction decreases arsenic mobilization in flooded paddy soils with high potential for microbial Fe reduction. Environ. Pollut. 251, 952–960. https://doi.org/10.1016/j.envpol.2019.05.086.

Xu, X., et al., 2020. The influence of soil temperature, methanogens and methanotrophs on methane emissions from cold waterlogged paddy fields. J. Environ. Manag. 264, 110421 https://doi.org/10.1016/j.jenvman.2020.110421.

Yan, W., et al., 2005. Differential response of rice germplasm to straighthead induced by arsenic. Crop Sci. 45, 1223–1228.

Yang, S.-S., Chang, H.-L., 1998. Effect of environmental conditions on methane production and emission from paddy soil. Agric. Ecosyst. Environ. 69, 69–80. https://doi.org/10.1016/S0167-8809(98)00098-X.

Yun, S.-I., et al., 2012. Further understanding CH4 emissions from a flooded rice field exposed to experimental warming with elevated [CO2]. Agric. For. Meteorol. 154-155, 75–83. https://doi.org/10.1016/j.agrformet.2011.10.011.

Zhang, N., et al., 2023. Effect of warming on rice yield and methane emissions in a Chinese tropical double-rice cropping system. Agric. Ecosyst. Environ. 348, 108409 https://doi.org/10.1016/j.agee.2023.108409.

Zhang, X., Reid, M.C., 2022. Inhibition of methanogenesis leads to accumulation of methylated arsenic species and enhances arsenic volatilization from rice paddy soil. Sci. Total Environ. 818, 151696 https://doi.org/10.1016/j.scitotenv.2021.151696.

Zhao, F.-J., Zhu, Y.-G., Meharg, A.A., 2013. Methylated arsenic species in rice: geographical variation, origin, and uptake mechanisms. Environ. Sci. Technol. 47, 3957–3966. https://doi.org/10.1021/es304295n.

Zheng, M.-Z., Li, G., Sun, G.-X., Shim, H., Cai, C., 2013. Differential toxicity and accumulation of inorganic and methylated arsenic in rice. Plant Soil 365, 227–238.

Zhou, Z., et al., 2014. Similarities in chemical composition of soil organic matter across a millennia-old paddy soil chronosequence as revealed by advanced solid-state NMR spectroscopy. Biol. Fertil. Soils 50, 571–581. https://doi.org/10.1007/s00374-013-0875-6.

Ziska, L.H., et al., 1998. Long-term growth at elevated carbon dioxide stimulates methane emission in tropical paddy rice. Glob. Chang. Biol. 4, 657–665. https://doi.org/10.1046/j.1365-2486.1998.00186.x.

Zobrist, J., Dowdle, P.R., Davis, J.A., Oremland, R.S., 2000. Mobilization of arsenite by dissimilatory reduction of adsorbed arsenate. Environ. Sci. Technol. 34, 4747–4753. https://doi.org/10.1021/es001068h.

Long-term paddy use influences response of methane production, arsenic mobility and speciation to future higher temperatures

José M. León Ninin[1], Alejandra Higa Mori[1], Johanna Pausch[2], Britta Planer-Friedrich[1]*

[1] Environmental Geochemistry, Bayreuth Center for Ecology and Environmental Research (BayCEER), University of Bayreuth, 95440 Bayreuth, Germany

[2] Agroecology, Bayreuth Center for Ecology and Environmental Research (BayCEER), University of Bayreuth, 95440 Bayreuth, Germany

* Corresponding author. Phone: +49-921-553999; E-mail address: b.planer-friedrich@uni-bayreuth.de

(16 Pages, 5 Tables, and 17 Figures)

Supplementary methods

Sequential Extraction Procedure (SEP)

This SEP proposed by Fulda, et al. [1] classifies binding mechanisms into the following operationally defined fractions: F1 ($CaCl_2$ 0.1 M) – mobile fraction (soluble or exchangeable, and soluble metalorganic complexes); F2 (1M Na-acetate) - easily mobilizable fraction (adsorbed and bound to carbonates or other minerals, weakly bound metalorganic complexes); F3 (0.025 M NH_4-EDTA) - organic fraction (low affinity sites); F4 (0.2 M NH_4-oxalate) - reducible fraction (bound to amorphous and crystalline Fe and Mn oxides), and F5 (30% H_2O_2, 2 M HNO_3, 3.2 M NH_4-Acetate) - oxidizable fraction (metal sulfides and organically bound to high affinity sites). For the general procedure, 0.2 g of dry soil were weighed into a 15 mL centrifuge tube and extracted following the steps and reactants described in the method (Summarized in Table S1). After each extraction, the samples were centrifuged (3500 rpm, 10 min) to separate the soil from the extract. The soil was washed with deionized water to prevent extractant carryover into the next step, while the extracts were filtered through 0.2 µm cellulose-acetate filters, diluted 1:10 with ultrapure deionized water, and stabilized with 15 µL of 30% H_2O_2 and 20 µL of 32.5% HNO_3 per mL of sample. Samples from Fraction 3 were not acidified to avoid the precipitation of EDTA. All extracts were analyzed for total As by ICP-MS as described before, using matrix-matched calibrations for each fraction. Non-extractable As (F6) was calculated by subtracting Σ F1 to F5 of the total As extracted from the original soils by microwave assisted digestion in 10 mL aqua regia (MARS Xpress, CEM).

Table S1: Summary of extractants and conditions for the SEP described by Fulda et al.[1]

Operationally defined fraction		Extractant	Extraction conditions
F1 (Mobile fraction)	Soluble and exchangeable; soluble metal-organic complexes	0.1 M $CaCl_2$	24 h shaking; 23 °C; SSR 1:25
F2 (Easily mobilizable fraction)	Specifically adsorbed, bound to $CaCO_3$ and other minerals labile at pH 5, weak metal-organic complexes)	1 M NaOAc (pH 5, adjusted with HOAc)	24 h shaking; 23 °C; SSR 1:25
F3 (Organically bound)	Low-affinity organic sites	0.025 M NH_4-EDTA (pH 4.6)	90 min shaking; 23 °C; SSR 1:25
		1 M NH_4OAc (pH 4.6)	10 min shaking; 23 °C; SSR 1:12.5
F4 (Reducible fraction)	Amorphous and crystalline Fe and Mn hydr(oxydes)	0.1 M ascorbic acid + 0.2 M NH_4Ox/HOx (pH 3.25)	2 h; 96 °C (heat block); SSR 1:25; dark
		0.2 M NH_4Ox/HOx (pH 3.25)	10 min shaking; 23 °C; SSR 1:12.5; dark
F5 (Oxidizable fraction)	Sulfides and organically bound to high-affinity sites	30% H_2O_2 (pH 2) + 2 M HNO_3	5 mL H_2O_2 + 3 mL HNO_3; 2 h; 85 °C (heat block)
			3 mL H_2O_2; 3 h; 85 °C (heat block)
		3.2 M NH_4OAc (in 20% v/v HNO_3)	5 mL NH_4OAc; 30 min; 23 °C

SSR: Soil:solution ratio. OAc: Acetate. Ox: Oxalate.

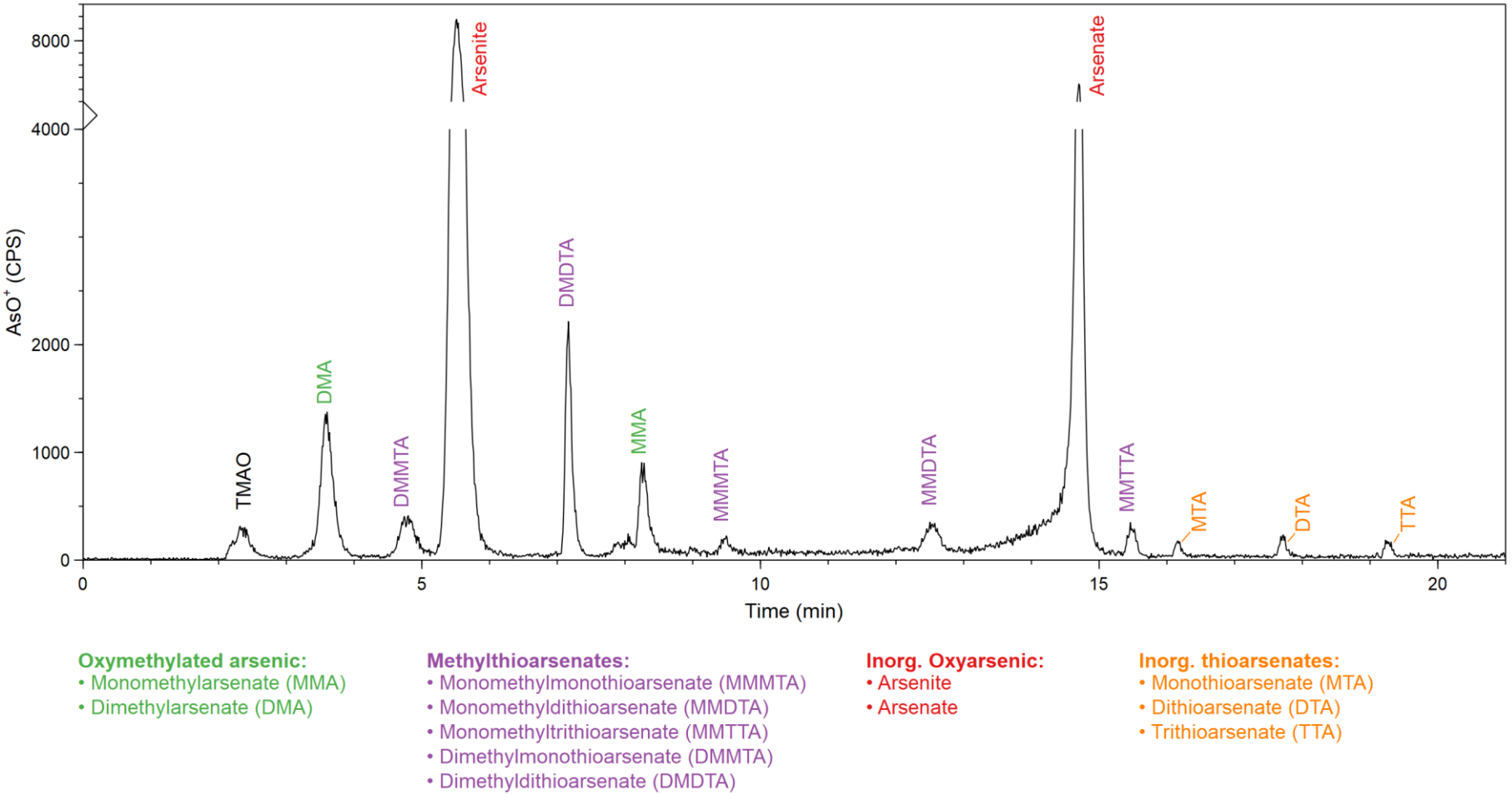

Figure SI1: Example chromatogram indicating the 12 separated As species and the four groups discussed in the study: Oxymethylated arsenic, methylthioarsenates, inorganic oxyarsenic, and inorganic thioarsenates. The peak labeled as "TMAO" corresponds to unidentified non-charged As compounds that elute with the dead volume; it is assumed that the majority of this As species is trimethylarsine oxide. Note that the complete elution takes 26 minutes, but the chromatogram here was shortened to 22 minutes for better graphical resolution of the relevant peaks.

Supplementary data

Table SI2: Selected soil properties of the topsoils from the non-paddies and paddies used in this study.

Soil	Horizon*	Horizon depth (cm)*	Soil pH*	Soil Org. C* (g kg^{-1})	Soil Fe* (g kg^{-1})	Soil As (mg kg^{-1})	Soil S (g kg^{-1})	Fe_O/Fe_{DCB}
NP50	Ap	0 - 9	7.3	10.6 ± 0.2	37	17	3.68	0.3 ± 0.1
NP700	Ap1	0 - 12	5.9	11.0 ± 1.9	28	15	2.45	0.30 ± 0.09
P50	Alp1	0 - 7	7.4	17.8 ± 0.5	38	17	3.52	0.43 ± 0.04
P100	Alp1**	0 - 9	5.0	17.6 ± 1.3	34	15 ± 2	2.64 ± 0.06	0.44 ± 0.04
P100	Alp2**	9 - 15	5.8	15.3 ± 1.1	35			
P300	Alp	0 - 18	5.8	22.6 ± 2.5	35	17	2.77	0.46 ± 0.06
P2000	Alp	0 - 15	5.1	30.0 ± 1.5	22	11	2.57	0.84 ± 0.05

*Data from Kölbl, et al. [2]. ** For this work, horizons Alp1 and Alp2 from P100 were mixed to obtain a material representative of the complete Alp horizon. Fe_O: Oxalate extractable iron, Fe_{DCB}: Dithionate-citrate-bicarbonate extractable iron. A complete characterization of all soils and horizons from this chronosequence can be found in Kölbl, et al. [2]. The data for paddy soils had been already compiled for León Ninin, et al. [3]

Table SI3: P-values of the two-way-ANOVAs carried out for the analyzed parameters across all incubation time in the paddy soil incubations at the three studied temperatures. Further statistical information regarding the ANOVAs can be found in the supplementary files.

	Source of variation		
Parameter	**Age**	**Temperature**	**Interaction**
Dissolved Fe	1.4×10^{-39}	0.003	0.002
DOC	1.5×10^{-67}	0.33	0.72
CO2	3.6×10^{-17}	1.5×10^{-15}	0.10
CO2 (day 10)	7.1×10^{-15}	2.5×10^{-14}	0.0003
CH4	0.12	0.0002	0.76
CH4 (day 10)	1.1×10^{-13}	2.4×10^{-17}	8.6×10^{-10}
Total As	6.8×10^{-5}	0.011	0.94
Methylated As (%)	7.7×10^{-17}	9.2×10^{-5}	0.47
Oxymethylated As (%)	4.5×10^{-17}	4.7×10^{-13}	0.003
Methylthioarsenates (%)	1.2×10^{-5}	6.9×10^{-11}	4.7×10^{-5}
Inorg. Oxyarsenic (%)	2.4×10^{-13}	0.018	0.42
Inorg. thioarsenates (%)	2.4×10^{-6}	1.5×10^{-8}	1.4×10^{-7}
Eh	0.072	0.39	0.92
pH	3.4×10^{-47}	0.92	0.76
Aqueous S	0.005	3.3×10^{-9}	0.39

Table SI4: P-values of the one- and two-way-ANOVAs carried out for the analyzed parameters across all incubation time in the non-paddy soil incubations at the three studied temperatures. Further statistical information regarding the ANOVAs can be found in the supplementary files.

	Source of variation		
Parameter	**Age**	**Temperature**	**Interaction**
Dissolved Fe	0.022	0.28	0.82
DOC	0.076	0.0067	0.61
CO2	1.1×10^{-5}	7.0×10^{-6}	0.23
CO2 (day 10)	2.2×10^{-5}	3.2×10^{-7}	0.47
CH4	0.46	0.018	0.15
CH4 (day 10)	0.32	0.40	0.31
Total As	0.003	0.00031	0.087
Methylated As - P700 (%)	-	0.017	-
Oxymethylated As - P700 (%)	-	0.064	-
Methylthioarsenates - P700 (%)	-	0.0006	-
Inorg. Oxyarsenic - P700 (%)	-	0.051	-
Inorg. thioarsenates - P700 (%)	-	0.0006	-
Eh	0.83	7.8×10^{-11}	0.38
pH	3.0×10^{-15}	3.6×10^{-6}	0.96
Aqueous S	0.015	0.39	0.65

One-way-ANOVAs were carried out for As speciation in NP since only P700 was analyzed.

Table SI5: DNA, microbial C (C_{mic}) and microbial N (N_{mic}) in the 0-20 cm in the paddy soil chronosequence under flooded conditions. This data has been previously published by Kölbl, et al. [2]

Soil	DNA content (mg kg^{-1})	C_{mic} (mg kg^{-1})	N_{mic} (mg kg^{-1})
P50	760 ± 24	720 ± 120	28 ± 18
P100	630 ± 120	1000 ± 330	110 ± 55
P300	810 ± 220	1800 ± 780	92 ± 36
P2000	1100 ± 140	5100 ± 1300	150 ± 30

All parameters are given in reference to soil dry weight. (n = 5).

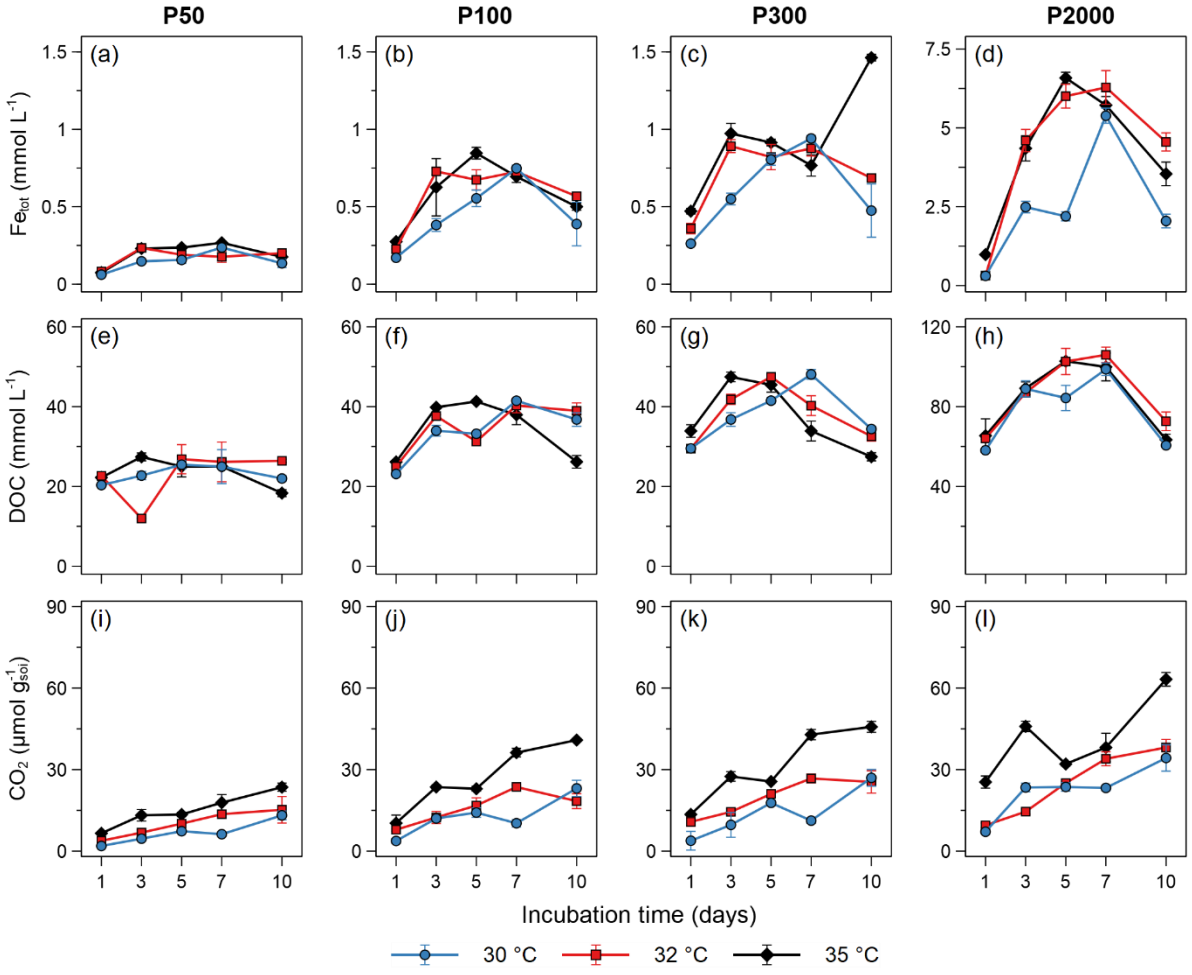

Figure SI2: Changes in selected biogeochemical parameters across incubation time in the paddy soil chronosequence incubated at different temperatures: dissolved Fe (a-d), DOC (e-h), and CO_2 (i-l). Data points represent means and error bars represent standard deviation (n=3). Note different axes for (d) and (h).

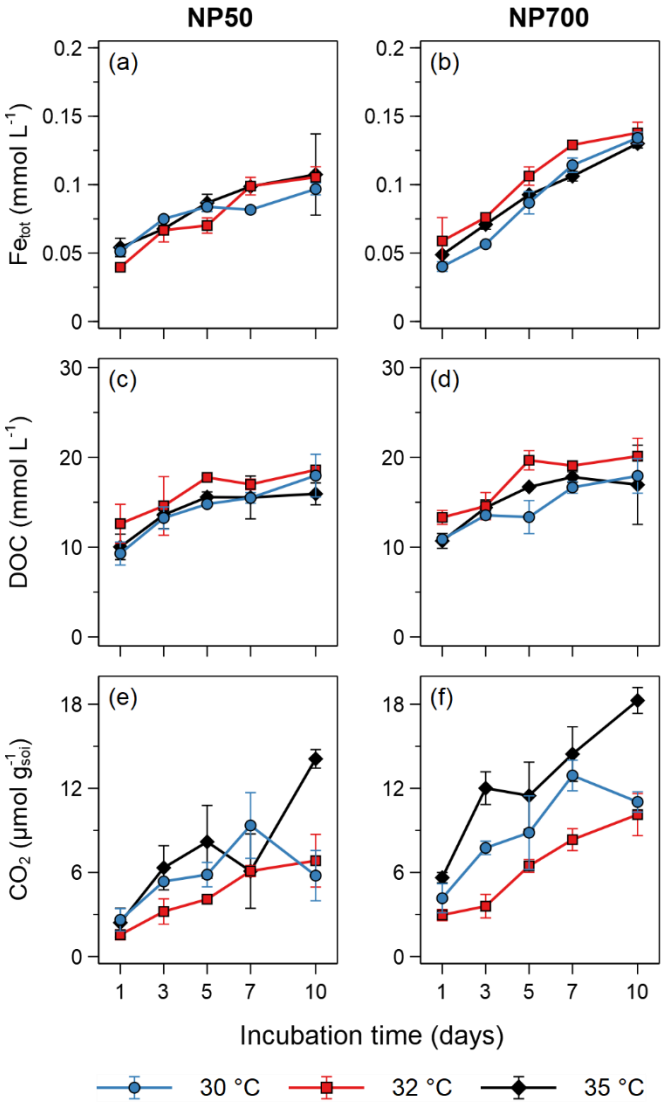

Figure SI3: Changes in selected biogeochemical parameters across incubation time in the non-paddy soil chronosequence incubated at different temperatures: dissolved Fe (a, b), DOC (c, d), and CO_2 (e, f). Data points represent means and error bars represent standard deviation (n=3).

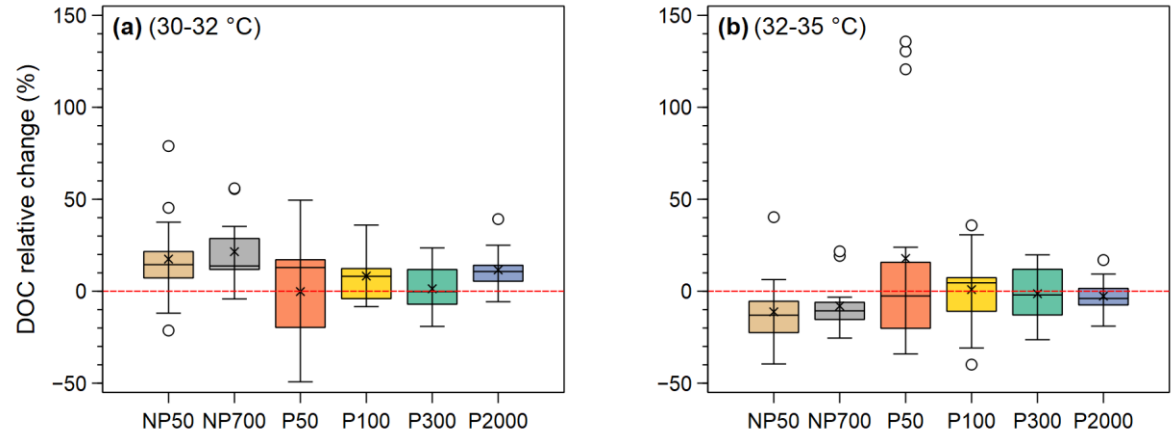

Figure SI4: Relative change in DOC concentration, integrated over all incubation times, based on both temperature comparisons: 30-32 °C (a) and between 32-35 °C (b). Each box summarizes the results of triplicates through the incubation time for each soil (n=15).

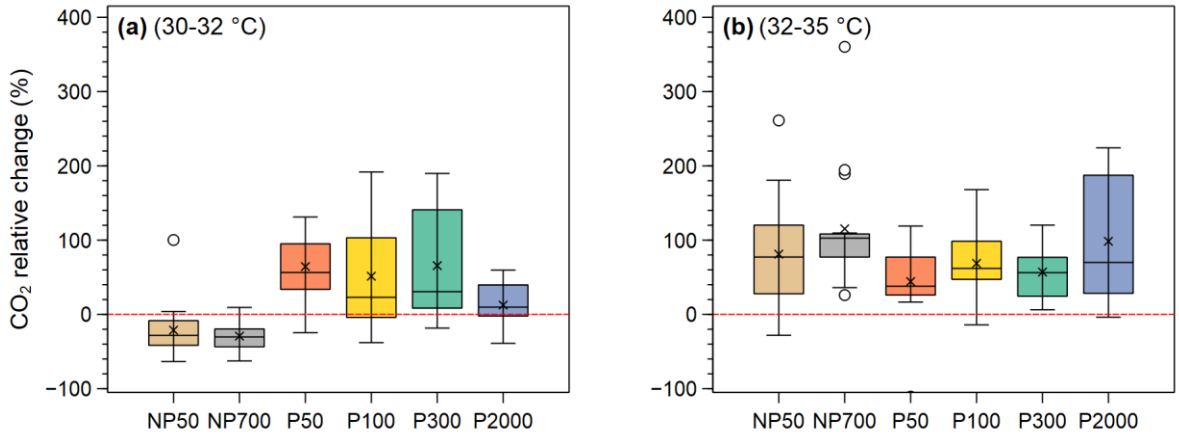

Figure SI5: Relative change in CO_2 production, integrated over all incubation times, based on both temperature comparisons: 30-32 °C (a) and between 32-35 °C (b). Each box summarizes the results of triplicates through the incubation time for each soil (n=15).

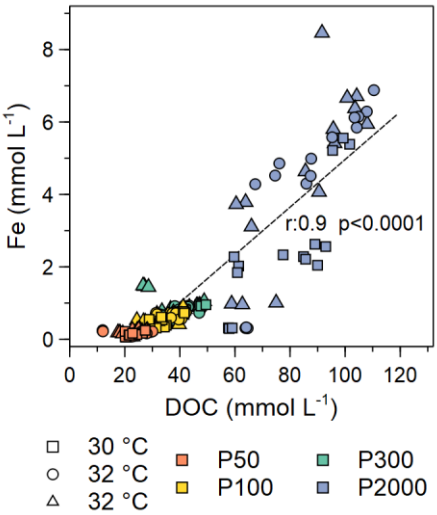

Figure SI6: Pearson correlation between dissolved Fe and DOC indicating release of DOC from reductive dissolution of Fe-SOC associations increasing with paddy soil age. Data is displayed as individual results of experimental triplicates from all 5 incubation times (n=15), colored-coded per soil.

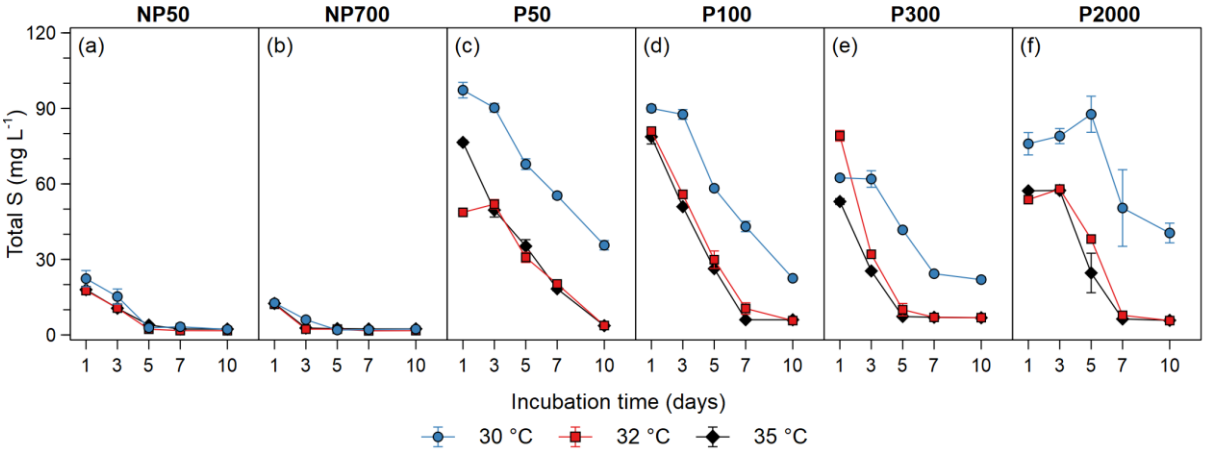

Figure SI7: Changes in total aqueous phase S across the non-paddy (a,b) and paddy (c-f) soil incubations at different temperatures. Data points represent means and error bars represent standard deviation (n=3).

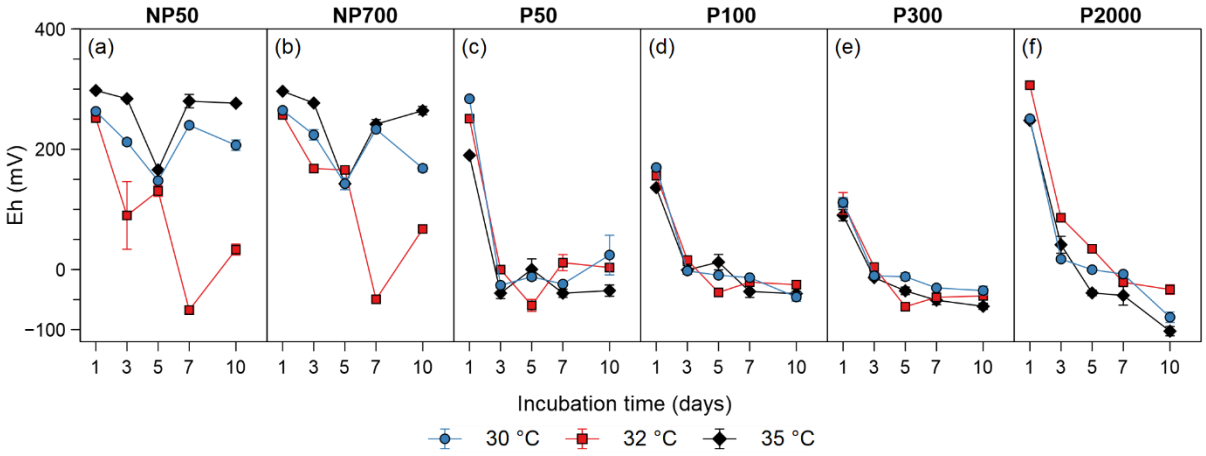

Figure SI8: Changes in redox potential across the non-paddy (a,b) and paddy (c-f) soil incubations at different temperatures. Data points represent means and error bars represent standard deviation (n=3).

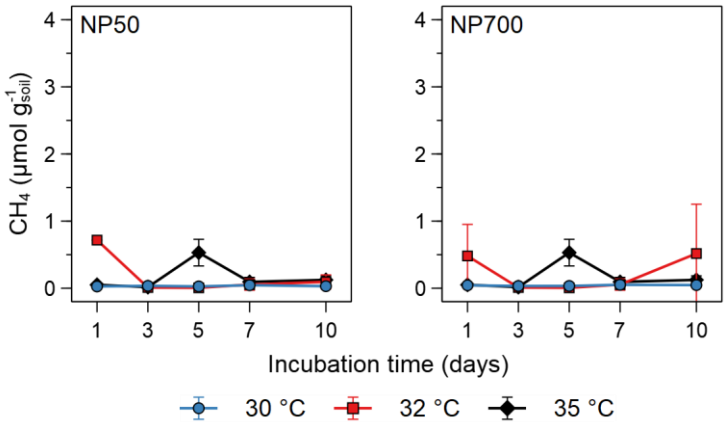

Figure SI9: Methane production in the non-paddy soil incubations at different temperatures. Data points represent means and error bars represent standard deviation (n=3).

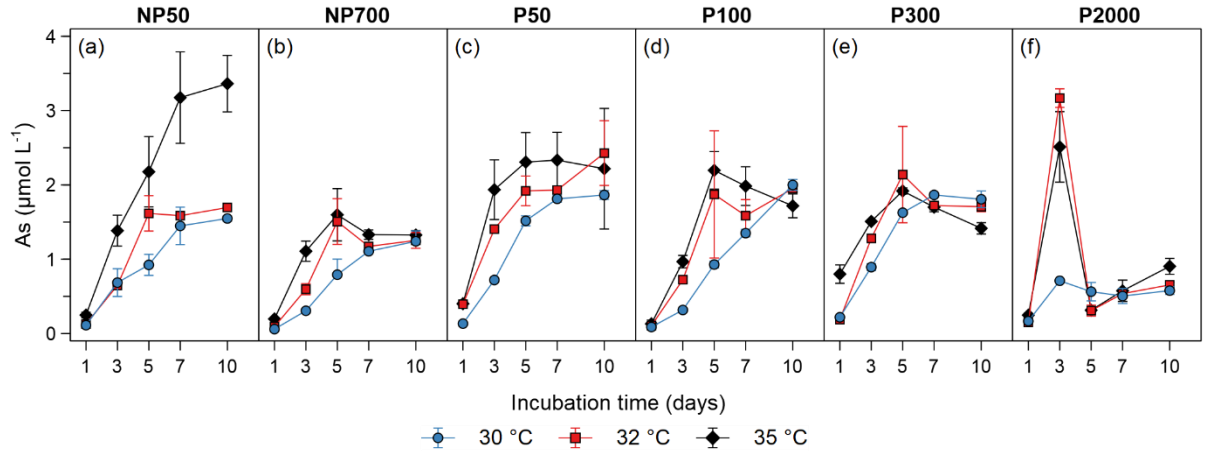

Figure SI10: Changes in total aqueous phase As across the non-paddy (a,b) and paddy (c-f) soil incubations at different temperatures. Data points represent means and error bars represent standard deviation (n=3).

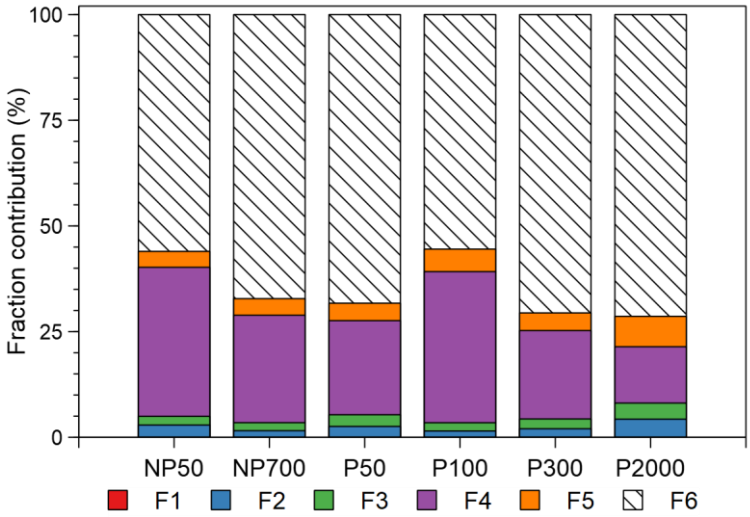

Figure SI11: Binding forms of As in the non-paddies and paddies. F1: Mobile fraction (Non detected), F2: Easily mobilizable fraction, F3: Organically bound to low affinity sites, F4: Reducible fraction, F5: Oxidizable fraction, F6: Non-extractable fraction (Total soil As - Σ F1 to F5).

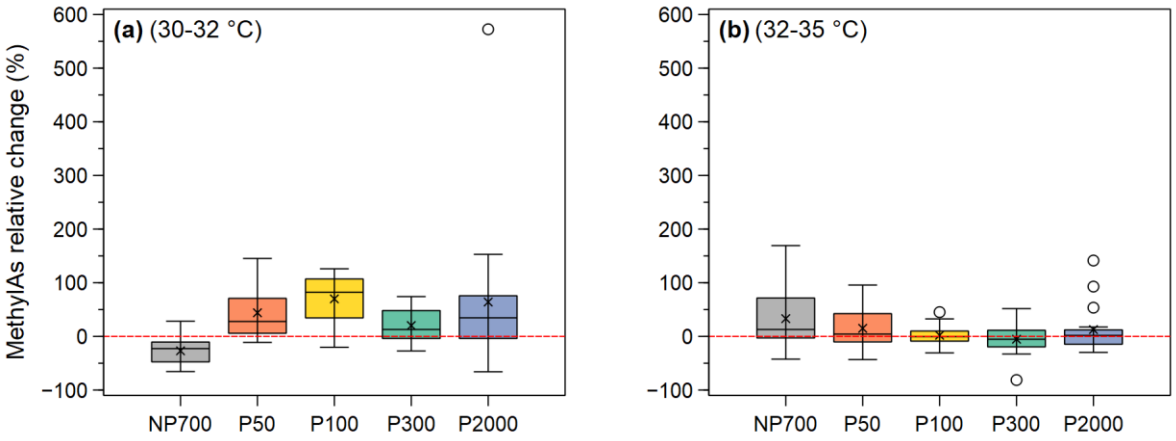

Figure SI12: Relative change in methylated As species contribution to total As, integrated over all incubation times, based on both temperature comparisons: 30-32 °C (a) and between 32-35 °C (b). Each box summarizes the results of triplicates through the incubation time for each soil (n=15).

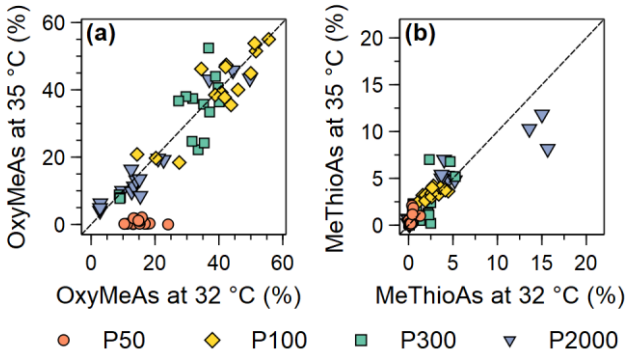

Figure SI13: Comparison of oxymethylated As (a) and methylthioarsenates contribution to total As between 32-35 °C. The data is displayed as individual results of experimental triplicates from all 5 incubation times (n=15), colored-coded per soil. The black dotted line represents a 1:1 line.

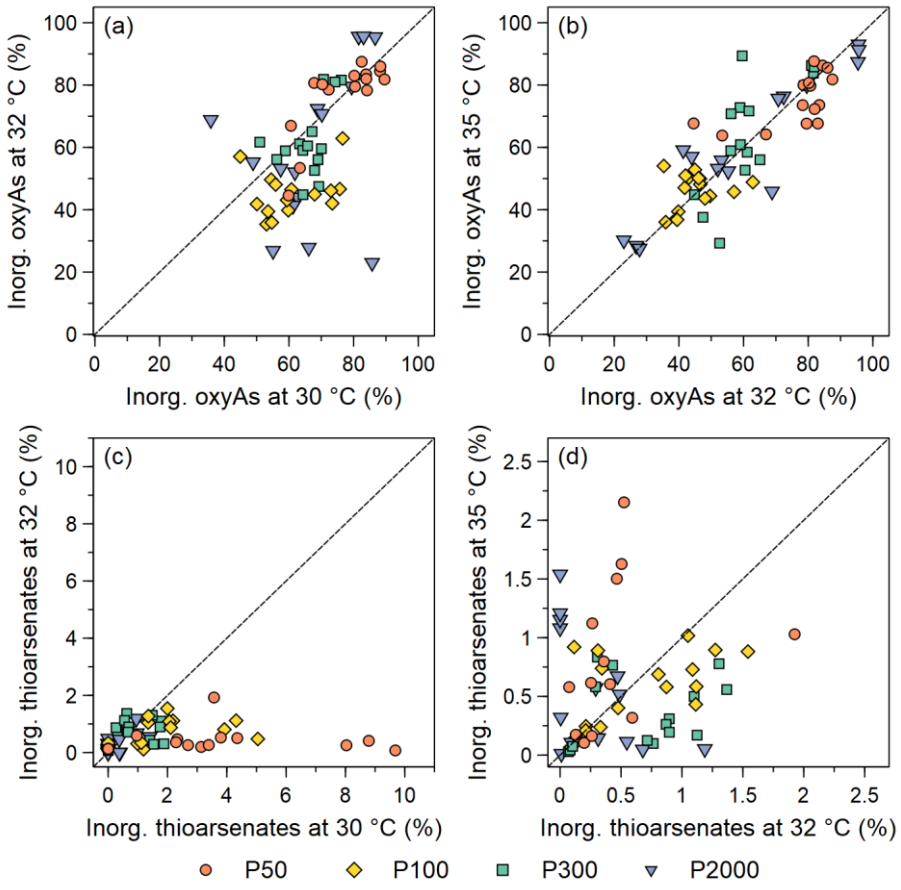

Figure SI14: Comparison of inorg. oxyarsenic (a, b) and inorg. thioarsenates (c,d) contribution to total As between 30-32 °C and between 32-35 °C. The data is displayed as individual results of experimental triplicates from all 5 incubation times (n=15), colored-coded per soil. The black dotted line represents a 1:1 line.

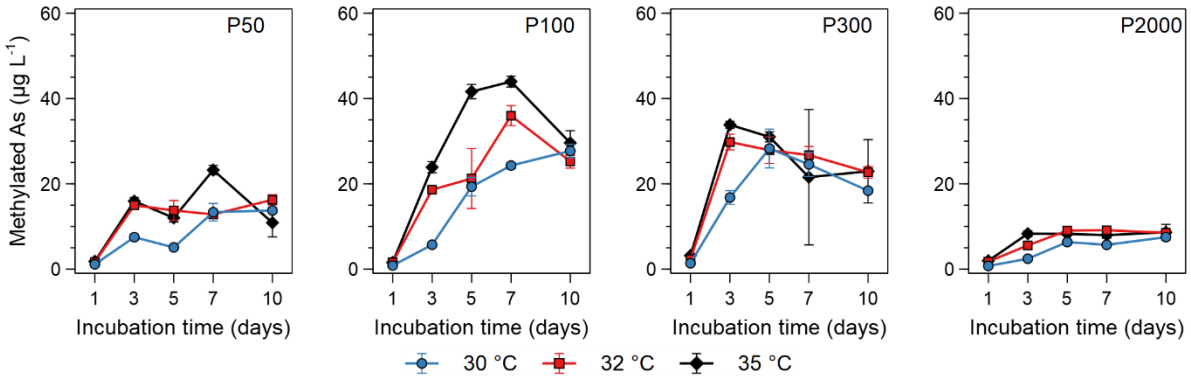

Figure SI15: Changes in concentration of methylated As species across all incubation time for paddy soil incubations at different temperatures. Data points represent means and error bars represent standard deviation (n=3).

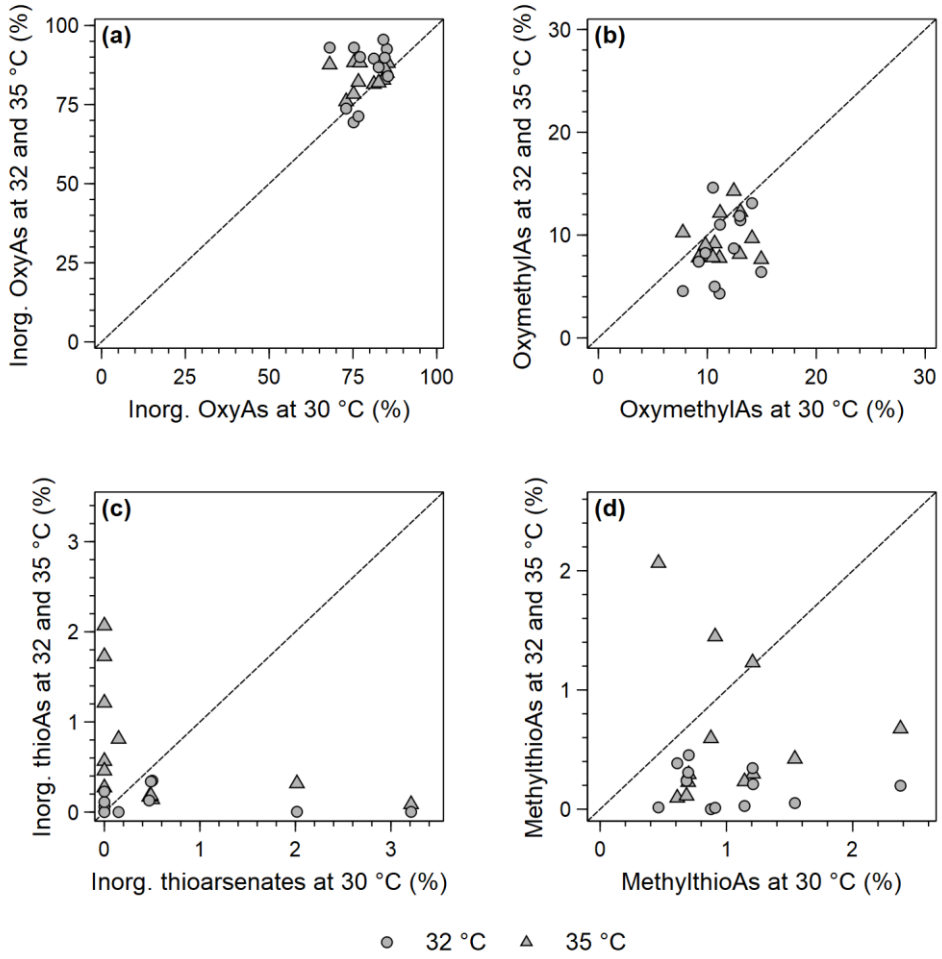

Figure SI16: Comparison of inorg. oxyarsenic (a), oxymethylated As (b), inorg. thioarsenates (c) and methylthioarsenates (d) contribution to total As between 30-32 °C and between 32-35 °C in the NP700 incubations. The data is displayed as individual results of experimental triplicates from all 5 incubation times (n=15). The black dotted line represents a 1:1 line.

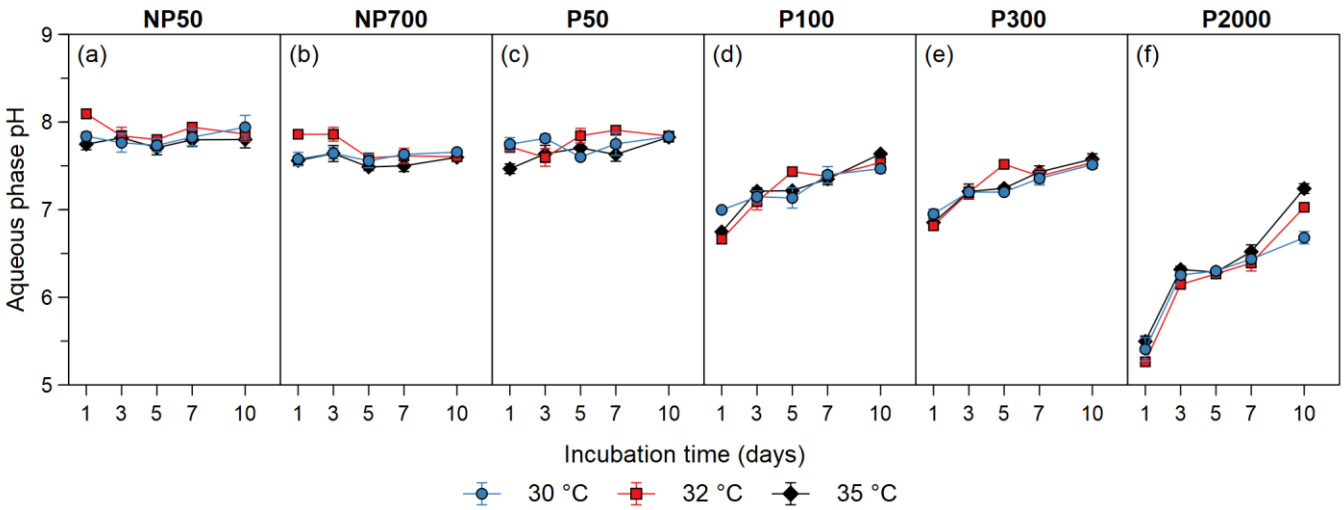

Figure SI17: Changes in aqueous phase pH across all incubation time for paddy soil incubations at different temperatures. Data points represent means and error bars represent standard deviation (n=3).

Additional references

1 Fulda, B., Voegelin, A., Ehlert, K. & Kretzschmar, R. Redox transformation, solid phase speciation and solution dynamics of copper during soil reduction and reoxidation as affected by sulfate availability. *Geochimica et Cosmochimica Acta* **123**, 385-402 (2013).

2 Kölbl, A. *et al.* Accelerated soil formation due to paddy management on marshlands (Zhejiang Province, China). *Geoderma* **228-229**, 67-89 (2014). https://doi.org:https://doi.org/10.1016/j.geoderma.2013.09.005

3 León Ninin, J. M. *et al.* Changes in arsenic mobility and speciation across a 2000-year-old paddy soil chronosequence. *Science of The Total Environment* **908**, 168351 (2024). https://doi.org:https://doi.org/10.1016/j.scitotenv.2023.168351

Study 3: Long-term paddy soil development buffers the increase in arsenic methylation and thiolation after sulfate fertilization

José M. León Ninin, Nathalie Kryschak, Stefan Peiffer, and Britta Planer-Friedrich

Reprinted with permission from

Journal of Agricultural and Food Chemistry (*72*, pp. 25045–25053)

Own contribution to Study 3:	
Concept and study design	80%
Data acquisition	95%
Analyses of samples	95%
Data analysis and figure preparation	95%
Discussion of results	95%
Manuscript writing	90%

This study was designed by J.M.L.N. and B.P.-F.; experiments and analyses of samples were carried out by J.M.L.N. with the support of N.K.; access to analytical facilities was provided by S.P. and additional analyses were carried out at the Limnological Research Station and the Ecological Microbiology group at the University of Bayreuth (see acknowledgments); data analyses, figure preparation, discussion of results, and manuscript writing were carried out by J.M.L.N. with the support of B.P.-F.; all authors contributed to the revisions of the published manuscript.

JOURNAL OF AGRICULTURAL AND FOOD CHEMISTRY

pubs.acs.org/JAFC Article

Long-Term Paddy Soil Development Buffers the Increase in Arsenic Methylation and Thiolation after Sulfate Fertilization

José M. León Ninin, Nathalie Kryschak, Stefan Peiffer, and Britta Planer-Friedrich*

Cite This: J. Agric. Food Chem. 2024, 72, 25045−25053 Read Online

ACCESS | Metrics & More | Article Recommendations | Supporting Information

ABSTRACT: Sulfate fertilization has been proposed to limit arsenic (As) mobility in paddy soils and accumulation in rice grains. However, As and sulfur (S) have complex biogeochemical interactions. Besides the desired precipitation of sulfides that sorb or incorporate As, S can enhance As biotic methylation and abiotic thiolation. Incubating 50- to 2000-year-old paddy soil chronosequence samples without and with S-addition showed the highest relative increases in the formation of low-sorbing, phytotoxic methylated oxyarsenates, and low-sorbing, cyto-, and phytotoxic thioarsenates in the youngest soil. These increases were related to low soil organic carbon (SOC) and iron (Fe) availability, high pH, and As methylation driven by sulfate-reducing bacteria. In older paddy soils, higher SOC and Fe availability buffered these net increases but only in healthy soils. Two paddy soils, where microbial activity and Fe availability had been anthropogenically disturbed, lacked this buffering effect. Therefore, soil history should be considered prior to sulfate fertilization.

KEYWORDS: *sulfate fertilization, rice cultivation, arsenic speciation, thioarsenates*

INTRODUCTION

Sulfur (S) is an essential nutrient for plants, and it is linked to plant health, yield, and efficient food production.[1,2] Atmospheric deposition is an important source of S in agricultural soils, originating either from natural sources or from anthropogenic activities such as fossil fuel combustion.[3,4] A decrease in fossil fuel use to decrease global warming, and policy and technical improvements for enhancing air quality have lowered S deposition in the last decades.[5] Considering that in the last two centuries, increased S deposition from anthropogenic sources has been coupled with the growth of intensive agriculture, sulfur depletion in agricultural soils as a consequence of these recent regulations could risk food security in the future.[3] Thus, S fertilization has been proposed to ensure enough S supply to croplands.[3]

In rice agriculture, S fertilization has been additionally proposed to decrease the accumulation of toxic arsenic (As) in grains.[6−9] Traditional cultivation in flooded paddy fields creates an anoxic environment that mobilizes As from the soil.[10,11] Once in the aqueous phase, rice plants can readily take up As and accumulate it in the grains, representing a significant dietary exposure.[12−14] Under these anoxic conditions, sulfate-reducing bacteria (SRB) produce sulfide that can be precipitated as iron (Fe)−sulfide phases, sorbing or incorporating As, or in the form of As−sulfide phases, directly removing As from the porewater and limiting its availability for rice plants.[9,15]

Different sulfur amendments have been studied in paddy soil systems, such as S-rich manure, S-based minerals such as gypsum, elemental sulfur (S^0), and sulfate salts, with the last two being the most widely studied.[6,16−18] Although sulfate salts have shown better performance, there are still contrasting reports on their effectiveness in removing As from the aqueous phase and in limiting its accumulation in rice grains. Tang et al.[17] observed around 20% decreases in As concentrations in porewater when adding 0.35 mmol Na_2SO_4 kg_{soil}^{-1} and around 75% decreases with a 3-fold higher application. Wang et al.[19] reported a decrease of porewater As only in the early stages of mesocosm experiments. Zhang et al.[16] showed either no effects or even an increase in porewater As when adding elemental sulfur and gypsum to pot experiments. Currently, it is not well understood why As biogeochemistry shows contrasting responses to sulfate addition in different soils.

It must be considered that S biogeochemistry is related to As in more ways than the precipitation of sulfides. Recent studies have shown that SRB are involved in As methylation,[20,21] forming methylated oxyarsenic species (mono- and dimethylarsenate, MMA and DMA, respectively) from arsenite in consecutive steps. The reduced S produced by the activity of SRB can also react with arsenite or with methylated oxyarsenic species to form inorganic and methylated thioarsenates, respectively.[19,22] Thioarsenates have been recently identified in paddy soil porewaters[19,23] and rice grains,[24] raising food safety concerns due to their high mobility and cytotoxicity.[25−27] Moreover, methylated As species,[28,29] especially dimethylthioarsenates, have been identified as phytotoxic, risking plant yield through so-called straighthead disease.[25,26,30] Increased formation of methylated oxyarsenic species (through enhanced SRB activity) and inorganic and methylated

Received: October 7, 2024
Revised: October 22, 2024
Accepted: October 23, 2024
Published: October 30, 2024

thioarsenates (due to an excess of reduced S as a byproduct of sulfate reduction) could hinder the sorption to or precipitation as sulfides and could explain the contrasting effectiveness of sulfate fertilization. Thus, thioarsenate formation could be an unwanted secondary effect from sulfate fertilization, with studies showing that sulfate addition to meso- and microcosm experiments increases thioarsenate content in paddy soil porewaters.[19,21] Considering that studies on sulfate fertilization often focus on total As concentration or use routine speciation analyses (overlooking thioarsenate formation), it is important to get a comprehensive understanding of how sulfate addition influences As biogeochemistry and, as a consequence, its mobility and toxicity for rice plants and consumers.

Arsenic mobility and speciation in paddies are influenced by different soil properties, such as As and Fe content and availability, soil organic carbon (SOC), soil pH, and microbial activity.[23,31] While these properties are influenced by geographical locations and agronomical practices, chronosequence studies have shown that they are subjected to a general soil development with long-term paddy use.[32−34] A particular chronosequence located in Cixi (province of Zhejiang, China) has been key in determining the main changes in pedological properties and developmental phases of paddy soil after land reclamation from salt marshes. This chronosequence is unique both in its time span, including soils with ages between 50 and 2000 years of use, and in the vast amount of available literature on soil properties and processes, which document its reliability to study the influence of long-term paddy use on soil properties.[32,34−37] Long-term paddy management causes SOC accumulation, decreases soil pH, and, as shown in our previous study, limits As mobility due to the formation of low crystallinity Fe phases.[23,32] The same study established that, concerning speciation, long-term paddy use decreases thiolation due to an increased availability of dissolved Fe which scavenges reduced S, but increases methylation due to a higher microbial activity supported by the accumulated SOC.[23] Long-term paddy soil development could offer important insights into which properties could limit dangerous As-related side effects from sulfate fertilization.

In this study, we incubated six paddy soils from the Cixi chronosequence, which comprise a wide range of pedological properties, with and without the addition of sulfate to evaluate how soil history influences the effects that sulfate fertilization could have on As mobility and speciation. Here, we refer to two different aspects of soil history: normal paddy soil development (based on four soils documented to to be used as paddies for50, 100, 300, and 2000 years) and the effects of additional anthropogenic influences that interfere with normal soil development,based on two soils from the same area that have gone through physical disturbance (topsoil removal) and chemical disturbances (oil spill; see Materials and Methods). We hypothesize that low Fe and SOC availability will increase arsenic methylation and thiolation in younger soils when sulfate is added. In contrast, older paddy soils may buffer this effect due to SOC accumulation, increased Fe availability, and a decrease in pH. However, chemical and physical disturbances that negatively affect microbial activity (oil spill) or decrease reducible Fe and SOC content (topsoil removal) could reverse this buffering effect. Through a comprehensive analysis of S, Fe, and As biogeochemistry, we link how changes in soil properties related to paddy soil development can regulate As mobility and speciation upon sulfate fertilization.

MATERIALS AND METHODS

Soil Samples. To assess the effect of S-fertilization on soils in different stages of soil development, we used soils from a Chinese paddy soil chronosequence. Located in Cixi (Zhejiang), this chronosequence is unique in the amount of existing data and its timespan. For the past 2000 years, salt marshes have been reclaimed into agricultural fields by sedimentation and the building of dikes, which allows the estimation of the age of the agricultural fields.[32,34,37] Throughout the text, soils are referred to as P (for paddies), followed by a number according to their estimated age. We used the ≤2 mm fraction of the topsoil of the main sites described by Cheng et al.[35] and Kölbl et al.,[32] with a duration of use (or "age") of 50, 100, 300, and 2000 years. Two additional soils from the area with ages of 700 and 1000 years were also used. However, the chronosequential integrity of these two soils was disturbed. P700 was contaminated with a fossil fuel spillage,[38−40] and the topsoil of P1000 was removed 5 years before sampling.[32,34] We use these two soils to understand how disrupted chronosequential development influences As mobility, speciation, and the effects of S-fertilization. The As binding mechanisms in the soil were determined by a sequential extraction procedure (SEP) following Fulda et al.[41] A detailed explanation of the procedure can be found in Table S1. Selected soil properties of the six soils are listed in Table S2. The high S content of the soils might be related to their coastal location and history as salt marshes. However, it has been established that soluble salts and elements are easily washed out during the first 50 years of paddy use.[32] Most of the S content in the soil is then likely bound to mineral phases of low solubility or to organic matter.

Incubation Experiments. Anoxic incubation experiments were conducted in 120 mL serum vials with 10 g of soil and 20 mL of N_2-purged aqueous phase. The aqueous phase consisted of Na_2SO_4 (+3 mmol of SO_4 kg_{soil}^{-1}, simulating sulfate fertilization, Merck) or NaCl (12 mmol kg_{soil}^{-1}, as ionic strength control, Merck). Both solutions had an ionic strength of 6 mmol L^{-1} and were prepared in ultrapure water (MQ, ≥18.2 MΩ cm, TOC < 3 μg/L) (Table S3). The selected concentration of sulfate added was based on previous studies that mimic sulfate fertilization in paddy soils.[17,19,21] The incubation vials were closed with rubber stoppers and aluminum caps inside a glovebox (95% N_2, 5% H_2, COY) and incubated at 30 °C (average maximum temperature in the Cixi region during the cropping season) standing in the dark for 10 days. This time point was selected based on previous studies showing that, in these soils, redox biogeochemical trends related to long-term paddy use are stable after 10 days.[23,42] After this time, the vials were taken out of the incubator, shaken, and allowed to reach room temperature (20 °C). The inner pressure of the vials was measured (Greisinger GMH, 3100 Series), and 5 mL of headspace was sampled using a gastight syringe and needle for CH_4 and CO_2 determination through a gas chromatograph with a flame ionization detector (GC-FID, SRI instruments 8610C) equipped with a methanizer.

Inside the glovebox, the content of the vials was homogenized to form a slurry and transferred into 50 mL centrifuge tubes. The tubes were closed and wrapped in parafilm, centrifuged at 4000 rpm for 10 min, and brought back inside the glovebox. The aqueous phase was separated from the soil with a syringe and needle, filtered under anoxic conditions inside the glovebox through 0.2 μm cellulose-acetate filters (Chromafil Xtra), and split into aliquots for the following described analyses. The soil was frozen, freeze-dried, and homogenized with a mortar and pestle for zerovalent sulfur (S^0) determination via HPLC−UV−vis after chloroform extraction.[43]

Aqueous Phase Analyses. Total Fe and Fe^{II} (using the ferrozine method[44,45]) and sulfide (methylene blue method[46]) were determined photometrically in triplicate using a multiplate reader (Infinite 200 PRO, Tecan). Colorimetric reactions and analyses were carried out outside the glovebox after anoxic sample stabilization according to the methods. If necessary, samples were diluted with MQ. A multimeter (HQ40d, Hach) was used to measure the pH (PHC301, Ag/AgCl electrode) and redox potential (MTC101).

https://doi.org/10.1021/acs.jafc.4c09537
J. Agric. Food Chem. 2024, 72, 25045−25053

For analyses of total As and S, a 2 mL aliquot was stabilized with 0.5% H_2O_2 and 0.8% HNO_3 and diluted before analysis by inductively coupled plasma-mass spectrometry (ICP-MS, 8900 Triple Quad, Agilent) in reaction mode with O_2. Arsenic was measured as AsO^+ (m/z = 91) and S as SO^+ (m/z = 48). Rhodium was used as an internal standard to compensate for signal drift, and a certified reference material (TMDA 62.2, Environment Canada) was used for quality control.

For As speciation analysis, a 700 μL aliquot was stabilized with 100 μL of hydroxybenzylethylenediamin (HBED, pH 7).[23] To ensure complexation of all the dissolved Fe, an HBED solution of 10 mmol L^{-1} was used to stabilize samples with Fe concentrations of <1 mmol L^{-1}, and a 59 mmol L^{-1} solution was used for those with higher Fe concentrations. The stabilized aliquot was flash-frozen in dry ice and kept at −20 °C until analysis. Samples were thawed inside the glovebox directly before analyses to avoid changes in speciation due to oxidation. Arsenic species were separated by ion chromatography (IC, 940 Professional IC Vario Metrohm) and quantified through ICP-MS. For the chromatographic separation, an AS16 column (Dionex AG/AS16 IonPac) was used, with a 2.5−100 mM NaOH gradient, 1.2 mL min^{-1} flow rate, and an injection volume of 50 μL.[47] Individual As species were assigned based on previously reported retention times.[19,48,49] Concentrations were calculated through a calibration containing arsenite ($NaAsO_2$, Fluka), arsenate ($Na_2HAsO_4{\cdot}7H_2O$, Fluka), MMA ($CH_3AsNa_2O_3{\cdot}6H_2O$, Supelco), and DMA ($C_2H_6AsNaO_2{\cdot}3H_2O$, Sigma-Aldrich). Concentrations of thiolated As species were calculated based on their oxyarsenic homologues. Throughout the text and figures, individual species have been grouped, depending on the biogeochemical processes related to their formation. Shortly, arsenite and arsenate are summarized as inorganic oxyarsenic (inorg. oxyAs), while MMA and DMA are summarized as methylated oxyarsenates (methyl. oxyAs). Mono-, di-, and trithioarsenate are summarized as inorganic thioarsenates. Monomethylmonothioarsenate (MMMTA), monomethyldithioarsenate (MMDTA), monomethyltrithioarsenate (MMTTA), dimethylmonothioarsenate (DMMTA), and dimethyldithioarsenate (DMDTA) are summarized as methylthioarsenates. The sum of methylated oxyarsenates and methylthioarsenates is termed total methylated As.

A 2 mL aliquot for acetate determination was filtered through a 0.45 μm polyamide syringe filter (Macherey-Nagel) and kept frozen until analysis by High-Performance Liquid Chromatography with a Refractive Index Detector (HPLC-RID, Agilent 1200) with a Rezex ROA Organic Acid column.[50] Acetate analyses were carried out from incubations under the same conditions but with tap water as aqueous phase, as part of an already published experiment.[23]

Determination of Sulfate Reduction Rates. The sulfate reduction rate (SRR) of each soil was determined. For this, a slurry prepared from 3 g of soil and 100 mL of N_2-purged deionized water was preincubated at room temperature for 7 days inside a glovebox. After preincubation, the slurry was homogenized, and a 10 mL aliquot was transferred to a septum vial, closed with a rubber stopper and aluminum cap, and spiked with 34 μL of a ^{35}S-labeled sulfate standard (50 kBq, Hartmann Analytic). The spiked slurries were incubated for 5 h at room temperature. The incubation was stopped by injecting 5 mL of a N_2-purged 10% zinc acetate solution (Grüssing) through the rubber stopper and mixing the content of the vial. ^{35}S-labeled products of sulfate reduction were determined following the reflux distillation method by Fossing and Jørgensen (1989).[51] Shortly, soil samples were extracted for 1 h in an N_2-purged distillation apparatus over a sand bath using 5 mL of 5 M HCl (AnalytiChem), 3 mL of ethanol (VWR), and 15 mL of a 1 M $CrCl_2$ (Sigma-Aldrich) solution in 0.5 M HCl. The evolving ^{35}S-labeled H_2S was trapped in 50 mL of 0.15 M NaOH (Merck) and measured by using a scintillation counter (Tri-Carb 2800TR) after dilution with a scintillation cocktail (ROTISZINT HighCapacity, Roth).

RESULTS AND DISCUSSION

S-Addition Effects on As Mobilization. Anoxic incubation caused As mobilization in all soils, with concentrations ranging between 0.48 ± 0.04 and 2.81 ± 0.08 μmol L^{-1}. Soils that follow a chronosequential development (namely, P50, P100, P300, and P2000) showed decreasing As mobility with increasing paddy soil age (Figure 1). This trend has been previously reported and is related to

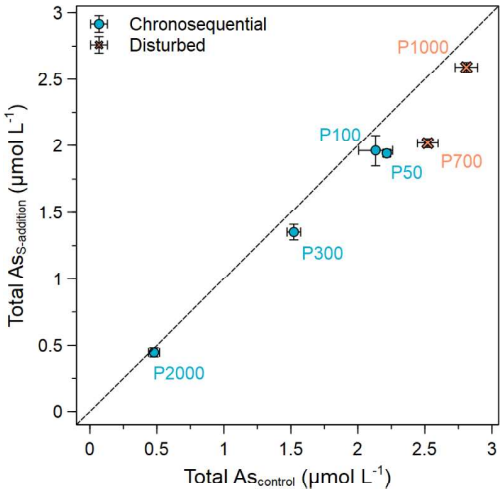

Figure 1. Changes in As mobilization with the addition of sulfate after 10 days of incubation. The black dotted line describes a 1:1 line for comparison between treatments. Data points are mean values, and error bars represent standard deviation (n = 3).

the increasing abundance of low crystallinity Fe phases with long-term paddy management that offer sorption sites.[23] P700 and P1000 are outliers due to their individual histories of anthropogenic disturbances.

P700 had soil As contents slightly higher than the chronosequence soils (Table S2), and the sequential extraction procedure showed that 7.5% of the solid phase As is weakly bound (∑F1 to F3) (Figure S1). It is not known whether the higher soil As content and increased mobility are related to the chemical spillage that affected the soil. In comparison, P2000 shows a higher contribution of weakly bound As (8.1%) but also has the lowest soil As content. Moreover, microbial activity (assessed through higher Eh) and particularly Fe reductive dissolution seemed to be hampered in P700 (Figure S2a), which could suggest that, in the soil's original conditions, there is no effective formation of secondary Fe minerals that could remove As from the porewater. P1000 had the highest solid phase As content of all studied soils with 38 mg kg^{-1} (more than double the average of all other soils) (Table S2). Kölbl et al.[32] showed in the chronosequence that redox-sensitive elements (such as Al, Mn, and Fe) migrate toward deeper soil layers as a consequence of the redox fluctuations related to paddy management. We suggest that the removal of the topsoil exposed a soil layer enriched with As, which had migrated for centuries from the previous topsoil. This As-enriched new topsoil had an increased As mobilization due to the lack of SOC and low crystallinity Fe phases to sorb As, as well as low microbial activity and high Eh values, which likely hamper the formation of secondary minerals to sorb As.

Sulfate addition caused a decrease between 8 and 20% of the total As concentrations in the aqueous phase of all soils (Figure

https://doi.org/10.1021/acs.jafc.4c09537
J. Agric. Food Chem. 2024, 72, 25045−25053

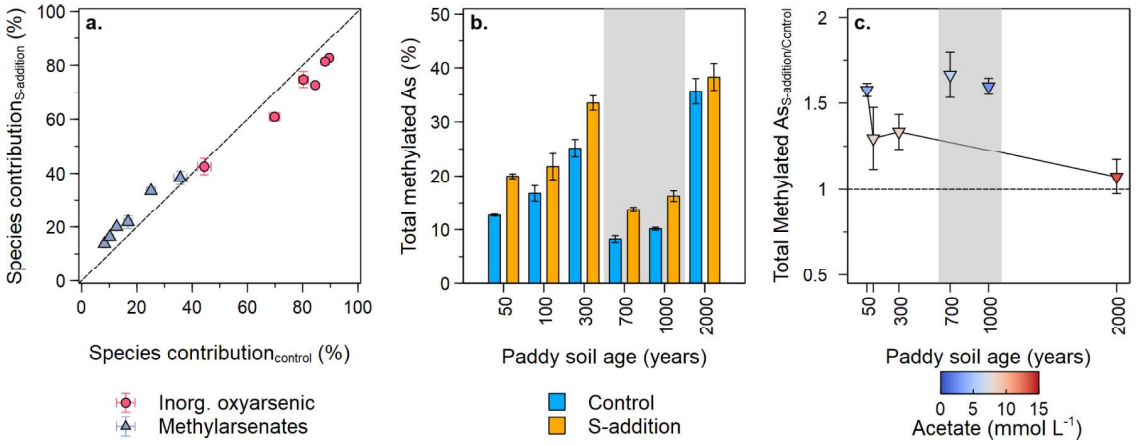

Figure 2. Changes in inorganic oxyarsenic and total methylated As contribution to total As with S-addition (a). The black dotted line in panel a describes a 1:1 line for comparison between treatments. Effect of S-addition increasing total As methylation depending on soil history in contribution to As speciation (b) and relative change (c) when comparing the % of methylated As with S-addition to that in the control. The dotted line in panel c represents a 1× ratio, meaning no relative change in methylation; data points above this line indicate an increase in methylation with S-addition. In panels b and c disturbed soils are gray-shaded. Aqueous acetate concentrations in the incubations are represented by the color in the data points in panel c. Data points and bars are mean values, and error bars represent standard deviation (n = 3).

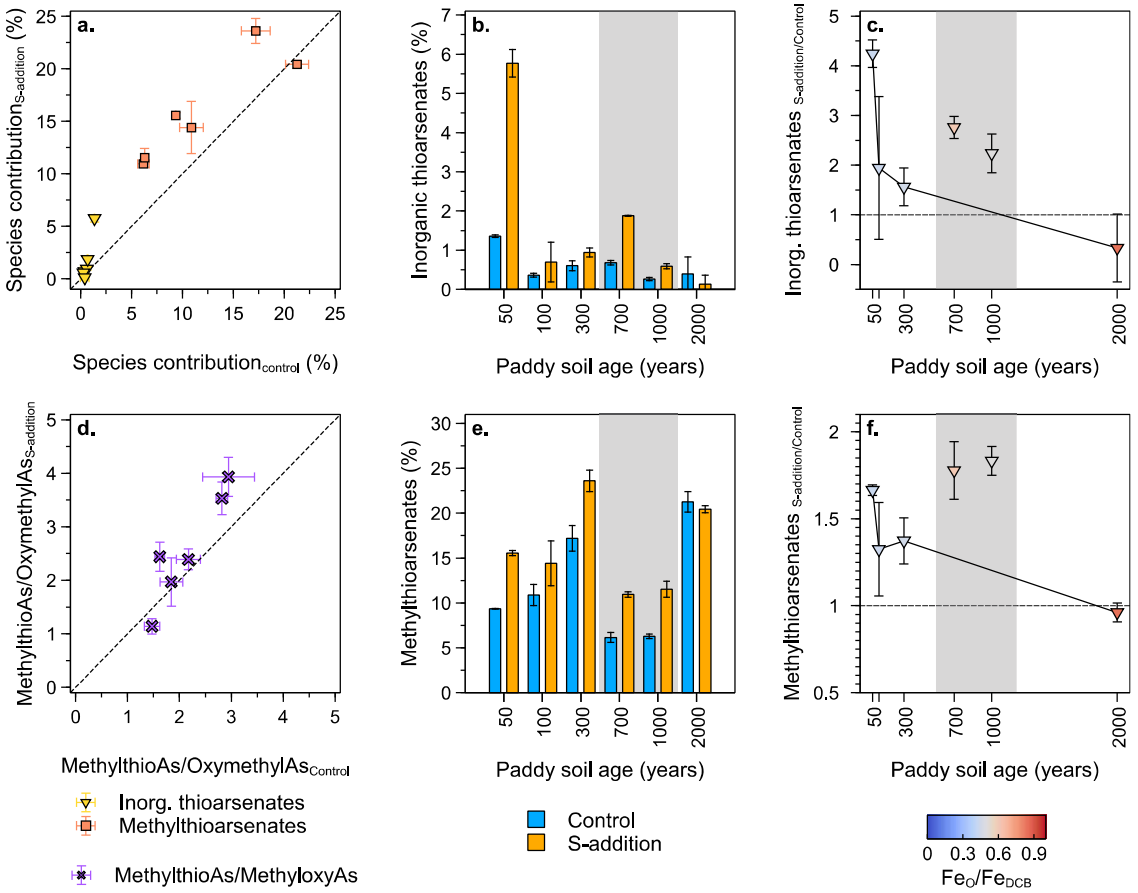

Figure 3. Changes in the inorganic and methylthioarsenate contributions to total As with S-addition (a). Effect of S-addition increasing formation of inorganic thioarsenates depending on soil history in contribution to As speciation (b) and as relative change (c) when comparing the % of inorganic thioarsenates As with S-addition with that in the control. Dominance of methylthiolated species over their oxymethylated counterparts with S-addition (d). Effect of S-addition increasing formation of methylated thioarsenates depending on soil history in contribution to As speciation (e) and as relative change (f) when comparing the % of inorganic thioarsenates As with S-addition with that in the control. The black dotted line in panels a and d describes a 1:1 line for comparison between treatments. In panels b, c, e, and f, disturbed soils are gray-shaded. The dotted line in panels c and f represents a 1× ratio, meaning no relative change in the formation of inorganic and methylated thioarsenates, respectively; data points above this line indicate an increase in thiolation with S-addition. Fe_o/Fe_{DCB} in the soils is represented by the color in the data points in panel c and f. Data points and bars are mean values and error bars represent standard deviation (n = 3).

https://doi.org/10.1021/acs.jafc.4c09537
J. Agric. Food Chem. 2024, 72, 25045−25053

1), with no significant difference or trends related to long-term paddy soil development (Figure S3). Another study has observed a similar decrease in As mobilization with the addition of similar S concentrations.[17] Generally, lower dissolved Fe concentrations in the S-addition incubations (Figure S2b) indicate its precipitation as secondary Fe−S phases, which would either incorporate or sorb As from the aqueous phase, decreasing its concentration. In the case of P2000, there was no decrease in dissolved Fe probably due to its excess in comparison to the added sulfate. The highest decrease was observed in P700, which was also the soil with the higher initial S concentrations in the aqueous phase (Figure S4).

S-Addition Effects on As Methylation. Sulfate addition caused an increase in As methylation (Figure S5) at the expense of inorganic oxyarsenic concentrations in the aqueous phase (Figure 2a), likely due to increased SRB activity and thus As methylation.[20,21] In the soils that follow a normal soil development, arsenic methylation increased with the paddy soil age as expected[23] (Figure 2b). However, the magnitude of the relative increase in As methylation was negatively correlated with long-term paddy development (Figure 2c). Younger paddies showed a relatively higher increase between 1.6- (P50) and 1.3-fold (P100, P300), while P2000 showed an increase of only 1.1-fold.

We have previously suggested through statistical observations that long-term paddy management influences the main microbial communities related to As methylation.[23] In younger paddies with low SOC, SRB are important As methylators. When paddies develop and SOC accumulates, fermentative bacteria, also suggested as methylators in paddy soils,[52] would gain relevance in the methylation process. The data presented here show that as acetate concentrations in the porewater increase with long-term paddy development, the relative effect that S-addition has on increasing As methylation is lower (Figure 2c), supporting this previous observation. Briefly,in younger paddies, since methylation is mainly carried out by SRB, S-addition generated an increase of higher magnitude. The effect becomes smaller with long-term paddy use as fermentative bacteria become more relevant for As methylation.

The disturbed soils had a lower As methylation capacity than if they followed a normal chronosequential development (Figure 2b) but showed an important and positive relative change in methylation with S-addition (1.6 and 1.7-fold increase, Figure 2c). P700 and P1000 had relatively low acetate contents, which can be related to their histories. In the case of P700, hindered microbial activity would mean that fermentative processes are also slowed down (suggested by its relatively low acetate concentration). In P1000, the removal of the topsoil and accumulated SOC means that substrates for fermentative bacteria are scarce. These results suggest that the relatively low methylation that takes place in these soils is driven by SRB, explaining the high increase in As methylation upon S-addition, comparable to that on P50.

Several studies have also identified that methanogens can influence As methylation dynamics through demethylation.[53−55] It could be argued that the increase in methylation is related to a decrease in methanogenic activity since S-addition has also been reported to limit methane emissions from paddy soils.[56−58] However, we found that S-addition did not cause significant changes in methane production in any soil, independently of chronosequential or disturbed development (Figure S6).

In general, decreasing contributions of carcinogenic inorganic oxyarsenic can be seen as a positive effect of S-addition. However, an increase in methylated As species can still represent a risk for food production due to their phytotoxicity, which can cause straighthead disease.[29] More importantly, methylated oxyarsenates are precursors of highly toxic methylthioarsenates.

S-Addition Effects on Arsenic Thiolation. S-addition caused an increase in the concentration (Figure S7) and contribution of inorganic and methylthioarsenates to total As (Figure 3a). In the 4 chronosequence soils, both the contribution of inorganic thioarsenates to As speciation and the magnitude of the relative change in their formation after S-addition were higher in younger paddies and decreased strongly with long-term paddy use (Figure 3b,c). In P50, inorganic thioarsenate contribution increased 4.2-fold with S-addition, compared to a 1.9-fold in P100. For P2000, there was even a decrease in thiolation with S-addition. We have previously reported that long-term paddy use decreases paddy soil thiolation potential, mainly because of the increased abundance of easily reducible Fe phases .[23] Upon reductive dissolution, these Fe phases release Fe^{II} into the aqueous phase (Figure S8), which then reacts with sulfide to precipitate as Fe−S phases. Thus, the availability of reduced S for As thiolation decreases with increasing paddy soil age. Supporting this, free sulfide was not detected in the porewater of any incubation, except for P50 with S-addition (7.8 ± 0.6 μmol L^{-1}), the soil that showed the highest relative increase in inorganic thioarsenates content. The results presented here show that the increasing content of amorphous Fe with increasing long-term paddy use (based on oxalate and dithionite−citrate−bicarbonate extractions; see Fe_o/Fe_{DCB} in Table S2) and by consequence the higher Fe^{II} concentrations in the aqueous phase can also buffer the possible negative effects that S-addition could have on increasing As thiolation after sulfate fertilization (Figure 3c).

The two disturbed soils showed higher relative changes in the formation of inorganic thioarsenates with S-addition compared to those from the chronosequence. P700 has a relatively high contribution of amorphous Fe phases (Figure 3c), fitting its chronosequential development, meaning that there would be easily reducible Fe phases that could release Fe^{II} and limit the thiolation potential by the formation of Fe−S phases. However, as described above, microbial processes seem to be hindered, and the soil shows a low level of Fe reductive dissolution. Moreover, P700 already has a high content of S. Low availability of Fe and high availability of reduced S enhanced As thiolation. In P1000, the removal of the topsoil decreased the content of amorphous Fe phases (Table S2). The low availability of reducible Fe phases means that there is no effective active mechanism that could scavenge reduced S.

Besides forming through a direct reaction between sulfide and arsenite, thioarsenates have also been reported to form through reaction with S^0.[19] In the paddy soil system, S^0 forms through the reoxidation of sulfide coupled with the reduction of Fe^{III} in the so-called cryptic S cycle.[59] Zerovalent S formation decreased with long-term paddy use (Figure S9a), since sulfide is less available for reoxidation after its precipitation as Fe−S phases that form due to the high availability of reduced Fe with long-term paddy use. S-addition increased S^0 content in all soils, and a higher contribution of

https://doi.org/10.1021/acs.jafc.4c09537
J. Agric. Food Chem. 2024, 72, 25045−25053

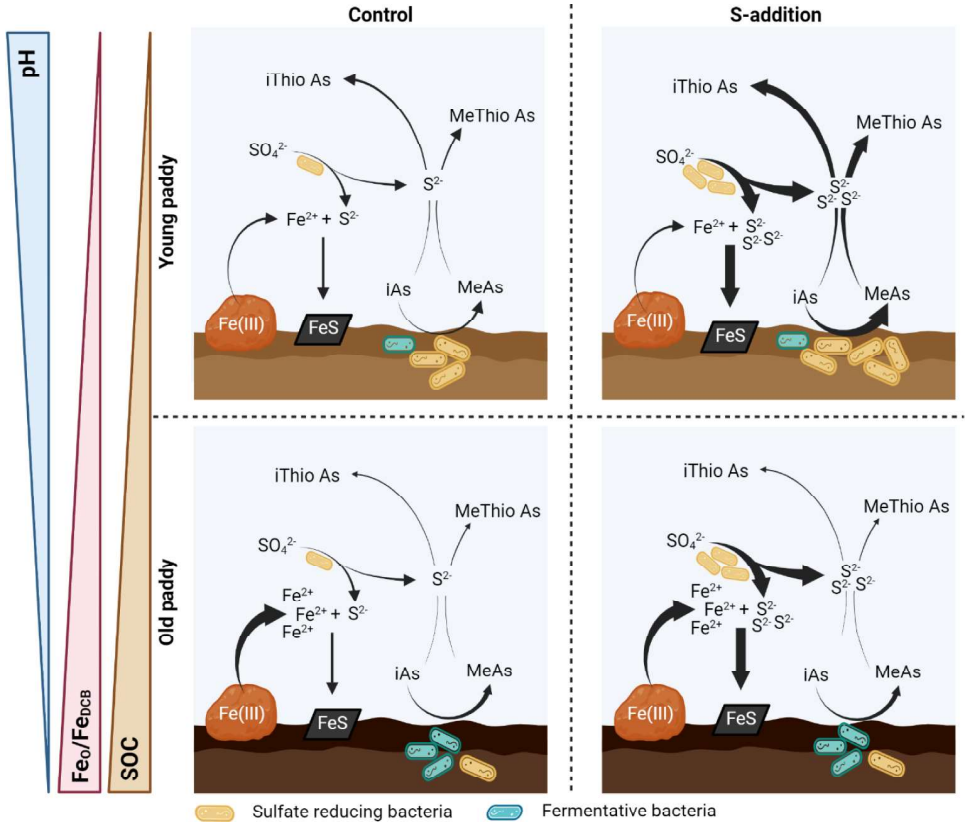

Figure 4. Conceptual model on the effects of sulfate addition on As biogeochemistry depending on soil age. Arrow thickness indicates the relative magnitude of the biogeochemical process.

inorganic thioarsenates was found in the soils with higher S^0 accumulation (Figure S9b).

Methylthioarsenate formation generally increased with S addition (Figure 3a). However, the increase in methylthioarsenates was not only a consequence of increased As methylation (with oxymethyl arsenates being substrates for the formation of methylthioarsenates). The ratio of methylthioarsenates to methyloxyarsenates also increased with the addition of sulfate (Figure 3d). In paddy soil neutral to acidic pH conditions (Table S2 and Figure S10), the formation of methyloxyarsenates is thermodynamically preferred to that of their inorganic counterparts.[48,49] With increasing concentrations of reduced S due to S-addition, methylthioarsenate contribution to total As increased as expected (Figure 3e). The preferential formation of methylthioarsenates over inorganic thioarsenates is also evident when comparing the relative increases with and without S-addition, since the relative change for methylthioarsenate formation (Figure 3f) decreases less steeply over chronosequential development than the one for inorganic thiorsenates (Figure 3c). Briefly, as the system becomes limited in reduced S due to increasing concentrations of dissolved Fe with long-term paddy use, inorganic thiolation will be hindered first, while the formation of methylthioarsenates is still thermodynamically preferred.

Incubations with the addition of ^{35}S-labeled sulfate showed that long-term paddy use increased SRR (Figure S11) from 5 ± 1 in P50 to 15.7 ± 0.7 nmol mL^{-1} d^{-1} in P2000. This increase is likely caused by increased microbial mass and activity with soil age, supported by a bigger pool of SOC.[23,36,60] A lower SRR in younger paddies means that there is a slow but steady supply of reduced S available for As thiolation, supporting the above-described observations. In contrast, sulfate is rapidly reduced in older paddies, meaning an early pulse of reduced S, which, together with the soil properties described above, hinders the formation of inorganic thioarsenates with long-term paddy use.

In summary, our results suggest that soils with properties similar to those of P50, P700, and P1000 could be at particular risk of increased methylthioarsenate formation upon S-addition. According to the results presented here, those characteristics include low Fe^{II} availability, low SOC, SRB-dominated methylation, and a slow but steady supply of reduced S through low SRR or active cryptic S cycling. While the formation of amorphous Fe phases with long-term paddy use is a consequence of SOC accumulation, we suggest then that Fe$_O$/Fe$_{DCB}$ is a better predictor of the S-addition effects in thiolation, since it directly accounts for potentially reducible Fe in the soil.

Implications for Rice Production. Our results highlight the importance of knowing soil properties before the application of sulfate fertilization to decrease As mobility, summarized in Figure 4. While the range of soil properties evaluated here did not have an important effect on the effectiveness of S-addition in decreasing total As concentrations in paddy soils, it did have important effects on As speciation and, thus, its mobility and toxicity for rice plants and consumers.

Younger soils showed the highest relative increase in the formation of low-sorbing, phytotoxic methylated oxyarsenates (1.6-fold for P50, compared to a 1.1-fold for P2000), as well as in low-sorbing, cytotoxic, and phytotoxic thioarsenates (4.2-fold increase for the formation of inorganic thioarsenates in

https://doi.org/10.1021/acs.jafc.4c09537
J. Agric. Food Chem. 2024, 72, 25045−25053

P50, compared with a decrease of 0.5-fold in P2000). This effect was linked to specific soil properties, including low SOC content and Fe availability, high pH, and mainly SRB-driven As methylation in young paddy soils. In contrast, older paddy soils with higher SOC and reducible Fe content and lower pH buffered the increase in As methylation and thiolation. Additionally, our results highlight how a low and constant supply of reduced S (through a low SRR) supports a higher thiolation potential in paddy soils, suggesting that timing might have a higher influence than concentration. Therefore, we recommend avoiding sulfate application to soils with properties similar to those of young paddy soils or evaluating these properties beforehand to avoid unwanted secondary effects in As speciation from sulfate fertilization. Further field experiments should evaluate these observations in the context of a plant–soil system, considering the whole extent of a rice cultivation season and the final product.

Disruption to the soil properties related to long-term paddy development overrides the buffering effect of long-term paddy use, with P700 and P1000 showing increases in methylation after S-addition of the same magnitude as P50 (1.6- and 1.7-fold, respectively) and increase of the magnitudes of their relative changes in thiolation (to 2.8- and 2.2-fold, respectively). Our study shows the importance of long-term paddy management in decreasing As thiolation potential, even when exogenous S is added to the soil. Thus, ensuring a healthy soil development and making efforts to sustain the related properties are important to decrease As mobility in paddy soils.

■ ASSOCIATED CONTENT

Data Availability Statement

The data generated and analyzed for the current study are also available from the corresponding author on reasonable request.

Supporting Information

The Supporting Information is available free of charge at https://pubs.acs.org/doi/10.1021/acs.jafc.4c09537.

Methods with the protocol for the sequential extraction procedure, selected soil properties, and information on the aqueous solutions used in the incubation setup; data and figures supporting the observations and discussion on the aqueous phase redox biogeochemistry of C, S, Fe, and As (PDF).

■ AUTHOR INFORMATION

Corresponding Author

Britta Planer-Friedrich – *Environmental Geochemistry, Bayreuth Center for Ecology and Environmental Research (BayCEER), University of Bayreuth, Bayreuth 95440, Germany;* orcid.org/0000-0002-0656-4283; Phone: +49-921-553999; Email: b.planer-friedrich@uni-bayreuth.de

Authors

José M. León Ninin – *Environmental Geochemistry, Bayreuth Center for Ecology and Environmental Research (BayCEER), University of Bayreuth, Bayreuth 95440, Germany;* orcid.org/0000-0003-3624-208X

Nathalie Kryschak – *Department of Hydrology, Bayreuth Center for Ecology and Environmental Research (BayCEER), University of Bayreuth, Bayreuth 95440, Germany*

Stefan Peiffer – *Department of Hydrology, Bayreuth Center for Ecology and Environmental Research (BayCEER), University of Bayreuth, Bayreuth 95440, Germany;* orcid.org/0000-0002-8326-0240

Complete contact information is available at: https://pubs.acs.org/10.1021/acs.jafc.4c09537

Author Contributions

This study was conceptualized by J.M.L.N. and B.P.-F. Incubation setup and solid, aqueous, and gas phase analyses were carried out by J.M.L.N. Determination of SSR was carried out by N.K. with the support of S.P. The manuscript and Supporting Information were written by J.M.L.N. with assistance from B.P.-F. All authors contributed to the manuscript revisions.

Notes

The authors declare no competing financial interest.

■ ACKNOWLEDGMENTS

We thank the German Academic Scholarship Foundation for the doctoral funding support for J.M.L.N. and funding within the Federal Ministry of Education and Research project BMBF (#031B0840 to B.P.-F.). We thank Livia Urbanski and Angelika Kölbl for providing the chronosequence soils. We thank Tillmann Lueders and Anita Gößner for the acetate analyses and Ben Gilfedder for providing access to the CH_4 and CO_2 analyses. Figure 4 and the Graphical Abstract were created using BioRender.

■ ABBREVIATIONS USED

DMA, dimethylatsenate; DMDTA, dimethyldithioarsenate; DMMTA, dimethyldithioarsenate; GC-FID, gas chromatograph with a flame ionization detector; HBED, hydroxybenzylethylenediamin; HPLC-DAD, high-performance liquid chromatography with a diode array detector; HPLC-RID, high-performance liquid chromatography with a refractive index detector; ICP-MS, inductively coupled plasma mass spectrometry; IC, ion chromatography; Inorg. oxyAs, inorganic oxyarsenic; Methyloxy As, methylated oxyarsenates; MMA, monomethylarsenate; MMDTA, monomethyldithioarsenate; MMMTA, monomethylmonothioarsenate; P, paddy; SRB, sulfate-reducing bacteria; SOC, soil organic carbon; SEP, sequential extraction procedure; SRR, sulfate reduction rate.

■ REFERENCES

(1) Haneklaus, S.; Bloem, E.; Schnug, E.*Sulfur: A Missing Link Between Soils, Crops, And Nutrition*Wiley Online Library200845–58–46

(2) Hitsuda, K.; Yamada, M.; Klepker, D. Sulfur Requirement of Eight Crops at Early Stages of Growth. *Agron. J.* **2005**, *97*, 155–159.

(3) Hinckley, E.-L. S.; Crawford, J. T.; Fakhraei, H.; Driscoll, C. T. A shift in sulfur-cycle manipulation from atmospheric emissions to agricultural additions. *Nat. Geosci.* **2020**, *13*, 597–604.

(4) Lamarque, J. F.; et al. Multi-model mean nitrogen and sulfur deposition from the Atmospheric Chemistry and Climate Model Intercomparison Project (ACCMIP): evaluation of historical and projected future changes. *Atmos. Chem. Phys.* **2013**, *13*, 7997–8018.

(5) Grennfelt, P.; et al. Acid rain and air pollution: 50 years of progress in environmental science and policy. *Ambio* **2020**, *49*, 849–864.

(6) Wisawapipat, W.; et al. Sulfur amendments to soil decrease inorganic arsenic accumulation in rice grain under flooded and nonflooded conditions: Insights from temporal dynamics of porewater

chemistry and solid-phase arsenic solubility. *Sci. Total Environ.* **2021**, *779*, 146352.
(7) Yan, S.; et al. Arsenic and cadmium bioavailability to rice (Oryza sativa L.) plant in paddy soil: Influence of sulfate application. *Chemosphere* **2022**, *307*, 135641.
(8) Fang, X.; et al. Simultaneously decreasing arsenic and cadmium in rice by soil sulfate and limestone amendment under intermittent flooding. *Environ. Pollut.* **2024**, *347*, 123786.
(9) Xu, X.; et al. Microbial sulfate reduction decreases arsenic mobilization in flooded paddy soils with high potential for microbial Fe reduction. *Environ. Pollut.* **2019**, *251*, 952−960.
(10) Kögel-Knabner, I.; et al. Biogeochemistry of paddy soils. *Geoderma* **2010**, *157*, 1−14.
(11) Xu, X.; McGrath, S.; Meharg, A.; Zhao, F. Growing rice aerobically markedly decreases arsenic accumulation. *Environ. Sci. Technol.* **2008**, *42*, 5574−5579.
(12) Stone, R. Arsenic and paddy rice: A neglected cancer risk? *Science* **2008**, *321*, 184−185.
(13) Ma, J. F.; et al. Transporters of arsenite in rice and their role in arsenic accumulation in rice grain. *Proc. Natl. Acad. Sci. U. S. A.* **2008**, *105*, 9931−9935.
(14) Meharg, A. A.; Hartley-Whitaker, J. Arsenic uptake and metabolism in arsenic resistant and nonresistant plant species. *New Phytol.* **2002**, *154*, 29−43.
(15) Sun, J.; Quicksall, A. N.; Chillrud, S. N.; Mailloux, B. J.; Bostick, B. C. Arsenic mobilization from sediments in microcosms under sulfate reduction. *Chemosphere* **2016**, *153*, 254−261.
(16) Zhang, D.; et al. Remediation of arsenic-contaminated paddy soil: Effects of elemental sulfur and gypsum fertilizer application. *Ecotoxicol. Environ. Saf.* **2021**, *223*, 112606.
(17) Tang, X.; et al. The response of arsenic bioavailability and microbial community in paddy soil with the application of sulfur fertilizers. *Environ. Pollut.* **2020**, *264*, 114679.
(18) Hu, Z.-Y.; et al. Sulfur (S)-induced enhancement of iron plaque formation in the rhizosphere reduces arsenic accumulation in rice (Oryza sativa L.) seedlings. *Environ. Pollut.* **2007**, *147*, 387−393.
(19) Wang, J.; et al. Thiolated arsenic species observed in rice paddy pore waters. *Nat. Geosci.* **2020**, *13*, 282−287.
(20) Chen, C.; et al. Sulfate-reducing bacteria and methanogens are involved in arsenic methylation and demethylation in paddy soils. *Isme J.* **2019**, *13*, 2523−2535.
(21) Chen, C.; et al. Sulfate addition and rising temperature promote arsenic methylation and the formation of methylated thioarsenates in paddy soils. *Soil Biol. Biochem.* **2021**, *154*, 108129.
(22) Stauder, S.; Raue, B.; Sacher, F. Thioarsenates in sulfidic waters. *Environ. Sci. Technol.* **2005**, *39*, 5933−5939.
(23) León Ninin, J. M.; et al. Changes in arsenic mobility and speciation across a 2000-year-old paddy soil chronosequence. *Sci. Total Environ.* **2024**, *908*, 168351.
(24) Colina Blanco, A. E.; Kerl, C. F.; Planer-Friedrich, B. Detection of thioarsenates in rice grains and rice products. *J. Agric. Food Chem.* **2021**, *69*, 2287−2294.
(25) Naranmandura, H.; et al. Comparative Toxicity of Arsenic Metabolites in Human Bladder Cancer EJ-1 Cells. *Chem. Res. Toxicol.* **2011**, *24*, 1586−1596.
(26) Moe, B.; et al. Comparative cytotoxicity of fourteen trivalent and pentavalent arsenic species determined using real-time cell sensing. *J. Environ. Sci.* **2016**, *49*, 113−124.
(27) Planer-Friedrich, B.; Kerl, C. F.; Colina Blanco, A. E.; Clemens, S. Dimethylated thioarsenates: a potentially dangerous blind spot in current worldwide regulatory limits for arsenic in rice. *J. Agric. Food Chem.* **2022**, *70*, 9610−9618.
(28) Zheng, M.-Z.; Li, G.; Sun, G.-X.; Shim, H.; Cai, C. Differential toxicity and accumulation of inorganic and methylated arsenic in rice. *Plant Soil* **2013**, *365*, 227−238.
(29) Gao, A.-X.; Chen, C.; Gao, Z.-Y.; Zhai, Z.-Q.; Wang, P.; Zhang, S.-Y.; Zhao, F.-J. Soil redox status governs within-field spatial variation in microbial arsenic methylation and rice straighthead disease. *Isme J.* **2024**, *18* (1), wrae057.
(30) Pischke, E.; et al. Dimethylmonothioarsenate Is Highly Toxic for Plants and Readily Translocated to Shoots. *Environ. Sci. Technol.* **2022**, *56*, 10072−10083.
(31) Eberle, A.; et al. Potential of high pH and reduced sulfur for arsenic mobilization − Insights from a Finnish peatland treating mining waste water. *Sci. Total Environ.* **2021**, *758*, 143689.
(32) Kölbl, A.; et al. Accelerated soil formation due to paddy management on marshlands (Zhejiang Province, China). *Geoderma* **2014**, *228−229*, 67−89.
(33) Winkler, P.; et al. Response of Vertisols, Andosols, and Alisols to paddy management. *Geoderma* **2016**, *261*, 23−35.
(34) Wissing, L.; et al. Organic carbon accumulation in a 2000-year chronosequence of paddy soil evolution. *CATENA* **2011**, *87*, 376−385.
(35) Cheng, Y.-Q.; Yang, L.-Z.; Cao, Z.-H.; Ci, E.; Yin, S. Chronosequential changes of selected pedogenic properties in paddy soils as compared with non-paddy soils. *Geoderma* **2009**, *151*, 31−41.
(36) Roth, P. J.; et al. Accumulation of nitrogen and microbial residues during 2000 years of rice paddy and non-paddy soil development in the Yangtze River Delta, China. *Global Change Biol.* **2011**, *17*, 3405−3417.
(37) Kalbitz, K.; et al. The carbon count of 2000 years of rice cultivation. *Global Change Biol.* **2013**, *19*, 1107−1113.
(38) Alley, R., et al. Climate Change 2007: The Physical Science Basis. Contribution of Working Group I to the Fourth Assessment Report of the Intergovernmental Panel on Climate Change: IPCC Secretariat: Geneva Switzerland2007.
(39) Mueller-Niggemann, C.; Bannert, A.; Schloter, M.; Lehndorff, E.; Schwark, L. Intra- versus inter-site macroscale variation in biogeochemical properties along a paddy soil chronosequence. *Biogeosciences* **2012**, *9*, 1237−1251.
(40) Mueller-Niggemann, C.; Schwark, L. Chemotaxonomy and diagenesis of aliphatic hydrocarbons in rice plants and soils from land reclamation areas in the Zhejiang Province, China. *Org. Geochem.* **2015**, *83−84*, 215−226.
(41) Fulda, B.; Voegelin, A.; Ehlert, K.; Kretzschmar, R. Redox transformation, solid phase speciation and solution dynamics of copper during soil reduction and reoxidation as affected by sulfate availability. *Geochim. Cosmochim. Acta* **2013**, *123*, 385−402.
(42) León Ninin, J. M.; Higa Mori, A.; Pausch, J.; Planer-Friedrich, B. Long-term paddy use influences response of methane production, arsenic mobility and speciation to future higher temperatures. *Sci. Total Environ.* **2024**, *943*, 173793.
(43) Lohmayer, R.; Kappler, A.; Lösekann-Behrens, T.; Planer-Friedrich, B. Sulfur species as redox partners and electron shuttles for ferrihydrite reduction by Sulfurospirillum deleyianum. *Appl. Environ. Microbiol.* **2014**, *80*, 3141−3149.
(44) Stookey, L. L. Ferrozine—a new spectrophotometric reagent for iron. *Anal. Chem.* **1970**, *42*, 779−781.
(45) Hegler, F.; Posth, N. R.; Jiang, J.; Kappler, A. Physiology of phototrophic iron(II)-oxidizing bacteria: implications for modern and ancient environments. *FEMS Microbiol. Ecol.* **2008**, *66*, 250−260.
(46) Cline, J. D. Spectrophotometric determination of hydrogen sulfide in natural waters 1. *Limnol. Oceanogr.* **1969**, *14*, 454−458.
(47) Planer-Friedrich, B.; London, J.; McCleskey, R. B.; Nordstrom, D. K.; Wallschläger, D. Thioarsenates in geothermal waters of Yellowstone National Park: determination, preservation, and geochemical importance. *Environ. Sci. Technol.* **2007**, *41*, 5245−5251.
(48) Wallschläger, D.; London, J. Determination of methylated arsenic-sulfur compounds in groundwater. *Environ. Sci. Technol.* **2008**, *42*, 228−234.
(49) Wallschläger, D.; Stadey, C. J. Determination of (oxy)-thioarsenates in sulfidic waters. *Anal. Chem.* **2007**, *79*, 3873−3880.
(50) Zeibich, L.; Schmidt, O.; Drake, H. L.; Löffler, F. E. Protein- and RNA-Enhanced Fermentation by Gut Microbiota of the Earthworm Lumbricus terrestris. *Appl. Environ. Microbiol.* **2018**, *84* (11), No. e00657.

https://doi.org/10.1021/acs.jafc.4c09537
J. Agric. Food Chem. 2024, 72, 25045−25053

(51) Fossing, H.; Jørgensen, B. B. Measurement of bacterial sulfate reduction in sediments: evaluation of a single-step chromium reduction method. *Biogeochemistry* **1989**, *8*, 205−222.
(52) Reid, M. C.; et al. Arsenic methylation dynamics in a rice paddy soil anaerobic enrichment culture. *Environ. Sci. Technol.* **2017**, *51*, 10546−10554.
(53) Zhang, X.; Reid, M. C. Inhibition of methanogenesis leads to accumulation of methylated arsenic species and enhances arsenic volatilization from rice paddy soil. *Sci. Total Environ.* **2022**, *818*, 151696.
(54) Chen, C.; Li, L.; Wang, Y.; Dong, X.; Zhao, F.-J. Methylotrophic methanogens and bacteria synergistically demethylate dimethylarsenate in paddy soil and alleviate rice straighthead disease. *Isme J.* **2023**, *17* (11), 1851−1861.
(55) Chen, C.; et al. Suppression of methanogenesis in paddy soil increases dimethylarsenate accumulation and the incidence of straighthead disease in rice. *Soil Biol. Biochem.* **2022**, *169*, 108689.
(56) Gauci, V.; et al. Sulfur pollution suppression of the wetland methane source in the 20th and 21st centuries. *Proc. Natl. Acad. Sci. U. S. A.* **2004**, *101*, 12583−12587.
(57) Scholz, V. V.; Meckenstock, R. U.; Nielsen, L. P.; Risgaard-Petersen, N. Cable bacteria reduce methane emissions from rice-vegetated soils. *Nat. Commun.* **2020**, *11* (1), 1878.
(58) Denier van der Gon, H. A.; van Bodegom, P. M.; Wassmann, R.; Lantin, R. S.; Metra-Corton, T. M. Sulfate-containing amendments to reduce methane emissions from rice fields: mechanisms, effectiveness and costs. *Mitig. Adapt. Strateg. Glob. Chang.* **2001**, *6*, 71−89.
(59) Wind, T.; Conrad, R. Localization of sulfate reduction in planted and unplanted rice field soil. *Biogeochemistry* **1997**, *37*, 253−278.
(60) Wissing, L.; et al. Organic carbon accumulation on soil mineral surfaces in paddy soils derived from tidal wetlands. *Geoderma* **2014**, *228−229*, 90−103.

https://doi.org/10.1021/acs.jafc.4c09537
J. Agric. Food Chem. 2024, 72, 25045−25053

Supporting information to

Long-term paddy soil development buffers the increase in arsenic methylation and thiolation after sulfate fertilization

José M. León Ninin[1], Nathalie Kryschak[2], Stefan Peiffer[2], Britta Planer-Friedrich[1]*

[1] Environmental Geochemistry, Bayreuth Center for Ecology and Environmental Research (BayCEER), University of Bayreuth, 95440 Bayreuth, Germany

[2] Department of Hydrology, Bayreuth Center for Ecology and Environmental Research (BayCEER), University of Bayreuth, 95440 Bayreuth, Germany

* Corresponding author. Phone: +49-921-553999; E-mail address: b.planer-friedrich@uni-bayreuth.de (B. Planer-Friedrich).

(10 Pages, 3 Tables, 11 Figures)

Supplementary methods

Sequential extraction procedure

A sequential extraction procedure was carried out following Fulda, et al. [1]. For this, 0.2 g of dry soil were weighed into a 15 mL centrifuge tube and extracted following the steps and reactants described in the method (summarized in Table S1). After each extraction, the samples were centrifuged (3500 rpm, 10 min) to separate the soil from the extract. The soil was washed with deionized water to prevent extractant carryover into the next step, while the extracts were filtered through 0.2 µm cellulose-acetate filters, diluted 1:10 with ultrapure deionized water, and stabilized with 15 µL of 30% H_2O_2 and 20 µL of 32.5% HNO_3 per mL of sample. Samples from Fraction 3 were not acidified to avoid the precipitation of EDTA. All extracts were analyzed for total As by ICP-MS as described in the main text, using matrix-matching calibrations for each fraction. Non-extractable As (F6) was calculated by subtracting Σ F1 to F5 of the total As extracted from the original soils by microwave-assisted extraction in 10 mL aqua regia (MARS Xpress, CEM). The operationally defined fractions are also summarized in Table S1.

Table S1: Summary of fractions, extractants, and conditions for the SEP described by Fulda et al.[1]

Operationally defined fraction		Extractant	Extraction conditions
F1 (Mobile fraction)	Soluble and exchangeable; soluble metal-organic complexes	0.1 M $CaCl_2$	24 h shaking; 23 °C; SSR 1:25
F2 (Easily mobilizable fraction)	Specifically adsorbed, bound to $CaCO_3$ and other minerals labile at pH 5, weak metal-organic complexes)	1 M NaOAc (pH 5, adjusted with HOAc)	24 h shaking; 23 °C; SSR 1:25
F3 (Organically bound)	Low-affinity organic sites	0.025 M NH_4-EDTA (pH 4.6)	90 min shaking; 23 °C; SSR 1:25
		1 M NH_4OAc (pH 4.6)	10 min shaking; 23 °C; SSR 1:12.5
F4 (Reducible fraction)	Amorphous and crystalline Fe and Mn hydr(oxydes)	0.1 M ascorbic acid + 0.2 M NH_4Ox/HOx (pH 3.25)	2 h; 96 °C (heat block); SSR 1:25; dark
		0.2 M NH_4Ox/HOx (pH 3.25)	10 min shaking; 23 °C; SSR 1:12.5; dark
F5 (Oxidizable fraction)	Sulfides and organically bound to high-affinity sites	30% H_2O_2 (pH 2) + 2 M HNO_3	5 mL H_2O_2 + 3 mL HNO_3; 2 h; 85 °C (heat block)
			3 mL H_2O_2; 3 h; 85 °C (heat block)
		3.2 M NH_4OAc (in 20% v/v HNO_3)	5 mL NH_4OAc; 30 min; 23 °C

SSR: Soil:solution ratio. OAc: Acetate. Ox: Oxalate.

Table S2: Selected soil properties of the topsoils from the paddy soils used in this study.

Soil	Horizon*	Horizon depth (cm)*	Soil pH*	Soil Org. C* (g kg^{-1})	Soil Fe* (g kg^{-1})	Soil As (mg kg^{-1})	Soil S (g kg^{-1})	Fe_O/Fe_{DCB}
P50	Alp1	0 - 7	7.4	17.8 ± 0.5	38	17	3.52	0.43 ± 0.04
P100	Alp1**	0 - 9	5.0	17.6 ± 1.3	34	15 ± 2	2.64 ± 0.06	0.44 ± 0.04
P100	Alp2**	9 - 15	5.8	15.3 ± 1.1	35			
P300	Alp	0 - 18	5.8	22.6 ± 2.5	35	17	2.77	0.46 ± 0.06
P700	*Alp1***	*0 - 10*	*6.7*	*23.2 ± 1.9*	*34*	*19*	*3.11*	*0.60* ± 0.03
P700	*Alp2***	*10 – 16*	*6.6*	*18.0 ± 1.8*	*33*			
P1000	*Alp*	*0 – 10*	*5.2*	*14.0 ± 0.6*	*31*	*38*	*2.21*	*0.50* ± 0.04
P2000	Alp	0 - 15	5.1	30.0 ± 1.5	22	11	2.57	0.84 ± 0.05

*Data from Kölbl, et al. [2]. ** For this work, horizons Alp1 and Alp2 from P100 and P700 were mixed to obtain a material representative of the complete Alp horizon. Fe_O: Oxalate extractable iron, Fe_{DCB}: Dithionate-citrate-bicarbonate extractable iron. A complete characterization of all soils and horizons from this chronosequence can be found in Kölbl, et al. [2]. The data for the chonosequential paddy soils (P50, P100, P300, and P2000) had already been compiled for León Ninin, et al. [3]. Disturbed soils (P700 and P1000) are typed in *italics* and gray-shaded.

129

Table S3: Solutions used as aqueous phase for the study.

	Main treatment			NaCl amendment		Final ionic strength (mmol L^{-1})
	Target concentration (mmol kg_{soil}^{-1})	In incubation (mmol per 10 g_{soil})	In incubation (mmol L^{-1} in 20 mL)	In incubation (mmol per 10 g_{soil})	In incubation (mmol L^{-1} in 20 mL)	
NaCl	12	0.12	6	-	-	6
Na_2SO_4	3	0.03	1.5	0.03	1.5	6

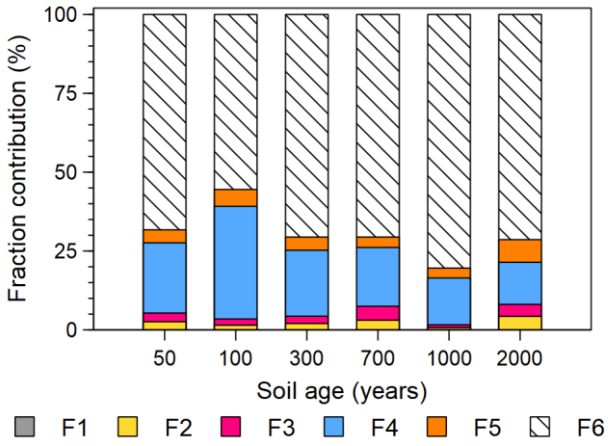

Figure S1: Binding forms of As across the paddy soil chronosequence. F1: Mobile fraction (non-detected), F2: Easily mobilizable fraction, F3: Organically bound to low affinity sites, F4: Reducible fraction, F5: Oxidizable fraction, F6: Non-extractable fraction (Total soil As - Σ F1 to F5). Data from P50, P100, P300 and P2000 has been already published in León Ninin, et al. [4]

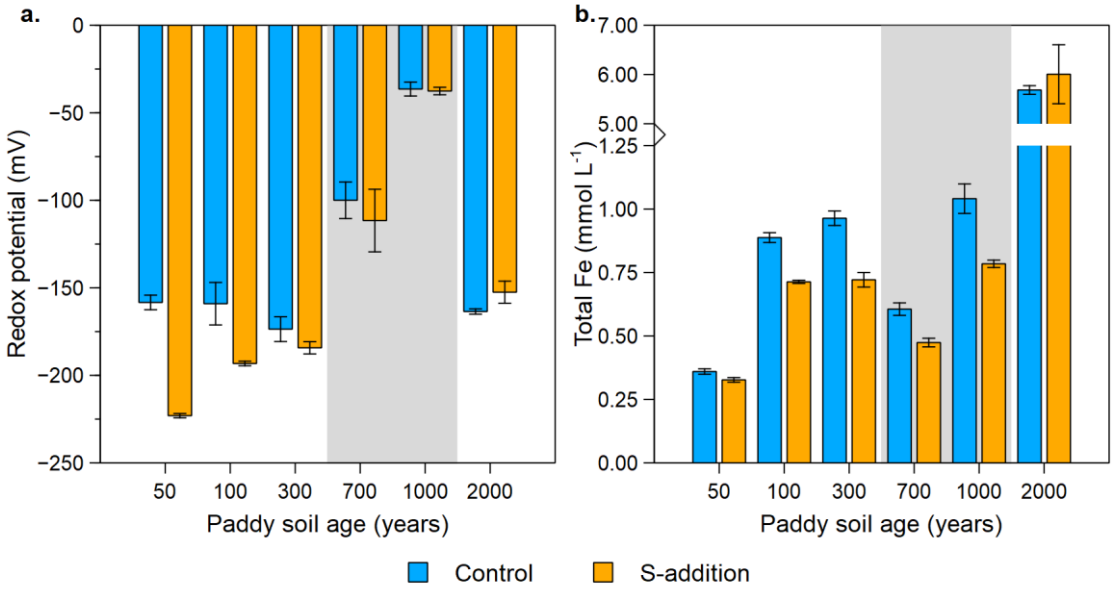

Figure S2: Redox potential (a) and dissolved total Fe (b) in the aqueous phase after 10 incubation days. Disturbed soils are gray-shaded. Data points and bars are mean values, and error bars represent standard deviation (n = 3).

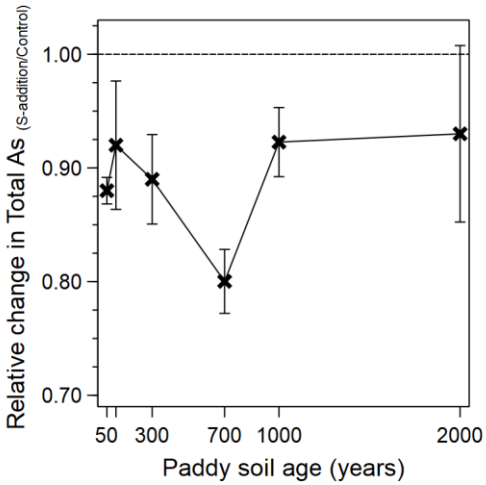

Figure S3: Decrease in total As concentration with S-addition across paddy soil age. Data points and bars are mean values, and error bars represent standard deviation (n = 3). The dotted line represents a 1x ratio, meaning no relative change in total As; data points under this line indicate a decrease in As concentrations with S-addition.

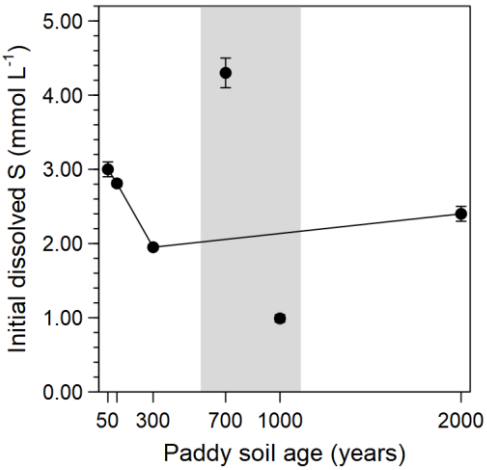

Figure S4: Initial aqueous phase S. Disturbed soils are gray-shaded. Data points and bars are mean values, and error bars represent standard deviation (n = 3).

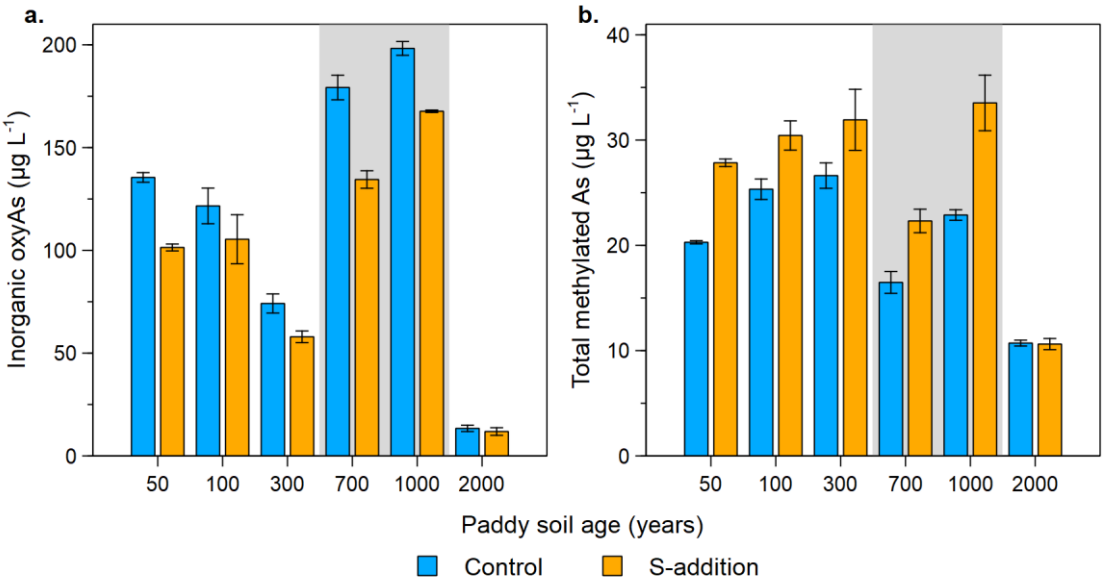

Figure S5: Changes in inorganic oxyarsenic concentration with S-addition (a), due to increased methylation (b). Disturbed soils are gray-shaded. Bars are mean values, and error bars represent standard deviation (n = 3).

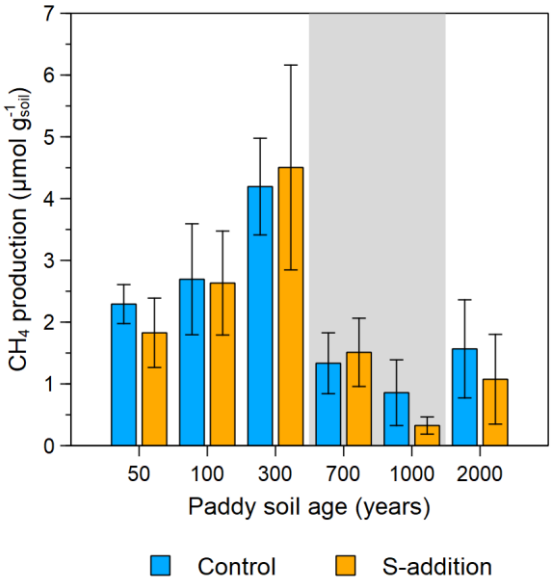

Fig S6: Methane production in the six studied soils with and without S-addition. Disturbed soils are gray-shaded. Data points and bars are mean values, and error bars represent standard deviation (n = 3).

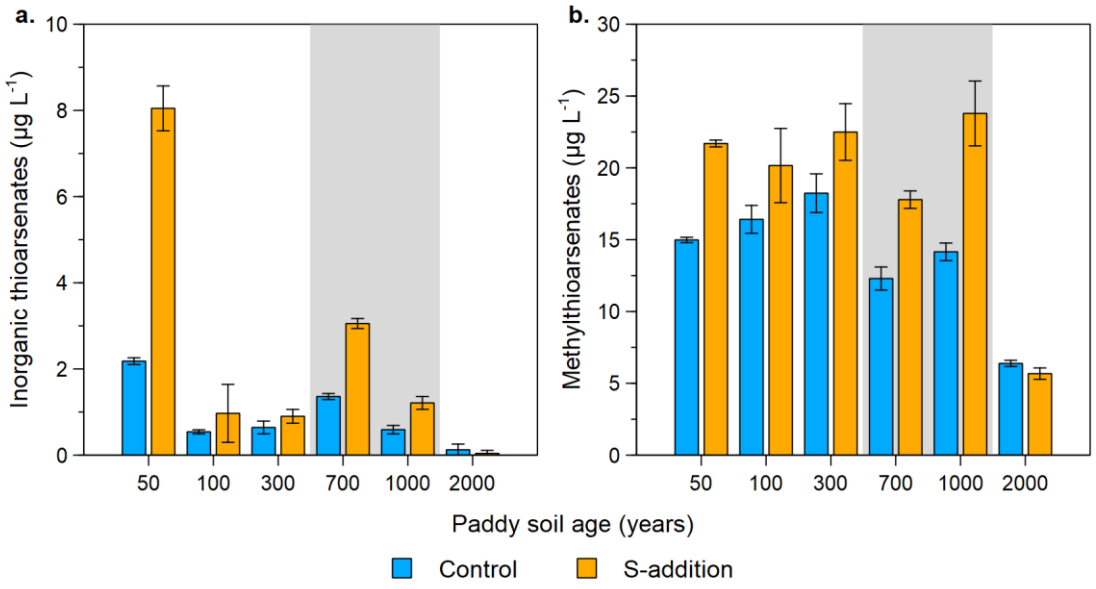

Figure S7: Changes in inorganic thioarsenates (a) and methylthioarsenates (b) concentration with S-addition. Disturbed soils are gray-shaded. Bars are mean values, and error bars represent standard deviation (n = 3).

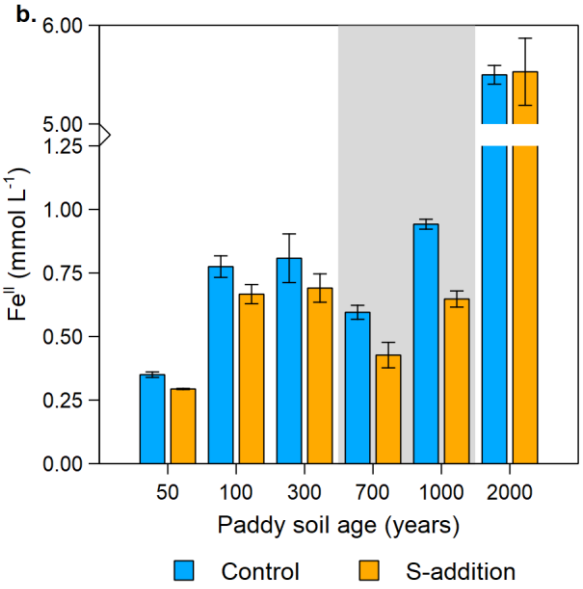

Fig. S8: Aqueous phase Fe^{II} after 10 days of incubation with and without S-addition. Disturbed soils are gray-shaded. Data points and bars are mean values, and error bars represent standard deviation (n = 3).

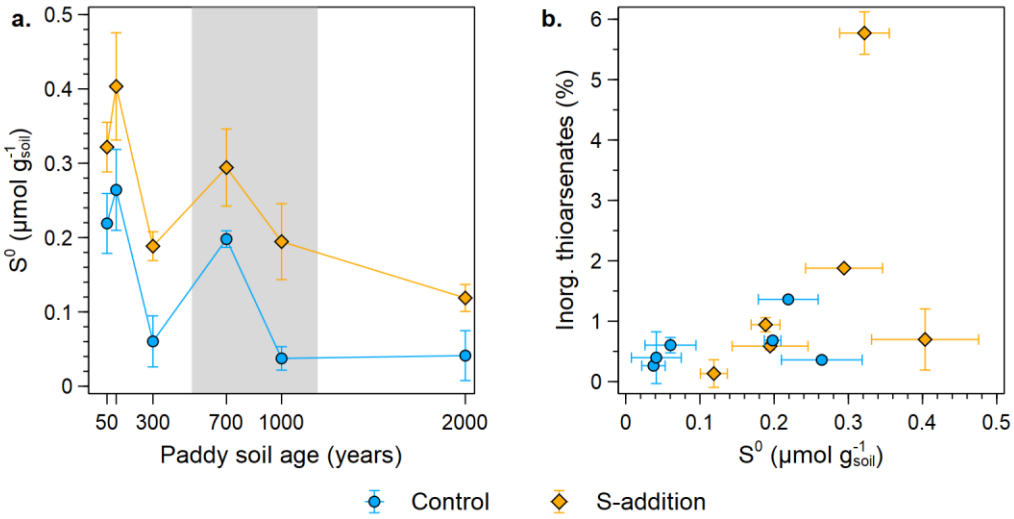

Fig. S9: Formation of S^0 in the solid phase after incubation (a). Influence of S^0 in the formation of inorganic thioarsenates (b). Disturbed soils in (a) are gray-shaded. Data points and bars are mean values, and error bars represent standard deviation (n = 3).

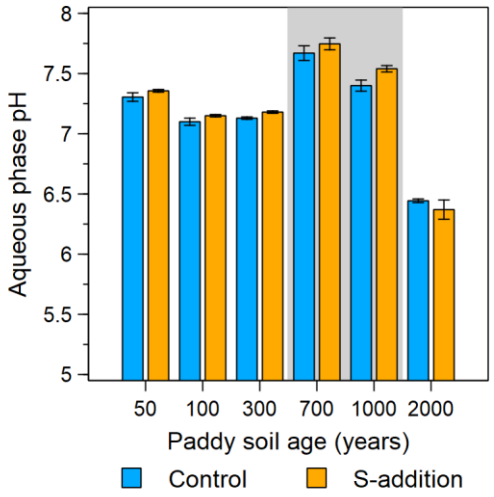

Fig. S10: Aqueous phase pH after 10 days of incubation with and without S-addition. Disturbed soils are gray-shaded. Data points and bars are mean values, and error bars represent standard deviation (n = 3).

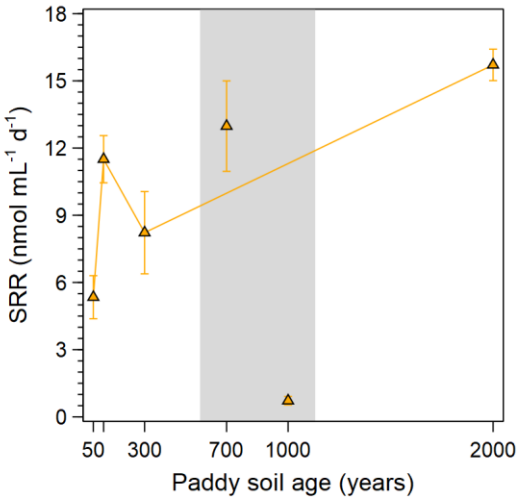

Fig. S11: Sulfate reduction rate (SRR) from studied soils. Disturbed soils are gray-shaded. Data points and bars are mean values, and error bars represent standard deviation (n = 3).

Supplementary References

1 Fulda, B., Voegelin, A., Ehlert, K. & Kretzschmar, R. Redox transformation, solid phase speciation and solution dynamics of copper during soil reduction and reoxidation as affected by sulfate availability. *Geochimica et Cosmochimica Acta* **123**, 385-402 (2013). https://doi.org:https://doi.org/10.1016/j.gca.2013.07.017

2 Kölbl, A. *et al.* Accelerated soil formation due to paddy management on marshlands (Zhejiang Province, China). *Geoderma* **228-229**, 67-89 (2014). https://doi.org:https://doi.org/10.1016/j.geoderma.2013.09.005

3 León Ninin, J. M. *et al.* Changes in arsenic mobility and speciation across a 2000-year-old paddy soil chronosequence. *Science of The Total Environment* **908**, 168351 (2024). https://doi.org:https://doi.org/10.1016/j.scitotenv.2023.168351

4 León Ninin, J. M., Higa Mori, A., Pausch, J. & Planer-Friedrich, B. Long-term paddy use influences response of methane production, arsenic mobility and speciation to future higher temperatures. *Science of The Total Environment* **943**, 173793 (2024). https://doi.org:https://doi.org/10.1016/j.scitotenv.2024.173793

Study 4: Sulfur depletion through repetitive redox cycling unmasks the role of the cryptic sulfur cycle for (methyl)thioarsenate formation in paddy soils.

José M. León Ninin, Carolin Dreher, Andreas Kappler, and Britta Planer-Friedrich

Reprinted with permission from

Environmental Science: Processes & Impacts (Advance article)

Own contribution to Study 4:	
Concept and study design	90%
Data acquisition	95%
Analyses of samples	95%
Data analysis and figure preparation	95%
Discussion of results	90%
Manuscript writing	95%

This study was designed by J.M.L.N. and B.P.-F.; experiments and analyses of samples were carried out by J.M.L.N. with the support of C.D.; assistance during the long-term experiment was provided by technical assistants, HiWis, and research students (see acknowledgments); access to analytical facilities was provided by A.K. and additional analyses were carried out at the Limnological Research Station (see acknowledgments); data analyses and figure preparation were carried out by J.M.L.N. with support from C.D.; discussion of results and writing of the draft were carried out by J.M.L.N. with the support of B.P.-F.

Environmental Science Processes & Impacts

ROYAL SOCIETY OF CHEMISTRY

PAPER

View Article Online
View Journal

Cite this: DOI: 10.1039/d4em00764f

Sulfur depletion through repetitive redox cycling unmasks the role of the cryptic sulfur cycle for (methyl)thioarsenate formation in paddy soils†

José M. León Ninin, *[a] Carolin Lisbeth Dreher, [b] Andreas Kappler[b] and Britta Planer-Friedrich‡[a]

Inorganic and oxymethylated thioarsenates form through the reaction of arsenite and oxymethylated arsenates with reduced sulfur, mainly as sulfide (S^{II-}) but also as zerovalent sulfur (S^0). In paddy soils, considered low-S systems, microbial reduction of the soil's "primary" sulfate pool is the principal S^{II-} source for As thiolation. Under anoxic conditions, this primary pool is readily consumed, and the precipitation of iron (Fe) sulfides lowers S^{II-} availability. Nonetheless, sulfate can be constantly replenished by the reoxidation of S^{II-} coupled with the reduction of Fe^{III} phases in the so-called cryptic S cycle (CSC). The CSC supplies a small secondary sulfate pool available for reduction and, according to previous studies, As thiolation. However, sulfate concentrations commonly found in paddy soils mask the biogeochemical processes associated with the CSC. Here, we depleted a paddy soil from excess S, Fe, and As from a paddy soil through repetitive flooding and draining (*e.g.*, redox cycling). After 10, 20, and 30 such cycles, we followed thioarsenate formation during an anoxic incubation period of 10 days. Higher S/As ratios increased As thiolation contribution to total As up to 10-fold after 30 cycles. During the anoxic incubation, the depleted soils showed a transient first phase where the reduction of the primary sulfate pool led to inorganic thioarsenate formation. In the second phase, methylthioarsenate formation correlated with partially oxidized S species (S^0, thiosulfate), suggesting CSC-driven sulfate replenishment, re-reduction, and thiolation. Methylthioarsenates formed even as inorganic thioarsenates de-thiolated, indicating thermodynamic preference under S-limited conditions. This study highlights the role of the CSC in sustaining thioarsenate formation in low-S systems.

Received 9th December 2024
Accepted 20th March 2025

DOI: 10.1039/d4em00764f

rsc.li/espi

Environmental significance

Cryptic sulfur cycling has been suggested to replenish sulfate pools in low-S systems like paddy soils, supporting the formation of highly mobile and toxic thioarsenates. Here we show that sulfide production through the reduction of the soil's primary sulfate pool supports a high but transient formation of inorganic thioarsenates. Once this primary sulfate pool is exhausted, lower sulfide concentrations cause de-thiolation. In a depleted system, we observed that the re-reduction of sulfate recycled through the cryptic sulfur cycle supported the formation of methylthioarsenates. These results suggest that methylthioarsenates can form even in very low-S environments, increasing mobility, toxicity, uptake by rice plants, and accumulation in rice grains.

Introduction

Arsenic (As) is a ubiquitously distributed element in the environment that is toxic for humans.[1–3] The mobility and toxicity of As are highly redox-dependent, making it a contaminant of interest in redox-active environments, such as groundwater systems or natural and managed wetlands.[1,4,5] The main As intake sources for humans are As-contaminated groundwater and As-enriched rice grains.[3,6] Understanding how redox dynamics in groundwater and rice cultivation systems influence As biogeochemistry could help decrease the risk of As intake for consumers.[5,7–10]

The mobility and toxicity of As depend on its speciation.[11] Under sub-oxic and anoxic conditions, As is mobilized mainly by the reductive dissolution of As-bearing Fe^{III} (oxy)hydroxides as arsenate or arsenite.[12–14] These two species (summarized as inorganic oxyarsenic) are known carcinogens.[2,3] Arsenite can be biotically methylated in consecutive steps to form the oxymethylated arsenates, mono- and dimethylarsenate (MMA and DMA, respectively).[15–17] Oxymethylated arsenates are currently

[a]*Environmental Geochemistry, Bayreuth Center for Ecology and Environmental Research (BayCEER), University of Bayreuth, 95440 Bayreuth, Germany. E-mail: jose.leon-ninin@uni-bayreuth.de; Tel: +49-921-553995*

[b]*Geomicrobiology, Department of Geosciences, University of Tübingen, 72076 Tübingen, Germany*

† Electronic supplementary information (ESI) available: ESI and figures supporting the above-described observations and discussion based on soil properties and the aqueous phase redox biogeochemistry of C, S, Fe, and As. Mössbauer spectra from original and depleted soils, and supplementary discussion on the use of μXRD for identification of mineral phases. See DOI: https://doi.org/10.1039/d4em00764f

‡ Deceased.

considered as less toxic to humans.[11,18] Arsenic methylation is carried out by microbes carrying the *S*-adenosylmethionine methyltransferase (*arsM*) gene.[15,19,20] Different microbial groups can methylate As depending on environmental conditions. For example, in geothermal springs, methanogens have been identified as methylators.[21] In paddy soils, sulfate-reducing bacteria (SRB)[22,23] and fermentative bacteria[20] have been shown to methylate As. Methanogens have been identified in paddy soils as de-methylators, transforming oxymethylated arsenates back to arsenite.[22,24,25]

Current studies on As speciation often focus on arsenate, arsenite, MMA, and DMA, and the biogeochemical processes governing their contribution to total As. However, another group of As species called thioarsenates has been shown to contribute significantly to As speciation in different environmental systems.[26–29] Thioarsenates form when reduced sulfur (S) species, mainly as sulfide (S^{II-}), but also as zerovalent S (S^0), substitute one or more hydroxyl groups in an As oxyanion.[26,27,30] The formation of thioarsenates requires, thus, the reaction of arsenite or methylated oxyarsenates with reduced S species, to form inorganic or methylated thioarsenates, respectively.[27,31] Depending on the system, these reduced S species could be of abiotic origin or produced by microbially mediated sulfate reduction.[21,28,32]

The formation of either inorganic or methylated thioarsenates is determined by the distribution of As species, availability of reduced S species, and pH conditions.[27,31] Inorganic thioarsenates are preferentially formed in environments with excess S^{II-} at neutral to alkaline pH when arsenite consecutively reacts with S^{II-} and S^0 to form mono-, di-, tri-, and tetrathioarsenate (MTA, DTA, TTA, and TetraTA, respectively) depending on S/As ratios.[27,30] The role of S^0 in inorganic thioarsenate formation is either related to the formation of MTA, or the oxidation of the unstable intermediate thioarsenites to thioarsenates.[30] Alkaline, sulfidic geothermal springs have been described as hotspots for the formation and identification of inorganic thioarsenates.[21,32]

The formation of methylthioarsenates is largely governed by the availability of oxymethylated arsenates, which are readily thiolated in the presence of S^{II-}.[31,33,34] Consecutive reactions of MMA with S^{II-} produce monomethylthioarsenate (MMMTA), monomethyldithioarsenate (MMDTA), and monomethyltrithioarsenate (MMTTA). Similarly, the thiolation of DMA produces dimethylmonothioarsenate (DMMTA) and dimethyldithioarsenate (DMDTA). Field and laboratory observations suggest that the S^{II-} excess required to form methylthioarsenates decreases with the number of methyl groups attached to As.[33,35] For example, DMA requires a lower S^{II-} excess to be thiolated than MMA.[33] A lower S^{II-} requirement to form methylthioarsenates, together with the low stability of inorganic thioarsenates at pH values < 8,[32] suggests that at neutral and acidic pH, methylthioarsenate formation is thermodynamically preferred to that of inorganic thioarsenates.

Thioarsenate formation and identification in relatively low-S terrestrial environments, such as wetlands and paddy soils, has been controversial. In such systems, SRB carrying out dissimilatory sulfate reduction (DSR) have been identified to be the main producers of S^{II-} for As thiolation.[23,28,36,37] However, the anoxic conditions required for DSR also trigger reductive dissolution of Fe(III) minerals.[38] Reduced Fe scavenges S^{II-} through the precipitation of FeS phases,[39–41] decreasing its availability to form thioarsenates.[28,36] Moreover, both wetlands and paddy soils are considered methanogenic environments where DSR accounts for only a small fraction of anaerobic respiration since the low sulfate contents in the soil, and hence aqueous phase concentrations are readily depleted.[23] Despite these assumptions, thioarsenates have been shown as important contributors to the mobility and export of As in groundwater[5] and wetland systems,[29,35] as well as being formed in flooded rice fields,[28,36,42] and accumulated in rice grains.[43] Their presence in paddy soils and rice grains has raised concern, given their high mobility, phyto-, and cytotoxicity, comparable, in the case of dimethylthioarsenates, to that of arsenite.[35,44,45] Moreover, thioarsenates have been observed and suggested to contribute to As mobility in systems with high dissolved Fe concentrations, where the availability of S^{II-} should be limited.[5,36] Thus, a better understanding of the biogeochemical processes influencing As thiolation is required.

Micro- and mesocosm experiments have suggested that the cryptic S-cycle (CSC) plays an important role in the formation of thioarsenates, providing small amounts of S^{II-} and S^0 for As thiolation.[28,36] Such a CSC is related to the reoxidation of S^{II-} to S^0 coupled with the reduction of Fe^{III} (oxyhydr)oxides, releasing Fe^{II} into the aqueous phase.[46–49] Zerovalent S can be consecutively further oxidized to thiosulfate and sulfate, thus being recycled and available again as a substrate for DSR.[28,46,50] Thus, even when most of the original "primary" pool of sulfate content has been consumed, S^{II-} abiotic reoxidation forms a "secondary" pool of sulfate. The re-reduction of this recycled sulfate through DSR offers a constant source of reduced S species. While the role of CSC in As thiolation has been implied,[5,28,36,51] to the best of our knowledge, it has not been directly evaluated, yet.

In the environment, the CSC has been reported in marine systems,[52] low sulfate lakes,[53] and wetlands.[54,55] Holmkvist and Ferdelman[52] described how the reoxidation of S^{II-} explains the abundance of SRB in marine sediments with low but constant sulfate availability. The authors associated the presence of stable sulfate background concentrations with the presence of Fe^{III} phases and S^{II-} in sediment samples. The same study suggests that the CSC might take place independent of sulfate limitations, but that S-rich environments might mask the small secondary pool of freshly produced sulfate. According to the authors, only S-depleted environments allow the identification of the CSC. In paddy soils, the CSC has been reported due to root oxygen loss, which creates redox interfaces in which sulfate is constantly reduced to S^{II-}, and partially reoxidized to form S^0, thiosulfate, and sulfate.[46,56,57] However, the identification in the bulk soil and the role of a secondary sulfate pool in thioarsenate formation has been elusive due to the masking effect of the bigger primary sulfate pool, despite products of partial S^{II-} reoxidation being found in the bulk soil.[28,36] In this sense, a S-depleted paddy soil system is required to identify the role of the CSC and its associated secondary sulfate pool in As thiolation.

Here, we present the results of a long-term microcosm experiment. Through repetitive redox cycling and aqueous phase removal, we decreased a paddy soil's background concentrations (*i.e.*, depleting it) of S, Fe, and As, aiming to investigate the role of the CSC in As thiolation. Our hypothesis is that in a S-depleted system with a smaller primary sulfate pool, CSC will provide a constant source of S^{II-} and S^0, forming thioarsenates. Following changes in S, Fe, and As speciation, we show that even in low-sulfate, high-methanogenic systems, thioarsenates form and even dominate As speciation, with CSC providing small amounts of sulfate which, through DSR, form S^{II-} for thioarsenate formation.

Materials and methods

Long-term microcosm experiment

Soil from the paddy cultivation area in Cixi, Province of Zhejiang, China, was used for a long-term microcosm experiment. This soil is the youngest paddy soil (50 years of paddy use – P50) of a chronosequence which has been previously used to understand how long-term paddy use affects pedologic properties[58–60] and redox biogeochemistry.[36,37,51] With its early stage of paddy development, the soil has shown a high potential for the formation of thioarsenates, due to low amounts of SOC and reducible Fe, and high pH.[36,37] For the microcosm experiments, the <2 mm fraction of the topsoil (0–7 cm) was used. Soil properties have been published elsewhere[36,58] and can be found summarized in Table S1.†

Microcosms were prepared inside a glovebox (COY, with 95% N_2, 5% H_2) by mixing 10 g of paddy soil, 0.13 g of finely milled rice straw to support microbial activity, and 20 mL of N_2 purged tap water inside 120 mL septum vials. The rice straw had an As content of 2.76 μg g^{-1}, while the tap water background concentrations of S, Fe, and As were 14.3, 0.04, and 0.0003 μmol L^{-1}. The vials were closed with butyl rubber stoppers and aluminum caps and incubated standing in the dark in an oven at 30 °C. To deplete the soil from excess S, Fe, and As, microcosms went through 30 redox cycles for one and a half years. Each redox cycle consisted of an anoxic period of 10 days followed by an oxic period of 5 days.

Redox fluctuations were carried out in the following way. After 10 days of anoxic incubation under the above-described conditions, the vials were taken from the oven, allowed to reach room temperature (20 °C), and shaken before removing the aluminum caps and butyl rubber stoppers. After allowing the soil to settle, the overlaying water was removed using a pipette. Finally, milled rice straw (0.13 g) was mixed into the soil to replenish the available C pool for microbes. The open vials were taken into the oven and incubated oxically for 5 days. After the oxic period, the vials were refilled with 20 mL of N_2 purged tap water inside the glovebox, closed with butyl rubber stoppers and aluminum caps, and anoxically incubated again at 30 °C for 10 days.

An additional, constantly anoxic (CA), setup was used as control. These vials went through 10 anoxic incubation days before being opened inside the glovebox to release the accumulated gases and add new rice straw before being closed again and returned to the oven. On the fifth day of the oxic cycle of the main setup, the rubber stoppers of the CA bottles were punctured with a needle inside the glovebox to release accumulated gases. This release was done in order to keep similar starting conditions between CA and the redox-cycled bottles throughout the experiment and at the moment of sampling.

Samplings

After 10, 20, and 30 redox cycles (C10, C20, and C30, respectively), sacrificial time-resolved samplings took place in which aqueous phase and soils were taken at days 1, 3, 5, 7, and 10 days of the anoxic cycle. Thus, in total 15 sacrificial vials were used per redox cycle sampling. The triplicates of the CA setup were sampled only on day 10 after 20 and 30 cycles (CA20 and CA30, respectively). These sampling days were selected based on previous reports from redox dynamics in similar setups with the same soil.[36,37,51] On each sampling day, the corresponding triplicate vials were taken out of the glovebox, mixed, and allowed to reach room temperature. The pressure inside the vials was measured with a handheld pressure meter (Greisinger GMH, 3100 Series) before taking a 5 mL headspace sample with a needle and a gastight syringe. This sample was injected into an evacuated glass vial and stored until CH_4 and CO_2 determination using a gas chromatograph with a flame ionization detector (GC-FID, SRI Instruments 8610C) equipped with a methanizer.

The vials were then brought inside the glovebox, mixed to form a slurry, and their contents poured into a 50 mL centrifuge tube. The tubes were closed and wrapped with Parafilm before being centrifuged outside the glovebox (4000 rpm, 10 min). Back inside the glovebox, the aqueous phase was separated from the soil using a syringe and needle and used for the different analyses described in each section below.

Aqueous phase analyses

The aqueous phase was filtered through 0.2 μm cellulose-acetate filters (Chromafil® Xtra) and split into different aliquots for the following biogeochemical analyses. A 2 mL aliquot was stabilized with 15 μL of 30% H_2O_2 and 20 μL of 65% HNO_3 and diluted before the determination of total As and S by Inductively Coupled Plasma Mass Spectrometry (ICP-MS, 8900 Triple Quad, Agilent). The determination was carried out using reaction mode with O_2, with As being measured as AsO^+ ($m/z = 91$) and S as SO^+ ($m/z = 48$). Rhodium was used as an internal standard to compensate for signal drift, and a certified reference material (TMDA 62.2, Environment Canada) was used for quality control.

A 700 μL aliquot for As and S speciation was stabilized with a 10 mM solution of hydroxybenzylethylenediamine (HBED, pH 7) and directly frozen in dry ice.[36] For analyses, the samples were thawed inside the glovebox to avoid changes in the speciation due to oxidation. Arsenic and S speciation was determined by ICP-MS after chromatographic separation by ion chromatography (IC, 940 Professional IC Vario Metrohm) using an AS16 column (Dionex AG/AS16 IonPac column) with a 2.5–100 mM NaOH gradient, a 1.2 mL min^{-1} flow rate, and an injection volume of 50 μL.[32] Concentrations were calculated through a calibration containing arsenite, arsenate, MMA, DMA, sulfate, and thiosulfate. Thioarsenates were identified based on

previously reported retention times,[27,28,31] and their concentrations were determined through their oxyarsenic homologs. Throughout the text, As species are often grouped depending on the biogeochemical processes ruling their formation. The sum of oxymethylated and methylthiolated arsenates is referred to as total methylated As, while the sum of inorganic and methylated thioarsenates is referred to as total thiolated As.

Total dissolved Fe, Fe^{II}, and S^{II-} were determined photometrically using the ferrozine[61,62] and the methylene blue method.[63] After stabilization according to the methods, colorimetric reactions were done outside the glovebox. Photometric determinations were carried out in triplicate using a multiplate reader (Infinite® 200 PRO, Tecan). Sulfide was not detected throughout the experiment (LOD = 1.2 μmol L^{-1}).

The rest of the filtered aqueous phase was used for the determination of pH and redox potential using a multiparameter (HQ40d, Hach) connected to the corresponding electrodes (PHC301, Ag/AgCl electrode and MTC101, respectively).

Solid phase analyses

Subsamples from all post-incubation soils were immediately frozen after being separated from the aqueous phase, and later freeze-dried and homogenized. Zerovalent sulfur (S^0) was determined *via* HPLC-UV-Vis after chloroform extraction.[64] Soil-extracted S^0 is operationally defined as chloroform-extractable S (which includes zerovalent S in polysulfides, S bound to solid phase, and S_8).

Total Fe content in the original soil and after redox cycling was determined after microwave-assisted digestion (MARS Xpress, CEM) in 10 mL aqua regia. The digested samples were filtered through 0.2 μm cellulose-acetate filters (Chromafil® Xtra) and diluted 1 : 10 with ultrapure deionized water (Millipore, 18.2 MΩ cm) before analysis by ICP-MS as described above. Changes in Fe mineralogy due to repetitive redox cycling were assessed by Mössbauer spectroscopy using samples from day 10 of the anoxic cycle from C10 and C30, as well as the original soil (C0). Dried mineral powders were loaded into Plexiglas holders (area 1 cm^2), forming a thin disc. Holders were inserted into a closed-cycle exchange gas cryostat (Janis cryogenics) under a backflow of He to minimize exposure to air. Spectra were collected at 5 and 77 K using a constant acceleration drive system (WissEL) in transmission mode with a ^{57}Co/Rh source. All spectra were calibrated against a 7 μm thick α-^{57}Fe foil that was measured at room temperature. Analysis was carried out using Recoil (University of Ottawa) and the Voigt Based Fitting (VBF) routine.[65] The half width at half maximum (HWHM) was constrained to 0.12 mm s^{-1} during fitting. Due to some uncertainties regarding the mineral phases of the Fe^{II} and the Fe^{III} (oxyhydr)oxides, additional μXRD measurements were carried out and can be found in the ESI Discussion.† The reference minerals were partly taken from the XRD Match! Software and partly from the mineralogical database "Rruff".

Statistical analyses

Unless stated otherwise, all data are presented as mean values ± standard deviation ($n = 3$). Pearson correlation coefficients were used to assess the significance of all variable correlations presented. Tukey *post hoc* analyses were used to evaluate changes in As speciation with increasing redox cycling. Pearson correlation and Tukey *post hoc* analyses were carried out using R (version 4.2.1) in RStudio (R Development Core Team, 2008).

Results & discussion

Depletion of S, Fe, and As with repeated redox cycling

Repeated redox cycling and removal of the aqueous phase after each anoxic period effectively depleted the soil of aqueous Fe, S, and As, and in consequence, concentrations in the aqueous phase. Aqueous Fe concentrations from the original soil (C0), peaked at 0.55 ± 0.09 mmol L^{-1} at 7 days of incubation (Fig. 1a). At day 7 Fe concentrations in the aqueous phase from the depleted soils (C10, C20, and C30) were lowered by 49, 43, and 61%, respectively. On average, 89% of the Fe in the aqueous phase was Fe^{II} throughout the experiment (Fig. S1†). Moreover, in the aqueous phase from the depleted soils, Fe concentrations increased constantly during the 10 day anoxic incubation period. Aqueous phase S decreased strongly with repeated redox cycling. Starting at 2.53 ± 0.08 mmol L^{-1} at day 1 in C0, the aqueous phase of the depleted soils lost, on average, 96% of this initial dissolved S concentration, decreasing the size of the primary S pool. In the depleted soils, a stable pool of dissolved S of around 0.10 mmol L^{-1} was found in the system at the beginning of each cycle. This observation suggests that during the oxic incubation period, sulfide phases were re-oxidized, releasing partially or fully oxidized soluble S forms, replenishing a small fraction of the primary sulfate pool, which was available for reduction in the next anoxic cycle (Fig. S2†).[56,57] In C0 and C10, dissolved S concentration decreased during the first incubation days, indicating consumption of sulfate from the primary pool, before stabilizing by day 7 around 0.14 and 0.04 mmol L^{-1}, respectively. In C20 and C30, stable dissolved S concentrations under 0.03 mmol L^{-1} were reached after day 3, showing a faster consumption of a smaller primary sulfate pool. Despite being depleted of electron acceptors, microbial activity was observed throughout the experiment, as shown by the decreasing Eh values throughout the 10 day anoxic period, and higher CO_2 and CH_4 production with increased redox cycling (Fig. S3†).

Dissolved As concentrations also decreased with increasing redox cycling and depletion. In C0, concentrations increased sharply with anoxic incubation time, peaking on day 7 at 2.11 ± 0.09 μmol L^{-1}. In C10, C20, and C30, dissolved As concentrations at the same incubation time were only 13, 5, and 6% of those in C0, respectively. More importantly, opposite to the trend observed in C0, As concentrations in the aqueous phase of the depleted soils decreased throughout the 10 day anoxic incubation period.

In the CA controls (Fig. S4†), dissolved Fe concentrations by the end of each cycle remained constant for CA20 and CA30 (0.7 ± 0.1 and 0.7 ± 0.03 mmol L^{-1}, respectively) showing an increase compared to C0 (0.47 ± 0.06 mmol L^{-1} at day 10). Dissolved S concentrations in CA20 and CA30 were 0.13 ± 0.01 and 0.16 ± 0.01 mmol L^{-1}, respectively. These concentrations are comparable to the stable values found on C0 from day 7 of

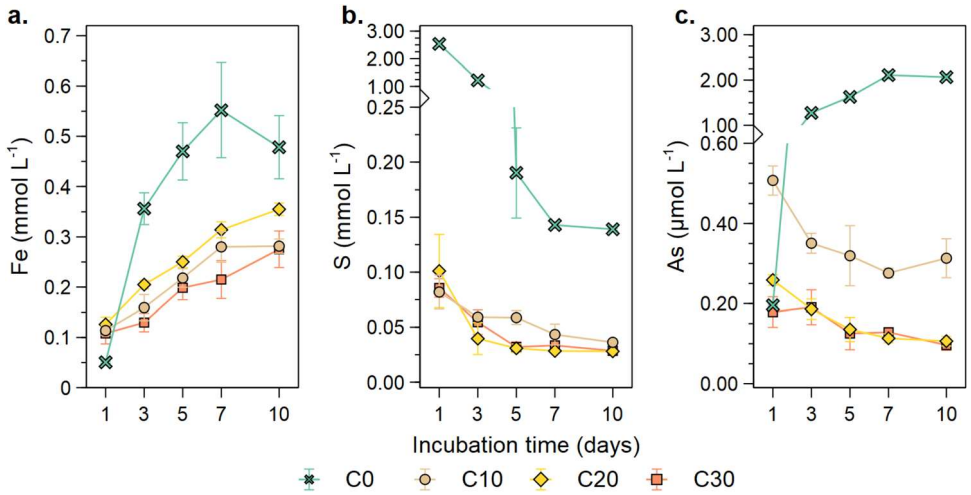

Fig. 1 Depletion of dissolved Fe (a), S (b), and As (c) through repeated redox cycling and washout. Data points are average values and bars indicate standard deviation ($n = 3$).

the anoxic period reported above. Dissolved As concentration also decreased with longer CA cycling, but to a lesser extent than in depleted soils. In CA20 and CA30, aqueous phase As concentrations were 0.40 ± 0.02 and 0.57 ± 0.07 µmol L^{-1}, compared to 2.07 ± 0.03 µmol L^{-1} at day 10 in C0.

The depletion of S, Fe, and As in the soils and hence the lower concentrations in the aqueous phase were a consequence of redox cycling and the removal of the standing water. Under anoxic incubation conditions, reductive dissolution of Fe(III) minerals took place, releasing Fe^{II} and the associated As into the aqueous phase.[7] By removing the standing water at the end of each anoxic cycle, the dissolved fraction of Fe^{II} and As was removed from the system. The repetition of this process with repetitive redox cycling caused the depletion of the bioavailable Fe^{III} fraction in the soils, lowering how much Fe^{III} could be reductively dissolved in the next anoxic period. The decrease of dissolved S throughout the 10 days of the anoxic periods indicates DSR and suggests the precipitation of sulfides, likely through reaction with dissolved Fe^{II}.[66,67] By removing the standing water at the end of each anoxic cycle, the non-precipitated S was removed from the system. The constant increase of dissolved Fe throughout the anoxic periods in the depleted soils suggests that FeS precipitation could be limited in these soils compared to C0, due to a lower availability of sulfate and hence, sulfide. In the CA setups, the stable concentrations of Fe and S in the aqueous phase suggest that their biogeochemistry might have reached an equilibrium in these setups, with FeS precipitation no longer taking place. The precipitation of Fe or As sulfide phases could be responsible for the lower As concentrations in the aqueous phase compared to C0.[41,66,68]

Changes in As speciation with repeated redox cycling

Repeated redox cycling directly affected As speciation. These results are presented as the percentage contribution of group species to total As, to correct for As depletion. Summarizing the data of the 10 anoxic incubation days of each cycle, the median contribution to total methylated As showed no trends with increasing redox cycling, with median values staying around 20–30% of total As (Fig. 2a). However, total As thiolation increased sharply with increasing redox cycling (Fig. 2b). Total contribution of thioarsenates to total As was 4% in C0, significantly increasing ($p < 0.05$) to 10, 40, and 39% in C10, C20, and C30, respectively.

Breaking down these species groups into subgroups shows that while there was no net trend in total methylated As, there was a significant decrease ($p < 0.05$) in the contribution of oxymethylated arsenates (Fig. 2c), from a median contribution of 26% in C0 to only 7% in C30. In contrast, the contribution of methylthioarsenates (Fig. 2d) increased significantly ($p < 0.05$) with increasing redox cycling between C0 and C20 from 3 to 25%. Since the contribution of total methylated species remained constant throughout the repetitive redox cycling, the opposite trends observed for these two subgroups suggest that the decrease in the contribution of oxymethylarsenates is caused by their thiolation to form methylthioarsenates. Moreover, the significant increase ($p < 0.05$) in the median contribution of inorganic thioarsenates, from 0.6 to 24% from C0 to C30 (Fig. 2e), caused a sharp increase in the contribution of total thiolated species. Strikingly, the thioarsenate contribution to total As in these depleted systems, was much higher than values commonly reported for paddy soils, which are often <10%.[28,36]

An increasing S/As molar ratio in the depleted soils (C10–C30) significantly correlated ($p < 0.0001$) with the increased contribution of inorganic thioarsenates (Fig. 3a). In C0, despite high S/As ratios, the contribution of inorganic thioarsenates to total As was low, since S here was mostly found as sulfate (Fig. S2†). In the CA controls, S/As values were in the same magnitude as those of C20 and C30, but the contribution of inorganic thioarsenates in the CA setups was similar to that in C10. Besides higher S/As ratios, the high contribution of thioarsenates in the depleted soils compared to C0 can be linked to the lower bioavailable Fe (Fig. S5a†), since at low aqueous Fe^{II}

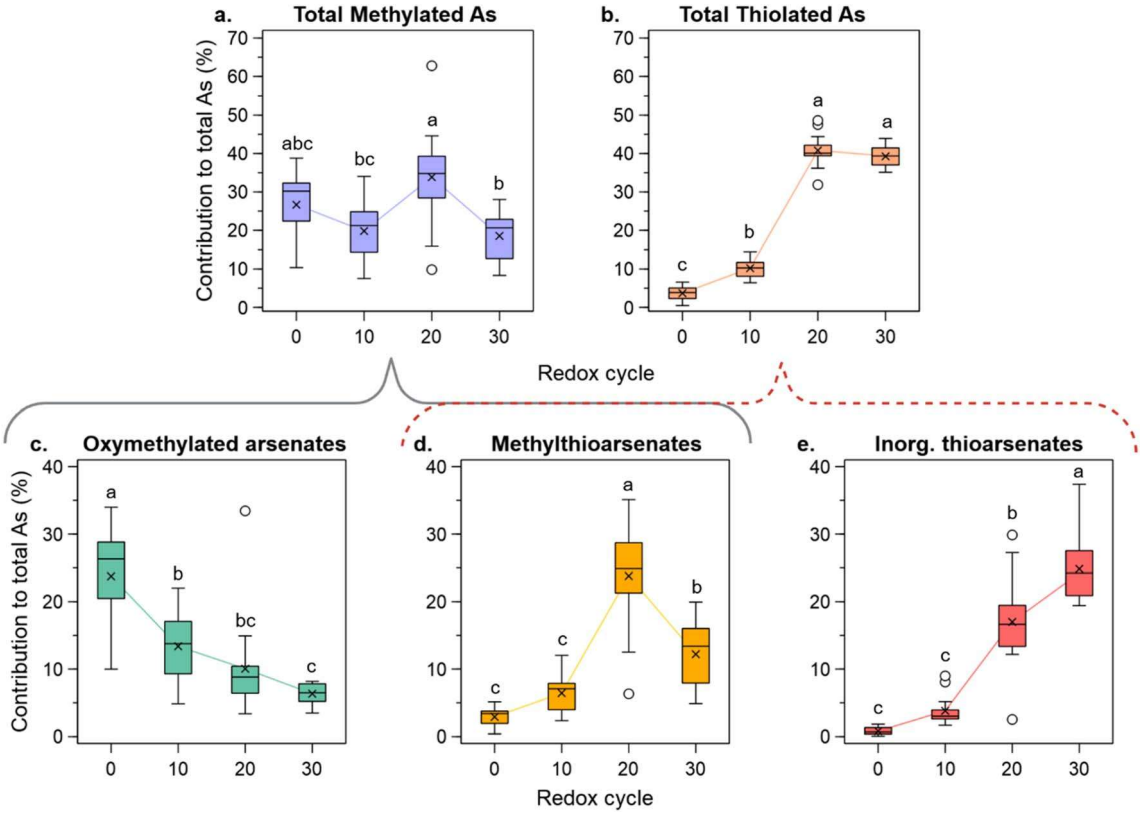

Fig. 2 Changes in total methylated (a) and total thiolated (b) As with increasing redox cycling. Species groups are further subdivided into oxymethylated arsenates (c), methylthioarsenates (d), and inorganic thioarsenates (e). Each box in the plot summarizes the results of triplicate throughout the 10 days of anoxic incubation ($n = 15$), with "×" showing the mean value and white circles showing outliers (1.5 interquartile range). Different letters on top of the boxes indicate statistical significance based on Tukey *post hoc* analyses ($p < 0.05$).

concentrations, more reduced S is available for thiolation. Excess S over Fe correlated positively and significantly with high inorganic thioarsenate formation (Fig. S5b†). Repeated redox cycling caused a higher ratio of inorganic thioarsenates over their oxyarsenic homologs, particularly at the beginning of the anoxic incubation period in C20 and C30. Nonetheless, arsenate and arsenite were still the dominating inorganic species throughout the experiment (Fig. S6†).

Moreover, changes in the contribution of inorganic thioarsenates throughout the 10 days of the incubation period show further insights into how increased redox cycling influenced their formation. In the depleted soils, the contribution of inorganic thioarsenates to total As was higher at the beginning of the 10 day anoxic period (Fig. 3b). The depleted soils, especially C20 and C30, showed a higher contribution of highly thiolated inorganic thioarsenates (DTA and TTA), which decreased throughout the anoxic incubation. The constantly anoxic controls did not show a similar trend, with MTA being constantly the dominant inorganic thioarsenate and rather a decrease in inorganic thiolation with increasing cycling (Fig. S7†).

Increasing S/As ratios also had a significant influence on the contribution of methylthioarsenates ($p < 0.001$) (Fig. 3c). In C0, despite the high S/As ratio, the formation of methylthioarsenates was low. Moreover, the contribution of methylthioarsenates to total As changed throughout the anoxic incubation period, showing differences from the trends reported above for inorganic thioarsenates (Fig. 3d). With increasing redox cycling, the formation, contribution, and degree of thiolation of methylthioarsenates increased. In particular in C20 and C30, highly thiolated monomethylated arsenates (MMDTA and MMTTA) contributed significantly to total As. During most of the anoxic incubation period in C20 and C30, methylthioarsenates dominated over methyloxyarsenates. The contribution of methylthioarsenate to total As did not decrease with increasing incubation time, and the degree of thiolation was relatively constant throughout the anoxic period.

The above-described results for the formation and stability of inorganic and methylated thioarsenates show the contrasting behaviors of these two species groups. The formation of inorganic thioarsenates coincides kinetically with the consumption of the primary sulfate pool in the first three days of incubation (Fig. S8†), with high inorganic thioarsenate concentrations being present at high concentrations of sulfate. We suggest that this period of high DSR triggers the formation of highly thiolated inorganic thioarsenates, due to a relative excess of S^{II-} related to the high sulfate consumption. Once S^{II-} becomes limited, due to the consumption of most of the primary sulfate pool and likely the precipitation of FeS phases in the presence of a relative excess of dissolved Fe, inorganic thioarsenate

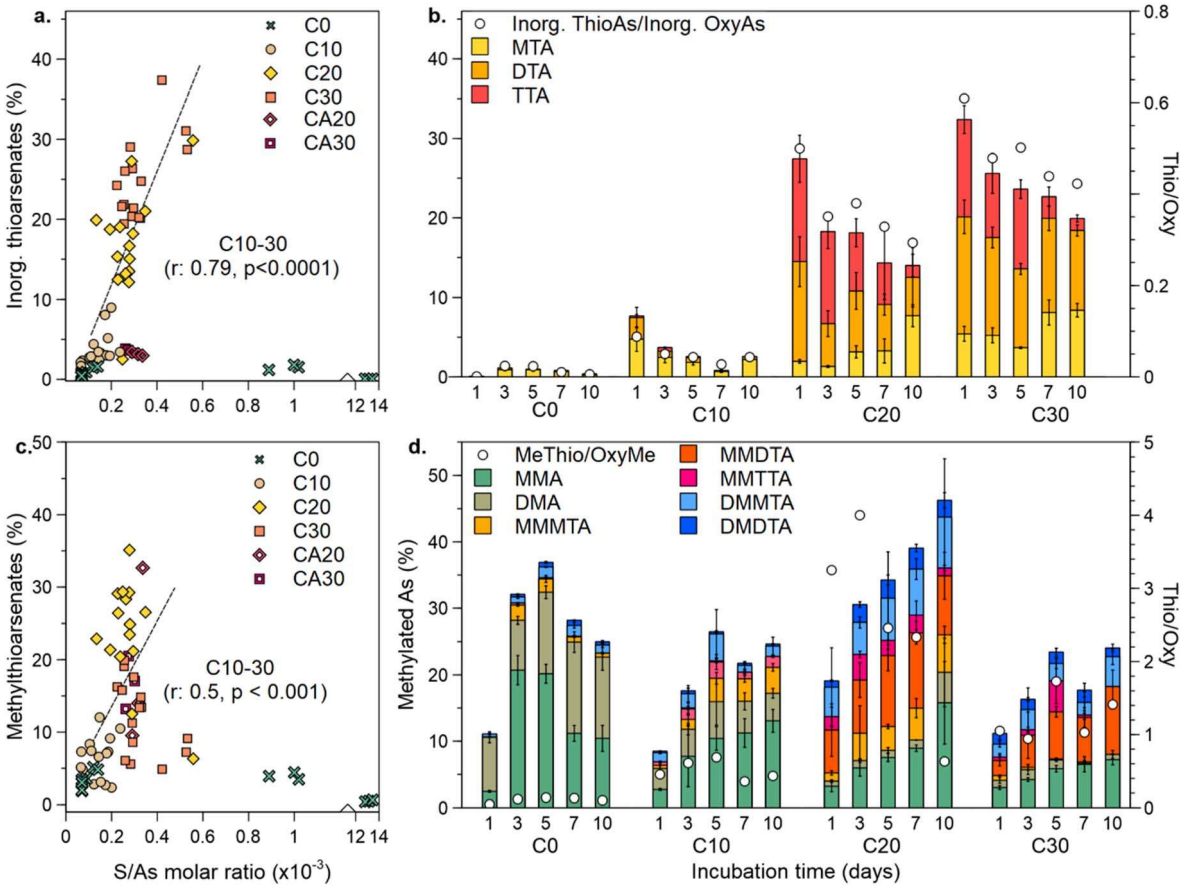

Fig. 3 Effect of repeated redox cycling on thioarsenate formation. Influence of S/As ratios on the contribution of inorganic and methylated thioarsenates to total As (a, c, respectively) and temporal dynamics of individual inorganic and methylated As species (b, d, respectively). Regression lines in (a and b) are drawn for samples from depleted systems (C10–C30).

concentrations decrease, indicating de-thiolation (Fig. S8†). Around the same time of the anoxic incubation, the contribution of methylthioarsenates increased. Methylthioarsenate formation was limited at the start of the anoxic period due to low MMA and DMA concentrations, but once these species are available, they are readily thiolated.[36] Moreover, methylthioarsenates still formed when the system seemed to be S^{II-} limited (Fig. S8†), as suggested by the dethiolation of inorganic thioarsenates and low sulfate concentrations.

Taking C20 and C30 as examples of highly depleted systems, although there is a decrease in the contribution of inorganic thioarsenates and an increase in methylthioarsenates, the contribution of total thiolated As species remains constant during the anoxic incubation period (Fig. S9†). Similar observations of inorganic thioarsenate dethiolation coupled with the formation of methylthioarsenates have been recently reported along the outflow channel of a geothermal spring.[69] Under neutral pH conditions commonly found in paddy soils and in the incubation setups of this experiment (Fig. S10†), methylthioarsenates require a lower excess of S^{II-} to form and, thus, are thought to be more thermodynamically stable and preferred thiolation products.[31–33] We suggest that under S^{II-} limited conditions in the depleted soils, the formation of MMA and DMA could trigger the de-thiolation of inorganic thioarsenates. Such competition for S^{II-} could take place as the inorganic thioarsenates de-thiolate due to a shift in the equilibrium caused by lower S^{II-} concentrations. The S^{II-} released by the de-thiolation could then react with MMA or DMA to form methylthioarsenates, which are stable at lower S^{II-} concentrations.

Changes in S speciation and influence on thioarsenate formation

Zerovalent S and thiosulfate, products of the partial reoxidation of S^{II-}, were found in the incubations. Despite the depletion of dissolved S in the aqueous phase with increasing redox cycling, S^0 accumulated in the solid phase (Fig. 4a). In C20 and C30, S^0 formation did not decrease by the washout of over 95% of the aqueous phase S. More importantly, S^0 was higher in depleted soils than in C0. Thus, the formation and accumulation of S^0 were independent of the S washout with increased redox cycling. This newly formed S^0 pool stayed relatively stable throughout the 10 day anoxic incubation, indicating comparable rates of production and consumption. In the depleted soils, S^0 content correlated positively ($p < 0.05$) with sulfate concentration in the aqueous phase (Fig. 4b).

Similarly, thiosulfate was found in the aqueous phase, being slightly higher at the beginning of the anoxic incubation and decreasing with time (Fig. 4c). Thiosulfate concentrations

peaking at the beginning of the incubation could be related to the partial oxidation of S^{II-} during the oxic incubation period. Nonetheless, thiosulfate is reported to be highly reactive, transforming easily back into S^{II-} or further oxidizing into sulfate.[56] Thus, thiosulfate concentrations around 0.025 μmol L^{-1} towards the end of the anoxic incubation period suggest its formation under anaerobic conditions. Thiosulfate concentrations also significantly correlated ($p < 0.0001$) with sulfate concentrations (Fig. 4d). A stable pool of S^0 and thiosulfate formation under anoxic conditions, and their significant correlations with aqueous sulfate concentrations, suggest an active CSC in the depleted soils.

Reduction of Fe^{III} is the main proposed partner for S^{II-} reoxidation under anoxic conditions.[52,70] Increasing concentrations of dissolved Fe during the anoxic incubation periods in the depleted soils indicate Fe^{III} reduction. This reduction could be partially associated with Fe respiration. However, trends in CH_4 production suggest that Fe reductive dissolution is not a central respiration pathway in the depleted soils. In C0, CH_4 production had a lag phase (Fig. S3†) normally associated with the use of other thermodynamically preferred respiration pathways,[71,72] followed by a phase of exponential CH_4 production. Bioavailable Fe^{III} (oxyhydr)oxides are known to delay methanogenesis.[73,74] In the depleted soils, this lag was not present, showing a linear increase in CH_4 production between day 1 and 10 of the anoxic incubation, suggesting the low availability of other electron acceptors for anaerobic respiration such as Fe^{III} and sulfate. These observations suggest that abiotic Fe^{III} reduction associated with the CSC might dominate over biotically mediated Fe reductive dissolution.

In the solid phase, Mössbauer spectroscopy showed that repeated redox cycling mainly caused changes in the distribution of Fe^{III} (oxyhydr)oxides (Tables S2, S3 and Fig. S11†). Crystalline Fe^{III} (oxyhydr)oxides contributed 24.6% to C0 and were decreased in half by C10. Further cycling slightly decreased their contribution. In contrast, poorly crystalline Fe^{III} (oxyhydr) oxides increased from 2.8% in C0 to 5.4% in C10, with a slight increase with further cycling. Moreover, there were slight increases in the contribution of other identified phases, such as Fe^{II} and adsorbed Fe^{III} with increased redox cycling (Table S3†). These Fe phases could offer a chemically reactive Fe^{III} pool for S^{II-} reoxidation, as proposed by Hansel *et al.*[70] for low sulfate freshwater sediments. Similarly, Holmkvist and Ferdelman[52] correlated a slowly reacting Fe pool with S^{II-} reoxidation.

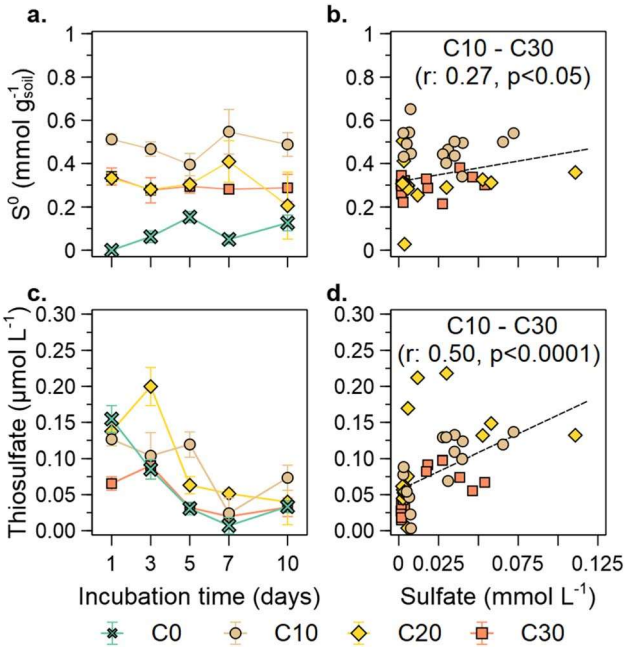

Fig. 4 Changes in S speciation with increasing redox cycling. Time-resolved zerovalent S during incubation (a) and soil content compared with aqueous sulfate (b). Time-resolved thiosulfate concentrations during incubation (c) and concentration compared to sulfate (d). In (a and c), data points are average values and bars indicate standard deviation ($n = 3$). For (b and d), only data points from the depleted systems (C10–C30) are used.

Sulfate reduction, sulfide reoxidation, and thioarsenate formation

The above-described results for As speciation suggest that the formation of inorganic and methylated thioarsenates might be ruled by different sources of reduced S species, depending mainly on thermodynamic stability and sulfate reduction kinetics. According to these results, early thiolation in paddy soils could be driven by the reduction of a big primary pool of sulfate, taking place in the first days of anoxic incubation. Later, as this primary sulfate pool is consumed, thiolation is driven by the reduction of a smaller secondary sulfate pool as a consequence of the CSC. The As speciation in the depleted soils of this experiment offers insights into this dependency.

High contribution of methylthioarsenates correlated positively ($p < 0.01$) with excess S^0 over methyloxyarsenates (as a molar ratio of the precursors (S^0) and reactants (MMA + DMA) required for methylthioarsenate formation) (Fig. 5a). This correlation was not present when considering inorganic thioarsenate formation through the reaction of S^0 and arsenite (Fig. 5b). In contrast, a higher contribution of inorganic thioarsenates was found at low S^0/arsenite ratios. Similarly, methylthioarsenate formation correlated positively ($p < 0.05$) with excess thiosulfate over methyloxyarsenates (Fig. 5c), but not with inorganic thioarsenate formation when comparing thiosulfate/arsenite (Fig. 5d). These positive correlations do not imply thiolation directly through the reaction of MMA and DMA with S^0 or thiosulfate, but rather S^0 and thiosulfate as intermediate S species of CSC for the formation of sulfate, which will be biotically reduced to S^{II-}, and form thioarsenates.

A direct evaluation of thiolation through S^{II-} was not possible since it was not detected in any setup. Low S^{II-} has been previously linked to the CSC since the small and constant amounts of S^{II-} produced readily react and thus, do not accumulate.[52,56] Sulfate concentrations were used to evaluate the role of the reduction of the primary sulfate pool on As thiolation, under the assumption that most of the available sulfate would be reduced by SRB to form S^{II-}. Nonetheless, this correlation does not consider that not all produced S^{II-} would be available for As thiolation, due to, for example, FeS precipitation. High

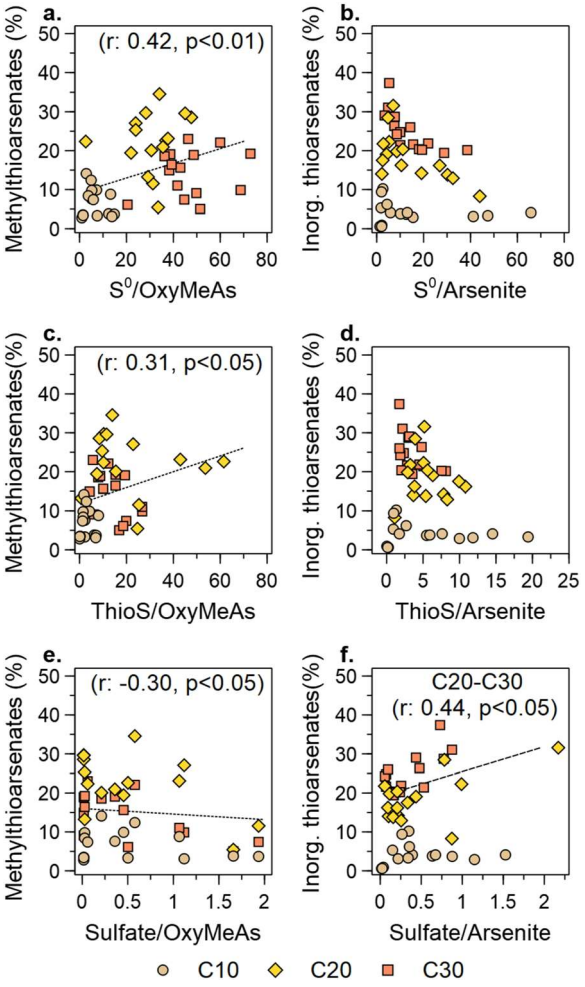

Fig. 5 Influence of excess S^0, thiosulfate (ThioS), and sulfate over oxymethylated arsenates (OxyMeAs) in the formation of methylthioarsenates (a, c, and d, respectively). Influence of excess S^0, thiosulfate (ThioS), and sulfate over arsenite in the formation of inorganic thioarsenates (b, d, and f, respectively).

sulfate over oxymethylated arsenate ratio correlated negatively ($p < 0.05$) with methylthioarsenate formation, while high inorganic thioarsenate formation correlated positively ($p < 0.05$) with excess sulfate over arsenite, but only when considering C20 and C30 as highly S depleted systems (Fig. 5e and f).

These correlations suggest that in a S-depleted paddy soil, the formation of inorganic and methylated thioarsenates takes place through the reduction of two different sulfate pools, summarized in Fig. 6 and contextualized for our 10 day incubation period. Since inorganic thioarsenates formed mainly at the beginning of the anoxic incubation period, and they lacked a correlation with intermediate, partially oxidized S products of the CSC, we suggest that their formation is strongly related to the reduction of the primary sulfate pool (Fig. 6, process 1), which was likely replenished through the oxidation of sulfide phases during the oxic period. The relatively high availability of S^{II-}, low dissolved Fe, and high S/As ratios then favored the formation of highly thiolated inorganic thioarsenates (DTA and TTA).

After 5 days, and once the primary pool of sulfate had been consumed by SRB, S^{II-} had been likely scavenged by FeS precipitation, and methylated oxyarsenates were present, inorganic thioarsenates dethiolated. Furthermore, the positive correlation between methylthioarsenate formation and partially oxidized products of the CSC suggest that the main source of S^{II-} for their formation in later stages of the anoxic incubation is the secondary sulfate pool formed through the CSC (Fig. 6, process 2). While this secondary sulfate pool would theoretically be available for the formation of inorganic thioarsenates, the lower excess S^{II-} necessary for the formation of methylthioarsenates favors their formation in an S-depleted system. Moreover, due to the depletion of S, the primary sulfate pool becomes a less relevant source of S^{II-} with increasing redox cycling.

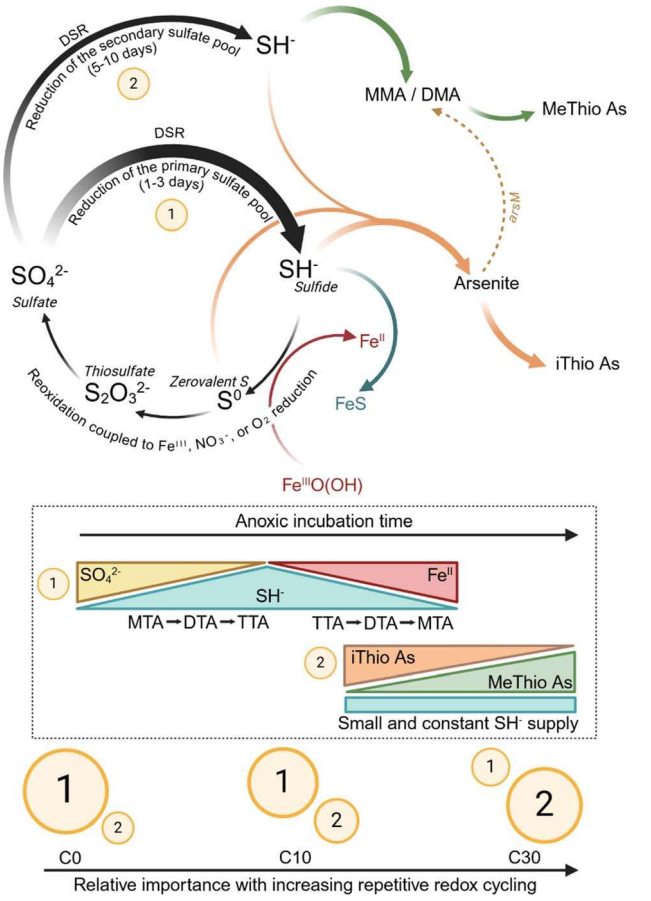

Fig. 6 Conceptual model indicating the formation of inorganic thioarsenates (iThio As) and methylthioarsenates (MeThioAs) with S^{II-} from either a primary (1) or secondary (2) sulfate pool. The top diagram in the figure displays the biogeochemical reactions involved in the production of S^{II-} and thioarsenates. The thickness of the arrows qualitatively illustrates the importance of a reaction. Sulfur species are protonated assuming pH 7, reflecting the neutral values during the experiment (Fig. S10†). In the center, diagrams indicate changes in concentrations of key players in the reactions throughout the 10 day anoxic incubation period. Circles at the bottom of the figure show how the reduction of the primary sulfate pool decreases in importance as the soil is depleted, while S^{II-} produced due to the reduction of a secondary sulfate pool gains importance.

Conclusion

The results presented here show the importance of considering thioarsenate formation when studying As speciation. It is often assumed that thioarsenates do not form in low-S systems such as wetlands or paddy soils, considered to be methanogenic environments. Here, we show that through the CSC, a supply of reduced S species is available for thiolation even in S-depleted systems and once the primary sulfate pool is consumed by SRB activity. These observations help explain the presence of thioarsenates in paddy soil porewaters even when sulfate reduction is no longer taking place. In systems with low As, where there is a high S/As ratio, thioarsenates can significantly contribute to speciation and, thus, mobility, long-range transport, and toxicity, depending on environmental conditions. In the context of paddy soils, a large share of thioarsenates can be related to a higher As uptake by rice plants, risking food safety. The results presented here do not imply that CSC only takes place in S-depleted systems. Cryptic S cycling likely takes place in S-rich systems as well, but its effects are masked by high S concentrations and changes in S speciation dominated by SRB activity during the consumption of the primary sulfate pool.

More importantly, this study highlights the differences in the kinetics and thermodynamics of the formation of inorganic and methylated thioarsenates. Systems with a high and constant reduced S supply might be dominated by inorganic thioarsenates, as is the case in many geothermal systems. However, if methylated oxyarsenates are present, and reduced S becomes scarce, our results suggest the dethiolation of inorganic thioarsenates to form methylthioarsenates. These observations show the complex biogeochemistry behind As thiolation, which depends on reduced S availability and the presence of specific As species, which in turn are strongly governed by microbially mediated reactions and the biogeochemistry of C and Fe.

Data availability

The data collected during the above-described experiments and used for this study are published on Zenodo at **https://doi.org/10.5281/zenodo.14336088**.

Author contributions

This study was conceptualized by J. M. L. N. and B. P.-F.; incubation setup and solid, aqueous, and gas phase analyses were carried out by J. M. L. N. Mössbauer spectroscopy and μXRD analyses were carried out by C. L. D. with the support of A. K. The manuscript and ESI† were written by J. M. L. N. with assistance from B. P.-F.; all authors contributed to the manuscript revisions.

Conflicts of interest

The authors declare no competing interests.

Acknowledgements

We thank the German Academic Scholarship Foundation for the doctoral funding support for J. M. L. N. and funding within the Federal Ministry of Education and Research project BMBF #031B0840 to B. P.-F. We are grateful to Sylvia Hafner, Jens Hamberger, Tobias Mayer, Hai Anh Nguyen, Milagros Galarza, and Alejandra Higa Mori for their experimental support during the long-term experiment. We thank Livia Urbanski and Angelika Kölbl for providing the chronosequence soil, and Ben Gilfedder for providing access to the CH_4 and CO_2 analyses. The Graphical Abstract and Fig. 6 were created using BioRender.

References

1 J. T. Trevors and B. J. Alloway, Heavy Metals in Soils: Trace Metals and Metalloids in Soils and their Bioavailability, *Heavy Metals in Soils*, 2013.
2 A. Aitio, K. Cantor, M. D. Attfield and P. A. Demers, Arsenic, metals, fibres, and dusts, *IARC Monogr Eval Carcinog Risks Hum.*, 2012, vol. 100, Pt C, pp. 11–465.
3 R. Stone, Arsenic and paddy rice: A neglected cancer risk?, *Science*, 2008, **321**(5886), 184–185.
4 I. Kögel-Knabner, W. Amelung, Z. Cao, S. Fiedler, P. Frenzel, R. Jahn, *et al.*, Biogeochemistry of paddy soils, *Geoderma*, 2010, **157**(1), 1–14.
5 A. A. Nghiem, H. Prommer, M. R. H. Mozumder, A. Siade, J. Jamieson, K. M. Ahmed, *et al.*, Sulfate reduction accelerates groundwater arsenic contamination even in aquifers with abundant iron oxides, *Nat. Water*, 2023, **1**(2), 151–165.
6 J. Podgorski and M. Berg, Global threat of arsenic in groundwater, *Science*, 2020, **368**(6493), 845–850.
7 P. L. Smedley and D. G. Kinniburgh, A review of the source, behaviour and distribution of arsenic in natural waters, *Appl. Geochem.*, 2002, **17**(5), 517–568.
8 J. F. Ma, N. Yamaji, N. Mitani, X.-Y. Xu, Y.-H. Su, S. P. McGrath, *et al.*, Transporters of arsenite in rice and their role in arsenic accumulation in rice grain, *Proc. Natl. Acad. Sci. U. S. A.*, 2008, **105**(29), 9931–9935.
9 A. A. Meharg and F. J. Zhao, *Arsenic & Rice*, Springer Netherlands, 2012.
10 F.-J. Zhao, Y.-G. Zhu and A. A. Meharg, Methylated arsenic species in rice: geographical variation, origin, and uptake mechanisms, *Environ. Sci. Technol.*, 2013, **47**(9), 3957–3966.
11 B. Moe, H. Peng, X. Lu, B. Chen, L. W. L. Chen, S. Gabos, *et al.*, Comparative cytotoxicity of fourteen trivalent and pentavalent arsenic species determined using real-time cell sensing, *J. Environ. Sci.*, 2016, **49**, 113–124.
12 S. Goldberg and C. T. Johnston, Mechanisms of arsenic adsorption on amorphous oxides evaluated using macroscopic measurements, vibrational spectroscopy, and surface complexation modeling, *J. Colloid Interface Sci.*, 2001, **234**(1), 204–216.
13 Y. Takahashi, R. Minamikawa, K. H. Hattori, K. Kurishima, N. Kihou and K. Yuita, Arsenic behavior in paddy fields

during the cycle of flooded and non-flooded periods, *Environ. Sci. Technol.*, 2004, **38**(4), 1038–1044.
14 J. Zobrist, P. R. Dowdle, J. A. Davis and R. S. Oremland, Mobilization of arsenite by dissimilatory reduction of adsorbed arsenate, *Environ. Sci. Technol.*, 2000, **34**(22), 4747–4753.
15 C. Lomax, W.-J. Liu, L. Wu, K. Xue, J. Xiong, J. Zhou, *et al.*, Methylated arsenic species in plants originate from soil microorganisms, *New Phytol.*, 2012, **193**(3), 665–672.
16 J. Qin, B. P. Rosen, Y. Zhang, G. Wang, S. Franke and C. Rensing, Arsenic detoxification and evolution of trimethylarsine gas by a microbial arsenite S-adenosylmethionine methyltransferase, *Proc. Natl. Acad. Sci. U. S. A.*, 2006, **103**(7), 2075–2080.
17 K. Viacava, K. L. Meibom, D. Ortega, S. Dyer, A. Gelb, L. Falquet, *et al.*, Variability in arsenic methylation efficiency across aerobic and anaerobic microorganisms, *Environ. Sci. Technol.*, 2020, **54**(22), 14343–14351.
18 H. Naranmandura, M. W. Carew, S. Xu, J. Lee, E. M. Leslie, M. Weinfeld, *et al.*, Comparative Toxicity of Arsenic Metabolites in Human Bladder Cancer EJ-1 Cells, *Chem. Res. Toxicol.*, 2011, **24**(9), 1586–1596.
19 F.-J. Zhao, E. Harris, J. Yan, J. Ma, L. Wu, W. Liu, *et al.*, Arsenic methylation in soils and its relationship with microbial arsM abundance and diversity, and As speciation in rice, *Environ. Sci. Technol.*, 2013, **47**(13), 7147–7154.
20 M. C. Reid, J. Maillard, A. Bagnoud, L. Falquet, P. Le Vo and R. Bernier-Latmani, Arsenic methylation dynamics in a rice paddy soil anaerobic enrichment culture, *Environ. Sci. Technol.*, 2017, **51**(18), 10546–10554.
21 L. Wang, Q. Guo, G. Wu, Z. Yu, J. M. L. Ninin and B. Planer-Friedrich, Methanogens-Driven Arsenic Methylation Preceding Formation of Methylated Thioarsenates in Sulfide-Rich Hot Springs, *Environ. Sci. Technol.*, 2023, **57**(19), 7410–7420.
22 C. Chen, L. Li, K. Huang, J. Zhang, W.-Y. Xie, Y. Lu, *et al.*, Sulfate-reducing bacteria and methanogens are involved in arsenic methylation and demethylation in paddy soils, *ISME J.*, 2019, **13**(10), 2523–2535.
23 C. Chen, B. Yang, Y. Shen, J. Dai, Z. Tang, P. Wang, *et al.*, Sulfate addition and rising temperature promote arsenic methylation and the formation of methylated thioarsenates in paddy soils, *Soil Biol. Biochem.*, 2021, **154**, 108129.
24 C. Chen, B. Yang, A. Gao, L. Li, X. Dong and F.-J. Zhao, Suppression of methanogenesis in paddy soil increases dimethylarsenate accumulation and the incidence of straighthead disease in rice, *Soil Biol. Biochem.*, 2022, **169**, 108689.
25 C. Chen, L. Li, Y. Wang, X. Dong and F.-J. Zhao, Methylotrophic methanogens and bacteria synergistically demethylate dimethylarsenate in paddy soil and alleviate rice straighthead disease, *ISME J.*, 2023, 1851–1861.
26 S. Stauder, B. Raue and F. Sacher, Thioarsenates in sulfidic waters, *Environ. Sci. Technol.*, 2005, **39**(16), 5933–5939.
27 D. Wallschläger and C. J. Stadey, Determination of (oxy) thioarsenates in sulfidic waters, *Anal. Chem.*, 2007, **79**(10), 3873–3880.
28 J. Wang, C. F. Kerl, P. Hu, M. Martin, T. Mu, L. Brüggenwirth, *et al.*, Thiolated arsenic species observed in rice paddy pore waters, *Nat. Geosci.*, 2020, **13**(4), 282–287.
29 A. Eberle, J. Besold, J. M. León Ninin, C. F. Kerl, K. Kujala and B. Planer-Friedrich, Potential of high pH and reduced sulfur for arsenic mobilization – insights from a Finnish peatland treating mining waste water, *Sci. Total Environ.*, 2021, **758**, 143689.
30 B. Planer-Friedrich, C. Härtig, R. Lohmayer, E. Suess, S. H. McCann and R. Oremland, Anaerobic Chemolithotrophic Growth of the Haloalkaliphilic Bacterium Strain MLMS-1 by Disproportionation of Monothioarsenate, *Environ. Sci. Technol.*, 2015, **49**(11), 6554–6563.
31 D. Wallschläger and J. London, Determination of methylated arsenic-sulfur compounds in groundwater, *Environ. Sci. Technol.*, 2008, **42**(1), 228–234.
32 B. Planer-Friedrich, J. London, R. B. McCleskey, D. K. Nordstrom and D. Wallschläger, Thioarsenates in geothermal waters of Yellowstone National Park: determination, preservation, and geochemical importance, *Environ. Sci. Technol.*, 2007, **41**(15), 5245–5251.
33 S. D. Conklin, M. W. Fricke, P. A. Creed and J. T. Creed, Investigation of the pH effects on the formation of methylated thio-arsenicals, and the effects of pH and temperature on their stability, *J. Anal. At. Spectrom.*, 2008, **23**(5), 711–716.
34 Y.-T. Kim, H. Lee, H.-O. Yoon and N. C. Woo, Kinetics of Dimethylated Thioarsenicals and the Formation of Highly Toxic Dimethylmonothioarsinic Acid in Environment, *Environ. Sci. Technol.*, 2016, **50**(21), 11637–11645.
35 P. V. T. Knobloch, L. H. Pham, C. F. Kerl, Q. Guo and B. Planer-Friedrich, Seasonal Formation of Low-Sorbing Methylthiolated Arsenates Induces Arsenic Mobilization in a Minerotrophic Peatland, *Environ. Sci. Technol.*, 2024, 1669–1679.
36 J. M. León Ninin, E. M. Muehe, A. Kölbl, A. Higa Mori, A. Nicol, B. Gilfedder, *et al.*, Changes in arsenic mobility and speciation across a 2000-year-old paddy soil chronosequence, *Sci. Total Environ.*, 2024, **908**, 168351.
37 J. M. León Ninin, N. Kryschak, S. Peiffer and B. Planer-Friedrich, Long-Term Paddy Soil Development Buffers the Increase in Arsenic Methylation and Thiolation after Sulfate Fertilization, *J. Agric. Food Chem.*, 2024, 25045–25053.
38 D. R. Lovley, Microbial Fe(III) reduction in subsurface environments, *FEMS Microbiol. Rev.*, 1997, **20**(3–4), 305–313.
39 E. D. Burton, S. G. Johnston and B. D. Kocar, Arsenic mobility during flooding of contaminated soil: the effect of microbial sulfate reduction, *Environ. Sci. Technol.*, 2014, **48**(23), 13660–13667.
40 M. L. Farquhar, J. M. Charnock, F. R. Livens and D. J. Vaughan, Mechanisms of arsenic uptake from aqueous solution by interaction with goethite, lepidocrocite, mackinawite, and pyrite: an X-ray absorption

spectroscopy study, *Environ. Sci. Technol.*, 2002, **36**(8), 1757–1762.
41 B. C. Bostick and S. Fendorf, Arsenite sorption on troilite (FeS) and pyrite (FeS2), *Geochim. Cosmochim. Acta*, 2003, **67**(5), 909–921.
42 J. Wang, D. Halder, L. Wegner, L. Brüggenwirth, J. Schaller, M. Martin, *et al.*, Redox dependence of thioarsenate occurrence in paddy soils and the rice rhizosphere, *Environ. Sci. Technol.*, 2020, **54**(7), 3940–3950.
43 A. E. Colina Blanco, C. F. Kerl and B. Planer-Friedrich, Detection of thioarsenates in rice grains and rice products, *J. Agric. Food Chem.*, 2021, **69**(7), 2287–2294.
44 B. Planer-Friedrich, C. F. Kerl, A. E. Colina Blanco and S. Clemens, Dimethylated thioarsenates: a potentially dangerous blind spot in current worldwide regulatory limits for arsenic in rice, *J. Agric. Food Chem.*, 2022, **70**(31), 9610–9618.
45 E. Pischke, F. Barozzi, A. E. Colina Blanco, C. F. Kerl, B. Planer-Friedrich and S. Clemens, Dimethylmonothioarsenate is highly toxic for plants and readily translocated to shoots, *Environ. Sci. Technol.*, 2022, **56**(14), 10072–10083.
46 T. Wind and R. Conrad, Localization of sulfate reduction in planted and unplanted rice field soil, *Biogeochemistry*, 1997, **37**(3), 253–278.
47 S. W. Poulton, Sulfide oxidation and iron dissolution kinetics during the reaction of dissolved sulfide with ferrihydrite, *Chem. Geol.*, 2003, **202**(1), 79–94.
48 G. Jiang, K. R. Sharma, A. Guisasola, J. Keller and Z. Yuan, Sulfur transformation in rising main sewers receiving nitrate dosage, *Water Res.*, 2009, **43**(17), 4430–4440.
49 M. Mora, L. R. López, J. Lafuente, J. Pérez, R. Kleerebezem, M. C. M. van Loosdrecht, *et al.*, Respirometric characterization of aerobic sulfide, thiosulfate and elemental sulfur oxidation by S-oxidizing biomass, *Water Res.*, 2016, **89**, 282–292.
50 S. L. Saalfield and B. C. Bostick, Changes in iron, sulfur, and arsenic speciation associated with bacterial sulfate reduction in ferrihydrite-rich systems, *Environ. Sci. Technol.*, 2009, **43**(23), 8787–8793.
51 J. M. León Ninin, A. Higa Mori, J. Pausch and B. Planer-Friedrich, Long-term paddy use influences response of methane production, arsenic mobility and speciation to future higher temperatures, *Sci. Total Environ.*, 2024, **943**, 173793.
52 L. Holmkvist, T. G. Ferdelman and B. B. Jørgensen, A cryptic sulfur cycle driven by iron in the methane zone of marine sediment (Aarhus Bay, Denmark), *Geochim. Cosmochim. Acta*, 2011, **75**(12), 3581–3599.
53 J. S. Berg, D. Jézéquel, A. Duverger, D. Lamy, C. Laberty-Robert and J. Miot, Microbial diversity involved in iron and cryptic sulfur cycling in the ferruginous, low-sulfate waters of Lake Pavin, *PLoS One*, 2019, **14**(2), e0212787.
54 G.-H. C. Ng, C. E. Rosenfeld, C. M. Santelli, A. R. Yourd, J. Lange, K. Duhn, *et al.*, Microbial and Reactive Transport Modeling Evidence for Hyporheic Flux-Driven Cryptic Sulfur Cycling and Anaerobic Methane Oxidation in a Sulfate-Impacted Wetland-Stream System, *J. Geophys. Res.*, 2020, **125**(2), e2019JG005185.
55 M. Pester, K.-H. Knorr, M. W. Friedrich, M. Wagner and A. Loy, Sulfate-reducing microorganisms in wetlands – fameless actors in carbon cycling and climate change, *Front. Microbiol.*, 2012, **3**, 72.
56 T. Wind and R. Conrad, Sulfur compounds, potential turnover of sulfate and thiosulfate, and numbers of sulfate-reducing bacteria in planted and unplanted paddy soil, *FEMS Microbiol. Ecol.*, 1995, **18**(4), 257–266.
57 W. Guo, A. R. Cecchetti, Y. Wen, Q. Zhou and D. L. Sedlak, Sulfur Cycle in a Wetland Microcosm: Extended 34S-Stable Isotope Analysis and Mass Balance, *Environ. Sci. Technol.*, 2020, **54**(9), 5498–5508.
58 A. Kölbl, P. Schad, R. Jahn, W. Amelung, A. Bannert, Z. H. Cao, *et al.*, Accelerated soil formation due to paddy management on marshlands (Zhejiang Province, China), *Geoderma*, 2014, **228–229**, 67–89.
59 L. Wissing, A. Kölbl, P. Schad, T. Bräuer, Z.-H. Cao and I. Kögel-Knabner, Organic carbon accumulation on soil mineral surfaces in paddy soils derived from tidal wetlands, *Geoderma*, 2014, **228–229**, 90–103.
60 Y.-Q. Cheng, L.-Z. Yang, Z.-H. Cao, E. Ci and S. Yin, Chronosequential changes of selected pedogenic properties in paddy soils as compared with non-paddy soils, *Geoderma*, 2009, **151**(1), 31–41.
61 L. L. Stookey, Ferrozine—a new spectrophotometric reagent for iron, *Anal. Chem.*, 1970, **42**(7), 779–781.
62 F. Hegler, N. R. Posth, J. Jiang and A. Kappler, Physiology of phototrophic iron(II)-oxidizing bacteria: implications for modern and ancient environments, *FEMS Microbiol. Ecol.*, 2008, **66**(2), 250–260.
63 J. D. Cline, Spectrophotometric determination of hydrogen sulfide in natural waters, *Limnol. Oceanogr.*, 1969, **14**(3), 454–458.
64 R. Lohmayer, A. Kappler, T. Lösekann-Behrens and B. Planer-Friedrich, Sulfur species as redox partners and electron shuttles for ferrihydrite reduction by sulfurospirillum deleyianum, *Appl. Environ. Microbiol.*, 2014, **80**(10), 3141–3149.
65 K. Lagarec and D. G. Rancourt, Extended Voigt-based analytic lineshape method for determining N-dimensional correlated hyperfine parameter distributions in Mössbauer spectroscopy, *Nucl. Instrum. Methods Phys. Res. Sect. B Beam Interact. Mater. Atoms*, 1997, **129**(2), 266–280.
66 X. Xu, P. Wang, J. Zhang, C. Chen, Z. Wang, P. M. Kopittke, *et al.*, Microbial sulfate reduction decreases arsenic mobilization in flooded paddy soils with high potential for microbial Fe reduction, *Environ. Pollut.*, 2019, **251**, 952–960.
67 J. Sun, A. N. Quicksall, S. N. Chillrud, B. J. Mailloux and B. C. Bostick, Arsenic mobilization from sediments in microcosms under sulfate reduction, *Chemosphere*, 2016, **153**, 254–261.
68 W. Wisawapipat, N. Chooaiem, S. Aramrak, N. Chittamart, S. Nookabkaew, N. Rangkadilok, *et al.*, Sulfur amendments to soil decrease inorganic arsenic accumulation in rice grain under flooded and nonflooded conditions: Insights

from temporal dynamics of porewater chemistry and solid-phase arsenic solubility, *Sci. Total Environ.*, 2021, **779**, 146352.

69 K. Yan, Q. Guo, L. Wang, Y. Liu and B. Planer-Friedrich, Potential for formation of methylated thioarsenates in geothermal environments, *Geochim. Cosmochim. Acta*, 2024, in press.

70 C. M. Hansel, C. J. Lentini, Y. Tang, D. T. Johnston, S. D. Wankel and P. M. Jardine, Dominance of sulfur-fueled iron oxide reduction in low-sulfate freshwater sediments, *ISME J.*, 2015, **9**(11), 2400–2412.

71 F. N. Ponnamperuma, The Chemistry of Submerged Soils, in *Advances in Agronomy*, ed. N. C. Brady, Academic Press, vol. 24, 1972, p. 29–96.

72 Jr. W. H. Patrick and A. Jugsujinda, Sequential reduction and oxidation of inorganic nitrogen, manganese, and iron in flooded soil, *Soil Sci. Soc. Am. J.*, 1992, **56**(4), 1071–1073.

73 D. R. Lovley and E. J. Phillips, Competitive mechanisms for inhibition of sulfate reduction and methane production in the zone of ferric iron reduction in sediments, *Appl. Environ. Microbiol.*, 1987, **53**(11), 2636–2641.

74 P. M. van Bodegom, J. C. M. Scholten and A. J. M. Stams, Direct inhibition of methanogenesis by ferric iron, *FEMS Microbiol. Ecol.*, 2004, **49**(2), 261–268.

Supporting information to

Sulfur depletion through repetitive redox cycling unmasks the role of the cryptic sulfur cycle for (methyl)thioarsenate formation in paddy soils

José M. León Ninin[1*], Carolin Dreher[2], Andreas Kappler[2], Britta Planer-Friedrich[1‡]

[1] Environmental Geochemistry, Bayreuth Center for Ecology and Environmental Research (BayCEER), University of Bayreuth, 95440 Bayreuth, Germany

[2] Geomicrobiology, Department of Geosciences, University of Tübingen, 72076 Tübingen, Germany

* Corresponding author. Phone: +49-921-553995; E-mail address: jose.leon-ninin@uni-bayreuth.de (J.M. León Ninin).

‡ Deceased

(8 Pages, 3 Tables, 12 Figures)

Supplementary Data

Table S1: Selected soil properties of the original soil used for the long-term incubation experiment.

Soil name	Horizon*	Horizon depth (cm)*	Soil pH*	Soil Org. C* (g kg^{-1})	Soil Fe* (g kg^{-1})	Soil As** (mg kg^{-1})	Soil S** (g kg^{-1})	Fe_O/Fe_{DCB}**
P50	Alp1	0 - 7	7.4	17.8 ± 0.5	38	17	3.52	0.43 ± 0.04

*Data from Kölbl, et al. [1]. **Data from León Ninin, et al. [2]. Oxalate extractable iron (Fe_O), Dithionate-citrate-bicarbonate extractable iron (Fe_{DCB}).

Table S2: Parameters collected during Mössbauer spectra analysis.

Sample	Phase	CS (mm/s)	QS/ ε (mm/s)	H (T)	σ*	Relative area (%)	χ^2
C0 (77 K)	$Fe^{III}_{adsorbed}$/clays	0.46	0.72			**52.6**	0.64
	Fe^{II}_{total}	1.24	2.87			30.1	
	Crystalline Fe^{III}(oxyhydr)oxides	0.39	-0.17	52.1	3.0	17.3	
C0 (5 K)	Fe(III)/clays	0.48	0.72			**45.5**	0.77
	Fe^{II}	1.30	2.81			27.2	
	Crystalline Fe^{III}(oxyhydr)oxides	0.49	-0.08	51.9	3.0	24.5	
	Poorly crystalline Fe^{III}(oxyhydr)oxides	0.35	-0.14	48.0	0.0	2.8	
C10 (77 K)	Fe^{III}/clays	0.47	0.73			**52.1**	0.52
	Fe^{II}	1.23	2.84			33.6	
	Crystalline Fe^{III}(oxyhydr)oxides	0.53	-0.071	51.9	2.2	14.3	
C10 (5 K)	Fe^{III}/clays	0.42	0.73			**53.8**	0.79
	Fe^{II}	1.30	2.79			28.0	
	Crystalline Fe^{III}(oxyhydr)oxides	0.53	-0.072	51.9	2.2	12.8	
	Poorly crystalline Fe^{III}(oxyhydr)oxides	0.35	0.019	58.4	3.0	5.4	
C30 (77 K)	Fe^{III}/clays	0.44	0.71			**50.7**	0.55
	Fe^{II}	1.24	2.84			32.1	
	Crystalline Fe^{III}(oxyhydr)oxides	0.43	-0.069	51.5	2.3	17.2	
C30 (77 K)	Fe^{III}/clays	0.48	0.71			**53.3**	0.83
	Fe^{II}	1.30	2.78			30.4	
	Crystalline Fe^{III}(oxyhydr)oxides	0.43	-0.14	51.5	2.3	9.5	
	Poorly crystalline Fe^{III}(oxyhydr)oxides	0.33	-0.034	49.1	3.0	6.8	

Center shift (CS), quadrupole splitting (QS), hyperfine field (H), sigma, the relative area and the goodness of the fit χ^2.

Table S3: Relative areas (%) of mineral phases and total Fe content in samples C0, C10, and C30.

Mineral phase & Fe soil content	C0	C10	C30
$Fe^{III}_{adsorbed}$/clays	45.5	53.8	53.3
Fe^{II}_{total}	27.2	28.0	30.4
Crystalline Fe^{III}(oxyhydr)oxides	24.6	12.8	9.5
Poorly Crystalline Fe^{III}(oxyhydr)oxides	2.8	5.4	6.8
Total Fe content (g kg^{-1})	33 ± 2	27 ± 2	23 ± 1

Values for Total Fe content in the soil are given as average ± standard deviation (n = 3).

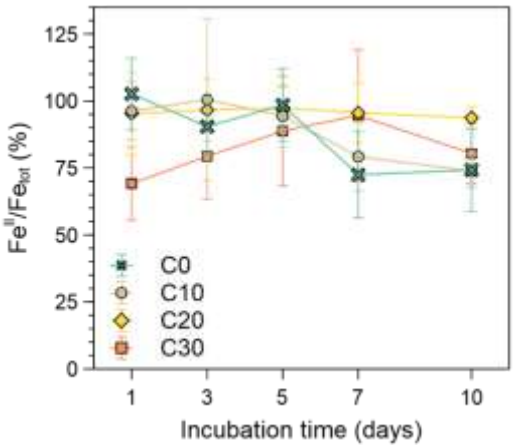

Figure S1: Fraction of reduced Fe in total dissolved Fe throughout incubation time for all redox cycled soils. Data points are average values and bars indicate standard deviation (n = 3).

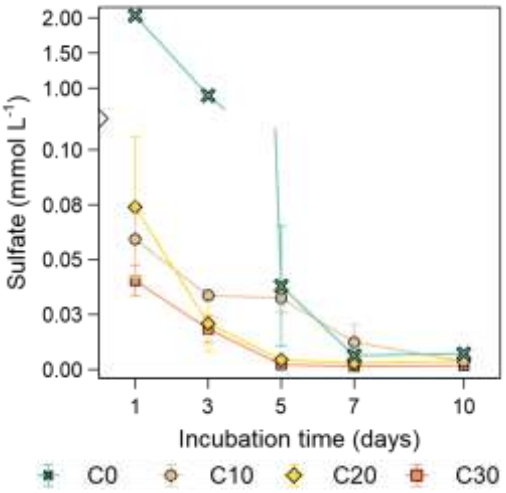

Figure S2: Time-resolved sulfate concentrations during the anoxic incubation period for all soils. Data points are average values and bars indicate standard deviation (n = 3).

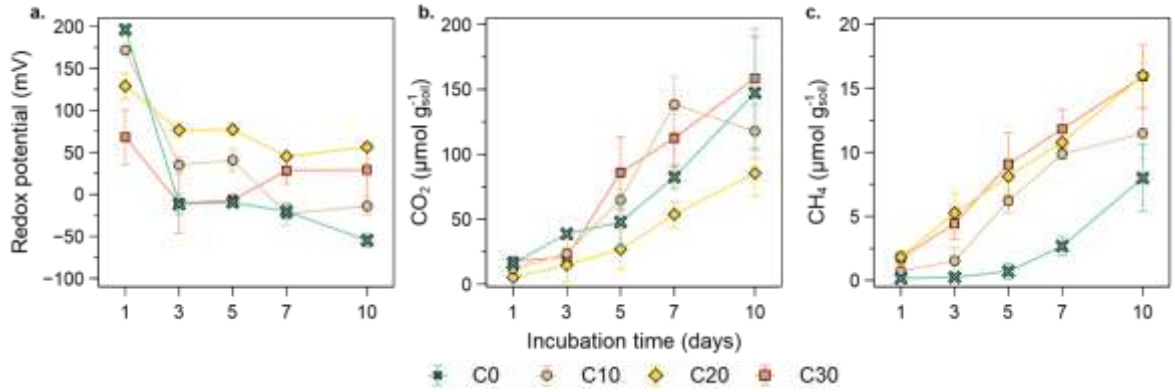

Figure S3: Temporal changes on redox potential (a), CO_2 production (b) and CH_4 production (c) for all redox cycled soils. Data points are average values and bars indicate standard deviation (n = 3).

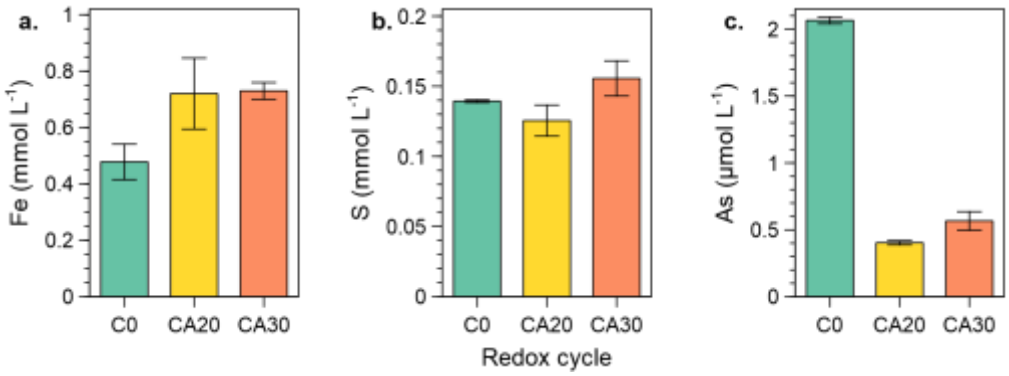

Figure S4: Comparison of aqueous phase Fe (a), S (b), and As (c) in C0 and constantly anoxic setups at day 10 of the anoxic cycle. Bar height is the average value, and bars indicate standard deviation (n = 3).

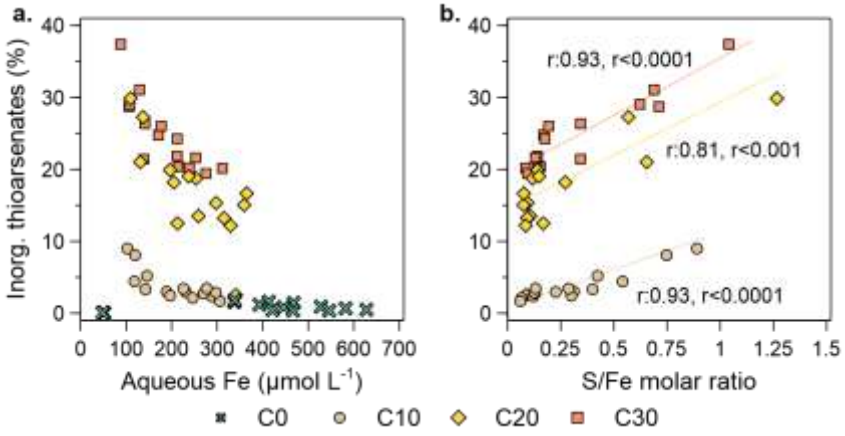

Figure S5: Influence of Fe depletion on thioarsenate formation in soils after repeated redox cycling (a) and effect of excess S over Fe on thioarsenate formation for each repleted soil (b).

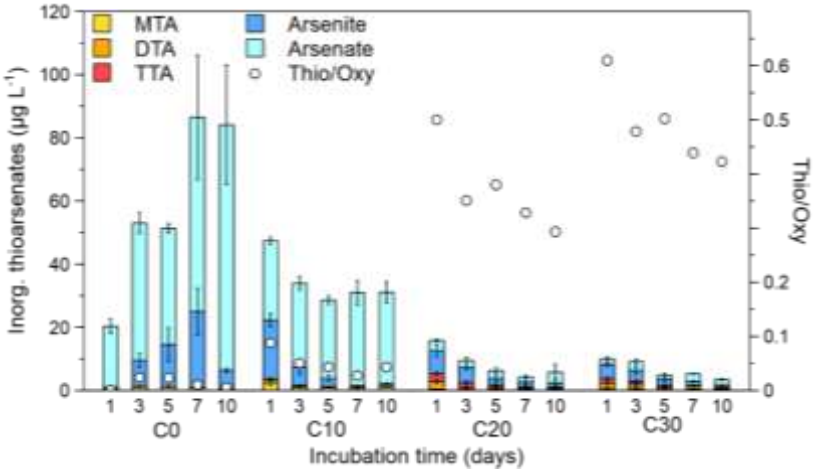

Figure S6: Temporal dynamics and contribution of all inorganic arsenic species to total As in the depleted soils.

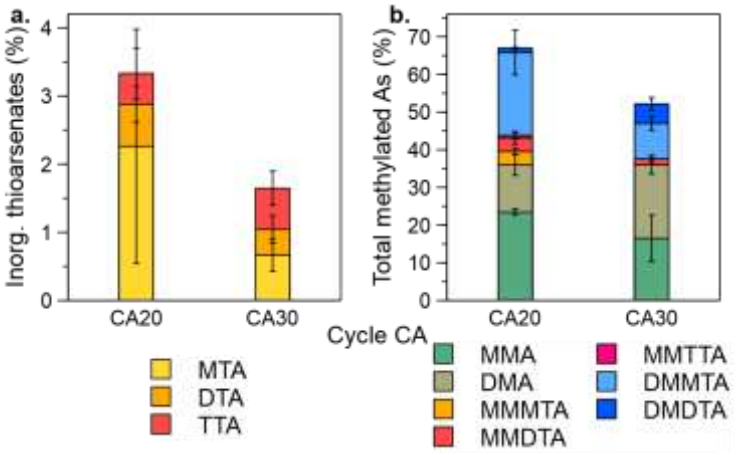

Figure S7: Inorganic thioarsenate and methylated As contribution to total As by anoxic incubation day 10 in CA setups.

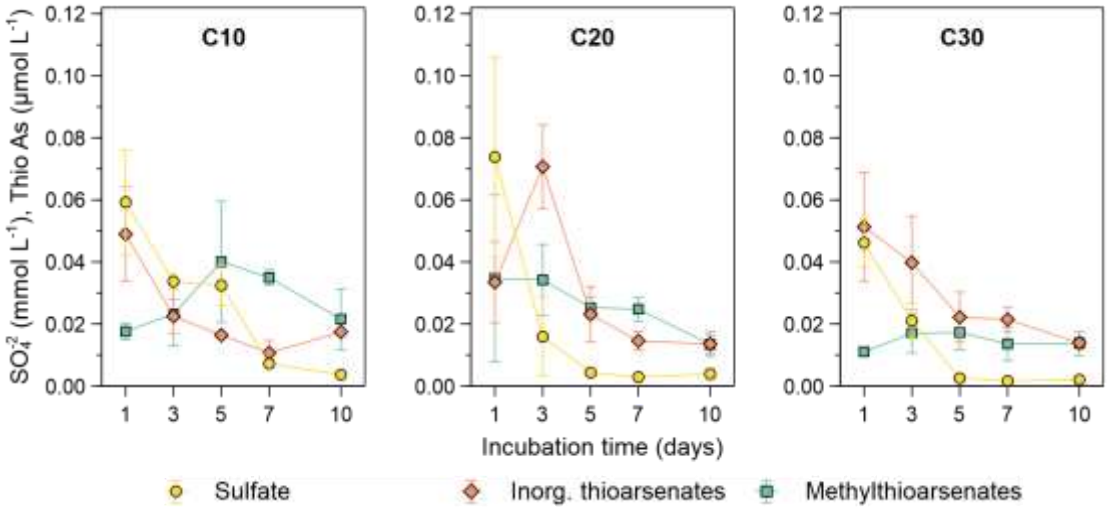

Figure S8: Temporal changes of inorganic and methylated thioarsenate concentrations in the soils after repeated redox cycling. Data points are average values and bars indicate standard deviation (n = 3).

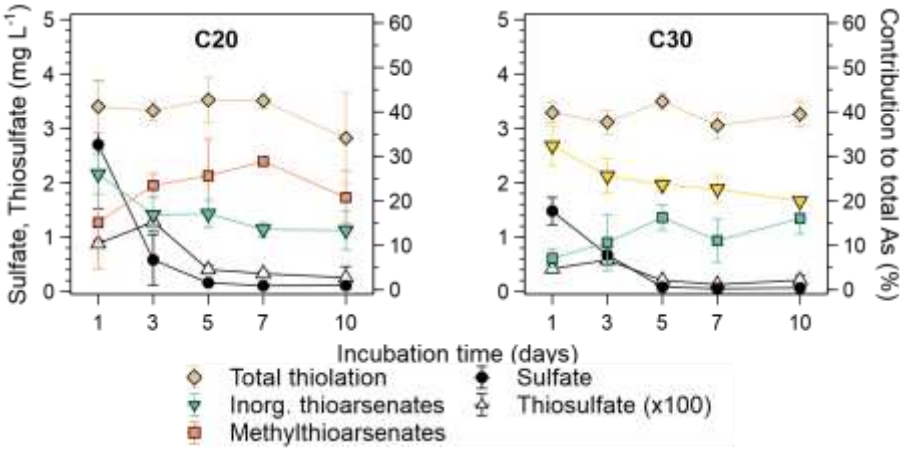

Figure S9: Temporal dynamics in the contribution of inorganic, methylated and total thiolated As species, and comparison with aqueous phase S species.Data points are average values and bars indicate standard deviation (n = 3).

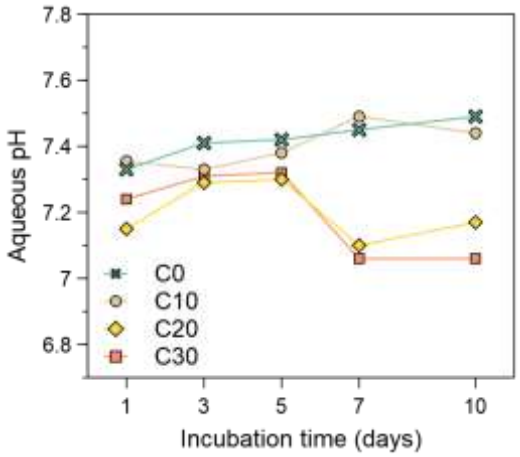

Figure S10: Temporal changes in aqueous phase pH with increasing redox cycling. Data points are average values and bars indicate standard deviation (n = 3).

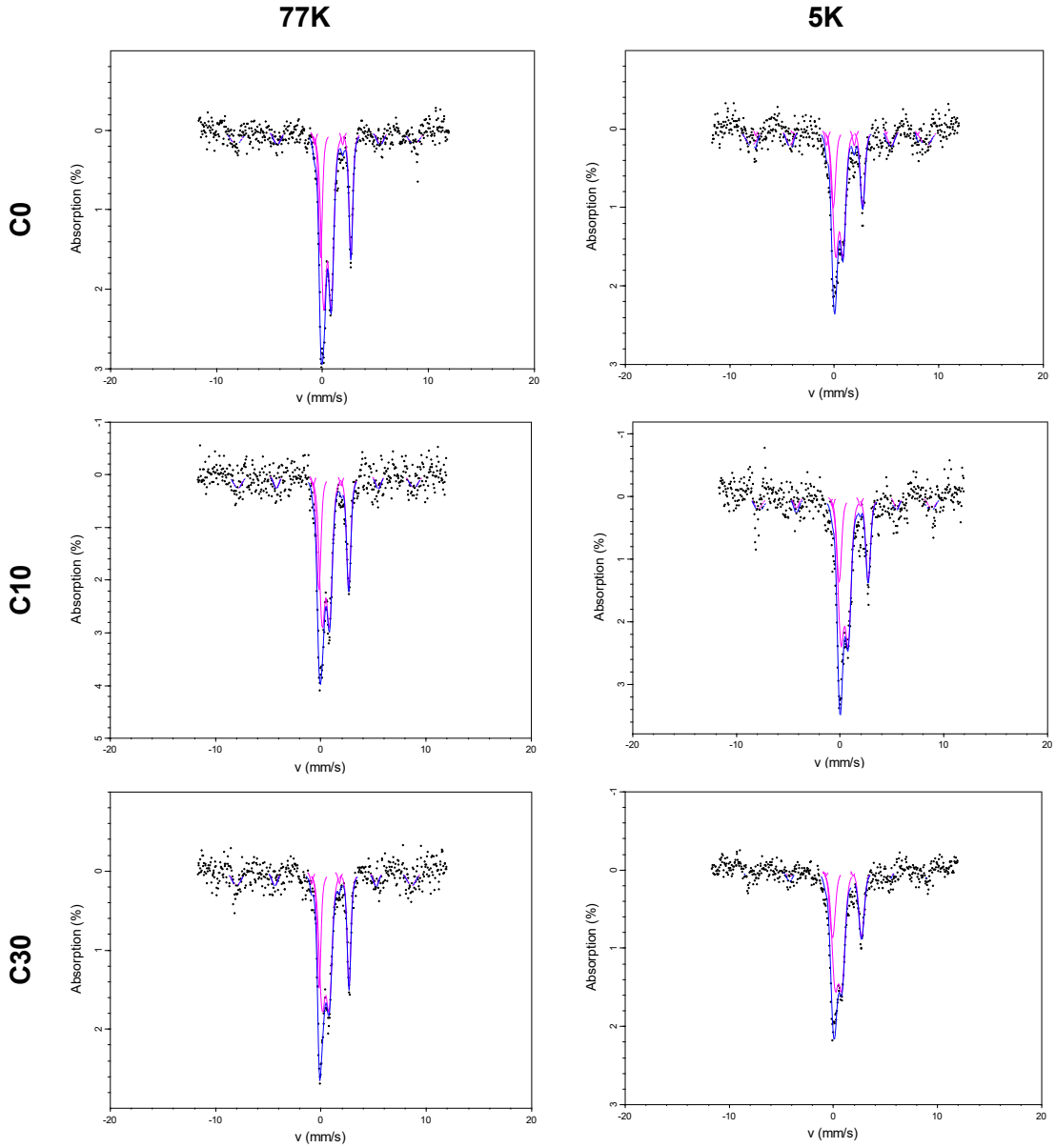

Figure S11: Mössbauer spectra and fitting of samples C0, C10, C30. Measurements taken at 77 and 5 K. Black dots show the original measurement. Blue and pink lines are the overall and individual fits, respectively.

Supplementary Discussion

Due to some uncertainties regarding the mineral phase of the Fe^{II} and the Fe^{III} (oxy)hydroxide, additional µXRD measurements were carried out (Figure S12). All samples were dominated by quartz. Therefore, some reflections were ambiguous. Other mineral phases found were wüstite ($Fe^{II}O$), siderite ($Fe^{II}CO_3$) and hematite ($Fe^{III}_2O_3$). Wüstite has a very similar pattern to periclase (MgO), so the main Fe^{II} phase was most likely siderite. The µXRD patterns did not show clear signs of clay minerals. However, the strong signal of quartz might have covered low abundant mineral phases.

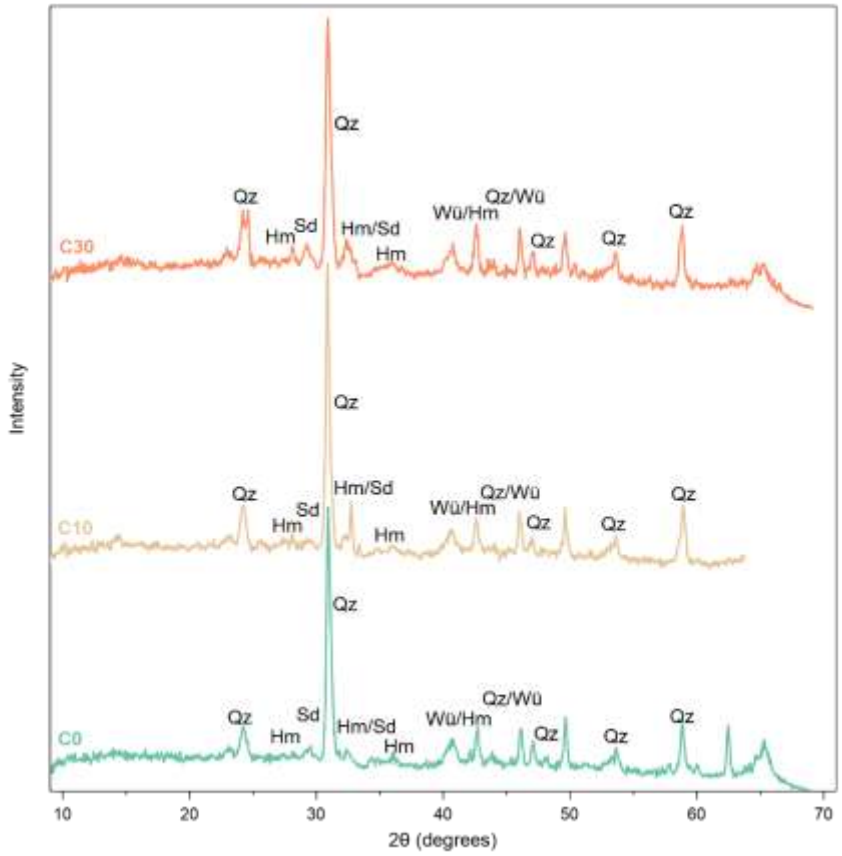

Figure S12: µXRD patterns of C0, C10, and C30 (from bottom to top). Quarz (Qz), Hematite (Hm), Siderite (Sd), Wüstite (Wü).

Supplementary References

1 Kölbl, A. *et al.* Accelerated soil formation due to paddy management on marshlands (Zhejiang Province, China). *Geoderma* **228-229**, 67-89 (2014). https://doi.org:10.1016/j.geoderma.2013.09.005

2 León Ninin, J. M. *et al.* Changes in arsenic mobility and speciation across a 2000-year-old paddy soil chronosequence. *Science of The Total Environment* **908**, 168351 (2024). https://doi.org:10.1016/j.scitotenv.2023.168351

List of Publications

The following papers have been published during the work on this thesis:

León Ninin, J.M.; Muehe, E.M.; Kölbl, A.; Higa Mori, A.; Nicol A.; Gilfedder, B.; Pausch, J.; Urbanski, L.; Lueders, T.; Planer-Friedrich, B. Changes in arsenic mobility and speciation across a 2000-year-old paddy soil chronosequence. *Sci. Total Environ.* **2024**, *908*, 168351.

León Ninin, J.M.; Higa Mori, A.; Pausch, J.; Planer-Friedrich, B. Long-term paddy use influences response of methane production, arsenic mobility and speciation to future higher temperatures. *Sci. Total Environ.* **2024**, *943*, 173793.

León Ninin, J.M.; Kryschak, N.; Peiffer, S.; Planer-Friedrich, B. Long-term paddy soil development buffers the increase in arsenic methylation and thiolation after sulfate fertilization. *J. Agric. Food Chem.* **2024** *72* (45), 25045-25053

León Ninin, J.M.; Dreher, C.; Kappler, A.; Planer-Friedrich, B. Sulfur depletion through repetitive redox cycling unmasks the role of the cryptic sulfur cycle for (methyl)thioarsenate formation in paddy soils. *Environ. Sci.: Processes Impacts*, **2025***,* Advance Article.

Other publications and manuscripts realized or submitted during the time as PhD student:

Eberle, A.; Besold, J.; León Ninin J.M.; Kerl, C.F.; Kujala, K.; Planer-Friedrich, B. Potential of high pH and reduced sulfur for arsenic mobilization–Insights from a Finnish peatland treating mining waste water. *Sci. Total Environ.* **2021**, *758*, 143689.

León Ninin, J. M.; Colina Blanco, A. E.; Held, A.; Planer-Friedrich, B. Environmental Forensics: Mock Trial of a Chromium Contamination Case as a Tool for Interdisciplinary Teaching and Improvement of Soft Skills. *J. Chem. Educ.* **2022**, *99* (10), 3452–3460.

Wang, L.; Guo, Q.; Wu, G.; Yu, Z.; León Ninin, J.M., Planer-Friedrich, B. Methanogens-Driven Arsenic Methylation Preceding Formation of Methylated Thioarsenates in Sulfide-Rich Hot Springs. *Environ. Sci. Technol.* **2023**, *57* (19), 7410-7420.

Drabesch, S.; Lechtenfeld, O.; Bibaj, E.; León Ninin, J.M.; Lezama-Pacheco, J.; Fendorf, S.; Planer-Friedrich, B.; Kappler, A.; Muehe, E.M. Climate induced microbiome alterations increase cadmium bioavailability in agricultural soils with pH below 7. *Commun. Earth Environ*. **2024,** *5* (1), 637.

Drabesch, S.; Mueller, S.; León Ninin, J.M.; Planer-Friedrich, B.; Kappler, A.; Muehe, E.M. Combined and individual effects of temperature and elevated atmospheric CO_2 on Cd mobility and soil biogeochemistry in an agricultural soil. *Submitted to Environ. Sci. Technol.*

Supervised Master Theses

The following theses have been co-supervised during the work on this thesis:

1. Traut, A. (2020). Trace element availability in a 2000-year-old paddy soil chronosequence. *The results of this project are included in Studies 1, 2, and 3.*
2. Ploompu, G. (2020). Effect of freeze-thawing cycles on the mobilization of As and P from peat.
3. Higa Mori, A. (2021). Arsenic speciation and methane release from a paddy soil chronosequence under changing climate conditions. *The results of this project are included in Study 2.*

Supervised Bachelor Thesis

The following thesis has been co-supervised during the work on this thesis:

1. Einert, N. (2020). Understanding vanadium geochemistry in estuaries and lakes in Croatia

(Eidesstattliche) Versicherungen und Erklärungen

(§ 9 Satz 2 Nr. 3 PromO BayNAT)

Hiermit versichere ich eidesstattlich, dass ich die Arbeit selbstständig verfasst und keine anderen als die von mir angegebenen Quellen und Hilfsmittel benutzt habe (vgl. Art. 97 Abs. 1 Satz 8 BayHIG).

(§ 9 Satz 2 Nr. 3 PromO BayNAT)

Hiermit erkläre ich, dass ich die Dissertation nicht bereits zur Erlangung eines akademischen Grades eingereicht habe und dass ich nicht bereits diese oder eine gleichartige Doktorprüfung endgültig nicht bestanden habe.

(§ 9 Satz 2 Nr. 4 PromO BayNAT)

Hiermit erkläre ich, dass ich Hilfe von gewerblichen Promotionsberatern bzw. -vermittlern oder ähnlichen Dienstleistern weder bisher in Anspruch genommen habe noch künftig in Anspruch nehmen werde.

(§ 9 Satz 2 Nr. 7 PromO BayNAT)

Hiermit erkläre ich mein Einverständnis, dass die elektronische Fassung meiner Dissertation unter Wahrung meiner Urheberrechte und des Datenschutzes einer gesonderten Überprüfung unterzogen werden kann.

(§ 9 Satz 2 Nr. 8 PromO BayNAT)

Hiermit erkläre ich mein Einverständnis, dass bei Verdacht wissenschaftlichen Fehlverhaltens Ermittlungen durch universitätsinterne Organe der wissenschaftlichen Selbstkontrolle stattfinden können.

…….
Ort, Datum, Unterschrift